# RAPID SEISMIC VULNERABILITY ASSESSMENT OF SCHOOL BUILDINGS IN QUÉBEC

**By**

**Helene Tischer**

Department of Civil Engineering and Applied Mechanics

McGill University

Montréal, Québec, Canada

April 2012

A thesis submitted to McGill University in partial fulfillment of the requirements of the degree of Doctor of Philosophy

# Abstract

The seismic performance of schools deserves special attention because of their unique occupancy characteristics and important post-earthquake role. Past experience has shown that school buildings are especially vulnerable to earthquakes; they are often irregular structures, and most of them were designed and built prior to the introduction of modern building codes that adequately address earthquake-resistant design and seismic hazard. This research addresses the concerns related to school earthquake safety for the province of Québec by developing a seismic screening method for the evaluation of the public school buildings.

Rapid visual screening methods are intended to be coarse screening procedures requiring little resources and time per building. The adapted seismic screening method that was developed is a score assignment procedure, with the final score dependant on the seismicity, lateral load resisting system type, building height, construction year, potential structural deficiencies (horizontal and vertical irregularities, deterioration and short concrete columns), potential for pounding and local soil conditions. Scores are calculated based on the capacity spectrum method, a nonlinear static analysis procedure. The methodology is inspired by the *Rapid Visual Screening of Buildings for Potential Seismic Hazard* (FEMA154) procedure, which has been adapted and enhanced to serve as a screening tool for schools in Québec. It reflects these building's specific characteristics and takes into consideration the province's seismicity as stipulated in the 2010 edition of the National Building Code of Canada (NBC).

The method is grounded on the extensive characterization of 101 individual school buildings, pertaining to 16 different school sites. These schools are designated as post-critical shelters and a secondary objective was to assess whether they can achieve this function in case of a design-level earthquake. Schools were characterized by site visits, study of building plans, and consultation of the city's microzonation map. Furthermore, an ambitious experimental program sought to determine the dynamic properties of all buildings and the characterization of the local soil conditions through ambient vibration measurements (AVM). Finally, a

comprehensive inventory of unreinforced heavy masonry partition walls was made. From the collected information general characteristics of schools could be established, which were corroborated by an extensive literature review. AVM records on buildings permitted an assessment of some of the generic capacity curves used for the calculation of the scores by comparing their elastic range to the experimental fundamental frequencies. Local soil conditions determined from AVM where in good agreement with other sources of information. The experimental procedure was also found to be simple enough so its application is feasible in a rapid seismic screening context.

The application of the screening method to the sample of schools classified 18 buildings as having a very high, 18 a high, 44 a moderate and 21 a low priority for future intervention. This information, together with average scores per school site, determines which sites are more likely to be adequate as post-earthquake shelters. A more detailed analysis of the results and comparison with two relevant existing rapid seismic screening methods (FEMA154 and the *Manual for Screening of Buildings for Seismic Investigation*, NRC92) clearly highlight some advantages of the developed method. Analysis of the scores' variances confirms that most of the evaluated parameters are significantly influential in the final scores. In particular, the classification of the structural weaknesses and the potential for pounding according to their severity proved effective to differentiate the buildings, something that was sought when developing the method because of the high incidence of these parameters in schools and because these are not properly considered in existing methods.

# Résumé

La performance sismique des écoles exige une attention particulière compte tenu de leur usage et de leur rôle-clé dans un contexte post-séisme. L'observation des dommages suite à des violents séismes survenus ailleurs dans le monde a révélé que les bâtiments scolaires sont particulièrement vulnérables; il s'agit souvent de structures comportant d'importantes irrégularités géométriques et la plupart ont été conçues et construites avant l'introduction de normes de conception parasismique modernes. Cette recherche se concentre sur l'évaluation des bâtiments scolaires du Québec et vise à développer une méthode simplifiée et rapide, adaptée au contexte québécois, pour classifier la vulnérabilité sismique de ces bâtiments en vue de prioriser des évaluations plus détaillées si nécessaires.

Les méthodes d'évaluation rapide dite visuelle, sont des méthodes de triage qui utilisent des critères simplifiés mais relativement certains et qui requièrent peu de ressources par bâtiment. La méthode présentée dans cette thèse procède par assignation de pointages suivant divers critères et paramètres, et le pointage final d'un bâtiment donné est la somme de son pointage de référence (le BSH : *basic structural hazard* score) qui dépend du type de système de résistance aux forces sismiques latérales, et d'une série de pointages correctifs. Ces pointages correctifs sont en fait des ajustements au pointage de référence qui tiennent compte des particularités du bâtiment évalué comme sa hauteur, son année de construction, la présence possible de faiblesses structurales (irrégularités verticales et horizontales, détérioration des matériaux, présence possible d'effets de poteaux courts dans les ossatures en béton armé), risque de cognement avec bâtiments adjacents, et effets d'amplification des accélérations dus aux conditions géotechniques locales. Les pointages de référence et les pointages correctifs sont définis pour 15 catégories de systèmes structuraux assurant la résistance aux charges sismiques horizontales, et ce pour trois zones d'aléa sismique (aléa faible, modéré et élevé). Les pointages ont été calculés à partir de la méthode de la capacité spectrale et l'analyse de la réponse inélastique des bâtiments ayant subi des dommages. Cette approche s'inspire de la méthodologie utilisée par FEMA 154 (*Rapid Visual Screening of Buildings for Potential Seismic Hazard)*: toutefois elle est grandement améliorée et adaptée au contexte particulier des écoles du Québec. La

méthode proposée reflète les caractéristiques particulières des bâtiments construits au Québec et tient compte des données d'aléa sismique stipulées dans l'édition 2010 du Code National du Bâtiment (CNB) du Canada.

Le développement de la méthode est basé sur une analyse exhaustive de 101 bâtiments scolaires faisant partie de 16 écoles situées sur l'île de Montréal. Il s'agit en fait de 16 écoles secondaires désignées par le Centre de sécurité civile de la Ville de Montréal pour servir de centre d'hébergement d'urgence en cas de catastrophe nécessitant l'évacuation de résidents de leur logis. Cet échantillonnage spécial définit un objectif secondaire de cette recherche qui consiste à évaluer (en appliquant la méthode développée) lesquels parmi ces centres d'hébergement sont susceptibles de rester fonctionnels pour servir leur usage suite à un fort tremblement de terre. Les données détaillées sur les 101 bâtiments ont été obtenues à partir d'inspections sommaires, par l'étude des dessins structuraux et architecturaux lorsque disponibles, et avec le microzonage sismique de l'île de Montréal. Les propriétés dynamiques de base des bâtiments ont été obtenues à partir d'une vaste campagne de mesures de vibrations ambiantes (MVA). Des MVA ont également été prises sur le sol à l'extérieur des bâtiments pour corroborer les informations géotechniques disponibles ou les classes sismiques des sites sur la carte de microzonage. Enfin, on a fait un inventaire détaillé de la géométrie des partitions et murs de remplissage en maçonnerie non armée, puisque ce type de mur est communément utilisé dans les bâtiments scolaires évalués. Ce type de mur est particulièrement vulnérable aux accélérations sismiques hors plan qui peuvent en causer l'effondrement et ainsi compromettre directement la sécurité des occupants ou gêner les manœuvres d'évacuation sécuritaire. À partir de cette collecte d'information, les caractéristiques des écoles s'avérant les plus pertinentes pour l'évaluation sismique ont été identifiées et ensuite corroborées par une revue de la littérature. Il en ressort que les bâtiments scolaires sont généralement de faible hauteur (de un à trois étages) et qu'ils partagent plusieurs caractéristiques susceptibles d'aggraver leur vulnérabilité sismique lorsqu'on les compare à d'autres types de bâtiments. Les structures des écoles évaluées montrent également peu de diversité quant au type de système de reprise des charges horizontales (deux systèmes seulement sont dominants) et l'année de construction. Les MVA ont permis d'estimer la limite inférieure de la période naturelle et de l'amortissement modal des bâtiments, information qui a ensuite été utilisée pour valider les courbes de capacités spectrales utilisées pour le calcul des pointages de référence (BSH) et l'assignation des pointages correctifs. Cette validation s'est faite en comparant la partie élastique des courbes de capacité avec les données expérimentales. Cette comparaison a montré que les fréquences propres mesurées étaient légèrement plus hautes mais généralement en accord avec les valeurs théoriques. Les classes de site sismiques estimées par MVA sont également en accord avec les données de microzonage sismique et autres informations géotechniques disponibles. La procédure expérimentale MVA s'est révélée assez simple (rapide et robuste) sur le terrain et son utilisation est tout à fait appropriée dans un contexte d'évaluation rapide comme la méthode proposée, surtout en l'absence de données géotechniques de base.

La méthode d'évaluation dans sa forme finale a ensuite été appliquée aux 101 bâtiments de l'étude. Les pointages obtenus indiquent les niveaux de priorité suivants: 18 de priorité très élevée, 18 de priorité élevée, 44 de priorité modérée, et finalement 21 de priorité faible. Les pointages individuels des bâtiments de même que les pointages moyens calculés pour l'ensemble des bâtiments d'une école donnée, permettent d'évaluer quelles sont les écoles (ou les sous-ensembles de bâtiments d'une école) susceptibles de pouvoir servir de centre d'hébergement post-sismique en cas de tremblement de terre majeur.

Une analyse détaillée des résultats obtenus avec la méthode proposée ainsi qu' une comparaison des résultats obtenus à l'aide des méthodes FEMA154 et NRC92 ont permis de mettre en évidence plusieurs de ses avantages. L'analyse statistique des variances des pointages correctifs confirme que tous les paramètres d'évaluation sélectionnés ont une influence significative sur le pointage final. En particulier, la considération de différents niveaux de sévérité des faiblesses structurales et des possibilités de cognement a permis de différentier la vulnérabilité des bâtiments à l'étude, ce qui était une motivation de départ importante pour cette recherche. Il est à noter que ces aspects ne sont pas bien différentiés par le FEMA 154 qui pénalise toute forme d'irrégularité verticale alors que les irrégularités horizontales ont peu d'influence. La méthode NRC92, quant à elle, pénalise systématiquement tous les bâtiments les plus anciens (construction avant 1970), alors que leurs autres caractéristiques spécifiques ont peu d'influence sur le classement final.

# Acknowledgments

I would like to thank my research co-supervisors, Prof. Denis Mitchell and Prof. Ghyslaine McClure, for their guidance and encouragement. I had the incredible luck to benefit from the close collaboration with these two outstanding professors, each one with distinctive interests and expertise. Their advice and positive criticism contributed significantly to the final outcome of this research. Our lively discussions also contributed to make the time spent on this project an enjoyable and enriching experience for me.

My work was carried out in collaboration with officials of several institutions. Special thanks go to the Civil Security Centre (Centre de Sécurité Civile) of the city of Montréal, which provided information on the city's schools designated as shelters and established contacts to the school boards. Officials at the school boards and schools were very kind to grant me access to building plans, and facilitate repeated visits to their institutions. Finally, I would like to thank the province's Ministry of Education (Ministère de l'Éducation, du Loisir et du Sport), in particular Mr. Gilles Marchand, for authorizing the work to be carried out.

The acquisition of ambient vibration measurements would have been impossible without the help of several graduate and undergraduate students: Diego Hausfather, Jeffrey Southern, Jean-François Belleau, Damien Gilles, Amin Asgarian, Suze Youance, Salman Saeed and Mohammad Talukder. I thank them all for helping me through long hours of demanding work and for their interest in my research.

I would like to acknowledge the financial support of the Natural Sciences and Engineering Research Council of Canada, through the Canadian Seismic Research Network (Strategic Networks Program), which allowed me to focus primarily on my research.

Finally, I would like to thank my family and extended family, for their much appreciated encouragement and their help, either directly with my research or indirectly by providing time and a stress-free environment for me to concentrate on my work.

# Table of Contents

# List of Figures

# List of Tables

# Chapter 1. Introduction

## 1.1. Research Motivation

The disastrous performance of schools during the M8.0 Sichuan (China) earthquake on 12$^{th}$ May 2008 resulted in the deaths of hundreds of children while at school (Revkin, 2008). The reason for this catastrophe was that the structures were not designed and built to withstand earthquakes of that magnitude: the first adequate Chinese seismic design code was implemented only after the 1976 Tangshan earthquake, and many buildings would likely have collapsed in a much smaller seismic event. Unfortunately, this case is not isolated. There have been many examples from different countries that have demonstrated that school buildings are especially vulnerable to damage in a moderate to strong earthquake (Dolce, 2004, López et al., 2004b, Revkin, 2008, Spence, 2004). Damage to school buildings is often more extensive than that suffered by other types of buildings, as experienced in the 1999 $M_w$ 7.6 Taiwan earthquake. Different explanations have been suggested. Most of the damaged schools were designed and constructed with less stringent design criteria than those considered appropriate today (ATC, 2004). Schools also tend to have an irregular structural configuration with large clear spans to accommodate spaces for a variety of functions, such as classrooms, offices, gymnasia and libraries (Dolce, 2004).

The protection of children is paramount because they provide for future generations and represent an especially vulnerable segment of society. It has also been argued that safe schools are a basic right that must be provided by the government, since school attendance is obligatory in many countries (Chakos, 2004). Acknowledging these facts, in 2005 the Organisation for Economic Co-operation and Development (OECD) published recommendations concerning guidelines on the earthquake safety of schools. In this document, the organization suggests that "member countries take steps to establish and implement programmes of school seismic safety" (OECD, 2005). The first step to ensure effective risk reduction in existing buildings is the assessment of this risk.

In Québec, previous studies and experience in past earthquakes have suggested that there is an urgent need to determine the seismic vulnerability of schools. This has also been acknowledged by the Ministry of Education, with a preliminary study conducted in 2006 (Chagnon, 2006), and ongoing research on several projects on this topic. The present research contributes to this effort by developing an adapted rapid seismic screening method specific to the characteristics of the province's schools and by carrying out a vulnerability assessment of the schools designated as post-critical shelters in Montréal. The designation as shelters is made by the city's emergency-preparedness department, CSC, (*Centre de Sécurité Civile*), and this project was carried out in close collaboration with this department.

Due to the large size of the Québec's school inventory (roughly 2,700 school sites, number of individual buildings unknown), it is necessary to address the seismic vulnerability in phases, starting by a seismic screening in order to identify buildings that are potentially at high risk. Only these high-risk buildings will undergo a more detailed evaluation of their mitigation needs and strategies. Rapid visual screening (RVS) methods available today, namely the Canadian *Manual for Screening of Buildings for Seismic Investigation,* NRC92, (NRC/IRC, 1992), and the North American *Rapid Visual Screening of Buildings for Potential Seismic Hazard*, FEMA154, (ATC, 2002a) have limitations when applied to Québec schools. Some of these shortcomings can be addressed by modifying these methods taking into account building types specific to Canada, and by considering the latest National Building Code (NBC) revisions of spectral accelerations in eastern Canada and the influence of soil conditions. For school buildings in particular, however, features promoting higher vulnerability could be overlooked if based only on an exterior visual evaluation. Failure to identify mass and stiffness irregularities induced by adjoining spaces of different geometries, or to identify separate adjacent structures when buildings are arranged in clusters are clear examples of such oversights.

## 1.2. Objectives

The main goal of the present research is to develop a seismic screening method adapted to schools in Québec. The purpose of this method is to single out critical school buildings by determining their probable behaviour when subjected to a design earthquake. Time and resources needed to evaluate each individual building have to be limited, so the application of the method is feasible for a large inventory of buildings. The method should consider Québec's seismicity and the specific characteristics of the school buildings. It should also be up to date with the 2010 NBC and adaptable to changes in future code editions.

A secondary objective of the present research, of special interest for the CSC, is to evaluate the seismic safety of all the schools designated as post-critical shelters on the island of Montréal, comprising 16 school sites and 101 individual buildings. The goal was to create a seismic portfolio for each individual building to determine if they are able to serve post-earthquake needs.

## 1.3. Methodology

### *1.3.1. Evaluation of Existing Information on Seismic Vulnerability of Schools*

As mentioned before, experience in past earthquakes has demonstrated that schools are particularly vulnerable and they have common features that could negatively influence their seismic behaviour. To identify these features and deficiencies, a thorough literature review of the behaviour of schools in past earthquakes, vulnerability assessment methods and retrofit programs for educational facilities was made. Although worldwide cases were studied, special attention was given to information specific to Québec.

### *1.3.2. Evaluation of Existing Rapid Seismic Screening Methods*

Two existing seismic screening methods were identified as being relevant in the given context: the method currently available for Canada, given in the *Manual for Screening of Buildings for Seismic Investigation,* NRC92, (NRC/IRC, 1992), and the method developed in the United States, *Rapid Visual Screening of Buildings for Potential Seismic Hazard*, presented in the FEMA154 report (ATC, 2002a). Preliminary assessments using the two methods were carried out on the 101 evaluated school buildings, and a careful evaluation of their advantages and drawbacks was made.

### *1.3.3. Examination of School Buildings*

Existing information on the seismic vulnerability of schools was corroborated and complemented with detailed assessments of the 101 individual buildings designated as post-critical shelters. These detailed assessments provided means to calibrate the rapid seismic screening method that was developed. School buildings were characterized in detail by site visits, evaluations of building plans, determinations of dynamic structural properties by ambient vibration measurements, characterization of infill walls and evaluations of local soil conditions by ambient noise data. An independent study evaluated the seismic risk associated with their operational and functional components. With the wealth of collected information, general characteristics of the schools (for example related to floor area, number of storeys and lateral load resisting system), as well as features that could negatively influence the seismic behaviour of the buildings were identified. Note that these schools were not randomly picked and therefore they do not represent the province's entire school building inventory, regarding building age and lateral load resisting system for example. This is discussed in more detail in **Chapter 8**.

### *1.3.4. In-Situ Dynamic Properties of Buildings*

The dynamic properties (periods, modes of vibration and viscous damping ratios for the first modes) of the 101 school buildings were determined by ambient vibration measurements. The fundamental periods obtained were compared to those obtained by approximate formulae given by the NBC and better fitting expressions were proposed. The period that characterizes the elastic range of generic capacity curves used in the developed seismic screening method was compared to the experimental periods. Finally the relation between the periods of torsional modes and the building height or number of storeys was examined, and viscous damping ratios were compared to the 5% value usually assumed for seismic design.

### *1.3.5. Determination of the Local Soil Conditions*

Local soil conditions of the 16 school sites were determined independently from information available on the building plans and from the city's microzonation map. Information on local soil conditions is often not readily available and this factor can be decisive in the seismic behaviour of a building (especially if very poor soil conditions are expected). Therefore an in-situ methodology, simple enough to be used in a rapid seismic screening context, was explored. This methodology determines the soil type based on ambient noise measurements taken on the soil surface. It was applied to all 16 school sites, and results were compared to those obtained from other sources of information.

### *1.3.6. Development of the Adapted Seismic Screening Method*

The adapted seismic screening method is inspired by the FEMA154 methodology and was developed as a score assignment procedure, with calculations based on the capacity spectrum method (ATC, 2005). The input demand spectra for the method were carefully selected to represent the latest available information on seismicity and demographics of Québec. Generic capacity and fragility curves developed for the United States (NIBS, 2003) were used to characterize the buildings, with benchmark years and design levels selected to reflect building practice in eastern Canada. Detailed treatment was given to structural weaknesses that are extremely common at schools, such as horizontal and vertical irregularities, short concrete columns and deterioration, as well as the potential for pounding.

### *1.3.7. Validation of the Developed Method*

Finally, the developed screening method was applied to the 101 school buildings that are post-disaster shelters in Montréal to validate the screening method and to confirm if these schools are appropriate to be used as shelters. The influence of all parameters that make up the final score for each building was assessed through analysis of variance. To demonstrate the improvements over existing methods, scores were recalculated with the FEMA154 and NRC92 methodologies and compared to results obtained by the adapted seismic screening method.

## 1.4. Organization of the Dissertation

The thesis consists of 8 chapters. **Chapter 1** states the research motivation, objectives, methodology and organization of the dissertation.

**Chapter 2** presents the background and literature review. The performance of school buildings in past earthquakes and seismic risk mitigation programs is described first. Some significant examples are described in more detail, and general observations are made. Available information on schools in Québec is then presented, describing experience in past earthquakes and previous studies relative to their expected earthquake performance. Then some information on existing rapid seismic screening methods and their development is given. Special emphasis is put on the two methods identified as being most relevant for the context of the present research, namely FEMA154 and NRC92. A detailed description of these methods is given, as well as their advantages and shortcomings when applied to the evaluation of school buildings in Québec. Finally, some concepts of the modal identification of buildings from ambient vibration testing are given.

A characterization of the studied school buildings is described in **Chapter 3**. The sources and methods used to gather the required information are described, followed by general characteristics of the inventory of buildings such as the construction year, lateral load resisting system and predominant structural weaknesses. A detailed database of the characteristics of heavy infill walls was generated and is also presented in this chapter. An independent study examined the seismic risk of operational and functional components, and the results are briefly discussed. Finally, a preliminary evaluation of the schools using the FEMA154 and NRC92 methods is presented.

In **Chapter 4** the in-situ dynamic properties of the same sample of school buildings are discussed. First the experimental procedure is described, comprising the data collection and analysis. Then the results are presented, with the characterization of all schools for their seismic portfolio, the evaluation of the approximate NBC formulae for fundamental period, and the comparison of the elastic part of the capacity curves used for the adapted seismic screening method with the experimentally determined results. The first torsional modes and their relation to the building height and fundamental mode were analyzed. Experimental viscous damping ratios were compared to the customary 5% damping, also used in the NBC.

In **Chapter 5**, information regarding the local soil conditions at the 16 studied school sites is presented. First, the description of the soil classification is given according to the NBC. Then the site classifications from existing sources of information are determined, including building plans and the city's microzonation map. Finally, a simple experimental procedure based on ambient noise records on the ground's surface is described and applied to all school sites. This procedure is simple enough to be feasible in a rapid seismic screening context, although its use is no prerequisite for the developed method. The selected NBC soil type for each school site is presented, considering all sources on information.

In **Chapter 6**, the development of the adapted seismic screening method for school buildings is presented. The selected methodology is described, with the final score for each building calculated as the sum of a basic structural hazard score and several score modifiers that take into consideration the building's specific characteristics such as age and structural deficiencies. These scores and modifiers are calculated based on the capacity spectrum method, and the required input is described, including the lateral load resisting system classification, the selection of the seismic design level and benchmark years, and the seismic zoning and spectral acceleration values used for the calculations. The calculated values of the basic scores and modifiers are then presented, together with a description on how the values were obtained. Finally, an independent methodology for the identification of school buildings where out-of-plane failure of heavy infill walls is critical is presented.

The developed method was applied to the sample of school buildings, as presented in **Chapter 7**. Here some general guidelines for the use of the methodology are also given, which can serve as some guidance for future use of the screening method. The final scores of the evaluated schools, as well as the influence of the basic structural hazard score and score modifiers, are analyzed and the benefits of the developed method are highlighted by comparing the results obtained using the adapted seismic screening method to those using existing rapid seismic screening methodologies.

Finally, **Chapter 8** summarizes the main conclusions and original contributions from the present research project. Limitations and recommendations for future work are also presented.

# Chapter 2. Background and Literature Review

As part of the literature review the performance of school buildings in past earthquakes and existing seismic risk mitigation projects were studied. The resulting conclusions and some well documented sample cases are presented in **Sections 2.1** and **2.2**. A complete list of cases and relevant citations can be found in **Appendix A**. In **Section 2.3** available information on schools in Québec, their performance in previous earthquakes and existing data on their probable seismic vulnerability are presented. This is followed by a review of existing seismic screening methods in **Section 2.4**, adapted from a previously published paper (Tischer et al., 2011). A detailed comparison between the two most relevant methods (NRC92 and FEMA154) is made, highlighting the advantages and shortcomings of each in the context of the evaluation of schools in eastern Canada. Finally, **Section 2.5** gives some background information on the experimental determination of dynamic properties of structures. It focuses on the data acquisition and digital signal processing for ambient vibration measurements, method used in this research.

## 2.1. Performance of School Buildings in Past Earthquakes

The poor performance of schools in past seismic events demonstrates the relevance of the present research. Information on the studied cases suggests that between 30% and 80% of schools subjected to strong earthquakes needed repair or had to be demolished. The number of school buildings with extensive damage and failure has also been disproportionally high compared to the general building stock. This has been the cause of deaths and injuries of thousands of children worldwide in the last century alone. Recent earthquakes, like the February 27, 2010 8.8 moment magnitude ($M_w$) Chilean event, demonstrate that the problem is far from solved. In this event that luckily happened outside school session, more than 2000 schools were seriously damaged. The series of strong earthquakes that occurred in recent years around the world also demonstrates that the issue is global and needs to be addressed in all communities exposed to high seismic hazards.

The protection of children is paramount in society because they represent an especially vulnerable segment of society. It has been argued that safe schools must be considered a basic right in countries where school attendance is obligatory (Chakos, 2004). The closure of schools after a seismic event also results in psychological stress of children. Children that lose their social network because of relocation may be more isolated and show higher dependency on adults (Bulut et al., 2005). In addition, school buildings play a key role in restoring the normal functioning of society after an earthquake: they can be used as emergency shelters and their operation enables parents to return to work.

From the studied cases it can be concluded that schools that behave unsatisfactorily usually are structures that were built with minimum or without seismic consideration. Either no or deficient seismic code provisions were in place, or the expected level of shaking was largely underestimated. The consequences of the lack of strength and ductility are aggravated by the high incidence of structural irregularities, for example because of the need to accommodate large open spaces such as gymnasia and libraries adjacent to smaller classrooms. Finally, insufficient maintenance and modifications to the original structures that increase the loading or reduce the resistance have been identified as two other common problems. Some key cases are exposed in more detail in the following sections. A complete review with extensive references is presented in **Appendix A**, together with data on seismic mitigation projects.

### *2.1.1. Italy*

One of Europe's biggest earthquake disasters of modern times was the collapse of the Iovene primary school in the town of San Guiliano during the October 31, 2002 5.5 $M_w$ Molise earthquake, killing 27 pupils and one teacher. This school was designed in 1957 and built between 1959 and 1960. Specific factors that contributed to the collapse are that the location was not classified as a seismic zone by the building codes prior to 2003, the local soil conditions amplified the ground motion, poor masonry construction was used in combination with a heavy concrete roof, and a second storey was added (Dolce, 2004). A total of 300 school buildings were surveyed after the earthquake, 20% of which were found to have suffered significant damage. Nearly all of them (295) were constructed without any consideration of seismic provisions since they were located on sites classified as low hazard prior to the event. In most cases modifications such as the addition of storeys or the reduction of resisting area of structural masonry walls further weakened the structures and aggravated the situation (Augenti et al., 2004). This earthquake caught nationwide attention, and compelled the state to revise seismic zoning and design norms.

### *2.1.2. Venezuela*

The 6.8 $M_w$ Caraico earthquake that struck Venezuela on July 9, 1997 caused the collapse of four schools. In the town of Caraico, closest to the epicentre, five reinforced concrete buildings collapsed. Two of these buildings were schools, and 46 students were killed. The first school, a two-storey concrete frame with infill masonry construction of 1958, with two independent buildings, failed due to the low resistance and stiffness in the longitudinal direction, short column effects induced by the masonry infill and limited ductility due to inappropriate detailing. The second school, also a concrete frame with infilled masonry construction, was designed in 1978 and built seven years later in 1985. The school had two buildings that were three storeys high and had a C shape plan view. The likely causes of the collapse were low ductility, short columns and a first soft storey effect created by the masonry infill (López et al., 2004b).

Approximately 70% of schools in Venezuela, roughly 20,000 individual campuses, are located in high and very high seismic hazard zones. Since schools in Venezuela have traditionally been built based on only a few generic design concepts, it is estimated that several hundred existing schools are similar to those damaged in Caraico, identified as old-type and box-type structures by their designs. A study of these two school types led to the conclusion that they pose a significant risk to life safety, even in moderate earthquakes. A project has been proposed to identify and classify existing schools in terms of seismic vulnerability, assess the level of risk and propose measures to reduce risk to levels deemed acceptable by national standards (López et al., 2004a, López et al., 2004b).

### *2.1.3. United States (California)*

Several earthquakes have damaged or destroyed Californian school buildings throughout American historey. One notorious event was the March 10, 1933 6.3 $M_w$ Long Beach earthquake, which produced heavy damage to school buildings and led to the implementation of seismic regulations specifically addressed to educational facilities. It was estimated that in Los Angeles County 75% of the public schools suffered extensive damage or collapse. Luckily, the earthquake did not happen during school hours so there were no casualties. This event made the Legislature aware of the serious shortcomings in the design and construction of school buildings and the Field Act was passed shortly after (in 1933), with the purpose of providing protection of life and property for elementary, secondary and community college facilities. The Garrison Act, first passed in 1939, has led to the evaluation and retrofit of almost all pre-Field Act school buildings (Jephcott, 1986).

### *2.1.4. Other Catastrophic Earthquakes*

Various events stand out in historey as nothing short of disasters. They put into perspective the urgency of evaluating and retrofitting school buildings, and the terrible consequences that could arise if this issue is ignored.

The 7.8 $M_w$ Kashmir earthquake devastated Pakistan on October 8, 2005; it happened on a Saturday, at 8:50am local time, while children were at schools. Over 10,000 schools collapsed, killing more than 18,000 children and injuring more than 50,000. The 2004 9.3 $M_w$ Southeast Asia earthquake and tsunami destroyed more than 750 schools in Indonesia alone, damaging another 2,135. A total of 40,900 students and 2,500 teacher and administrative staff died. In Sri Lanka the Maldives and Thailand over 130 additional schools were destroyed in the same event. El Salvador was rocked by a 7.6 $M_w$ earthquake in 2001 that damaged 85 schools beyond repair, and seriously damaged 279 additional ones. Half of the casualties of this event were children. In Taiwan the 1999 7.6 $M_w$ Chi-Chi earthquake produced the collapse of 51 schools, damaging 786 other. This accounted for 22% of the countries elementary, middle and high schools. Additionally, 71% of the post-secondary institutions were damaged. Luckily the earthquake occurred at 1:47am and no casualties were reported. In Washington State (United States), the 7.1 $M_w$ Olympia earthquake of 1949 luckily hit at noon, while schools were not in session. Two children were killed at a school site, 10 schools were destroyed and 30 more were damaged. A total of 10,000 students were affected.

## 2.2. Seismic Risk Mitigation Programs for Schools

In 2005 the Organization for Economic Co-operation and Development (OECD) acknowledged the poor seismic performance of educational facilities and published recommendations on the earthquake safety of schools (OECD, 2005). In this document, OECD suggests that "member countries take steps to establish and implement programs of school seismic safety". Partly thanks to this initiative and partly because of the effect of damaging earthquakes, programs of seismic assessment and retrofit have been or are currently being carried out in several countries. Reports on these projects are often difficult to access, because they are treated with high confidentiality. However, in some isolated cases the opposite is true, and information is made available in great detail (see for example the seismic screening program of Oregon's essential facilities). Sharing the information leads to greater community involvement and which in turn results in swift actions being taken by local governments when schools are deemed to be at risk. Two cases that illustrate the importance of the involvement of parents and the community at large are the procedures used in Berkeley, California and in British Columbia.

The study of seismic assessment programs is especially interesting in the context of this research. From these experiences, it is seen that the seismic evaluation of schools always has been treated as a multi-stage (multi-tier) process, due to the large building stocks that need to be examined. The first phase is often very general, aimed at identifying schools that have an adequate level of safety and that do not require further study. It is either carried out based on information already available, or some simple form of data collection, mostly relying on visual inspection of the building geometry and exterior appearance. Results show that schools have some general features that are the same for almost every location examined. They are usually low-rise structures with high incidence of irregularities. The variation of lateral load resisting systems is limited, although the types present will not necessarily be the same from one country or jurisdiction to another. In some cases, a large proportion of the building stock was constructed based on a single generic design, which simplifies the assessment projects. The year of construction of schools is also not randomly distributed, but clearly linked to urbanisation, governmental educational policies and population fluctuations. Sometimes a distinction on the seismic vulnerability can be made based on the level of education offered (primary versus secondary for example in Canada), as the buildings are often composed of different building types and construction times.

In places where schools have already been retrofitted, as in California (USA) and New Zealand, the positive effect of this retrofit has been demonstrated in later seismic events. Retrofitted buildings have clearly fared better than school buildings where no interventions have been carried out. There are also no reports of injuries and fatalities at the retrofitted schools.

Some cases of seismic risk mitigation programs are presented in the following sections. For more information see **Appendix A**.

### *2.2.1. British Columbia (Canada)*

The only comprehensive seismic assessment and retrofit program for schools in Canada is the British Columbia (BC) School Seismic Mitigation Program, sponsored by the province's Ministry of Education. This project stands out for being initiated by an active community advocating for seismically sound schools. The community involvement was started by a single mother of two, worried by the school collapse after the 2002 Molise earthquake in Italy. She engaged other parents, and founded the *Families for School Seismic Safety* advocacy group. In 2004, after a little less than two years of community pressure, the Ministry of Education engaged in the evaluation of the seismic vulnerability of all public schools located in the province's high-risk zones, corresponding to 850 of the province's total of around 2,500 schools. A special-purpose rapid seismic assessment software was developed to conduct this evaluation. This tool, known as UBC-21, was used to evaluate low-rise buildings based on five parameters: the seismic zone (the province was divided in six regional seismic zones), the structural lateral-load resisting system, the capacity, the year of construction (before or after 1990) and the structural irregularities (Ventura et al., 2004). Among the 850 schools evaluated with UBC-21, about 700 were found at moderate or high risk: 293 high, 265 moderate/high, and 149 moderate (Pandey and Ventura, 2010).

Based on these results, in 2004 the Ministry approved a $1.5 billion seismic mitigation program over 10 to 15 years (initially estimated to be completed in 2019) with the goal of retrofitting all at risk schools, recognizing that schools need to be reassessed before taking these measures. Given the size of the project, the Ministry also funded the development of "a state-of-the-art performance-based seismic engineering technology for achieving optimum safety within a cost-effective mitigation framework" (Taylor et al., 2006). The development of this technology was entrusted to the Association of Professional Engineers and Geoscientists of BC (APEGBC) with the collaboration of the Department of Civil Engineering of the University of British Columbia (CEUBC).

Due to the perceived urgent need to begin the retrofitting of BC schools , interim "Bridging Guidelines" were developed and first published in 2005, with the aim to reassess the seismic vulnerability of the schools and develop specific reinforcement strategies (APEGBC and UBC, 2005). Continued research allowed the recent publication of the first edition of the Seismic Retrofit Guidelines (APEGBC and UBC, 2011). Further work is currently being carried forward, and a second edition is already envisioned. The three main objectives of the guidelines, currently applicable only to low-rise school structures with limited irregularities, are enhancing life safety by reducing the probability of structural collapse, achieving cost-effective retrofits and developing a user-friendly approach to the evaluation and retrofit of schools. It was also envisioned to adopt a common engineering approach for the seismic evaluation and retrofit of all the province's schools.

The project was developed by a unique collaboration between government, APEGBC, CEUBC, the local structural engineering community and international experts. The provincial government, through its Ministry of Education, is the promoter and funds the project. The Ministry also plays a key role in enforcing the use of the developed guidelines. The research needed for the project was conducted by the CEUBC, including the development of the methodology, performing numerical analyses and experimental testing. The work was then reviewed by an external peer review committee, comprising several practicing engineers from California, and two committees of local engineers registered with the APEGBC, an internal peer review committee and the technical review board. In total over 50 highly qualified engineers were involved in the project. To train BC's engineering community at large for the application of the developed guidelines, several seminars have been offered.

One of the main advantages of the guidelines is the use of a performance-based approach. The threshold for potential collapse in a building undergoing earthquake excitation is determined using inelastic deformation predictions, rather than relying on pseudo-elastic forces calculated according to current building codes. The predictions were established based on the incremental dynamic analysis (IDA) technique, with over nine million analyses performed. Local soil and seismicity were considered by de-aggregating the uniform seismic hazard mapping information by considering each type of earthquake source separately (crustal, subcrustal and subduction earthquakes). The nonlinear characteristics of almost all the structural systems of existing schools as well as retrofit solutions were established based on laboratory tests and existing information from a comprehensive literature review. The structural systems are treated as an assembly of sub-systems, called prototypes, that represent the principal building elements. Prototypes are defined for the lateral deformation-resisting system (LDRS), the vertical load-bearing elements, unreinforced masonry walls susceptible to out-of-plane rocking, floor diaphragms and foundations.

To perform the seismic analyses, 10 earthquake records were selected for each earthquake source. The records were then scaled to the uniform hazard velocity spectra in a period range of one to two seconds. Each prototype is subjected to 30 ground motions at a specific intensity, and the results expressed as the probability of deformation occurrence are combined. This is repeated with ground motion intensities varying from 30% to 250% of code levels (probability of exceedance of 2% in 50 years, corresponding to a return period of 2475 years) using 10% increments. The reference soil type C was used for the analyses, and modification coefficients were established for other soil types.

The non-linear behaviour of the prototypes, described through cyclic force-deformation response curves, was established using experimental data already available complemented with additional laboratory testing. A two-storey building was selected for the analysis and deemed appropriate to represent one to three-storey schools with some adaptations. IDA was performed for each prototype varying the lateral capacity from 2% to 100% of the building's gravity weight. To determine if a given LDRS is adequate, a design drift limit was selected. Defining the probability of drift exceedance (PDE) as the probability that the drift limit for a given LDRS will be exceeded over 50 years for all levels of shaking and for all types of earthquakes, the IDA analyses were used to determine the lateral capacity needed to keep the PDE below 2% in 50 years, deemed to correspond to life safety performance. This minimum required capacity for the LDRS can be compared to its actual capacity to determine the system's adequacy. A second condition was imposed to relate the guidelines to the National Building Code of Canada (NBC). This condition limits the probability that a LDRS peak drift will exceed the governing drift limit over 50 years to 25% at a level of shaking and the specified type of earthquake in the NBC, corresponding to a mean return period of 2475 years. Results were made available to the final user through a web-based application, called the seismic performance analyzer. **Figure 2.1** shows the output plot of the analyzer when using the seismic assessment option for a sample element. The user needs to input the location, soil type, prototype, resistance of the prototype factored with respect to the seismic weight attributed to this element, storey height and design drift limit. The blue curve in the plot represents the PDE of the given prototype versus its factored resistance. The green triangle represents the specific element studied, in this case with a factored resistance of 13%, as defined by the user. Since the PDE for this element is below 2%, the element does not need retrofit. The analyzer can be used in a similar manner to determine the factored resistance necessary for a given element to achieve a given design drift limit.

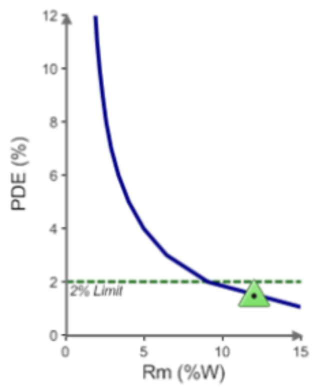


**Figure 2.1.** Sample output of the seismic performance analyzer, from (APEGBC and UBC, 2011)

Finally, the so-called toolbox method allows combining different structural systems to evaluate existing structures and different retrofit options to select the most cost-effective one. The toolbox method aims to include all structural systems and components and generate their lateral resistance in a drift-compatible manner. This is achieved by selecting the appropriate governing deformation limit, which corresponds to the lowest deformation limit of all considered prototypes.

### *2.2.2. Oregon (United States)*

The state of Oregon has recently undertaken the seismic screening of its essential post-critical facilities, including most of its K-12 public schools and community colleges. A total of 1,101 schools and 179 colleges, representing more than 2,300 buildings, were evaluated using the FEMA154 screening tool (see **Section 2.4**), and detailed results were published on the internet in 2007 (McConnell, 2007). The state was divided in three seismic zones: moderate, high and very high near the coast. However, scores assigned for the high and very high regions were the same, with calculations considering a median short period (0.2 s) spectral acceleration response value of 1.23 g and a median one-second spectral acceleration response value of

0.45g. It was found that 31% of the evaluated educational facilities have a low, 22% a moderate, 35% a high and 12% a very high collapse potential in a design-level earthquake.

Analyzing the detailed data available for each school building, it was concluded that the constructions can be described by a limited number of lateral load resisting systems. The three most common lateral load resisting types were reinforced masonry bearing walls with wood or metal deck floors and roofs, wood post and beams, and concrete shear walls, making up for 81% of the evaluated buildings. Over 50% of the buildings were constructed between 1940 and 1970. The presence of irregularities is very widespread, with 60% of the buildings having at least one vertical irregularity and 71% having at least one plan irregularity. The most common vertical irregularity is building with setbacks, and the most common horizontal irregularities are buildings with re-entrant corners and lateral load resisting elements that are out of plane.

Some initial steps to reduce the seismic risk of essential facilities have already been taken in Oregon. In 2009, an initial sum of 15 million US dollars was allocated to the seismic retrofit of public school buildings through the seismic rehabilitation grant program. The seismic mitigation work at high-occupancy schools is programmed to be completed by 2032, over a period of 20 years.

### *2.2.3. Italy*

As mentioned before, the San Guiliano school collapse in 2002 generated much attention around seismic safety of school buildings in Italy. A general appraisal of the condition of Italian school buildings revealed that some global factors affect their vulnerability. The seismic zonation used for design has changed significantly over the last century, and older buildings were probably designed considering an inappropriate seismic hazard. Historically Italian seismic codes have also not been adequate for ensuring seismic safety. Although some topics on seismic safety of existing buildings were included since 1986, codes did not change significantly until 2003. Therefore most of the typical Italian schools, reinforced-concrete and masonry buildings constructed before 1980, were practically designed without any seismic considerations. Other common features of schools that affect their seismic performance are irregularities in plan and elevation, insufficient separation joints between adjacent buildings and schools located in buildings which originally had a different use and occupancy. Finally, structural changes pose problems particularly for masonry buildings. Modifications can introduce geometric irregularities and often the mass is increased while the amount of structural walls is decreased. The observed lack of adequate standards of construction, execution and maintenance aggravates existing problems (Dolce, 2004).

Two local studies were conducted in the city of Sanremo (Balbi et al., 2004) and in the province of Potenza (Dolce et al., 2004). In both cases a multi-tier evaluation procedure was proposed¸ with each tier being more complex, and aimed at excluding buildings with acceptable seismic risk in view of detailed seismic engineering studies. The first step used basic data, already available to government agencies, to exclude properly design buildings from the subsequent evaluation. In Sanremo the following phase used an index based screening procedure. It was recognized that existing methods had to be modified for the evaluation of schools to account for worrisome features particularly common in schools buildings, for example buildings that had a different original use and were subsequently modified and extended. The buildings that did not pass this screening were subjected to a detailed structural survey and some in-situ testing. In Potenza, the second phase was the evaluation of potentially at risk buildings using non-destructive testing (as ambient vibration testing) and collecting more detailed information. Finally, the third phase was the detailed evaluation and retrofit of buildings when necessary.

A nationwide prioritisation procedure for the retrofit of educational facilities throughout Italy is currently under development. A two-tier procedure has been proposed, considering that Italy has almost 50,000 school buildings to be assessed. Similar to previous studies, the first phase only takes some key characteristics of the structures into account, using a database collected by the Italian Ministry of Education. The second phase requires more specific information for each school. It has only been applied locally, since the information needed has been collected for a limited number of masonry structures so far (Borzi et al., 2011).

### *2.2.4. California (United States)*

The Field Act provided seismic regulation for Californian schools as early as 1933. Since several moderate and strong earthquakes have happened since then, this case provides insight on the positive effect that seismic regulations can have on the earthquake performance of schools. After the 1984 6.2 $M_w$ Morgan Hill Earthquake for example, six public schools constructed under the Field Act provisions were examined and found to have performed relatively well, with no structural damage to any of the schools, although some limited non-structural damage was observed (Meehan, 1985).

Comparison of the performance of post-Field Act schools with older buildings shows the positive effect of these regulations. Defining the damage loss as the ratio of the cost of repairs or reconstruction to the replacement value of the building, **Table 2.1** shows the comparative performance of several buildings evaluated after significant earthquakes (Jephcott, 1986). For all cases, studied cases were limited to locations with Modified Mercalli (MM) intensities of VIII or higher. For the Imperial Valley earthquake, information for 16 buildings at nine school sites was available. For the Kern County earthquake all schools that were subjected to strong intensity shaking were considered, for a total of 37 schools. The San Fernando Earthquake only affected two school sites with high intensities. For the Coalinga earthquake, nine school sites containing 78 individual buildings were analyzed. As can be seen in **Table 2.1**, for all events the Field Act buildings suffered no significant damage (excluding one building with moderate structural damage after the Coalinga earthquake). Older, pre-Field Act buildings fared far worse, with several buildings having to be demolished.

**Table 2.1.** Comparative performance of pre- and post-Field Act buildings during earthquakes (Jephcott, 1986)

| | **Average Damage Loss** | |
|---|---|---|
| **Earthquake** | **Pre-Field Act** | **Post-Field Act** |
| Imperial Valley (1940, 7.1 $M_w$) | 29% | 1% |
| Kern County (1952, 7.7 $M_w$) | 50% | 1% |
| San Fernando (1971, 6.6 $M_w$) | 100% | 4% |
| Coalinga (1983, 6.7 $M_w$) | 100% | 3% |

Although the positive effect of the Field and the Garrison Acts are undeniable, there are concerns about the potentially poor behaviour of some older Field Act buildings that have not yet been subjected to strong shaking. Despite the encouraging results of post-Field Act buildings in earthquakes, advances in structural analysis and design since 1933 lead to the conclusion that events with longer durations than those of the past could cause certain buildings to collapse. Buildings identified as especially vulnerable include concrete tilt-up construction, non-ductile reinforced concrete frame buildings, older wood structures with unrepaired dry rot or termite damage, buildings with irregular configurations and pre-fabricated buildings with poor foundation systems. Regulations regarding non-structural elements were also very limited in early Field Act schools, only addressing excessive deflections of the structural bracing systems, since it was recognized that they will lead to widespread non-structural damage. So, for example, deflections in vertical bracing systems were limited to 0.005 times the free storey height at the equivalent static force loading. Half this value was proposed for walls containing openings with normal window glass. Even at moderate shaking the failure of non-structural elements can be fatal to occupants if their design is not addressed properly (Mujumdar and McGavin, 1999).

The parents of children attending schools in Berkeley, California, acted on the above-mentioned concerns after the 1989 Loma Prieta Earthquake. Thanks to the community's involvement, all public schools of the area were evaluated and retrofitted starting in 1992. Funds were raised by means of a special tax, which was approved by 70% of Berkeley's voters. A general mitigation program was also started, including the retrofit of other essential facilities (Chakos, 2004). So, for example, all the cities fire stations were retrofitted starting in 1992, in 1996 funds were provided to retrofit the City Hall, and in 2000 the retrofit of the building housing the Police and Fire administrative staff was concluded. However, other public buildings still need to be assessed and retrofitted.

### *2.2.5. New Zealand*

New Zealand's entire territory has been classified as having high seismic hazard, experiencing a large number of earthquakes. This has led to continuous revision and updating of building codes and standards and the retrofit or replacement of existing buildings suspected to have poor seismic behaviour. As an example, unreinforced masonry structures were banned in 1935, and most of the schools of this structural type were replaced or strengthened since then. It was thus assumed that most if not all of New Zealand's schools complied with adequate seismic standards, but there were no records to confirm this assumption. Therefore in 1995 a preliminary assessment of the seismic safety of school buildings and other important structures was carried out by mandate of the Ministry of Education. The findings were used to commission a nationwide study between 1998 and 2001.

The later nationwide evaluation surveyed all the 21,000 individual buildings of the more than 2,000 state primary and secondary schools. The so-called Nelson blocks, 137 buildings constructed in the late 1960s with a standard design concept, were excluded from this study since they were evaluated independently. It was found that generally Nelson blocks needed to be seismically retrofitted, and a standard retrofit solution was designed. One significant finding of the previous 1995 assessment was that most of New Zealand's schools are one and two-storey lightweight constructions. Experience in past earthquakes has demonstrated that one-storey construction of this type perform well, unless heavy elements or poor connections to the foundation are present. Therefore, in the 1998 inspection all buildings fitting this general type, that is the vast majority of the building stock, were deemed adequate unless some specific hazardous features were present. These features could be identified by a visual inspection, without requiring detailed analysis. Because of the high live load of the upper levels (compared to roof loads in New Zealand) this is not applicable to buildings with two or more storeys (Connell Wagner Limited, 2003). Results of the survey showed that previous general assumptions on school safety were correct, with only four buildings found to have an unacceptable level of structural risk, and around 11% of the buildings with at least one structural defect requiring remedial work. Considerable investments have been made since 2001 to remedy these defects (Mitchell, 2004).

The retrofitted school buildings were put to test in the city of Christchurch and surrounding area first during the September 4, 2010 7.1 $M_w$ Canterbury earthquake and the subsequent 6.3 $M_w$ devastating aftershock on February 22, 2011 (Ingham, 2011). Both events caused significant damage to buildings, especially the aftershock with hypocentre at about 10 km from Christchurch's city centre, partly because some structures were already weakened from the previous event. Although the 2010 Canterbury earthquake did not cause human losses, 181 fatalities were reported during the second event. However, school buildings fared surprisingly well given their shaking levels. The second earthquake occurred during school hours, at 12:51pm, but no casualties were reported in any primary or secondary school. Damage to schools was also limited and mainly non-structural. It was reported that 163 schools suffered some damage, 11 of which were damaged significantly. Most of the schools reopened after only three weeks.

## 2.3. Schools in Québec

### *2.3.1. Seismicity and Past Earthquakes*

To assess the seismic risk of a building it is essential to consider the characteristics of the construction and the likelihood of occurrence of a significant seismic event. In eastern Canada on average three earthquakes of magnitude 5 or above are likely to occur within 10 years (NRC, 2009). The province of Québec however is considered a moderate seismic zone. Most of its population is located along the St. Lawrence River valley and continuing along the Ottawa River valley, the province's most active seismic zone. The Charlevoix region has the highest localized seismicity. According to NBC 2010 Uniform Hazard Spectral acceleration values assigned to LaMalbaie are Sa(0.2s) = 2.30 g for short periods and Sa(1.0s) = 0.52 g at a period of 1.0 s, with a probability of exceedence of 2% in 50 years. However, this is a rather confined zone of about 60 km in radius. More typical values are those of the two largest cities of the province, Montréal with Sa(0.2s) = 0.64 g and Sa(1.0s) = 0.14 g, and Québec City, with Sa(0.2s) = 0.55 g and Sa(1.0s) = 0.15 g. These two cities account for half of the province's population.

Moderate and strong earthquakes have occurred in the past in Québec, and they will most certainly occur in the future. The strong events (with Magnitude above 6) have a relatively long return period, which gives the general population the impression that earthquakes are not a threatening hazard in the region, heavily struck by winter storms and floods in the last 15 years. The 1998 Great Ice Storm was the worst ever natural hazard to strike Eastern Canada and North East United States, causing catastrophic losses estimated at nearly 3 billion Canadian dollars in Québec alone (Chang et al., 2007). Some examples of strong earthquakes are the 1929 Grand Banks earthquake (7.2 $M_w$), the 1935 Timiskaming earthquake (6.2 $M_w$), the 1944 Cornwall-Massena earthquake (5.6 $M_w$) and most recently the 1988 Saguenay earthquake (6.0 $M_w$) (Bruneau and Lamontagne, 1994). The Saguenay earthquake is perhaps the only one that the active population can remember, but its consequences were very small compared to those of the 1998 ice storm.

Although Québec's earthquakes in the past have not caused human life losses, extensive property damage has been reported. For example, and although not comparable with the monetary losses of the 1998 ice storm, the 1988 Saguenay earthquake produced damage estimated in the tens of millions of Canadian dollars, even if its epicentre was in a wildlife reserve and far away from major cities (Bruneau and Lamontagne, 1994). In future seismic events with the same magnitude as those in the past, damage is expected to be greater and more widespread due to population growth in post-WWII, prior to the introduction of adequate seismic design standards. Infrastructure expansion has also often been in locations only recently identified as soft soil regions with the tendency to amplify the ground motions (Bruneau and Lamontagne, 1994, Rosset et al., 2011). The importance of these site effects on the seismic hazard has been demonstrated in many seismic events, as for example the earthquake that devastated Mexico City in 1985, where amplifications up to five times the motion recorded on rock outcropping were recorded on soft clay (Finn and Wightman, 2003). Local site effects are discussed in more detail in **Chapter 5**.

Experience of past earthquakes suggests that in Québec school vulnerability is probably not different than in other communities located in moderate seismic areas. There was considerable damage reported to the Collegiate and Vocational School in Cornwall after the 1944 Mw 5.8 Cornwall-Massena earthquake as heavy masonry debris fell through the roof of the gymnasium (Bruneau and Lamontagne, 1994). The findings of the 1988 Saguenay earthquake damage reconnaissance visit team (Mitchell et al., 1989) are troubling for Québec schools when considering that the measured peak accelerations at rock sites did not exceed 0.16 g in the horizontal direction and 0.10 g in the vertical direction. Damage to three schools in Chicoutimi is described in the report, while 16 schools suffered some damage. The report draws attention to the hazards of unreinforced masonry construction (the Cornwall school had been a striking example), and warns about the abundance of this kind of construction in both infill walls and interior partitions, particularly in schools and hospitals. A more detailed damage evaluation of public schools affected by the Saguenay earthquake (Tinawi and Mitchell, 1990) indicated that 16 of the 25 schools of the Chicoutimi School Board suffered architectural damage, with repairs and retrofit costing 3 million Canadian dollars. The study also reports a total of 2.8 million Canadian dollars in architectural damage to all 17 schools of the Baie des Ha! Ha! School Board.

### *2.3.2. Seismic Profile of Québec's Schools*

The seismic safety of public Québec schools with elementary and secondary education programs was first addressed in 2006 in a study commissioned by the province's Ministry of Education, *Ministère de l'Éducation, du Loisir et du Sport* (MELS) (Chagnon, 2006). In this study, the public school infrastructure, comprising more than 3500 buildings constructed between 1857 and 2005, was classified into five groups according to the characteristics presented in **Table 2.2**. The principal consideration for this classification was the year of construction, which was linked to specific architectural types. Mixed type lateral load resisting systems are also found but they are not classified per se because they are not numerous.

**Table 2.2.** Structural classification of public schools in Québec (Chagnon, 2006)

| Type | Category | Construction Year | Lateral Load Resisting System | Percentage |
|---|---|---|---|---|
| 1 | Old | 1950 and before | Steel moment resisting frames | 17.6% |
| 2 | Duplessis | 1955 - 1963 | Wood post and beam | 31.8% |
| 3 | Institutional | 1950 - 1964 | Concrete moment resisting frames | 21.0% |
| 4 | Polyvalente | 1964 - 1979 | Concrete shear walls | 19.0% |
| 5 | Recent | 1980 and after | Steel braced frame | 10.6% |

Another study on the seismic behavior of schools in Québec was presented in (Brayard, 2008). Using Chagnon's classification, complemented with site visits and plan reviews, the relative vulnerability of schools in each of the five categories was established. Based on **Equation 2.1**, the base shear ratio ($V_R$) was calculated for each type of school assumed be located in Montréal and Québec City.

$$V_R = \frac{V_C}{V_{2005}} \cdot 100 \ \ [\%] \tag{2.1}$$

Where:

$V_C$: base shear calculated according to the National Building Code of Canada (NBC) in effect for the construction year, and

$V_{2005}$: base shear as specified by the 2005 NBC.

The seismic priority index (SPI) of the NRC92 visual seismic screening method was calculated for each generic type of school. The SPI, an overall score related to the building's vulnerability, considers the local seismicity, soil conditions, type of lateral load resisting system, presence of irregularities, building importance and non-structural hazard (see **Section 2.4** for further details). Probable damages for each type were also predicted, according to a literature review on damage to schools in past earthquakes. The principal findings are summarized in **Table 2.3**.

**Table 2.3.** Seismic behavior of schools in Québec by type (Brayard, 2008)

| **Type** | **$V_R$ Montréal** | **$V_R$ Québec City** | **SPI** |
|---|---|---|---|
| 1 | 9.2 to 13.3% | 10.5 to 17.3% | 11.7 |
| 2 | 23.1 to 24.3% | 27 to 28.3% | 11.2 |
| 3 | 25.1 to 29.3% | 29.4 to 33.3% | 14.6 |
| 4 | 10.2 to 22.3% | 24.0 to 26.2% | 7.5 and 4.2$^{+}$ |
| 5 | 17.8 to 47.8% | 41.6 to 83.2% | 4.2 and 5.1$^{++}$ |

$^{+}$: SPI for schools of Type 4 constructed before 1970 and after 1970

$^{++}$: SPI for school of Type 5 constructed before 1990 and after 1990

As expected, there is a direct relation between the age of the building and $V_R$. The lower $V_R$ values of older buildings point to a higher seismic vulnerability. However for older buildings, a design load case other than seismic loading could have been critical for the design of the lateral load resisting system and thus it is possible that the lateral resistance of the building is in fact higher. In this case assuming the resistance of the buildings in direct relation to the design base shear is not appropriate as values obtained will be too conservative. The comparison is also questionable since it was not considered that before 1965 $V_R$ values were based on working stress design, while later codes are based on ultimate strength procedures (up to 1980) and limit state design (1980 to present).

According to results obtained for the SPI values schools of types 1, 2 and 3 can be considered as having moderate priority for mitigation, and schools type 4 and 5 having low priority. However, the generalization of the SPI values is questionable due to the high sensitivity of the method to parameters that would considerably vary from one school to another, such as the soil type, site effects, and irregularities of the building.

## 2.4. Seismic Screening Methods

Seismic screening methods based on rapid visual screening or score assignment procedures, are intended to be coarse screening procedures using little resources per building. This is achieved by evaluating a limited number of features that influence seismic performance and assigning an overall score or state of vulnerability to each building. An ideal screening method will identify all those buildings that are potentially seismically hazardous, while limiting the number of buildings that will have to undergo a more detailed evaluation (NZSEE, 2006).

Seismic screening methods can be classified as observed or predicted vulnerability procedures, or hybrid methods, depending on the type of source information used. Observed vulnerability procedures use statistics of damage in past earthquakes, sometimes combined with expert opinion, to determine the probable behaviour of structures under future events. The main setback of this approach is the possible lack of observed data, as is the case in Canada, especially in the east, and the subjectivity in data interpretation. The observation-based approach also lacks analytical justification. Predicted vulnerability methods try to overcome these shortcomings by using analytical procedures to determine the probable behaviour of a structure subjected to a design-level earthquake loading. The limitation of this approach is the time and computational effort required by detailed analysis. Therefore a balance between effort, that need to be relatively low per evaluated building, and accuracy, that should be as high as possible, has to be found (Mendes-Victor et al., 2009).

The first comprehensive rapid visual screening method for seismic vulnerability assessment of buildings was developed in the United States in the late 1980s by the Applied Technology Council (ATC) under contract for the Federal Emergency Management Agency (FEMA) (ATC, 2002a, ATC, 2002b). The work was mainly motivated by the advances in design codes that made it possible to design safe new buildings. This method, published as the FEMA154 report, *Rapid Visual Screening of Buildings for Potential Seismic Hazard*, is probably the most widespread screening tool, and there is considerable guidance on its application (e.g. (Joshi and Kumar, 2010, Olshansky and Wu, 2004)). The method has also served as a prototype for the development of screening tools in many other countries, as for example in Switzerland (Lang, 2002) and Italy (Faccioli et al., 1999) and it is also used in this research. The current official Canadian seismic screening method, *Manual for Screening of Buildings for Seismic Investigation* (NRC92) (NRC/IRC, 1992), is largely based on the first edition of FEMA154. Other efficient methods have been developed independently, for example in New Zealand and in Japan. The procedure of the New Zealand Society for Earthquake Engineering (NZSEE, 2006) assesses existing buildings by comparing them to current New Zealand standards. In Japan the Seismic Index Methodhas been developed and used to evaluate low- and mid-rise reinforced concrete buildings in Japan since 1975 (Calvi et al., 2006). The method is a multi-tier screening procedure that estimates the vulnerability of an existing building by a seismic performance index calculated for every storey in each main direction and based on key characteristics of the building.

In the context of developing a seismic screening method and evaluating the schools of the province of Québec, FEMA154 and NCR92 were found to be most relevant. A more detailed description of the two methods follows.

### 2.4.1. FEMA154

FEMA154 was first published in 1988 (ATC, 1988a, ATC, 1988b), and was significantly improved in 2002 with the release of its second edition. Screening can be completed by means of a sidewalk survey, although entering the building to observe actual details of the lateral load resisting system and gravity framework and consulting existing plans and other documentation is recommended. Based on this inspection a data collection form is completed. Initially the lateral load resisting system has to be identified and related to one of the 15 predefined building types. A basic structural hazard score ($BSH$) is provided for each building type. To consider specific characteristics of the building that could affect its seismic performance, the score is then altered by adding or subtracting score modifiers to obtain the final structural score. Score modifiers are related to building height, vertical and horizontal irregularities, year of construction and soil type. Typical scores range from 0 to 6, higher final scores corresponding to a better seismic performance. It is generally recommended that buildings with a score of 2 or less should be evaluated in more detail as they may present features that promote seismic vulnerability.

In the first edition of FEMA154 published in 1988, the $BSHs$ were calculated as the negative of the logarithm (base10) of the probability of damage ($D$) exceeding 60% of the building's value, given a ground motion represented by the National Earthquake Hazards Reduction Program (NEHRP) effective peak acceleration, as shown in **Equation 2.2**.

$$BSH = -log_{10}[P(D \geq 60\%)] \tag{2.2}$$

To determine the probability of occurrence of different levels of damage given a specified ground motion, expert opinion was used in form of the ATC-13 report (ATC, 1985). It is important to note that this report was concerned exclusively with buildings constructed according to Californian building practices, and again expert opinion was sought out to make the results applicable to other regions of different seismicity. The score modifiers were also calculated based on expert-opinion criteria.

For the 2002 edition of FEMA154 a more rational approach is implemented which relies more on seismic analysis. The $BSH$ for each building type is defined as the negative of the logarithm (base 10) of the probability of collapse ($P$) of the building, given a ground motion corresponding to the maximum considered earthquake ($MCE$), as shown in **Equation 2.3**.

$$BSH = -log_{10}[P(collapse\ given\ MCE)] \tag{2.3}$$

The probability of collapse is the product of the probability of the building being in complete damage state and the fraction of the buildings of the same type that reach complete damage state[1] and effectively collapse.

To determine the probability of the building being in complete damage state given the spectral displacement $dpi$, $P(complete|dpi)$, $dpi$ is first calculated using the

[1] Complete damage state is defined as a building that is collapsed or is in imminent danger of collapse due to failure of its structural elements. Non-structural elements will also be severely affected. Complete damage state implies that the structure must be replaced.

capacity spectrum method, a nonlinear static analysis procedure (ATC, 1996), depicted in **Figure 2.2.a**. This method is based on the assumption that the maximum inelastic deformation of a nonlinear single-degree-of-freedom (SDOF) system can be estimated from the maximum elastic deformation of an equivalent linear elastic SDOF which has natural period and viscous damping ratio values ($T_{eq}$ and $\beta_{eq}$) higher than the nonlinear system in the small strain range ($T_o$ and $\beta_o$). The inputs of the method are the lateral force-deformation relationship of the structure, commonly known as the push-over curve, and the seismic load demand. Both are plotted in the form of spectral acceleration (Sa) vs. spectral displacement (Sd) curves. In this format natural periods can be represented by radial lines through the origin. The equivalent period is assumed to be the secant period ($T_{sec}$) at the intersection of the capacity spectrum curve and the seismic demand spectrum curve with reduced equivalent damping. The equivalent damping is estimated based on the area under the capacity curve. Since both the equivalent period ($T_{eq}$) and damping ($\beta_{eq}$) depend on the estimated maximum spectral displacement $dpi$, an iterative process is necessary to calculate $\beta_{eq}$.

The estimated spectral displacement $dpi$ is used to determine the cumulative probability of complete damage state from a fragility curve specific to the building type, as can be seen in **Figure 2.2.b**. This probability is multiplied by the fraction of buildings that will collapse if they reach their complete damage state, to obtain the probability of collapse of the building and calculate the $BSHs$. A similar procedure is used to calculate the score modifiers. The collapse fractions are based on judgment and limited earthquake data for each building type.

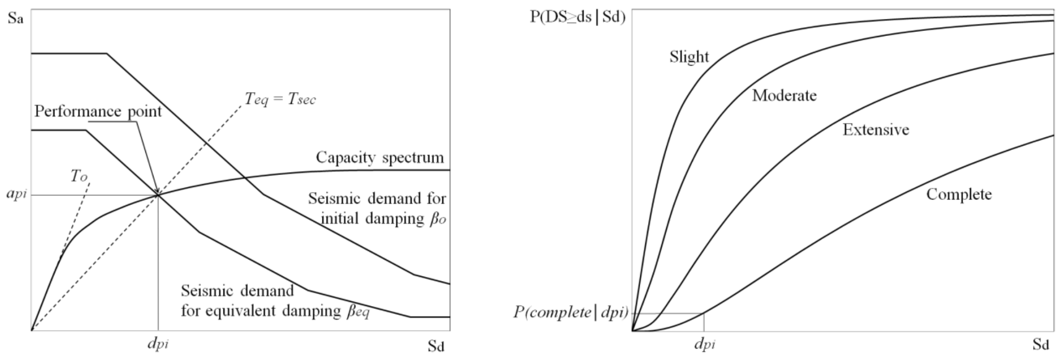


a. Capacity spectrum method b. Fragility curves

**Figure 2.2.** Estimation of the probability of complete damage state of a building class, adapted from (ATC, 2002b)

### *2.4.2. NRC92*

The NRC92 procedure was developed in Canada and published in 1992. Largely based on the 1988 edition of FEMA154, the practical implementation of NRC92 relies on a data collection form that can be filled out by visual inspection of the building. It is expected that the exterior as well as the interior are evaluated, and recommended that building plans be considered. The user first has to identify the lateral load resisting system and correlate it to 15 different building types, very similar to those of FEMA154. High importance is given to the identification of building irregularities, differentiating between seven different types. Non-structural hazards also have to be identified.

A structural index is computed by multiplying five factors related to local seismicity, soil conditions, type of lateral load resisting system, presence of vertical and horizontal irregularities and building importance. A non-structural index is also computed, based on the identified sources of non-structural hazards, the soil conditions and building importance. The final score, called the seismic priority index (SPI), is the sum of the structural index and the non-structural index. Contrary to FEMA154 scores, a high SPI indicates high priority for refined seismic vulnerability analysis of the building. NRC92 suggests that buildings with a score less than 10 be treated as low priority, 10 to 20 as moderate priority, 20 to 30 as high priority and an SPI score larger than 30 indicates a potentially hazardous building requiring immediate attention and a refined assessment.

Although the NRC92 guidelines state that the method is largely based on the first edition of FEMA154, specific details on how the method was adapted for Canadian seismicity and building design and construction practice are not provided. However, it is clear that score calculations are mainly based on engineering expert opinion. The seismicity, soil, type of structure and irregularities factors were all obtained by comparing code requirements of different editions of the National Building Code of Canada (NBC).

Currently an effort is being made to update the NRC92 guidelines considering the 2005 edition of the NBC, as well as developing computer software to apply the updated methodology (not publicly available at present time). The update relies on a comparison of the base shear calculated according to the 1990 and 2005 NBC, from which factors are derived to affect the original scores presented in the NRC92 methodology (Saatcioglu et al., 2010).

### 2.4.3. Advantages and Shortcomings of Each Method

#### *2.4.3.1. Procedures behind score calculations*

Supporting documentation for NRC92 is limited and this creates challenges for any attempt to update the procedure. An update of NRC92 is needed because it was largely based on the 1988 edition of FEMA154, which has itself been thoroughly revised in 2002. On the other hand, FEMA154 uses a more sound methodology for calculating the vulnerability scores than NRC92, with the calculations based on the capacity spectrum method as described in ATC-40 (ATC, 1996). However the application of ATC-40 has raised concerns in the past, showing poor agreement with other simplified analysis methods. Furthermore, when comparing with results of response historey analysis, significant differences could be found (Akkar and Miranda, 2005). Some studies demonstrated that the estimated maximum deformations can be underestimated by as much as 50% (Chopra and Goel, 2000). Recognizing these concerns, a thorough evaluation of the 2002 method was conducted and an updated procedure was published in the FEMA440 report (ATC, 2005). In this evaluation it was found that for short-period structures, with period less than 0.5s approximately, the peak displacements are largely overestimated in

ATC-40; this period range is typical of school buildings. For higher periods the methodology can either overestimate or underestimate the displacements, depending on the assumed hysteretic behaviour of the evaluated building. The main modification introduced by FEMA440 was to introduce updated expressions for the calculation of the equivalent or effective period ($T_{eff}$) and viscous damping ($\beta_{eff}$). Approximate equations, that are independent of the hysteretic curve and post-elastic stiffness ratio of the capacity curve used, are presented in the **Equations 2.4** to **2.6**, were μ is the ductility demand, $T_O$ and $\beta_O$ are the initial period and elastic viscous damping ratio for the nonlinear system, respectively.

For $1.0 < \mu < 4.0$:

$$\begin{aligned} \beta_{eff} &= 4.9(\mu - 1)^2 - 1.1(\mu - 1)^3 + \beta_0 \\ T_{eff} &= [0.20(\mu - 1)^2 - 0.038(\mu - 1)^3 + 1]T_0 \end{aligned} \tag{2.4}$$

For $4.0 \leq \mu \leq 6.4$:

$$\begin{aligned} \beta_{eff} &= 14.0 + 0.32(\mu - 1) + \beta_0 \\ T_{eff} &= [0.28 + 0.13(\mu - 1) + 1]T_0 \end{aligned} \tag{2.5}$$

For $\mu > 6.4$:

$$\begin{aligned} \beta_{eff} &= 19\left[\frac{0.64(\mu-1)-1}{[0.64(\mu-1)]^2}\right]\left(\frac{T_{eff}}{T_0}\right)^2 + \beta_0 \\ T_{eff} &= \left\{0.89\left[\sqrt{\frac{(\mu-1)}{1+0.05(\mu-2)}} - 1\right] + 1\right\}T_0 \end{aligned} \tag{2.6}$$

$T_{eff}$ and $\beta_{eff}$ were determined by a statistical analysis that minimized the error between the maximum response of an inelastic system and an equivalent linear system. Inelastic system responses were obtained through non-linear response-historey analyses of SDOF systems. A large number of SDOF systems were studied, with a wide range of periods of vibration, lateral strengths and hysteretic behaviour. These systems were subjected to several recorded earthquake motions that included near-fault and far-fault records with site conditions ranging from very soft soil to rock.

To get a better understanding of these equations, **Figures 2.3** and **2.4** show $\beta_{eff}$ and $T_{eff}$ for different values of $\beta_O$ and $T_O$ respectively. The vertical lines in the plot represent the limiting ductility demand values (4.0 and 6.4). From the plots it can be seen that the equivalent linear parameters are equal to their initial counterpart for ductility equal to one (the structure remains elastic). For both cases the equivalent parameters then drastically increase for ductility demands up to 4.0. $\beta_{eff}$ remains almost constant for higher ductility demands, while $T_{eff}$ increases linearly.

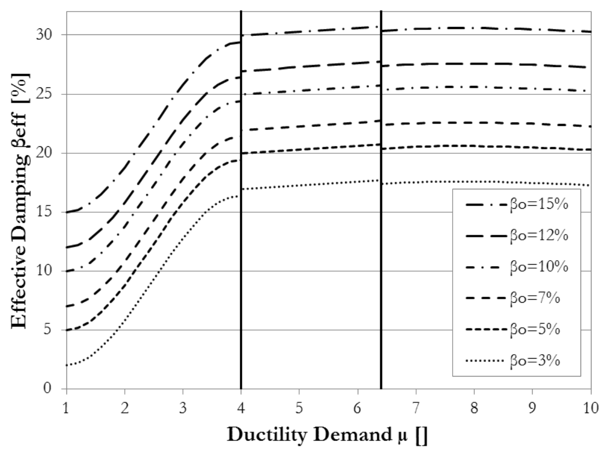


**Figure 2.3.** Effective damping values

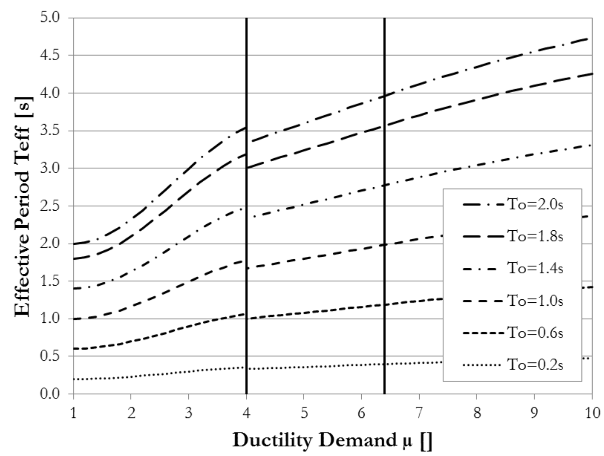


**Figure 2.4.** Effective period values

Based on these equations, scores for FEMA154 were recalculated. **Figure 2.5** shows a comparison between the $BSHs$ presented in FEMA154 and the updated values. On average the values increased 14% for high seismicity, 29% for moderate seismicity and 28% for low seismicity. Increased values indicate a better earthquake performance. This result was expected, since the $BSHs$ are calculated for low-rise buildings with relatively short periods, and the capacity spectrum method as presented in ATC-40 tends to overestimate the predicted maximum spectral displacement for short periods.

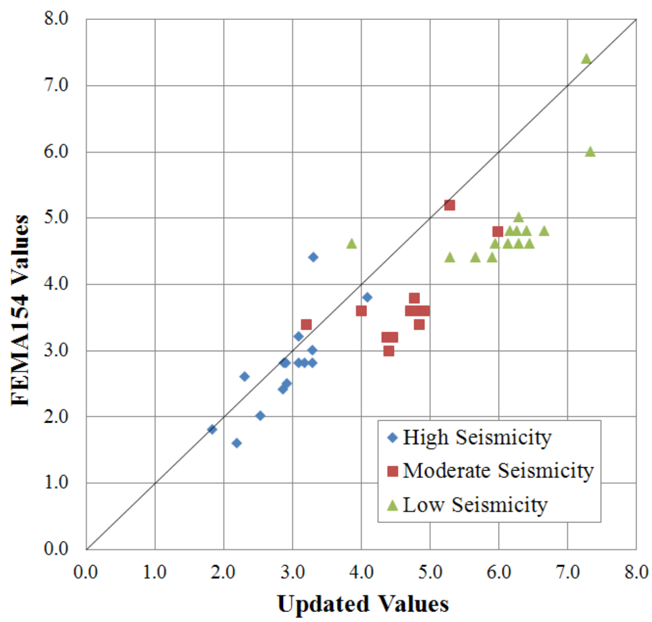


**Figure 2.5.** Comparison between the $BSHs$ of FEMA154 and calculated values from the updated capacity spectrum method

### *2.4.3.2. Spectral response acceleration values*

FEMA154 was developed for the United States. Three seismicity regions (high, moderate and low) are defined based on design spectral acceleration values for periods of 0.2s and 1.0s, S(0.2s) and S(1.0s). Limiting values were taken from FEMA310 (ASCE, 1998), ignoring local site effects. To determine the median spectral acceleration response values for each seismic region first each county was classified based on the maximum S(0.2s) and S(1.0s) values. The median of these maximum values was calculated for each region and used for the score calculations. The median spectral acceleration values and the $BSHs$ and modifiers have been recalculated considering the seismicity of Québec's cities and towns as specified in the 2005 edition of the NBC, considering the same spectral acceleration limits of the three seismicity regions defined in FEMA154 (Karbassi and Nollet, 2008).

Although the spectral accelerations in Canada and the United States are calculated with the same hazard level, i.e. a probability of exceedance of 2% in 50 years, there are differences in the calculations that result in cross-border inconsistencies, as for example the use of the median seismicity values in Canada versus the mean values in the United States. Furthermore when using FEMA154 in Canada, one important consideration to be addressed is that in the United States the spectrum is reduced by 2/3 for building design (BSSC, 2009), while this reduction is not used in Canada except for low-period structures. This has an impact on the calculated scores, and the use of the same spectral acceleration limits to define the three seismicity regions is questionable, since these limits were prescribed considering the 2/3 reduction factor. When analyzing the case of the island of Montréal for example, having moderate seismicity as per NBC 2010 (S(0.2s) = 0.64 g and S(1.0s) = 0.14 g for Site Class C), it would be classified by FEMA154 as moderate seismicity if applying the 2/3 reduction factor and high seismicity if not.

NRC92, although developed for the Canadian context, has yet to be updated to consider the revised uniform seismic hazard data which have been implemented in NBC 2010. The seismicity used by NRC92 is that specified in the 1990 NBC (NRC/IRC, 1990), with hazard maps developed in 1985. The effective seismic zone of the site of interest is calculated according to the peak ground acceleration and peak ground velocity with probability of being exceeded of 10% in 50 years. The new models developed for the 2005 NBC included the latest findings related to historical seismic events in Canada, new attenuation laws, a better description of the site conditions and the explicit consideration of uncertainty (Adams and Atkinson, 2003).

#### *2.4.3.3. Site classification*

Design spectral accelerations are determined by the expected seismic excitation and local geotechnical conditions at the site. Both in the US and in Canada local site conditions are classified into six seismic categories, from type A to F, ranging from hard rock (Site Class A) to poor soil (Site Class F). For the classification of each type, the parameters used are the measured shear wave velocity or the standard blow count. Ground motion amplification factors for short and long periods, $F_a$ and $F_v$

respectively, depend on the expected intensity of shaking and are defined for each site class. For the US, the reference soil is type B, meaning that $F_a$ and $F_v$ values are equal to one for soil type B (BSSC, 1998). In the seismic provisions of the 2005 NBC, the American classification system was adopted with small changes. However the reference soil in Canada is defined as type C (defined as very dense soil and soft rock, with shear wave velocity between 360 and 760m/s), to be consistent with previous editions of the NBC (Finn and Wightman, 2003). Therefore $F_a$ and $F_v$ values for the same soil type are lower in Canada than in the US. This implies that when using FEMA154 with spectral acceleration values and soil definitions for Canada the site effects may be overestimated.

The four different soil types considered by NRC92 have foundation factors $F$, ranging from 1.0 to 2.0. These factors are based on design practice of the early 1990s and do not consider the differences between short and long period building responses and the influence of the intensity of shaking.

#### *2.4.3.4. Configuration irregularities*

Schools are complex structures with many irregularities. While FEMA154 only differentiates between vertical and plan irregularities, NRC92 identifies seven different types of deficiencies: vertical and horizontal irregularity (torsion), short concrete columns, soft storey, susceptibility to pounding, major structural modifications and material deterioration.

In FEMA154 score modifiers for vertical irregularities are based on engineering judgment. For high and moderate seismic zones, the modifiers were chosen so that if it were the only modifier considered, the final score would be below the cut-off score of two. For low seismicity, modifiers similar to those of the moderate seismic zone were adopted. For the calculation of the plan irregularity modifiers, an increase of 50% in the spectral acceleration response values was used. This approach seems appropriate when evaluating general building stock (including commercial and residential), where irregularities in plan and elevation should be rather uncommon. When evaluating school buildings however, due to the prevalence of configuration irregularities, a more discriminating evaluation is desirable. Finding a balance between the simplicity of the method and the detailed identification of irregularities is challenging. An example of how this can be achieved is found in the screening procedure of New Zealand (NZSEE, 2006). Even in a first-tier evaluation, four critical structural features have to be identified (plan and vertical irregularities, short columns and pounding potential) and the effect on the structural performance of each has to be classified as severe, significant or insignificant. Clear guidance on how to classify the severity level is provided. For buildings with an L-shape plan, for example, the effect on structural performance is determined by comparing the length and the width of the wings.

#### *2.4.3.5. Potential for pounding*

When insufficient or no separation is provided between adjacent buildings they will likely suffer from pounding during a strong earthquake. This will induce high amplitude shock loadings, and experience in past earthquakes has demonstrated that this problem can even cause buildings to collapse. During the 1985 Mexico City earthquake, 15% of building collapses could be attributed to these severe pounding effects (Jeng and Tzeng, 2000).

While FEMA154 does not consider pounding, NRC92 incorporates it in calculating the score, and the limiting distance between buildings is defined in terms of the velocity-related seismic zone (dependent on the expected peak ground velocity) and number of storeys. Since 2005, NBC stipulates the seismic demand in terms of spectral acceleration values only, so other expressions have to be found to quantify the limiting building separation distance for potential pounding.

Experience in past earthquakes has demonstrated that the effect of pounding is most critical for adjacent buildings with different heights, periods and masses. Floors at different elevations may result in the slabs of one building impacting columns of the other building generating shear failure and partial or total collapse. In absence of these adverse factors, pounding usually will only induce local damage (Anagnostopoulos, 1996).

#### *2.4.3.6. Non-structural components*

Another important aspect considered by NRC92 while ignored by FEMA154 is the evaluation of seismic vulnerability related to damage to operational and functional building components. Addressing such functionality issues is a cost-effective first step for retrofit and directly translates into increased public safety. Furthermore, if the installations are classified as post-critical, as is the case with school buildings designated as post-critical shelters, non-structural damage must be limited. In eastern North America, a moderate seismic zone, non-structural damage can also be more widespread than structural damage or collapse, as has been demonstrated by experience in past earthquakes in Québec (Lin and Adams, 2011, Mitchell et al., 1989), where earthquakes have typically higher frequency content compared to the Pacific Coast.

#### *2.4.3.7. Building importance*

Schools fall into two distinct classes regarding building importance: post-disaster shelters and ordinary schools which all belong to the post-disaster building category according to NBC. The different performance objectives of these two occupancies should be acknowledged by the seismic screening method: school occupancy requires essentially safety performance while post-earthquake shelter occupancy requires a minimum of damage for nearly immediate occupancy and functionality after strong shaking. While ignored by FEMA154, NRC92 asks for the calculation of a building importance factor based on the occupancy and use of the building. For school buildings, the structural index is increased between 20 and 50%, compared with a normal occupancy building. For post-disaster buildings which have to remain fully functional after the earthquake, the increase is between 50 and 100%.

#### *2.4.3.8. Cut-off scores*

While FEMA154 only suggests one cut-off score, classifying a building either as safe or as requiring a more in depth examination, NRC92 defines four distinct categories: low, moderate, high priority for future intervention, and potentially hazardous. This more detailed classification gives a better sense of the vulnerability of each building and of the need for a more detailed seismic evaluation.

The scores of FEMA154 are directly related to the probability of the building to collapse given the maximum considered earthquake. A score of 1 indicates a probability of collapse of 1 in 10 or 10%, a score of 2 a probability of 1%, a score of 3 a probability of 0.1%, etc. Based on these numbers a detailed ranking system is presented in **Table 2.4**, which was used in the evaluation of schools and other critical public facilities in Oregon (McConnell, 2007).

**Table 2.4.** Proposed ranking to be used in Oregon with FEMA154 (McConnell, 2007)

| Classification | Probability of collapse | Score |
|---|---|---|
| Very high | 100% | ≤ 0.0 |
| High | 10% to 100% | 0.1 – 1.0 |
| Moderate | 1% to 10% | 1.1 – 2.0 |
| Low | below 1% | > 2.0 |

## 2.5. Modal Identification of Building Structures from Ambient Vibration Testing

Modal analysis is the study of the dynamic properties of a given structure excited by vibration. This technique has been widely used in mechanical engineering for several decades, with analysis techniques and testing equipment being progressively refined. Later, with the development of signal processing tools for output-only systems (refer to **Sections 2.5.1** and **2.5.2**), modal analysis has also gained popularity for the evaluation of civil structures.

The seismic performance of a civil structure depends on its horizontal stiffness and reactive mass, and how they are spatially distributed. Theoretical predictions of these factors, generally done with the help of finite element models, often disagree with measured natural frequencies. Assumptions made to model the torsional effects and the influence of the foundation could lead to errors that will imply a non-conservative design. It is therefore desirable to perform in situ tests to determine the characteristics of linear behaviour of structures under lateral loads (Brownjohn, 2003). In the present research, ambient records were collected at all of the school buildings that were investigated to get a better understanding of their behaviour. The dynamic properties were also used to validate generic capacity curves used to model different lateral load resisting systems.

### *2.5.1. Experimental Determination of Dynamic Properties of Buildings*

Experimental dynamic properties of civil structures can be determined from vibration measurements, a process called experimental modal analysis. Based on the type of excitation used as input, the technique can be further classified. Ambient vibration tests rely on ambient loads such as wind, traffic and microtremors for example, to induce vibration of the structure. The main advantage of the method is the simplicity of the experimental procedure. The main drawback is that the excitation is not known, and that the amplitude of the measured vibration is very low, with horizontal accelerations that can be of the order of $10^{-5}$g at the ground floor and $10^{-4}$g at the top floor in the case of buildings (Hans et al., 2005). Some instruments measure velocities instead of accelerations to minimize systematic relative errors. Forced vibration tests excite the structure, usually by means of a rotating mass to generate harmonic loads. Therefore both the input and the output are known. It also allows for higher excitation levels than ambient vibration measurements (around ten times higher), although these are still not in the inelastic range. Large structures such as buildings and bridges are very difficult to excite with an experimental set-up, and studies have shown that consistent results are obtained from ambient and forced vibration testing (Trifunac, 1972). Free vibration response tests, where a structure is studied in free decaying motion after an initial excitation, have similar advantages and shortcomings as forced vibration tests. Finally, a structure can be permanently monitored to capture the vibration during an earthquake of relevant magnitude. It is evident that while properties extracted from these strong motions will give a clear insight of the behaviour of a structure, monitoring is of limited benefit outside of zones of high seismicity with frequent earthquakes. For the present research, the method of choice was ambient vibration testing, due to the availability of the equipment necessary and the simplicity of the experimental setup.

Ambient vibration measurements have been used successfully to determine the dynamic properties of civil structures for over 35 years (Ivanovic et al., 2000). This has demonstrated that the method is reliable to establish natural frequencies and modal shapes, although the determination of damping is not as consistent (Brownjohn, 2003). The dynamic properties obtained can then be used, for example, to calibrate analytical models that will predict the response of a structure under service loads more reliably (Lord et al., 2004). Many studies of this type have been conducted for bridges, where predicting the dynamic behaviour is especially interesting because wind, earthquake and traffic loading can play a key role (Lu et al., 2006). Ambient vibration measurements have also been used to determine the effect of seismic retrofitting of structures, as natural frequencies increase with the retrofitting, indicating higher stiffness, while damping tends to decrease (Tischer et al., 2006). Another application of ambient vibration measurements is the real time health monitoring of a structure, where detected changes in the natural frequencies of the structure are correlated with possible damage (Montalvão et al., 2006).

The experimental characterization of dynamic properties of low-rise buildings, such as the structures investigated in this research, has not been explored in depth in the past and only some isolated studies could be reviewed here. This increases the relevance of the information collected in this research. It appears that the reason for the lack of previous research is the inherent difficulty of performing modal analysis based on ambient vibration records for low-rise buildings, due to the low amplitudes of the recorded motions and the potentially high influence of soil-structure interaction (Tobita et al., 2000). These difficulties have been partly overcome by more sensitive equipment and more sophisticated digital signal processing techniques.

As a word of caution, when extracting dynamic properties of structures from ambient vibration measurements, it must be considered that the natural frequency of structures will be correlated to the amplitude and duration of the input, generally decreasing with higher levels of excitation. These changes are significant, and have been measured with factors up to 3.5. They can be explained by the non-linear behaviour of the structure under strong excitation and by the soil-structure interaction effects (Trifunac et al., 2001a, Trifunac et al., 2001b). Therefore, natural frequencies determined from ambient vibration measurements are not equivalent to the frequencies of the deformed structure under strong shaking, especially if the structure suffers permanent damage. There is also not a clear consensus on the factor to relate both, although some ranges and maximum values have been proposed. However, due to the scarcity of experimental data under strong shaking, and its complete absence in zones of moderate and low seismicity, results of ambient vibration testing are considered relevant to determine a lower bound of the natural period of buildings.

### *2.5.2. Digital Signal Processing of Ambient Vibration Measurements*

As ambient vibration tests in civil structures have become increasingly popular over the years, so has the development of methods for the system identification from these tests. They differ from other control engineering applications where typically both the input load and the output response are known, since only the output response is measured. Even if measurements are taken on the ground level to capture excitations such as microtremors and traffic, it is virtually impossible to capture the input for other excitations such as wind and vibrations due to the usage of the structure. Therefore system identification techniques for ambient vibration records are based on the assumption that the input is a white noise. Another challenge is the small amplitude of ambient vibrations compared with the noise that contaminates the signals.

The first and most simple modal identification technique developed is known as "peak picking", and it is still applied to some extent today in combination with other analytical methods. It has been used since the development of the Fast Fourier Transform (FFT) algorithm in the 1960s (Cooley and Tukey, 1965). Several improvements boosted its usage starting in the mid-seventies. More recently, due to the shortcomings of the peak picking method and the enhanced computational capacity available, research on the topic has been vast (De Roeck and Ren, 2000). Several different techniques have been proposed and applied to civil structures with success, the most widespread of which are the frequency domain decomposition

(FDD and enhanced FDD) method (Brincker et al., 2001), which will be discussed in **Section 2.5.2.2**, and the stochastic subspace identification method (Van Overschee, 1993). The techniques and transforms used for the pre-processing and the processing of the acquired records are discussed in more detail in the next sections.

#### *2.5.2.1. Power Spectral Density and Peak Picking Technique*

The power spectral density (PSD) of a signal represents the distribution of the average power of the signal over frequency. The PSD plot (or periodogram) is the basis for the average normalised spectral density modal identification technique, simply called peak picking. Both concepts are standard textbook material, and the following discussion has been mainly adapted from (Proakis and Manolakis, 1996). Other excellent references are (Oppenheim and Schafer, 2010) and (Bendat and Piersol, 1993).

The PSD of a periodic signal $x(t)$ that can be decomposed into a summation of harmonics with fundamental period $T_p$ is determined from its average power $P_x$, defined by **Equation 2.4**. $c_k$ are the Fourier coefficients of the harmonic series' representations. This relation is known as the relation of Parseval[2].

$$P_x = \frac{1}{T_p}\int_{T_p} |x(t)|^2 dt = \sum_{k=-\infty}^{\infty} |c_k|^2 \tag{2.4}$$

The sequence $|c_k|^2$ is denominated PSD. An example of a PSD plot is presented in **Figure 2.6**, of an ambient vibration record acquired on the top floor of a high rise building (Tischer, 2007).

[2] Note that if the signal is discrete in time, Parseval's relation can be written as $\sum_{n=0}^{N-1}|x(n)|^2 = \sum_{k=0}^{N-1}|c_k|^2$, where $N$ is the period of the signal and $n$ are the sampling moments.

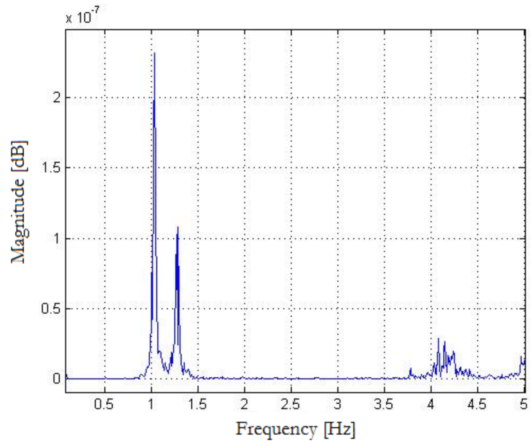


**Figure 2.6.** Sample PSD plot (Tischer, 2007)

Peaks in this plot allow identifying the signal's dominant frequencies, since the auto spectra of the ambient outputs go through an extreme value around these frequencies (Bendat and Piersol, 1993). Since in this application the input is considered a white noise, the peak frequencies represent the dominant natural frequencies of the structure for the measured horizontal motion. If different sensors are recording simultaneous records at different floors, the signal coherence will further help to establish if the observed peaks are actually natural frequencies, since the coherence will be close to one at the frequencies of interest. To determine the corresponding mode shapes, values of the transfer functions between simultaneous records at the studied frequencies are used. Assuming one of these records as the input and the other as the output signal, the transfer function is the relation between the two in terms of frequency[3]. The transfer function allows the identification of the modal shapes given the spatial distribution of the sensors since it will establish if the two signals are in phase at a given frequency of interest. Viscous damping ratios can be roughly estimated with the half-power bandwidth method applied to the corresponding peaks of the power spectral density plots (Chopra, 1995).

Peak picking has been used extensively for the modal identification of civil structures for around 40 years. However, drawbacks of the method have been identified by different investigators and more sophisticated analytical techniques have been

[3]In its most simple form, the transfer function between an input signal $x(t)$ and an output signal $y(t)$ that are continuous in time is $H(s) = Y(s) \,/\, X(s)$ , where $Y(s)$and $X(s)$ are the Laplace transform of $y(t)$ and $x(t)$ , respectively.

developed. Peak picking fails to identify closely-spaced modes and damping ratios when close modes are present or when the signal is affected by background noise. Furthermore, the peak selection is somewhat subjective and "operational deflection shapes" are obtained instead of mode shapes (Brownjohn, 2003, De Roeck and Ren, 2000).

#### *2.5.2.2. Time-Frequency Distributions*

The PSD allows identification of the frequencies with high average power content, but it is not possible to determine the stability of the signal over time. To represent the frequency content of the signal against time, time-frequency distributions (TFD) are used. Two different TFDs were used in the present study, the spectrogram and the Choi-Williams transform (Choi and Williams, 1989).

The spectrogram is the most widespread TFD. It is generated by dividing the signal in overlapping segments, windowing each segment, and calculating the short time Fourier transform of it, as given by **Equation 2.5**. A sample spectrogram generated from an ambient vibration record of a high -rise building is presented in **Figure 2.7**. Note that higher values are represented in red and horizontal lines indicate that the frequency content is stable over time.

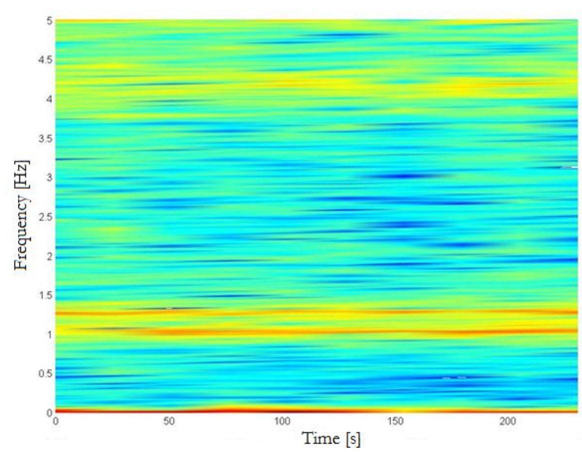


**Figure 2.7.** Sample Spectrogram (Tischer, 2007)

In recent years other TFDs have been developed and applied to the identification of dynamic properties of civil structures. The aim is to improve the resolution of the spectrogram plot, so that closely-spaced modes are recognisable or small changes in the natural frequency can be determined (as in health monitoring applications). One tool is the Choi-Williams transform from the Cohen class. The Cohen class time-frequency distributions use a bilinear transformation that depends on time and frequency variables. All the TFDs of this class, each for different applications and with specific characteristics, are defined by **Equation 2.5** (Choi and Williams, 1989):

$$P(t,w) = \frac{1}{4\pi} \iint A(\theta,\tau)\phi(\theta,\tau)\, e^{-j\theta t - j\tau\omega} d\tau d\theta \tag{2.5}$$

$A(\theta,\tau)$, the symmetric ambiguity function of the signal $x$, (defined as the Fourier transform of the signal's auto-correlation function[4] taken with respect to τ) and is defined as:

$$A(\theta,\tau) = \int x\left(t+\frac{\tau}{2}\right) x^{*}\left(t-\frac{\tau}{2}\right) e^{j\theta t} dt \tag{2.6}$$

The function $\phi(\theta,\tau)$, denominated kernel, is an arbitrary function that varies for each TFD of the Cohen class and that will define the specific characteristics of the TFD. For the Choi-Williams transform, the kernel is taken as:

$$\phi(\theta,\tau) = exp\left(\frac{-\tau^2\theta^2}{\sigma}\right) \tag{2.7}$$

In **Figure 2.8**, a sample Choi-Williams transform is presented together with the same record's spectrogram for comparison. The plots correspond to an ambient vibration record of the top storey of a high-rise building. Although the computational resources necessary for the Choi-William transform greatly surpass those needed for the spectrogram, the results are clearly improved with a higher resolution: the horizontal lines identifying the dominant sway natural frequencies of the building are much sharper in the left plot (Tischer et al., 2007).

[4]The auto-correlation function of a signal is its cross-correlation with itself. The auto-correlation is used to establish the similarity between observations as a function of the time separation between them.

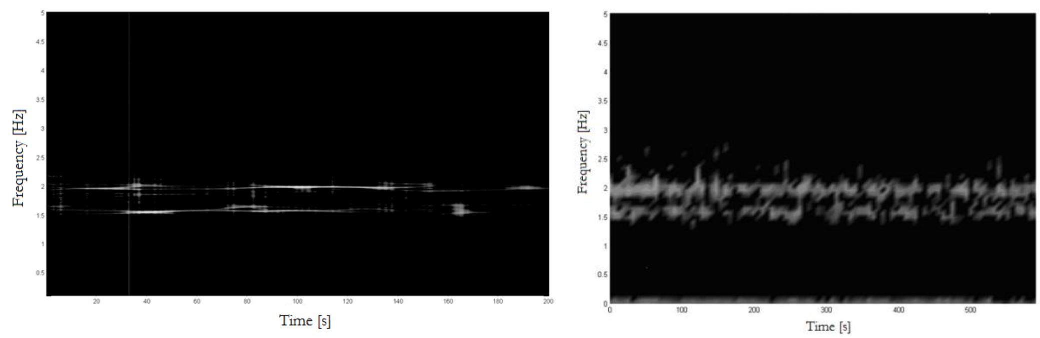


a. Choi-Williams transform b. Spectrogram

**Figure 2.8.** Sample Choi-Williams transform, compared to a spectrogram of the same signal, adapted from (Tischer et al., 2007)

#### *2.5.2.3. Frequency Domain Decomposition*

The frequency domain decomposition (FDD) is a modal identification technique that is as user-friendly as peak picking with some clear advantages. The spectral density function matrix is decomposed, meaning that the response spectrum is separated into a set of viscously-damped SDOF systems, each of which will represent one mode of the studied structure, even allowing the identification of closely-spaced modes. The application of the method is briefly explained in the following paragraphs. For the theoretical background and additional details on the implementation of the method, the reader is referred to (Brincker et al., 2001).

To apply the FDD technique, first the output PSD matrix $G$ is computed, a square matrix containing the auto and cross spectral density functions between all the response signals for the frequency range of interest. Invoking the spectral theorem, $G$ is then decomposed using the singular-value form at discrete frequencies $\omega_i$:

$$[G(j\omega_i)] = [U_i][S_i][U_i]^H \tag{2.8}$$

Where $U_i$ is a unitary matrix (a complex matrix) holding the singular vectors $u_{ij}$ and $S_i$ is a diagonal matrix holding scalar singular values $s_{ij}$, and the superscript $H$ denotes the Hermitian transform. In this form, the singular vectors are the orthonormal eigenvectors of $[G(j\omega_i)]$, and the singular values are the corresponding eigenvalues. Hence, the singular vectors are an estimate of the system's mode shapes, and the contribution of each mode shape to the overall energy can be estimated from the singular values (see **Figure 4.3** for example). At a given frequency where only one mode is dominant, the singular value corresponds to the auto PSD function. The truncated segment of the PSD that correlates to a mode of interest can be obtained from the PSD by comparing the mode shape estimate at the peak related to the mode to the singular vectors for the frequency lines around the peak using the modal assurance criterion (MAC). The natural frequency and viscous damping ratio of the mode can then be estimated using the truncated SDOF PSD function obtained around the peak, for example by converting it back to time domain and examining the zero-crossing times to estimate the period, and calculating the logarithmic decrement of the corresponding auto-correlation function to estimate the modal viscous damping ratio.

As mentioned before, extracting dynamic properties from ambient vibration records for low-rise buildings is rather difficult (see **Section 2.5.1**). The advantages of the FDD versus peak picking are therefore extremely important in the case of the school buildings studied in this research. However, it has to be considered that for FDD as well was for peak picking the unknown excitation is assumed to be a broadband, stationary Gaussian with noise. This implies that the input is statistically independent and uncorrelated at any two times and that its energy content is roughly equal for the entire frequency range of interest. This assumption may not always be accurate, but it will not affect the predicted natural frequencies. For the estimation of damping however, it has been cited as one source of error that makes the estimated values unreliable. Another source of error is the noise measurement, since it has a significant effect on the curve fitting techniques commonly used to determine damping values. Finally, the selection of the window length and type in the estimation of the spectral densities can also adversely affect the damping estimates (Rainieri et al., 2010).

# Chapter 3. Characterization of School Buildings

One cornerstone for the development of the adapted seismic screening method for schools was the characterization of a sample of approximate 100 buildings, located at 16 different school sites. The population of the schools that were studied was selected based on the fact that they are designated by the Civil Security Centre of Montréal (*Centre de Sécurité Civile de Montréal*) as shelters for evacuees in case of emergency, mostly because of their location and capacity to accommodate a large number of disaster victims. Note that due to this selection criterion, the sample of schools in our study is not random and is not deemed to be representative of the entire province's school building stock. However, since these are amongst the largest schools, there is a special interest in their examination.

The thorough evaluation of these schools permitted the creation of a seismic portfolio for each school. This is one outcome that will prove beneficial to Montréal's Civil Security Centre, which has been involved in the project since its initial stages. Not only will the Centre know if the schools designated as shelters meet minimum requirements regarding earthquake safety and are therefore suitable as shelters, but a more detailed assessment per building will also enable the determination of which parts of the school are more likely to suffer damage in case of an earthquake. It is noteworthy that an ongoing project at McGill University will characterize emergency shelters other than schools, allowing for a complete set of seismic profiles. The results of these projects will have a direct and important impact on the city's earthquake preparedness program.

The characterization of school buildings was carried out by a comprehensive study of the available building plans, complemented with site visits. The collected information was used to determine the building's general characteristics and common features presented in **Section 3.1**, and to do a preliminary assessment using existing rapid seismic screening methods presented in **Section 3.4**. Since heavy unreinforced masonry partition walls are prevalent in schools buildings, a detailed survey of these walls was conducted; these results are discussed in **Section 3.2**. An independent study (McClure et al., 2010) evaluated the operational and functional components at fourteen of the visited schools, and a summary of the results is presented in **Section 3.3**.

## 3.1. General Characteristics of Schools Studied

All but one of the schools studied comprised several buildings, usually with floor separation joints using one-inch (25 mm) gaps. Thus the 16 schools were composed of a total of 101 independent buildings. Since different buildings at each site were found to have significantly different characteristics, they were all evaluated independently. Some general descriptors related to the size of the schools are given in **Table 3.1**. For confidentiality reasons, the schools cannot be identified and code names were assigned to them in this dissertation. Considering 100 and 1000 students as the limiting values to differentiate the schools according to size[5], almost two-thirds of the evaluated schools can be classified as large and only one of them is considered small (S8_EAO). It is interesting to notice that due to the complexity of the schools, the number of buildings and location of separation joints could only be established after careful consideration of building plans combined with site visits. Usually rapid seismic screening protocols call for site visits only.

[5] Values suggested by D. Chagnon of Québec MÉLS.

**Table 3.1.** General characteristics of school buildings

| School ID | No. of Buildings | No. of Students* | Total Floor Area [$m^2$] |
|---|---|---|---|
| S1_A | 10 | 1,202 | 22,440 |
| S2_CL | 7 | 1,824 | 15,920 |
| S3_AV | 11 | 1,045 | 14,090 |
| S4_JM | 8 | 872 | 9,790 |
| S5_LR | 1 | 1,609 | 11,790 |
| S6_EM | 11 | 1,511 | 14,140 |
| S7_CaL | 6 | 1,484 | 8,710 |
| S8_EAO | 2 | 77 | 2,350 |
| S9_R | 7 | 1,066 | 14,040 |
| S10_JG | 6 | 1,523 | 3,450 |
| S11_PD | 4 | 518 | 11,680 |
| S12_LM | 4 | 852 | 9,480 |
| S13_SE | 7 | 1,868 | 17,470 |
| S14_MR | 6 | 835 | 15,400 |
| S15_DJ | 8 | 436 | 17,920 |
| S16_PT | 4 | 1,109 | 13,340 |

*: Information supplied by the Québec Ministry of Education (MÉLS).

### *3.1.1. Lateral Load Resisting Systems (LLRSs)*

**Figure 3.1** depicts all identified LLRSs and their percentage of occurrence. The schools studied pertain to a very limited number of LLRSs, 95% of them using only five different categories. The most common systems, which account for almost 80% of the studied buildings, are concrete frames with infill (unreinforced) masonry walls, concrete shear walls and steel moment frames. It is interesting to note that other studies suggest that the use of a limited number of LLRSs for schools is a worldwide practice (typical of institutional constructions), although the types may differ from one location to another.  In Oregon for example, it was found that most buildings are reinforced masonry bearing walls, wood post-and-beam construction, and concrete shear walls (McConnell, 2007). In Italy, all school buildings could be described as reinforced concrete or masonry construction (Borzi et al., 2011) as steel and timber are not used. This reduced variety in construction types will evidently simplify the seismic assessment procedure. However, the LLRS type alone will no longer be a parameter suitable for the differentiation of the seismic vulnerability of school buildings.

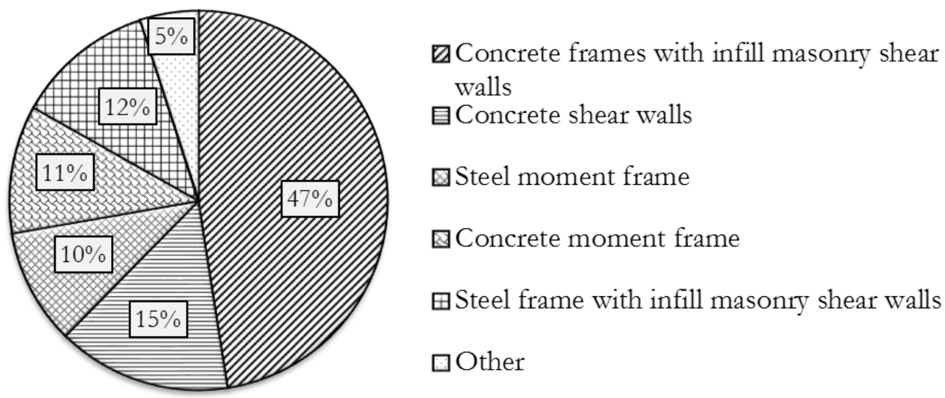


**Figure 3.1.** Distribution of LLRSs for the evaluated school buildings

### *3.1.2. Construction Year*

The distribution of the construction year of the school buildings studied is presented in **Table 3.2**. Although the schools were constructed between 1956 and 2001, 87% of them were built in the 1960s and 1970s, with almost half of them built between 1960 and 1969. The fact that large schools in Montréal (identified to be suitable as shelters) were built in this time bracket corresponds to the province's reform of its educational system in the early 1960s. A unified, integrated and public 5-year "secondary" educational system (years 8 to 12 renamed *Secondaire I* to *Secondaire V*) was implemented, and the large so-called "Polyvalente" school type was created. Many new school buildings with characteristics suitable for this educational model were then constructed to accommodate the new generation of teenagers of the post-WWII "baby boom".

**Table 3.2.** Distribution of construction year for the evaluated school buildings

| Construction Year | % of Buildings |
|---|---|
| Before 1960 | 1% |
| 1960 to 1969 | 48% |
| 1970 to 1979 | 39% |
| 1980 to 1989 | 10% |
| 1990 and after | 2% |

### *3.1.3. Height and Floor Area*

**Table 3.3** presents the distribution of the height of the schools, represented by the number of storeys. Most school buildings are low rise: roughly 85% of them are three storeys or less, with the tallest being six storeys. Low-rise buildings are typical for educational infrastructure in general, as can be seen for example from assessment projects in British Columbia (APEGBC and UBC, 2011) and New Zealand (Connell Wagner Limited, 2003). The distribution by floor area of independent buildings is presented in **Figure 3.2**, and varies between 200 and 5,300m$^2$, with an average value of 2,000m$^2$.

**Table 3.3.** Distribution of number of storeys for the evaluated school buildings

| Number of Storeys | % of Buildings |
|---|---|
| 1 | 22% |
| 2 | 46% |
| 3 | 18% |
| 4 | 9% |
| 5 | 2% |
| 6 | 3% |

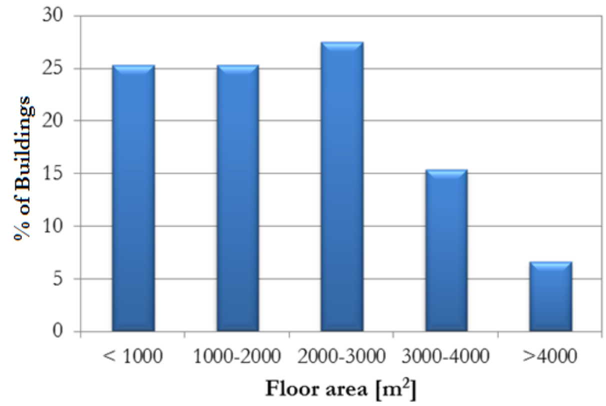


**Figure 3.2.** Distribution of floor area for the evaluated school buildings

### *3.1.4. Irregularities and Potential for Pounding*

One reason that has been proposed to explain the observed poor seismic performance of school buildings is that their complex structural features compromise seismic safety (ATC, 2004). The high incidence of these irregular features could be confirmed among the evaluated buildings. **Table 3.2** summarizes the most common features and their percentage of occurrence. It can be seen that irregularities in plan and elevation, as for example buildings with an irregular plan view or steps in elevation, are rather the norm than the exception. Around 80% of the examined buildings have some type of irregularity, with almost 40% having at least one vertical and one plan irregularity. This can partly be explained by the need to accommodate large open spaces such as gymnasium, cafeteria, auditorium, and library, with the much smaller classrooms and staff and administration office areas.

As mentioned before, all except one school comprise several individual buildings separated by floor separation joints. These joints are essentially "temperature and shrinkage" joints usually of 25 mm width, and therefore potentially not sufficient to exclude pounding effects in case of a large magnitude earthquake. As discussed in **Chapter 2**, these effects will probably be negligible in cases where buildings are of similar height and characteristics, and this differentiation was considered in the final evaluation method for schools.

**Table 3.4.** Features that could affect seismic performance and their occurrence in evaluated schools buildings

| Feature | % of Buildings |
|---|---|
| Irregular building plan | 50% |
| Steps in elevation | 46% |
| Potential for pounding with adjacent building(s) | 94% |
| Deterioration of structural elements | 22% |

### *3.1.5. Other Characteristics*

#### *3.1.5.1. Interior Layout*

The buildings studied house rooms of a variety of sizes for different uses and occupancies. This constitutes one factor that influences their irregularities. As expected, the most common use is for classrooms (typically without fixed seats), with 63% of space allocation on average. In addition, 22% of the buildings house one or several gymnasia, 16% cafeterias, 15% offices, 12% auditoriums, 7% swimming pools, and 53% other spaces such as storage, locker rooms, lavatories, and building services.

#### *3.1.5.2. Roof Details*

Over 95% of the examined buildings have a flat roof. However, for almost half of the buildings there were steps in the roof elevation: details that make the roof prone to snow accumulation are therefore common. Additionally, 15% of the buildings had large operational and functional components on the roof (e.g., large heating and air conditioning equipment and penthouses used as mechanical rooms).

#### *3.1.5.3. Environment*

The schools studied are all located on large campuses where seismic hazard from surrounding tall buildings or trees is not an issue. The topography in Montreal is rather flat, and accordingly, two-thirds of the buildings were found to be on practically level ground, while the remaining schools were located on slightly inclined slopes.

#### *3.1.5.4. Exterior and Interior Falling Hazards*

Most of the buildings have some sort of exterior surface cladding elements and architectural components that, if not adequately tied to the structure, would constitute a falling hazard during ground shaking endangering students and personnel and eventually blocking safe egress routes during evacuation. However, the type and state of the attachment elements is difficult to determine from a simple visual inspection, and could not be defined from the collected information. A special type of exterior element that could interfere with evacuation are canopies over exits: these were observed at 16% of the school buildings.

About one third of the buildings had lockers and other heavy slender elements located in hallways. These elements could topple over and need to be properly restrained to minimize their possible impact.

## 3.2. Heavy Infill Walls

In the initial site visits over 90% of the school buildings were identified as having heavy masonry partition walls, typically unreinforced except in staircases. Since past earthquakes have demonstrated that poor out-of-plane behaviour of these walls can be fatal even if there is no building collapse, it was decided to address this issue with more scrutiny in this research and a comprehensive survey of the wall dimensions and locations was conducted as an initial step. The walls were quantified by storey, noting their thickness, block type used, height, confinement at the top and orientation regarding the building's principal directions.

The wall survey confirmed that heavy infill masonry partitions are present in all the school buildings studied. The most common masonry type found was concrete block, accounting for 69% of the total surveyed wall length, followed by concrete block plus brick walls, accounting for 26%. No *terra cotta* masonry was observed. Typical thicknesses are 200 mm for concrete block walls and 300 mm for concrete block plus brick walls. The height of the walls varied between 1.2 m (in basements) and 7.5 m, but about 90% of them were between 2.5 and 4.0 m high. Most of these walls go up to the confining structural element, except for 4% where a gap was observed at the top of the walls.

The quantity of walls per storey, expressed either as wall length or wall area, was normalized by the floor area. Results are presented in **Figures 3.2** and **3.3**, where a normal distribution was fitted to each case. It can be seen that in both cases the distribution is similar, and mean and standard deviation values are presented in **Table 3.5**.

**Table 3.5.** Mean and standard deviation for normalized wall quantities

| Indicator | Units | Mean | Standard Deviation |
|---|---|---|---|
| Wall length/Floor area | $m/m^2$ | 0.22 | 0.10 |
| Wall Area/Floor Area | $m^2/m^2$ | 0.71 | 0.35 |

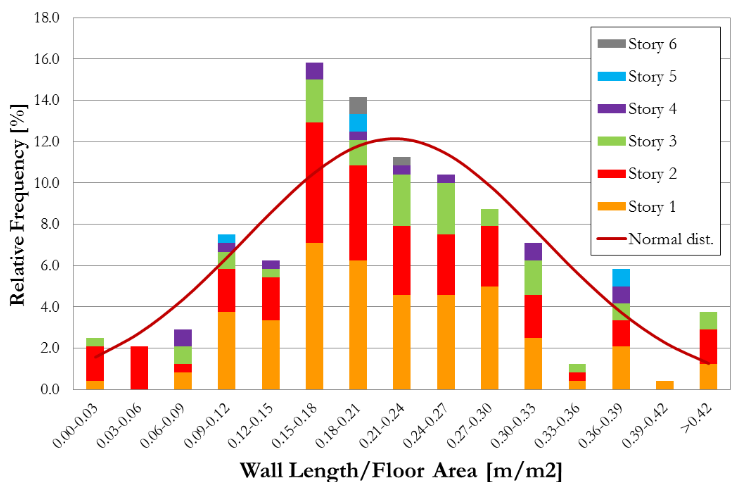


**Figure 3.3.** Distribution of normalized wall length per floor area values

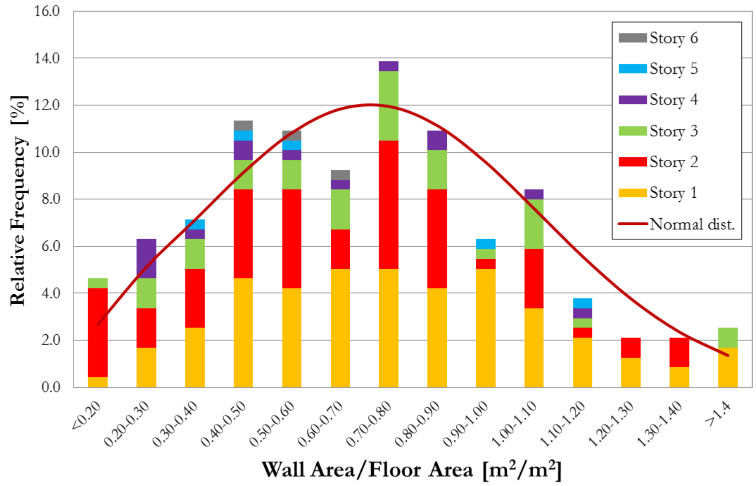


**Figure 3.4.** Distribution of normalized wall area per floor area values

If one storey has significantly less heavy infill walls than an adjacent storey, the difference in stiffness can induce a concentration of the lateral load deformation in the soft storey, leading to high storey drifts that the structure cannot withstand. To explore this possibility, the wall length over floor area ratios of the first and second storey where compared. Results are presented in **Figure 3.5**. For 16% of the studied cases the ratio at the second floor was under 50% of the value of the first floor, and for 18% of the cases the ratio at the second floor was over 150% the values of the first floor (over and under the dashed lines in **Figure 3.5**). Note that in the case of two-storey buildings, having a weaker top storey is not as critical as having a weaker first storey. Although rapid screening procedures try to identify weaker storeys by visual inspection of the amount of infill walls present, a detailed wall survey is not feasible in this context.

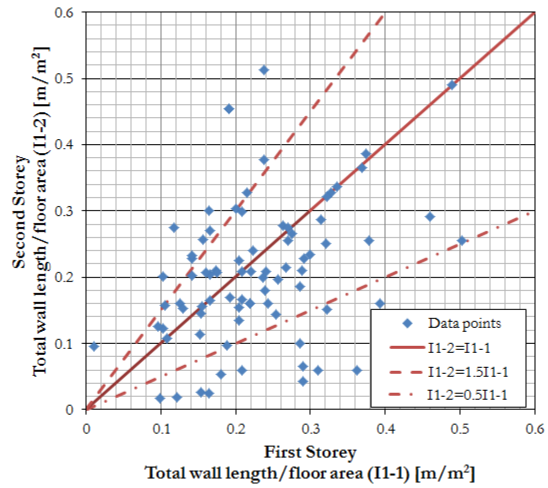


**Figure 3.5.** Comparison of total wall length/floor area ratios for first and second storey

Another undesirable feature is having an uneven relative distribution of the walls in both principal directions of the building in terms of overall dimensions. The wall length in the short direction was therefore compared to the wall length in the long direction, without reference to the actual horizontal stiffness of the lateral load resisting system. The distribution of the wall length ratio between these two directions is presented in **Figure 3.6**. The cumulative distribution is shown in **Figure 3.7**. It can be seen that the ratio is below 0.5 for only around 7% of the examined cases, and below 0.75 for 40% of the cases (marked with vertical lines in **Figure 3.7**).

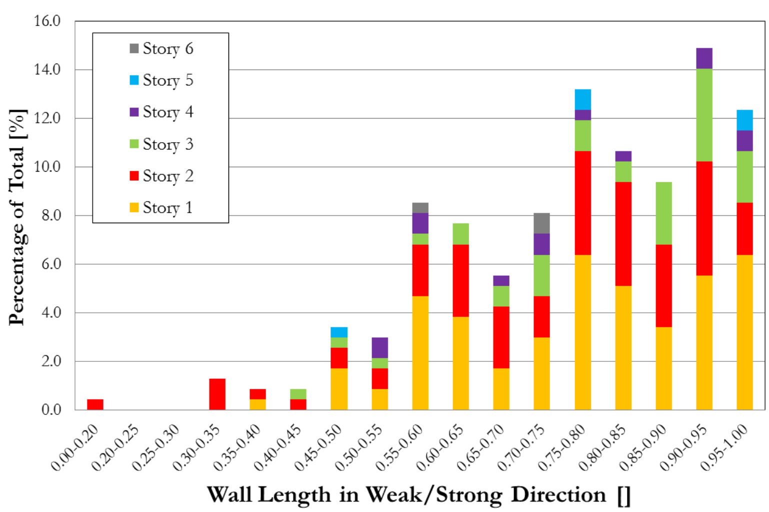


**Figure 3.6.** Distribution of the ratio of the wall length in the weak direction over the wall length in the strong direction

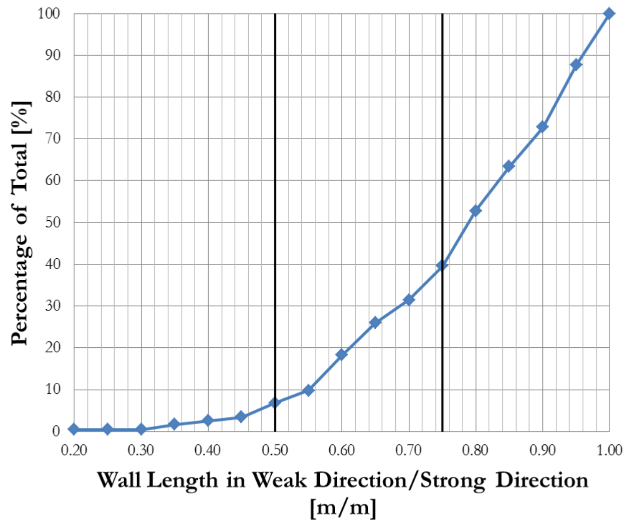


**Figure 3.7.** Cumulative ratio of the wall length in the weak direction over the wall length in the strong direction

## 3.3. Evaluation of Operational and Functional Components (OFCs)

A companion study evaluated the seismic vulnerability and risk of typical OFCs of fourteen of the sixteen schools (McClure et al., 2010), according to the procedure in the CAN/CSA S832-06 Standard, *Seismic risk reduction of operational and functional components (OFCs) of buildings* (CSA, 2006). This method is based on a visual inspection of the components. For each OFC a risk index (R) is determined as the product of the vulnerability index score and the consequences index score. The vulnerability index score is calculated based on the restraint of the OFC, the probability of impact or pounding with adjacent components, its likelihood of overturning, the relative flexibility of the OFC and its support, its location (elevation) in the building and the general soil and lateral load resisting system characteristics of the building. The consequences index score is mainly based on life safety and functionality criteria, in reference to the number of people threatened by the malfunction or failure of the OFC during or immediately after the earthquake, and the breakdown time that is tolerable according to the building's function and performance objectives. The individual OFCs are then classified as high risk for R over 50, moderate risk for R between 15 and 50, and low risk for R under 15. For high risk components mitigation measures are strongly recommended, while for moderate risk they remain optional.

A total of 91 independent school buildings were evaluated for OFCs, with the inspection and calculation of the R index for around 450 typical components. From the inspected OFCs, 20% were rated high and 54% moderate risk. Most of the high risk components were related to building services (e.g., mechanical and electrical components), and the most common problem identified was lack of restraint of the components.

## 3.4. Preliminary Evaluation Using Existing Rapid Seismic Screening Methods

Based on the collected information, preliminary building assessments using the FEMA154 and NRC92 rapid seismic screening procedures were performed. Please refer to **Chapter 2** for limitations in the use of these methods in the given context. Cut off scores were used as recommended for each method. Results of FEMA154 suggested that 53% of the buildings should undergo a detailed evaluation. NRC92 results classify 32% of the buildings with low priority for future interventions, 31% moderate priority, 23% high priority and 13% potentially hazardous. The clear relation between the results of both methods is presented in **Figure 3.8**. The large proportion of buildings requiring detailed evaluation, especially for the FEMA154 methodology, appears somewhat alarmist for a moderate seismicity environment like Montréal and provides further motivation for the development of better adapted screening methods that can identify more precisely which are the facilities that need detailed seismic vulnerability assessment.

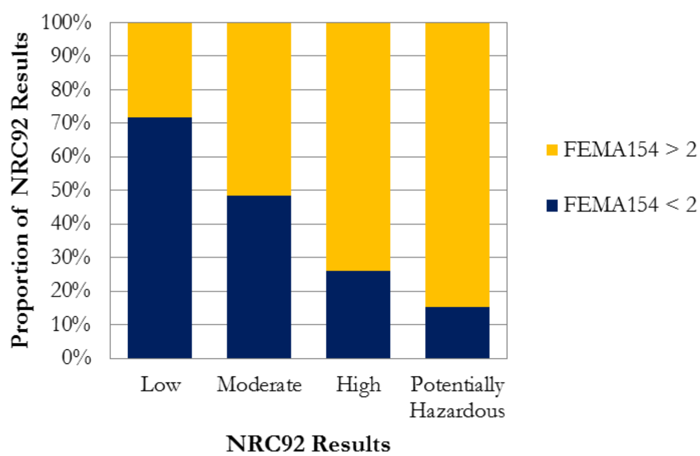


**Figure 3.8.** Comparative results of preliminary assessment using FEMA154 and NRC92

In general, the parameters that affect the scores (e.g., LLRS and construction year) are so correlated that it is difficult to establish a relation between them and the final scores. However, the positive effect of the refined classification of irregularities of NRC92 compared to FEMA154 can be appreciated when studying the influence of different vertical irregularities (e.g., steps in elevation view, building on a sloping terrain, and soft storey) on the final results. NRC92 classified 40% of school buildings with only one vertical irregularity as high priority and 70% with two vertical irregularities as high priority. Using FEMA154 the percentage of buildings in need of a detailed assessment was 90% and 100%, respectively for each case. This demonstrates that the NRC92 approach gives greater differentiation when more than one irregularity exists.

### 3.5. Summary

The study of a sample of 101 school buildings in Montréal showed that schools tend to be low-rise structures using a limited number of lateral load resisting system types. This reduced variety in construction types will simplify the seismic assessment procedure, but the LLRS type alone will no longer be a parameter suitable for the differentiation of the seismic vulnerability. As for construction years, they necessarily follow demographic and political changes. Typical Québec schools were constructed in the 1970s and before, having therefore strength and ductility deficiencies due to the lack of adequate seismic design criteria used at the time. The high incidence of structural features that could compromise seismic safety was confirmed, with 80% of the examined buildings having at least one type of irregularity. Heavy unreinforced masonry infill walls are extremely common. They were studied in detail due to the risk they pose when failing out-of-plane.

Results obtained by applying the existing seismic screening methods, NRC92 and FEMA154, are in reasonable agreement. However, results of FEMA154 seem somehow alarmist, with roughly half of the buildings being identified as needing a detailed assessment. NRC92 performs better in the identification and classification of irregularities.

# Chapter 4. In Situ Dynamic Properties of School Buildings

As part of the investigation of the schools designated as shelters on the island of Montréal, ambient vibration testing was conducted to extract in situ dynamic characteristics of the dominant low-frequency mode shapes (natural frequencies, damping ratios and modal shapes) excited by ground shaking due to earthquakes. The records were collected at all 101 school buildings in the summer months of 2009 and 2010. The experimental procedure, data analysis and results are presented in the following sections.

## 4.1. Experimental Procedure

### *4.1.1. Data Collection*

#### *4.1.1.1. Equipment*

Most of the buildings were tested using up to 6 Micromed Tromino ENGYN PLUS digital tromographs (Trominos), shown in **Figure 4.1**. These very compact instruments have 9 channels for the data acquisition: a set of 3 orthogonal high resolution electrodynamic velocimeters and high gain, a set of 3 orthogonal high resolution electrodynamic velocimeters and low gain and a set of 3 orthogonal digital accelerometers. To capture the ambient vibration data, the high gain velocimeters were used. **Table 4.1** summarizes the instrument's technical specifications as provided by the manufacturer.

Experience of other researches has demonstrated that the Trominos are appropriate to determine dynamic characteristics of buildings, as well as to record ambient noise for the characterization of soil. For example, Trominos were used to determine soil-structure interaction with measurements taken in four high-rise buildings and on soil (Castellaro and Mulargia, 2010). The performance of the instruments was tested in the range of 0.1 to 10 Hz on a piezoelectric shaking table with satisfactory results.


**Figure 4.1.** One Tromino sensor fitted with a radio transmitter (to the left) and one fitted with a GPS receiver (to the right)

**Table 4.1.** Technical specifications of Tromino sensors

| | |
|---|---|
| Amplifiers | All channels with differential inputs |
| Noise | < 0.5 μV r.m.s @128Hz sampling |
| Input impedance | $10^6$ Ohm |
| Frequency range | 0 – 360 Hz |
| Sampling frequency | 16384 Hz per channel |
| Oversampling frequency | 32x, 64x, 128x |
| A/D conversion | ≥ 24 bit equivalent |
| Max analog input | 51.2 mV (781 nV/digit) |
| Data recording | Internal memory |
| Operating environmental conditions | Temperature: -10 to 70$^o$C, humidity 0 to 90% without condensation |

Measurements at six of the buildings were performed using two Lennartz LE-3D/5s triaxial seismometers instead of Trominos, due to the equipment's availability. According to the manufacturer's technical specifications, these sensors have an eigenperiod of 5 s, a bandwidth of 0.2 to 40 Hz, a sensitivity of 400 V/(m/s), and a RMS noise at 1 Hz under 1 nm/s. The sensors were connected to a LEAS CityShark II data acquisition system each. For additional information on this type of sensor see

(Gilles, 2011), where they were used to perform extensive research on high-rise buildings in Montréal.

#### 4.1.1.2. *Experimental Setup*

The measurement nodes for each building were selected by inspection of the available building plans. The aim at the node selection is to gather records that will allow identifying dominant low-frequency sway and torsional modes. Typically, three nodes were examined along one of the principal directions at each floor and the roof. One sample setup is shown in **Figure 4.2**For one-storey buildings, typically a minimum of 4 sensors were placed on the roof at each corner of the building. Other configurations were used when necessary, for example for irregular buildings or when limited access was granted.

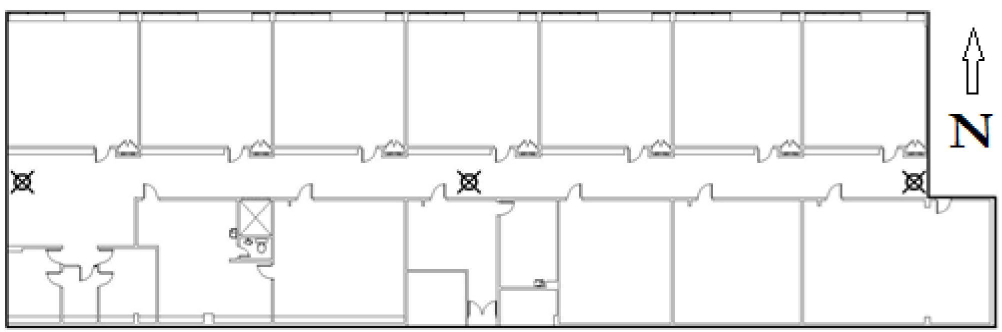


**Figure 4.2.** Typical setup of three sensors at one floor level (same location at every floor)

Since the number of sensors available was often insufficient to cover all the selected measurement points simultaneously, one sensor was left on a stationary location for all test setups (reference sensor), while the other sensors were placed at different nodes until all measurement points were covered (roving sensors). In this approach, it is important to locate the reference sensor on a node where all the modes of interest will be excited. Therefore the reference sensor was always located either at the top floor or at the roof, at one side on the building. To be able to later synchronize the different records, records were started either by remote control or manually using GPS time markers. Typical records were 8 minutes long, with a sampling frequency of 128 Hz.

### *4.1.2. Data Analysis*

#### *4.1.2.1. Pre-processing*

The collected data was downloaded using the Tromino's accompanying software, Grilla (Micromed S.p.A., 2011). The software also allows the synchronization of the records acquired manually, using the GPS time stamp.

The data was then imported to Matlab (MathWorks, 2011) for pre-processing, where signals where analyzed in time and frequency to exclude corrupt records and to roughly identify the frequencies of interest in both principal directions. Power spectral densities, spectrograms and the Choi-Williams transform were used for the analysis in frequency (see **Section 2.5.2** for the theoretical background).

The power spectral densities were calculated using Welch's method. For this approach, the input signal is divided in overlapping segments (usually 1024 data points in length, equal to 8 s for the typical sampling frequency), each of which is then processed through a Hamming window. The modified periodogram of each segment is then calculated and the average of all is used as an estimate of the power spectral density. Spectrograms were calculated directly as described in **Section 2.5.2.2**. To calculate the Choi-Williams transforms routines developed by the *Centre National de la Recherche Scientifique (CNRS)* were used. These routines can be downloaded at *<http://tftb.nongnu.org, 09/2011>*. To avoid the aliasing effect inherent to the Choi-Williams transform, the analytical representation of the studied signals was used (Figueiredo et al., 2004a, Figueiredo et al., 2004b). For a signal $x(t)$, the analytical representation $x_a(t)$ is given by **Equation 4.1**, where $\hat{x}(t)$ is the Hilbert transform of the signal $x(t)$ and $i$ is the imaginary unit.

$$x_a(t) = x(t) + i\hat{x}(t) \tag{4.1}$$

The final step of the pre-processing was the down-sampling of the records to match the lower-frequency band of interest for this application. .

#### *4.1.2.2. Processing*

The properties of the acquired records where extracted by the enhanced frequency domain decomposition (EFDD) technique as implemented in the ARTeMIS Extractor software (Structural Vibration Solutions A/S, 2010a). The procedure followed is described in the following paragraphs. For further details the reader is referred to the software's user's guide (Structural Vibration Solutions A/S, 2010b) and to the theoretical and background information of **Section 2.5.2**.

To perform the analysis, first the pre-processed data was imported to the software together with the geometric properties of the building model. As mentioned before, the data were then modified (down-sampling), from the sampling frequency at acquisition (usually 128Hz) to 32Hz. Since the actual frequency range that can be analyzed is given by the Nyquist Frequency, corresponding to half of the sampling frequency, this means that data were analyzed in the range of 0 to 16Hz.

The processing phase was started by calculating the spectral density matrices. The spectral density matrices are the spectral density functions at discrete, equally spaced frequency lines, and the number of frequency lines is chosen based on the resolution to be achieved (higher number of frequency lines will result in higher resolution). For the analyzed data, the number of frequency lines used was between 256 and 1024.

To apply the frequency domain decomposition (FDD) technique, singular value decomposition was then performed on the spectral density matrices. Since for the studied buildings usually multiple setups were available, the software averages the first singular value for all test setups. The same is done for the second, third, and successive singular values. An example averaged singular value plot is presented in **Figure 4.3**, where two frequencies of interest have been identified. Note that at each frequency the existing number of singular values is equal to the measured degrees of freedom in the test setup. To perform the classical FDD, the peaks of this plot are selected directly. Optionally, ARTeMIS allows to analyze the singular values for independent setups and to modify the selected peaks.

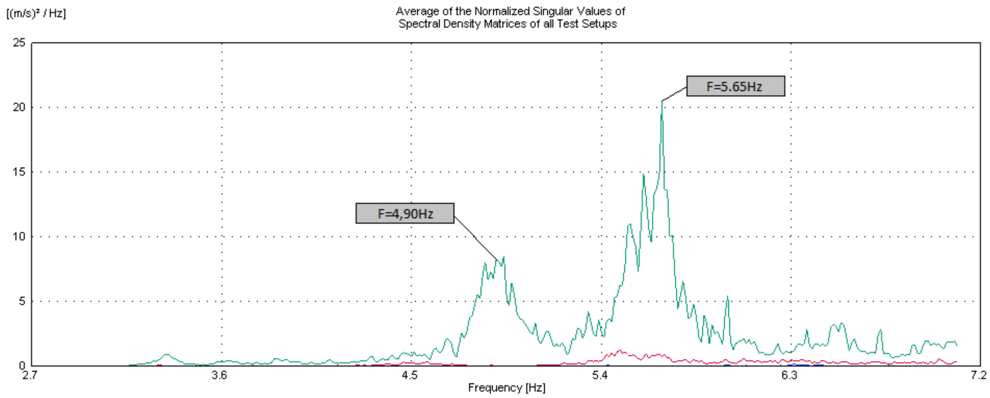


**Figure 4.3.** Sample average singular value plot

For the Enhanced FDD technique an additional step is introduced. First FDD peak picking is performed as described above. The mode shapes corresponding to the selected frequencies are then used to define the single-degree-of-freedom (SDOF) spectral bell functions. This is achieved through a correlation analysis on the modes using the modal assurance criterion, MAC. Natural frequencies and modal viscous damping ratios are then estimated performing a simple regression analysis on the SDOF spectral bell functions transformed to the time domain, which will be SDOF correlation functions. As an example, **Figure 4.4** shows the correlation function in the time domain and the linear regressions for the estimation of damping and the natural frequency for the first mode identified in **Figure 4.3** where peak picking yielded $f_1 = 4.9\,Hz$. Since the correlation functions in the time domain decay exponentially, similarly to the free response of a linear SDOF oscillator, the viscous damping ratio can be estimated from them using the logarithmic decrement technique. Peaks and their time of occurrence are identified from the correlation function. The natural logarithms of these peaks are then plotted against time (see **Figure 4.4**). From the logarithmic decrement technique it can then be shown that the modal damping ratio is related to the slope of this line, $m$, and the damped natural period, $T_d$, by **Equation 4.2**, where $\delta = -mT_d$.

$$\xi = \frac{\delta}{\sqrt{4\pi^2+\delta}} \tag{4.2}$$

The frequencies are estimated by from the zero crossings of the correlation function, by plotting them against time, as shown in **Figure 4.4**, and performing a linear regression. The slope of the regression is the number of cero crossings per second. Since there are two cero crossings per cycle, the frequency is equal to half the slope.

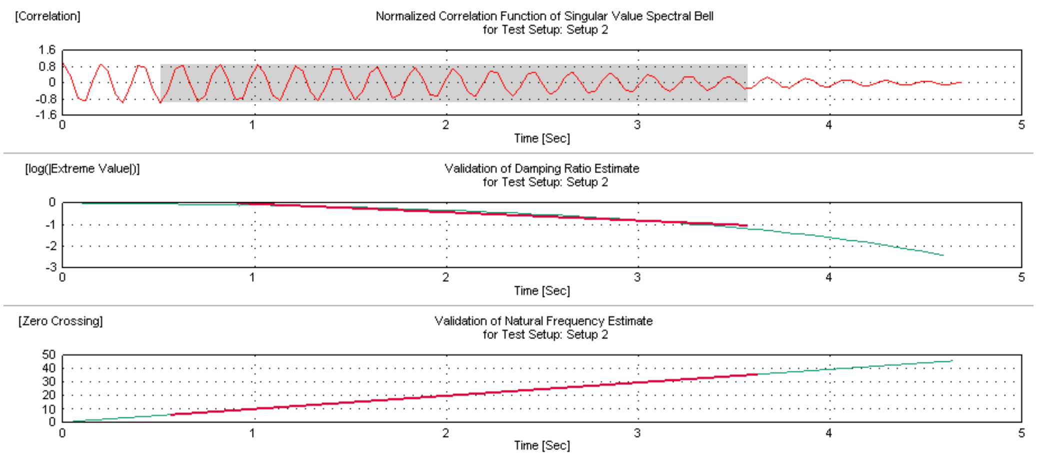


**Figure 4.4.** Sample normalized correlation function and linear regressions for the estimation of the damping ratio and natural frequency

## 4.2. Results and Discussion

### *4.2.1. Results*

As mentioned before, the extraction of dynamic properties of low-rise buildings from ambient vibration measurements is challenging, partly due to the low amplitude of the excitation and the effect of the soil. This was confirmed in the present study. Modes of vibration could only be established for 77 of 101 studied buildings, and only for 28% of the buildings two translational and one torsional mode could be determined from the gathered data. For other cases either one or two modes were identified, except one building where the first five modes were found. Similar studies in high-rise buildings have resulted in the determination of the first and second translational and torsional modes (at least 6 modes in total).

As an outcome of the study, a report for each building was developed, to be added to the seismic portfolio of each school. A sample of a summary sheet for one school and the report for the first building can be found in **Appendix B**. The fundamental period of vibration for all the tested buildings is presented in **Figure 4.5** where the data were assigned to seven types of lateral load resisting systems defined in **Table**

6.1. Both the relation to the building height and to the number of storeys are presented, given that the storey height varied considerably between buildings due to the special usage spaces, as for example gymnasia. As expected, in both cases there is a clear dependency between the period and the examined parameter. A similar trend can be observed for the first sway mode in the strong direction presented in **Figure 4.6**, and the first torsional mode shown in **Figure 4.7**. Modal viscous damping ratios associated with the fundamental sway mode are presented in **Figure 4.8**. For a more in depth analysis only two types of buildings were considered, concrete shear wall buildings (C2) and concrete frame buildings with unreinforced masonry infill walls (C3). Detailed data for these types of buildings are presented in **Appendix C**. All the other types were discarded because not enough buildings were examined to yield statistical significance. Even in the two considered cases the data sets are rather limited, with 22 and 32 buildings for C2 and C3 respectively. Further studies to increase the database are advisable.

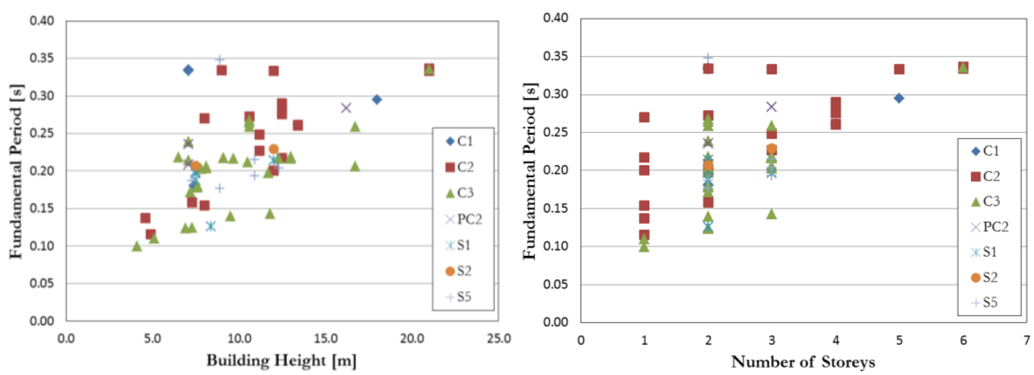


**Figure 4.5.** Experimental fundamental periods

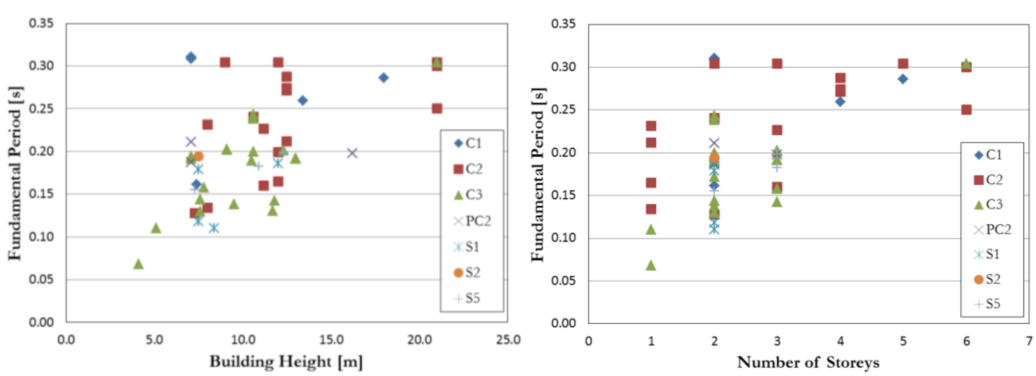


**Figure 4.6.** Experimental first periods in the strong direction

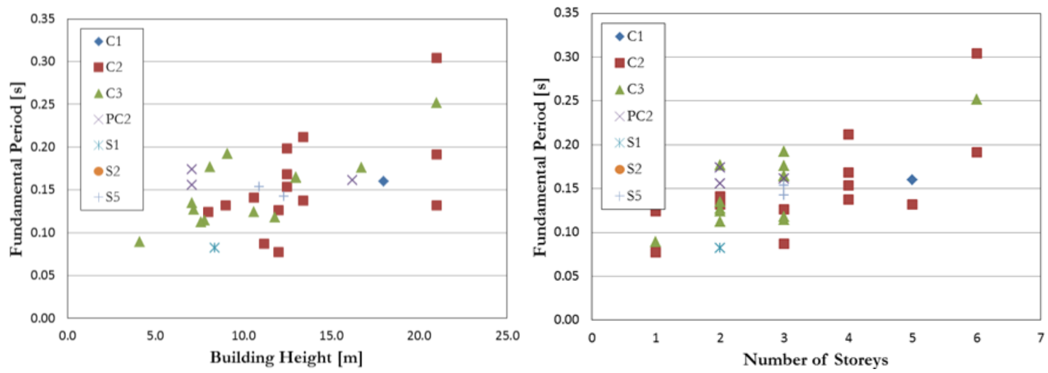


**Figure 4.7.** Experimental first torsional periods

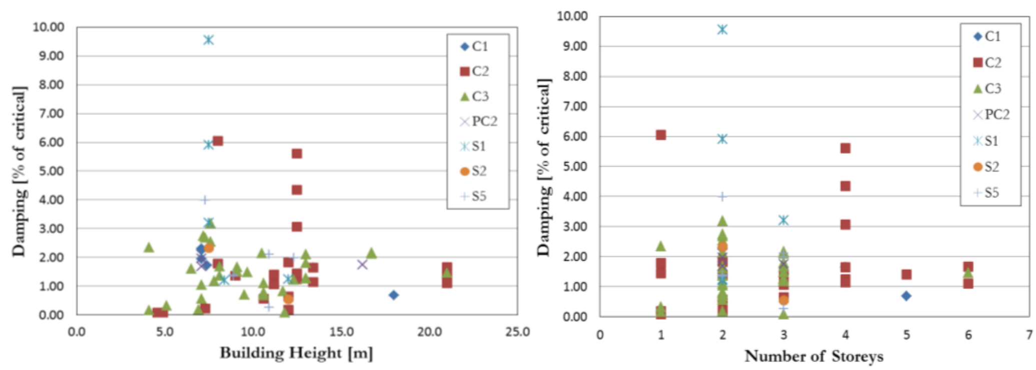


**Figure 4.8.** Experimental damping ratios determined for the fundamental mode

### *4.2.2. Evaluation of Elastic Region of Capacity Curves for Vulnerability Assessment*

#### *4.2.2.1. Capacity Curves for Vulnerability Assessment*

In seismic screening methods such as FEMA154 (ATC, 2002a) or large scale seismic assessment methods such as Hazus (NIBS, 2003), the expected behaviour of a building is described by generic capacity curves (see **Section 2.4.1**). Capacity curves give a relation between the force and the displacement in the structure and are defined by building type, height and quality of construction.

The collected data were used to assess how well the experimental first translational modes compare with the period that defines the elastic region of the Hazus capacity curves. This is relevant for the seismic screening method developed for schools because the same curves are used.

The capacity curves are given as a relationship between spectral displacements versus spectral accelerations. In this format, a radial line represents a constant frequency (note that the slope of the line is directly related to the frequency, therefore inversely related to the period). For a more detailed description of the curves and how they are defined see **Chapter 6**.

#### *4.2.2.2. Theoretical Versus Ambient Vibration Fundamental Frequencies*

Observations have shown that the fundamental period of a building structure tends to increase with the amplitude of the excitation as nonlinear response is mobilized by geometric and inelastic effects. It would therefore be inappropriate to compare results of ambient vibration testing directly with the theoretical values used in the capacity curves. However, since ambient vibration testing provides the means of supplying a significant sample of measured fundamental periods, and in view of the lack of other viable alternative methods, this approach has been used extensively in the past. Some considerations that will help to interpret the results are exposed. More details can be found in (Michel et al., 2010).

Ambient vibration tests will identify fundamental natural frequencies in the low amplitude domain, denominated $f_0$. On the other hand, the frequencies that represent the elastic part of generic capacity curves refer to the elastic fundamental frequency, $f_1$. This frequency reflects the behaviour of the building in its operational limit state, meaning that slight damage is already present, although there should be no plastification of structural elements.

Assuming a perfectly elasto-plastic model, a reinforced concrete structure will respond in the linear domain under excitations ranging from ambient vibrations to moderate earthquakes, at least until the ultimate wind loads are reached. Up to small earthquakes the behaviour will be strictly linear, with a constant frequency, corresponding to $f_0$. In moderate seismic events, although the behaviour can still be considered elastic, more small cracks will appear and the frequency, now referring to $f_1$, will decrease up to 35%. Finally, in the plastic domain the building will suffer major damage and the frequency will subsequently drop sharply. Some studies indicate that the "final" frequency at the onset of collapse will be of the order of

40% of the initial frequency, corresponding to a reduction of around 60% (Michel et al., 2010).

#### *4.2.2.3. Comparison of Elastic Range of Capacity Curves and Experimental Fundamental Frequencies*

For C2 buildings, 14 data points were available for low rise (C2L) and 9 for medium rise (C2M) buildings. For C3 buildings, 31 data points were available for low rise buildings (C3L). Only for these cases the comparison with the capacity curves were made. Further studies to enlarge the data sets are recommended. Note that for different capacity curves that reflect the quality of construction of different C2 or C3 buildings (given in terms of design code[6]) the frequency in the elastic range is the same. Results are presented in **Figure 4.9**.

For all cases, the experimental curves lie above the theoretical Hazus elastic curves. This indicates that the experimental frequencies are higher than the theoretical ones. Remembering that $f_o > f_1$, this result was expected. However, this does not imply that the theoretical capacity curves are conservative. For traditional seismic force design, conservative $f_1$ values are overestimated ones (i.e., underestimated periods), but for displacement-based design $f_1$ values should be underestimated. Considering this and some studies that suggest that $f_1 > 0.4f_o$ (Michel et al., 2010), it can be concluded that a conservative yet realistic estimate of $f_1$ requires $f_o$ values to be slightly above $f_1$ values. However, difference above 60% are not realistic, since this is the approximate value reached when the structure is close to collapse. For C2L buildings, the average difference is 37%, and 15% of the cases are above the 60% limit (2 buildings). For C2M buildings, the average difference is 48%, but there is no case above 60%. Finally, for C3L the average difference is 44%, and 20% of the cases (6 buildings) are above 60%. In conclusion, the measured frequency values seem to be slightly high (slightly low periods) but generally in good agreement with the theoretical capacity curves.

[6] See **Chapter 6** for a discussion on how the quality of construction is considered in the capacity curves.

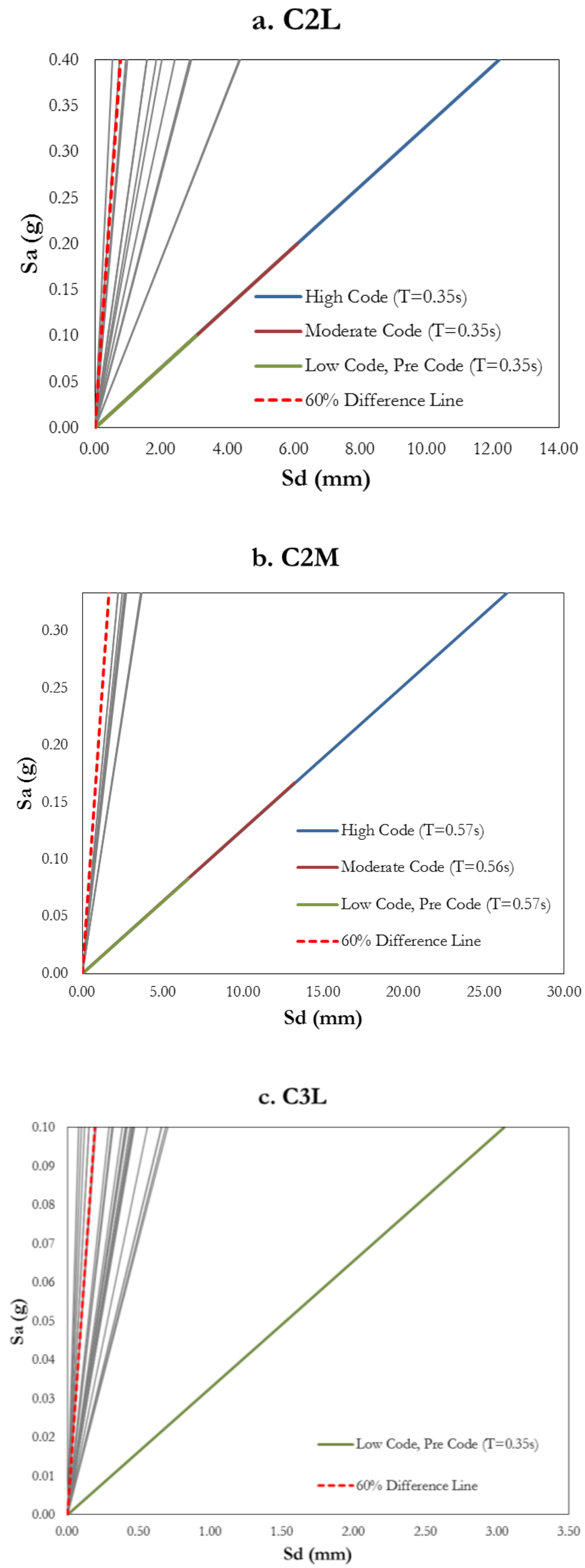


**Figure 4.9.** Elastic part of capacity curves for seismic assessment compared to experimental data (in grey).

### *4.2.3. Approximate Fundamental Period Formulae*

#### *4.2.3.1. NBC Period Formulae*

Dynamic analysis is the preferred seismic analysis method recommended in the 2010 NBC, although the equivalent static force procedure can still be used for buildings in low seismicity regions or buildings that are relatively stiff, with limited height and irregularities. For either of these analysis methods, the fundamental sway period of the building is a key parameter in seismic design. In the equivalent static force procedure, the fundamental period directly defines the magnitude of the design spectral acceleration from the uniform hazard spectrum. If response spectrum analysis is used for linear structures, the uniform hazard spectrum is used as a pseudo-acceleration design spectrum. The natural frequencies, determined from the eigenvalue analysis of an idealised finite element model, will define the maximum accelerations for each mode from the uniform hazard spectrum.

The NBC gives approximate empirical expressions to determine the fundamental period of the structure for different lateral load resisting systems for the application of the equivalent static force procedure. The two equations of interest in the present study are repeated here as **Equations 4.3 and 4.4**, where $T_a$ is the fundamental translational period and $h$ is the building height above ground level.

$$T_a = 0.075h^{3/4} \quad \text{for reinforced concrete moment-resisting frames,} \tag{4.3}$$

$$T_a = 0.05h^{3/4} \quad \text{for shear walls and other structures.} \tag{4.4}$$

Even if the fundamental period of the structure is determined by an alternative, potentially more reliable method, the code limits the value that can be used for the equivalent static force procedure to 1.5 or 2.0 times the value obtained from the appropriate equation above depending on the lateral load resisting system. These limits are also relevant when dynamic analysis is performed, since the NBC states that the base shear calculated must be at least 80% of the equivalent static base shear for regular structures and 100% for irregular ones.

The relationship between the fundamental period and the height of the building affected by an exponent of ¾ was derived in the late 1970s using Rayleigh's method and some rational assumptions, and it has been used ever since in different North American codes. Note that other equally plausible assumptions would lead to a different exponent. The expression was then calibrated by calculating the factor from a linear regression of measured fundamental periods of buildings. The problem lies in the fact that the number of buildings studied was very limited and later studies, where more data were available, showed a bad fit. The original buildings studied were also all located in California, and it is questionable if buildings located elsewhere would follow a similar trend (Gilles, 2011). This has been recognized by researches, and alternative simplified expressions have been derived based on experimental periods measured in buildings in different regions of the world. Keeping the relationship only in terms of the building height, some authors have proposed that the exponent of ¾ could be replaced by 1, without affecting the fit of the data (Hong and Hwang, 2000).

It must be recognized that expressions based solely on the building height (or number of storeys) over simplify the assessment of the structure's period, and the estimates can therefore not expected to be very accurate. Other more complex expressions include other factors that influence the fundamental period, as for example the dimensions of the vertical lateral load resisting elements (Goel and Chopra, 1998). However, expressions based solely on the building height are still commonly used because of their simplicity.

The effect of the inaccuracy of the simplified period equations on the base shear calculated for design will be significant. A study based on experimental ambient vibration data collected in high rise buildings in Montréal and uncertainty propagation found that the design seismic loads can be overestimated significantly if the empirical formulae are used. If the upper limits given by the NBC are used, the loading may be significantly underestimated (Gilles et al., 2011).

In the context of the present research, the fundamental periods obtained from ambient vibration data were compared to the simplified expressions based solely on the building height as presented in the NBC. It must be recognized that in addition to the problems already mentioned before, these formulae were calibrated on mid-rise, mostly shear buildings, which are very different to the ones examined here. Further considerations to compare periods obtained from ambient vibration data to code formulations are presented in the next section.

The discussion made on how the variability of the frequency with amplitude of excitation must be considered for the comparison between theoretical and ambient vibration fundamental frequencies (see **Section 4.2.1.2**) is also applicable in this case. The simplified formulae for fundamental frequencies of the building codes (as in **Equations 4.3** and **4.4** for the NBC) aim to represent $T_1 = {}^{1}/_{f_1}$. To assure that the base shears calculated using traditional design are conservative, the values of $T_1$ are also underestimated by about 10 to 20% (Michel et al., 2010). Since $T_0 < T_1$, using $T_o$ instead of $T_1$ is usually a conservative approach for conventional design governed by seismic forces. Note that for displacement-based design where drift limits govern, design periods higher than the real ones are conservative.

#### *4.2.3.2. Comparison between Experimental Data and Code Period Formulae*

**Figures 4.10** and **4.11** show the recorded fundamental periods for C2 and C3 building types, and the NBC code approximate expressions and allowed maxima. As a reference, the best fit line is also shown, see details in **Section 4.2.2.3**. In both cases the fit between the AVM recorded data and the NBC expressions is poor. Furthermore, the NBC expressions overestimate the periods.

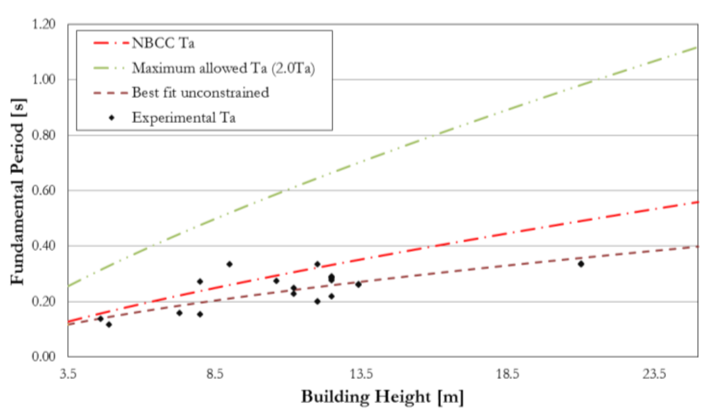


**Figure 4.10.** Experimental Data and NBC Formula for Concrete Shear Wall Buildings (C2)

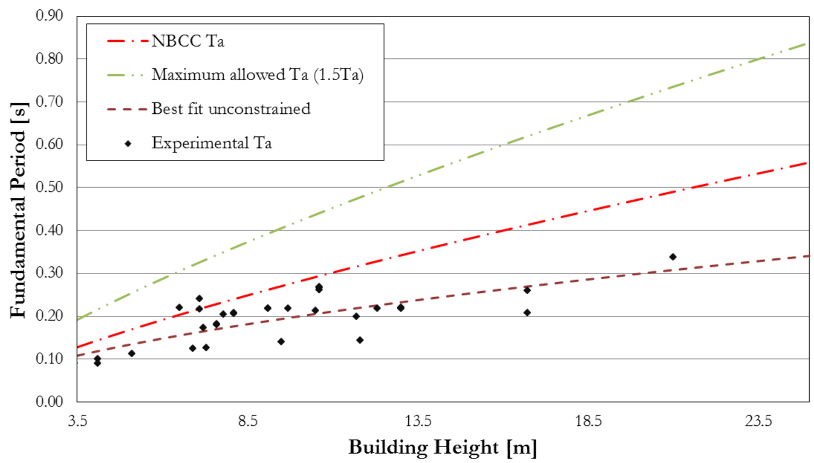


**Figure 4.11.** Experimental Data and NBC Formula for Concrete Frame Buildings with Unreinforced Masonry Infill Walls (C3)

#### *4.2.3.3. Proposed Improved Fundamental Period Formulae*

Multiple linear regressions were performed on the data sets for C2 and C3 buildings, to explore how expressions of the type $T_0 = ah^b$ fit the measured data, where $T_o$ is the measured fundamental period and $h$ is the height of the building above ground, in meters. Three cases where considered based on the allowed values for the exponent $b$. First, the best fit without constrains was found and then values of $b$ were constrained to 0.75 and 1. The procedure followed is similar to (Gilles, 2011), and additional details can be found in **Appendix D**, together with complete results with and without outliers. Herein, the presented results refer to data sets without outliers.

Results for both evaluated structural types are presented in **Table 4.2** and **4.3**, and **Figures 4.12** and **4.13**. In general terms the fit between the data and the proposed expressions is not high. As exposed in previous sections, this was expected since the approximate formulae oversimplify the complexity of the determination of the period. Another factor that is specific to the evaluated building set is the high variability of the storey height. For C2 buildings this is extreme, with buildings of 1, 2 and 3 storeys with the same height (12m). It is evident that these buildings will have a different dynamic behaviour.

It is quite interesting to see that the best fit unconstrained is close to the best fit constraining $b = 0.75$ with differences in $R^2$ and $s_e$ of less than 2% for both lateral load resisting systems. When using $b = 1.0$, the fit is clearly poorer, with $R^2$ of 0.64 for C2 and 0.50 for C3. Another observation made is that results for both examined lateral load resisting systems are similar. This could be explained by the stiffening effect of the masonry infill partition walls.

**Table 4.2.** Results of regression analyses for C2 buildings

| Type | Coefficient b | Coefficient a | $s_e$ | $R^2$ |
|---|---|---|---|---|
| Unconstrained | 0.69 | 0.043 | 0.145 | 0.797 |
| Constrained | 0.75 | 0.038 | 0.147 | 0.791 |
| Constrained | 1.00 | 0.020 | 0.194 | 0.639 |

**Table 4.3.** Results of regression analyses for C3 buildings

| Type | Coefficient b | Coefficient a | $s_e$ | $R^2$ |
|---|---|---|---|---|
| Unconstrained | 0.66 | 0.043 | 0.181 | 0.674 |
| Constrained | 0.75 | 0.035 | 0.184 | 0.662 |
| Constrained | 1.00 | 0.020 | 0.225 | 0.495 |

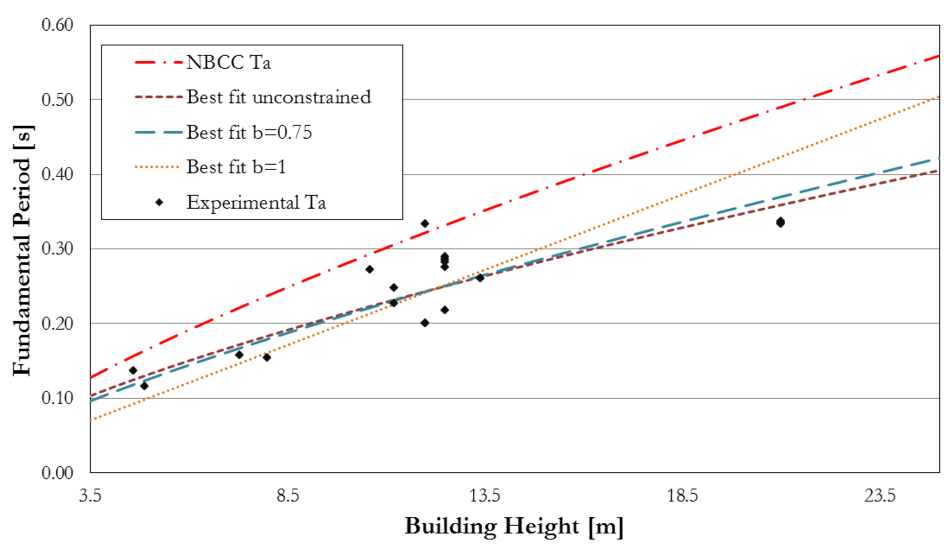


**Figure 4.12.** Regression analyses for C2 buildings

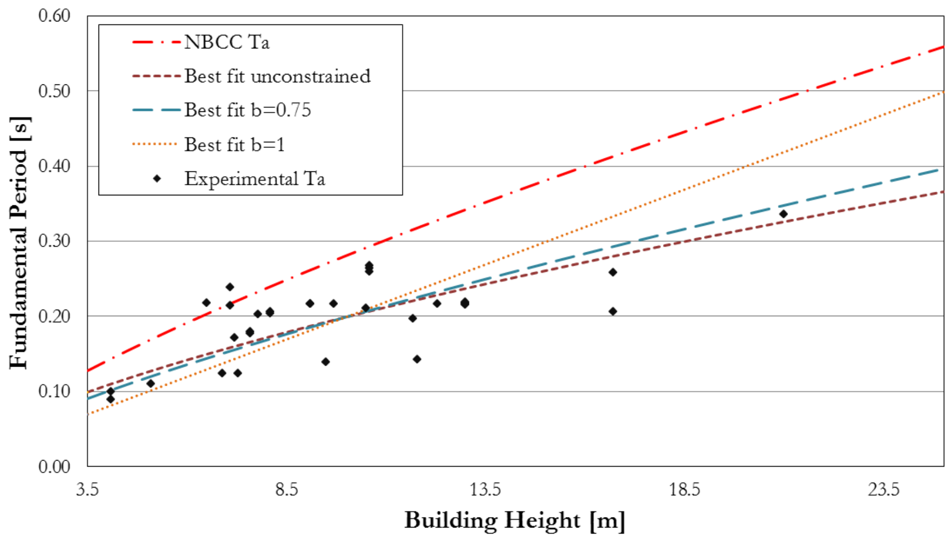


**Figure 4.13.** Regression analyses for C3 buildings

The possibility of fitting the data against the number of storeys instead of building height was considered, but results were disregarded due to the very poor fit of the data, see **Figure 4.14** where linear trend lines were fitted to both data sets with $R^2$ values of 0.35 and 0.47 respectively. Two problems were identified that lead to this poor fit. First, the distribution of the data over number of storeys gives a poor resolution, since most of the buildings are one to three storeys high. Second, the variability in the data is high, which can again be partly explained by the high variability of storey heights, as shown for the fit against building height.

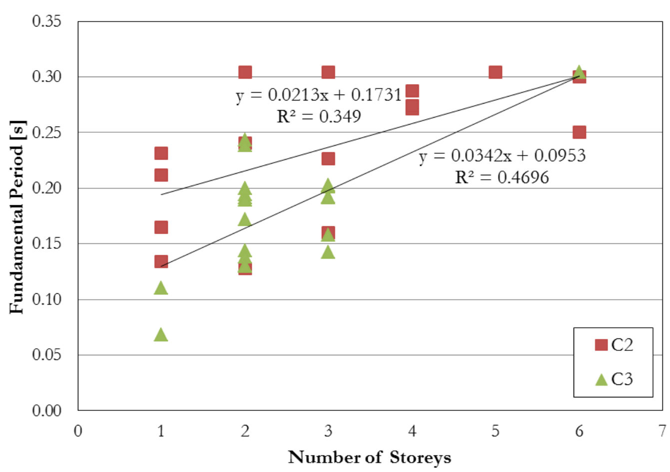


**Figure 4.14.** Fundamental period versus number of storeys

#### 4.2.3.4. *Comparison of Results with Results from Previous Studies*

For the city of Montreal, ambient vibration measurements have been used to determine the dynamic characteristics of high-rise concrete shear wall buildings. A similar linear regression as presented above was made, to determine the best fit curves to the data (Gilles, 2011). Results are given in **Table 4.4** for comparison. In the same study, it was proposed that the fundamental period of a structure should be estimated based on results with $b = 1$ and the data's standard deviation.

A first observation is that the fit to the data of high rise buildings is better, with $R^2$ values that are roughly 10% higher. This better fit could be explained by the difficulties of extracting dynamic properties from ambient vibration data for low rise buildings, as discussed before. The low-rise buildings investigated are potentially also less homogeneous than the high-rise buildings. The information was collected in schools with many irregularities, and where standard storey heights can vary considerably. However, it must be considered that the estimation of the natural period with the given expressions is in any case more accurate than the expressions proposed in the NBC. These expressions can therefore be useful if other school buildings should be seismically assessed and retrofitted.

**Table 4.4.** Results of regression analyses for high-rise concrete shear wall buildings in Montreal (Gilles, 2011)

| Type | Coefficient b | Coefficient a | $s_e$ | $R^2$ |
|---|---|---|---|---|
| Unconstrained | 1.032 | 0.017 | 0.229 | 0.898 |
| Constrained | 0.75 | 0.052 | 0.296 | 0.738 |
| Constrained | 1.00 | 0.019 | 0.230 | 0.892 |

### *4.2.4. First Torsional Mode*

Collected data for torsional modes is scarce, with information for 14 buildings of type C2 and 13 of type C3. In spite of this a linear regression was performed to determine the best fit curve following the same procedure as for the fundamental sway mode. Since in the literature the first torsional mode has been compared to the building height or to the fundamental period, linear regressions for both cases were made. Results are presented in **Table 4.5**, and **Figures 4.15** and **4.16**. Only an unconstrained analysis was performed due to the poor fit of the data, with values of $R^2$ ranging from 0.175 to 0.512. Moreover, using the F-statistic to test the fit of the linear regressions, it was demonstrated that the obtained optimal straight line has no statistical significance. The large scatter of the data is in agreement with the high incidence of irregularities in the buildings studied, and it reflects how difficult it is to account for them in a simplified manner. In both cases the torsional mode had a better correlation to the building height than to the first translational mode.

**Table 4.5.** Results of regression analyses for first torsional mode

| Lateral Load Resisting System | Investigated Parameter | Coefficient b | Coefficient a | $s_e$ | $R^2$ |
|---|---|---|---|---|---|
| C2 | Height | 0.599 | 0.032 | 0.316 | 0.256 |
| | Fundamental Period | 0.693 | 0.368 | 0.332 | 0.175 |
| C3 | Height | 0.477 | 0.050 | 0.205 | 0.512 |
| | Fundamental Period | 0.772 | 0.522 | 0.181 | 0.452 |

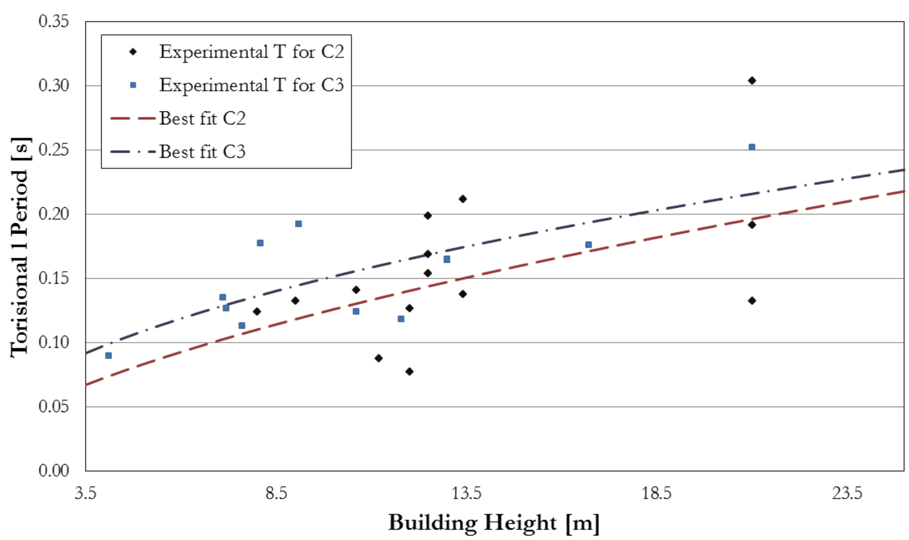


**Figure 4.15.** Regression analyses of first torsional period against building height

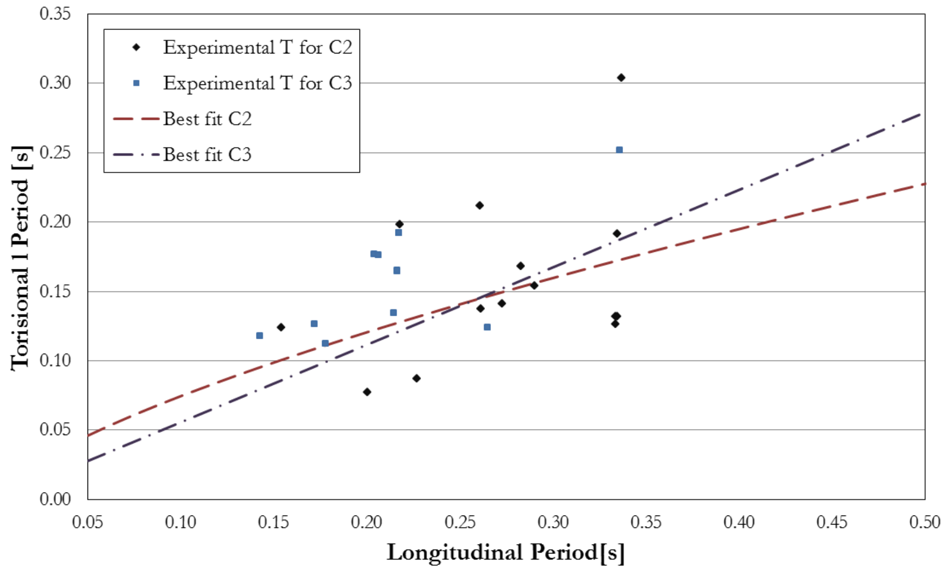


**Figure 4.16.** Regression analyses of first torsional period against first sway period

### *4.2.5. Viscous Damping Ratios*

Viscous damping ratios calculated from this study should be treated with care as their determination from ambient vibration data is not as reliable as the natural frequencies. This was confirmed when evaluating several independent tests for the same building. While the variability of natural frequencies was minimal, damping ratios tended to show large scatter. Nonetheless the results are presented and some very general conclusions are reached.

Considering the first longitudinal, transverse and torsional modes, a total of 56 damping values were collected for C2 buildings and 68 for C3 buildings. Data points with considerable standard deviation (≥50%) or where the estimate of the standard deviation was not available (indicating a poor estimate) were removed, resulting in 20 damping values for C2 buildings and 36 for C3 buildings, as presented in **Figures 4.17** and **4.18**. Note that about half of the calculated ratios were found to be inaccurate and were discarded, again showing the limited reliability of the damping estimates.

The scatter of the data sets is considerable. However, comparing the damping ratios to the customary 5% viscous damping used for seismic design, also considered in the NBC, it can be seen that obtained values tend to be lower. For C2 buildings, the average damping ratio is 1.9% and the median is 1.7%. For C3 buildings, the average and median values are both 1.3%. These values indicate that using a damping of 5% is not conservative even considering that viscous damping will increase for higher levels of shaking, up to a factor of two. The same was noted in (Gilles, 2011), where similar values as in the present study where obtained: the average viscous damping ratio of the fundamental sway mode extracted from AVM records in high rise C2 buildings in Montréal was 2.2%, with a median close to 2%.

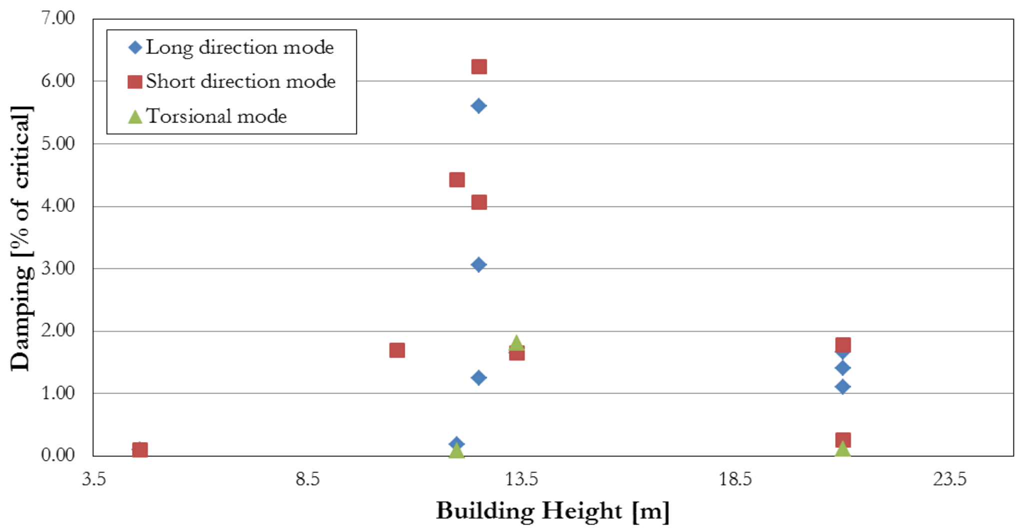


**Figure 4.17.** Damping ratios for C2 buildings

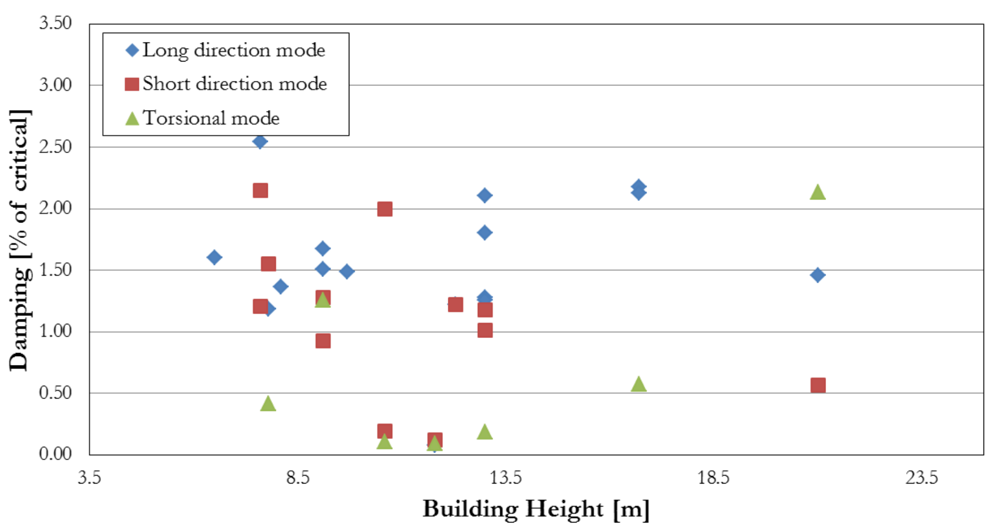


**Figure 4.18.** Damping ratios for C3 buildings

## 4.3. Summary

The principal outcome of the data analysis was the comparison of the elastic part of the capacity curves used for the adapted seismic screening method to experimentally obtained natural frequencies. This allowed a validation of the use of these generic curves. Furthermore, the dynamic characteristics of each school building were added to the seismic portfolio of each school. This information will be valuable should further actions toward seismic mitigation be taken. Finally, as a complementary work approximate code formulae for fundamental periods as presented in the NBC were compared to experimental data, and the first torsional modes and damping rations were also analyzed. Although this analysis has no direct influence on the developed seismic screening method, it was included due to its significance to seismic design in general.

# Chapter 5. Local Site Conditions

Local site conditions largely influence the behaviour of a structure under seismic loading. The 2010 NBC acknowledges this fact and design spectral acceleration values can be amplified up to roughly two times for structures located on poor soil, compared to structures located on a reference stiff soil (type C). Existing seismic screening methods also reflect the high importance of local site conditions. FEMA154 for example, will have an average reduction of the final score of 40% for structures located on poor soil (type E).

However, in a seismic screening context collecting soil data can be challenging. The difficulties that can arise were demonstrated during the evaluation of the selected schools. Although building plans were readily available, in most cases soil reports were not. For the school buildings studied, borehole data were only available for two out of 16 sites. Traditional in situ soil testing is not feasible in a seismic screening context due to the required resources. However, if no soil data are available the soil score modifier is very penalizing. Therefore an alternative approach was explored, consisting of extracting the soil's natural frequency from ambient noise measurements using the H/V technique (Nakamura, 2000). Site effects considered in the building code are based on estimates of the shear wave velocity of the soil, which can be estimated from the natural frequency of the soil and the bedrock depth

## 5.1. NBC Site Classification

For seismic effects, NBC classifies soil types into six site classes, from A to F, ranging from hard rock (type A) to poor soil (type F) (NRC/IRC, 2010a). For the classification of each type, the main parameter used is the measured (or estimated) average shear wave velocity in the top 30 m of soil, $V_{s30}$. Ground motion amplification factors for short and long periods, $F_a$ and $F_v$, dependent on the expected intensity of shaking, are defined for each site class. **Table 5.1** gives the $F_a$ and $F_v$ values for the city of Montréal, together with the description for each NBC soil type and representative values of $V_{s30}$. The reference soil is type C, meaning that $F_a$ and $F_v$ values are equal to one for this type.

**Table 5.1.** Ground amplification factors for Montréal, from (NRC/IRC, 2010a)

| Soil Type | Description | $V_{s30}$ | $F_a$ | $F_v$ |
|---|---|---|---|---|
| A | Hard rock | $V_{s30}$ > 1500m/s | 0.776 | 0.500 |
| B | Rock | 760m/s < $V_{s30}$ ≤ 1500m/s | 0.876 | 0.640 |
| C | Soft rock and very dense soil | 360m/s < $V_{s30}$ ≤ 760m/s | 1.000 | 1.000 |
| D | Stiff soil | 180m/s < $V_{s30}$ ≤ 360m/s | 1.124 | 1.360 |
| E | Soft soil | $V_{s30}$ ≤ 180m/s | 1.172 | 2.060 |
| F | Poor soil | [a] | [a] | [a] |

[a]: site-specific geotechnical investigation required.

## 5.2. Site Classification from Existing Sources of Information

Geotechnical or geological maps and reports are the preferred sources of information for seismic screening. For the schools studied, geotechnical data were extracted from the set of building plans, and summarized in **Table 5.2**. Another available source of information was Montréal's microzonation map, shown in **Figure 5.1** (Rosset et al., 2011). The map provides the NBC site class at any given location, based on estimates of the shear wave velocities.

**Table 5.2.** NBC soil type estimates from available geotechnical data

| School | NBC Soil Type | Comments |
|---|---|---|
| S2_CL | C or higher | Soil bearing capacity of 1.92 x $10^5$ Pa (to be verified) |
| S3_AV | C or higher | Borehole data plan available but not legible. Rock depth estimate: 7.5 m |
| S4_JM | D | Borehole data for building S available. Rock depth 6.5 to 9.5 m. |
| S5_LR | A or B,<br>C or higher | For building blocks A-B-C-D: Rock bearing capacity: 9.58 x $10^5$ Pa. For building blocks B-D-E: soil bearing capacity: 1.44 to 1.68 x $10^5$ Pa. |
| S6_EM | A or B | Borehole data available. Rock depth 2.5m or less, typical Rock quality designation: 100% |
| S9_R | A or B | All footings shall be taken down to the rock surface. Maximum rock bearing capacity for design purposes: 9.58 x $10^5$ Pa. |
| S12_LM | A or B | Rock depth: 1.30m or less, no information on quality of rock. |

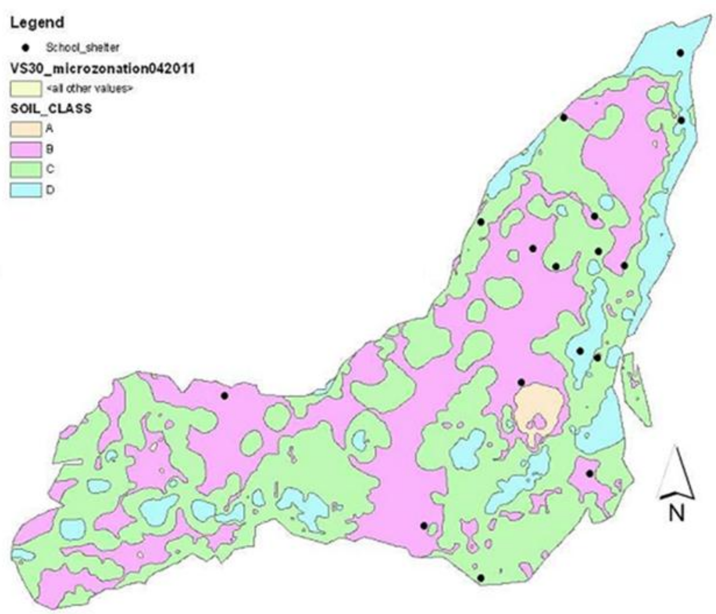


**Figure 5.1.** Montreal's microzonation map with the localization of evaluated schools (Rosset et al., 2011)

## 5.3. Site Classification from Ambient Noise Data

The feasibility of using ambient noise data to determine the soil type was explored. The natural frequency of the soil at each school site was extracted from ambient noise measurements using the H/V technique. This technique, introduced by Nakamura in 1989, has been widely used to determine dynamic characteristics of soils, because of its simplicity and fast results. The technique requires ambient ground motion data, that is then processed by dividing the horizontal components by the vertical component (hence the name, H/V technique). The fundamental resonant frequency of the soil can be estimated from the resulting ratio because of the multiple refractions of the S waves on the ground surface. A comprehensive description of the method is given in (Nakamura, 2000).

In this research single station measurements of 10 minutes with a sampling frequency of 120Hz were recorded using the same sensors as for AVM in the buildings, Micromed Tromino ENGYN PLUS tromographs (see Chapter 4 for a complete description of the instrument). To capture the ambient noise data, the high gain velocimeters were used. All recordings were taken on natural soil. Using the Micromed Grilla software, the H/V technique was applied to the records to extract the fundamental resonance frequency at each site. **Figure 5.2** shows the results for a sample site. The site's fundamental frequency, 10.31 ± 0.07 Hz, can be identified from the H/V spectrum (**Figure 5.2.a**). The spectrogram (**Figure 5.2.b**) shows the stability of the signal in time and the amplitude spectra (**Figure 5.2.c**) depict the properties of the three analyzed components, two horizontal and one vertical. Complete results of the estimated natural frequencies for all school sites are presented in **Table 5.3**.

The implementation of this procedure for the evaluated schools demonstrated how easy and fast it is, the only drawback is that specialized equipment has to be available. The entire setup, including surface preparation, equipment installation and 10-minute measurement took on average only 20 minutes. In most cases data processing was relatively simple as well, taking on average 5 minutes per measurement. Both tasks can be performed by non-specialists after a short training. The application of this method, although still to complex for its application to all visited sites in a large seismic screening program, is simple enough to be applied in this context to buildings (or locations) of special interest.

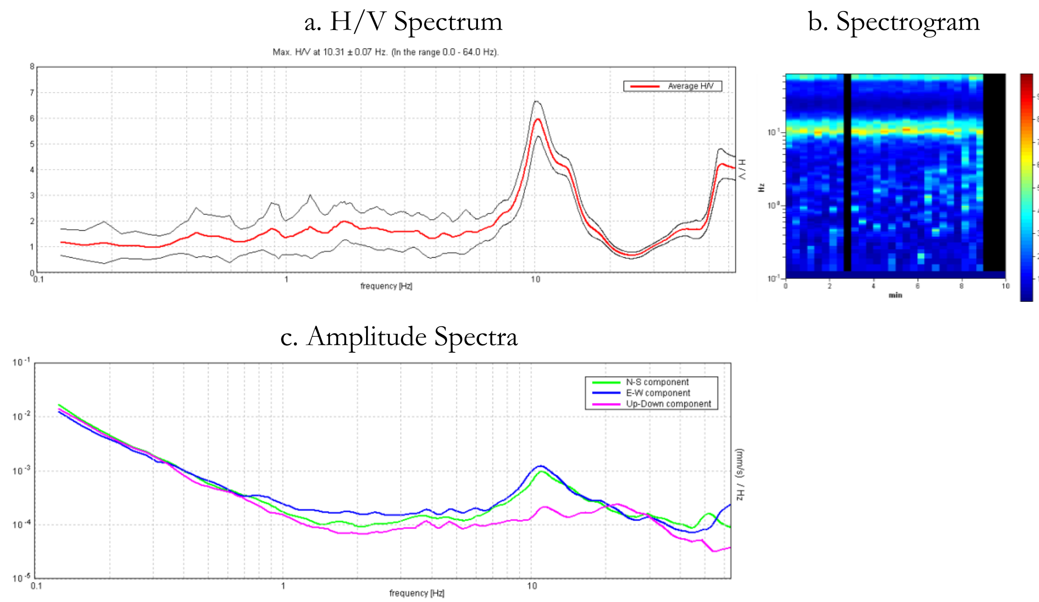


**Figure 5.2.** H/V analysis results for a sample school site

**Table 5.3.** Natural frequencies at school sites determined from ambient noise data

| School | Frequency [Hz] | Standard Deviation [Hz] |
|---|---|---|
| S1_A | 10.31 | 0.07 |
| S2_CL | 17.56 | 4.55 |
| S3_AV | 14.38 | 0.56 |
| S4_JM | 3.72 | 0.06 |
| S5_LR | 16.72 | 4.95 |
| S6_EM | 51.56 | 0.19 |
| S7_CaL | 3.09 | 0.64 |
| S8_EAO | 16.88 | 5.69 |
| S9_R | 29.30 | 10.50 |
| S10_JG | 23.09 | 5.67 |
| S11_PD | 14.48 | 0.08 |
| S12_LM | 37.81 | 0.15 |
| S13_SE | 42.78 | 0.08 |
| S14_MR | 5.31 | 1.40 |
| S15_DJ | 36.25 | 0.06 |
| S16_PT | 1.88 | 0.02 |

Having the natural frequency of the soil $f$, and assuming a single-layer soil model, the shear wave velocity of the soil $V_{s\ soil}$, can be estimated (if the thickness $h$ of the sedimentary layer is known) using **Equation 5.1** (Castellaro and Mulargia, 2009). For the present method, the rock depth at the different locations was estimated by interpolation of borehole data, using the natural neighbourhood method[7] (cross-referenced with (Prest and Hode Keyser, 1962)), resulting in a minimum and a maximum estimate for each location. The resulting estimates of rock depth are in good agreement with the geotechnical data, where available (compare **Table 5.2** and **Table 5.4**). The soil layer was assumed uniform.

$$f = \frac{V_{s\,soil}}{4h} \tag{5.1}$$

[7] Compounded by U. Tamima with data of the City of Montreal.

To determine the NBC soil type the weighted average shear wave velocity $V_{s30}$ was calculated according to **Equation 5.2** (NRC/IRC, 2010b). For limestone of the Trenton formation $V_{s\,rock}$ = 2200 m/s, for shale of the Utica formation $V_{s\,rock}$ = 1400 m/s, and for unknown rock type $V_{s\,rock}$ = 1000 m/s was assumed. the selection of these values and of the rock type at each site was based on maps presented by (Prest and Hode Keyser, 1962)[8].

$$V_{s30} = \frac{30m}{\frac{h}{V_{s\,soil}} + \frac{30-h}{V_{s\,rock}}} \tag{5.2}$$

From the $V_{s30}$ values the NBC soil type can be estimated as shown in **Table 5.1**. Categories A and B can only be used if the distance between the foundation and the rock depth is less than 3 m, even if $V_{s30}$ is higher than 760 m/s (NRC/IRC, 2010b). **Table 5.4** shows the average results obtained. They represent soil frequencies plus and minus their standard deviation as well as upper and lower bounds for the rock depth were used. The complete data can be found in **Appendix E**. For three schools the $V_{s30}$ value was slightly above a soil class limiting value. In these cases the lower category was assumed.

[8] 12 school sites on limestone, 2 on shale and 2 unknown rock type.

**Table 5.4.** NBC soil type estimates from ambient noise data, average values

| School | $h$ [m] | $V_{s\,soil}$ [m/s] | $V_{s30}$ [m/s] | NBC soil type |
|---|---|---|---|---|
| S1_A | 18.4 | 757 | 1018 | C |
| S2_CL | 13.1 | 969 | 1150 | C |
| S3_AV | 7.9 | 459 | 1097 | C |
| S4_JM | 7.9 | 118 | 389 | D |
| S5_LR | 2.6 | 351 | 1562 | B |
| S6_EM | 2.6 | 1083 | 2031 | A |
| S7_CaL | 7.9 | 104 | 330 | D |
| S8_EAO | 2.6 | 354 | 1547 | B |
| S9_R | 2.6 | 615 | 1711 | A |
| S10_JG | 7.9 | 786 | 1440 | C |
| S11_PD | 7.9 | 457 | 1100 | C |
| S12_LM | 2.6 | 794 | 1939 | A |
| S13_SE | 2.6 | 898 | 1977 | A |
| S14_MR | 13.1 | 293 | 509 | C |
| S15_DJ | 13.1 | 1902 | 1277 | C |
| S16_PT | 23.6 | 178 | 215 | D |

### 5.4. Summary

**Table 5.5** summarizes the estimated NBC soil types for all school locations from three different sources: Montreal's microzonation map, ambient noise data and geotechnical data. For the microzonation map, values in parentheses indicate alternative soil types for locations close to boundary lines. The different sources of information are in good agreement. To select the soil type for the vulnerability assessment of the schools, geotechnical data was given priority. Without this information, a conservative approach was employed, using the most penalizing condition.

In conclusion, these results show that ambient vibration tests data can be used successfully to estimate local soil conditions in cases where other sources of information are not available. However, considering that in a rapid seismic screening context resources required for each building's evaluation should be limited, it is not feasible to use this approach in a large scale seismic screening program. Key sites could be identified for the measurement of the soils natural frequency and subsequent estimation of the soil class.

**Table 5.5.** Summary of NBC soil type estimates

| School | Microzonation | Ambient Noise | Geotechnical Data | Used |
|---|---|---|---|---|
| S1_A | B (C) | C | N.A. | C |
| S2_CL | C | C | C or higher | C |
| S3_AV | B (C) | C | C or higher | C |
| S4_JM | D | D | D | D |
| S5_LR | C | B | A or B;<br>C or higher | C |
| S6_EM | B (C) | A | A or B | B |
| S7_CaL | C | D | N.A. | D |
| S8_EAO | B | B | N.A. | B |
| S9_R | B | A | A or B | B |
| S10_JG | C (B) | C | N.A. | C |
| S11_PD | C (D) | C | N.A. | C |
| S12_LM | C (B) | A | A or B | B |
| S13_SE | B | A | N.A. | B |
| S14_MR | B | C | N.A. | C |
| S15_DJ | D (C) | C | N.A. | D |
| S16_PT | D | D | N.A. | D |

N.A.: Not available

# Chapter 6. Adapted Seismic Screening Method for School Buildings

The proposed adapted rapid seismic screening method is a score assignment procedure, that can also be classified as a predicted vulnerability method, with score calculation based on the capacity spectrum method, as described in FEMA440 (ATC, 2005). Independently, some criteria were established to determine the vulnerability of heavy infill partition walls to out-of plane failure.

Basic structural hazard scores ($BSHs$) are calculated for 15 different building types, and for three seismicity levels. Score modifiers that account for features that could make a particular building more or less vulnerable are also calculated. A building's final score $S$ is given by the summation of the $BSH$ and the applicable score modifiers ($SM$) as shown in **Equation 6.1**. Limiting values of $S$ identify potentially vulnerable buildings that would require a more detailed seismic evaluation. The procedure is similar to the one followed in FEMA154. In this chapter, the details of the calculation are given. For the practical application of the method, please refer to **Chapter 7**.

$$S = BSH + \sum_i SM_i \tag{6.1}$$

## 6.1. General Procedure for the Calculation of the $BSH$ and Score Modifiers

A $BSH$ is calculated for each building type and each seismicity region, and is defined as the negative of the decimal logarithm of the probability of collapse of the building, given a ground motion corresponding to the maximum considered earthquake, $P(collapse\ given\ MCE)$, as shown in **Equation 2.3**, repeated here as **Equation 6.2**.

$$BSH = -log_{10}[P(collapse\ given\ MCE)] \tag{6.2}$$

To solve **Equation 6.2**, first the spectral displacement ($dpi$) is determined using the capacity spectrum method as described in FEMA440 (ATC, 2005), see details in

**Section 2.4**. The probability of a building type to be in a complete damage state, $P(complete|dpi)$, is then determined from the fragility curves using $dpi$ as input. Finally, the probability of collapse is defined as $P(complete|dpi)$ times the estimated fraction of the buildings in complete damage state that are expected to collapse in similar conditions:

$$P(collapse\ given\ MCE) = P(complete|dpi) \cdot collapse\ rate \tag{6.3}$$

This procedure is described in the flow chart of **Figure 6.1** for a given building type and seismic zone, and was implemented in MATLAB routines.

Score modifiers for building height, construction year, structural weaknesses (irregularities in plan and elevation, deterioration and presence of short concrete columns), potential for pounding and local soil conditions were obtained. To determine the score modifier for each case, first interim scores were calculated following the same procedure as for the *BSHs*, the only difference being that the input capacity and/or acceleration spectra were modified to consider the desired feature. For example, to consider different soil types, the acceleration spectrum was affected by the appropriate soil amplification factors. The score modifier was then obtained by subtracting the interim scores from the corresponding *BSH*.

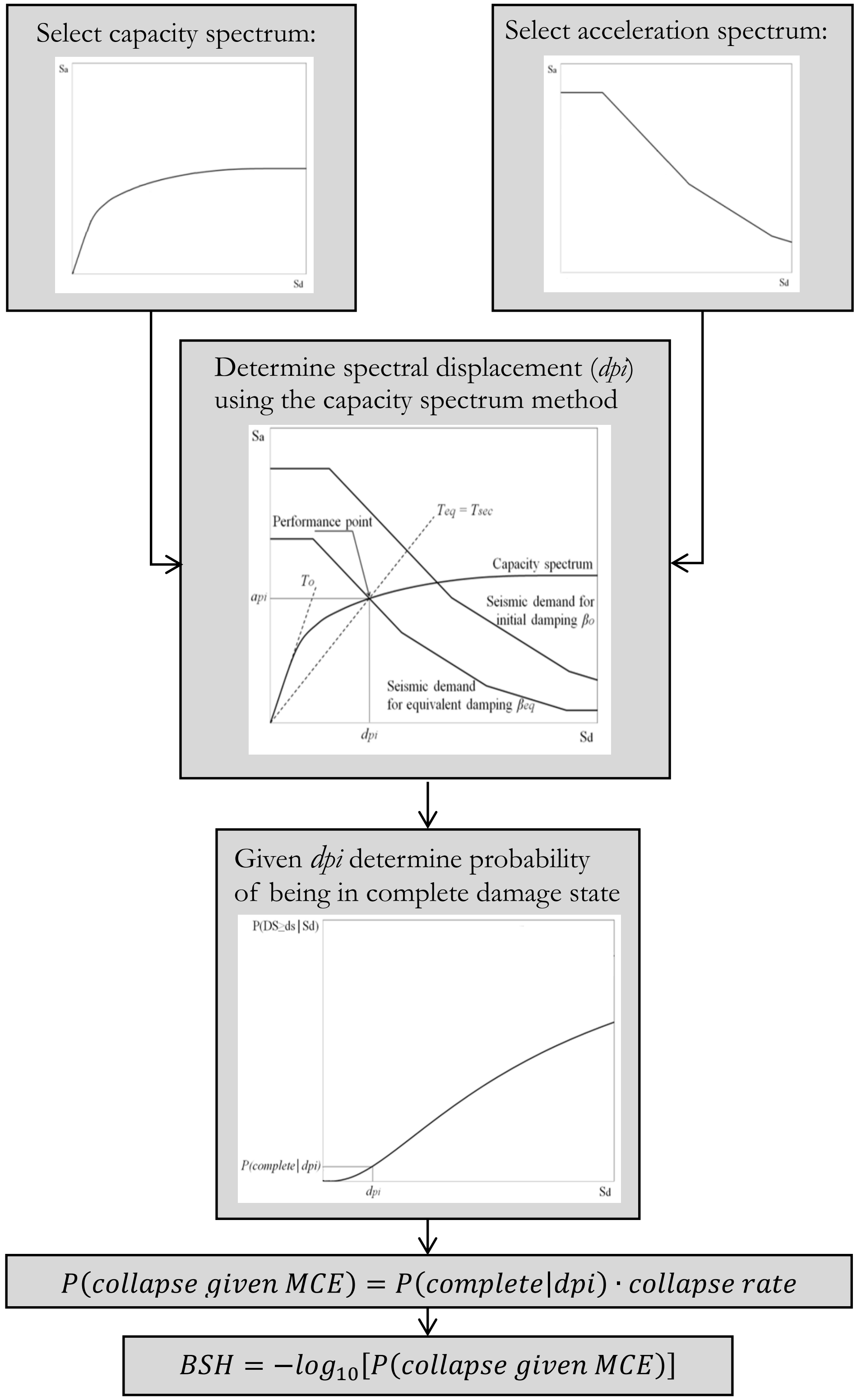


**Figure 6.1.** Determination of the *BSH* for a given building type and seismic zone

## 6.2. Lateral Load Resisting Systems (LLRSs) Classification and Descriptors

The classification of lateral load resisting systems in 15 building types of NRC92 was retained, see **Table 6.1**. This classification is also used in FEMA154, and is deemed appropriate for the Canadian context with some limited exceptions, as for example old cut-stone masonry buildings. Each model building type is described by capacity curves, fragility curves and collapse rates, values for them are given in **Appendix F**. These were taken from *Hazus-MH MR4 Technical Manual* (NIBS, 2003), and the reader is referred to this document for a detailed description of the procedure to determine them. Most of these curves have been deemed appropriate for their application in Québec and have been used to evaluate seismic vulnerability of buildings in the province (Karbassi and Nollet, 2008). However, to assess if the these curves are appropriate to describe school buildings in Québec, fundamental periods obtained from ambient vibration measurements were compared to the linear elastic part of the capacity curves with good agreement, see **Chapter 4** for details. It must be noted that the inelastic portion of the curves was not subjected to any evaluation.

**Table 6.1.** Building types, adapted from (NRC/IRC, 1992) and (ATC, 2002a)

| Type (NRC92) | FEMA154 Denomination | Description |
|---|---|---|
| WLF | W1 | Wood light frame |
| WPB | W2 | Wood, post and beam |
| SMF | S1 | Steel moment resisting frame |
| SBF | S2 | Steel braced frame |
| SLF | S3 | Steel light frame |
| SCW | S4 | Steel frame with concrete shear walls |
| SIW | S5 | Steel frame with infill masonry shear walls |
| CMF | C1 | Concrete moment resisting frame |
| CSW | C2 | Concrete shear walls |
| CIW | C3 | Concrete frame with infill masonry shear walls |
| PCW | PC1 | Precast concrete walls |
| PCF | PC2 | Precast concrete frame |
| RML | RM1 | Reinforced masonry bearing walls with wood or metal deck floors or roofs |
| RMC | RM2 | Reinforced masonry bearing walls with concrete diaphragms |
| URM | URM | Unreinforced masonry bearing walls |

The capacity curves are defined in terms of two control points, the yield and the ultimate capacity. A sample capacity curve can be seen in **Figure 6.2**, presented in acceleration-displacement response spectrum format as required by the capacity spectrum method. Up to the yield point the structure remains elastic. Note that the yield point reflects the true lateral strength of the building, rather than the nominal strength of the design capacity. The ultimate strength control marks the point where the building reaches the fully plastic behaviour.

Sets of capacity and fragility curves identified as High-Code, Moderate-Code, Low-Code and Pre-Code capture the variability of strength and ductility for each LLRS type. They represent an average building conceived based on modern code standards (as for example the 1976 Uniform Building Code (UBC) or the 1985 NEHRP provisions), but designed for different UBC seismic zones. **Table 6.2** shows the approximate basis and the expected performance for the different seismic design levels. For most of the LLRSs there are also different curves for different building heights.

**Table 6.2.** Approximate basis for seismic design levels, adapted from (NIBS, 2003)

| Seismic design level | Expected performance | Seismic Zone (UBC) |
|---|---|---|
| High-Code | High strength<br>High ductility | 4 |
| Moderate-Code | Moderate Strength<br>Moderate Ductility | 2B |
| Low-Code | Low Strength<br>Low Ductility | 1 |
| Pre-Code | Minimal Strength<br>Minimal Ductility | 0 |

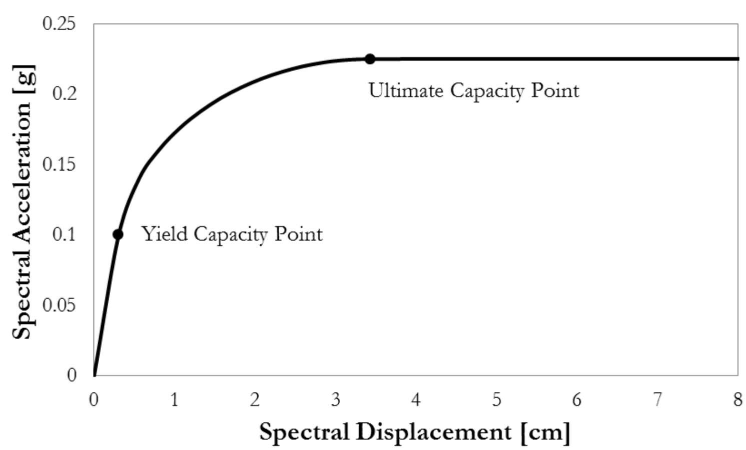


**Figure 6.2.** Sample capacity curve in acceleration-displacement response spectrum format (low-rise, low-code CIW building)

Fragility curves describe the probability of exceeding slight, moderate, extensive and complete damage given a spectral displacement, for each LLRS model building type. For the calculation of the proposed scores, only the complete damage state curves were used. They are modeled as a cumulative lognormal distribution and are defined in terms of the median and the lognormal standard deviation. Given a spectral displacement response, $S_d$, the probability of reaching or exceeding complete damage state is given by **Equation 6.4**.

$$P(ds|S_d) = \Phi\left[\frac{1}{\beta_{ds}} \cdot ln\left(\frac{S_d}{\bar{S}_{d,cds}}\right)\right] \tag{6.4}$$

where:

$\Phi$: standard normal cumulative distribution function,

$\beta_{ds}$: standard deviation of the natural logarithm of spectral displacement of complete damage state $cds$, and

$\bar{S}_{d,cds}$: median value of spectral displacement at which the building reaches the threshold of complete damage state $cds$.

A sample fragility curve is presented in **Figure 6.3**. In this figure, $\bar{S} = 16cm$ represents the median value for the selected example, $S_+$ represents the +1 standard deviation level of the fragility curve calculated as $S_+ = \bar{S} \cdot \exp(\beta_{ds}) = 39.8cm$ , and $S_-$ represents the -1 standard deviation level of the fragility curve calculated as $S_- = \bar{S}/\exp(\beta_{ds}) = 6.4cm$ . The corresponding probabilities of being in or exceeding the complete damage state are:

$$P(complete|S_- = 6.4cm) = 0.16$$

$$P(complete|\bar{S} = 16cm) = 0.50$$

$$P(complete|S_+ = 39.8cm\ ) = 0.84$$

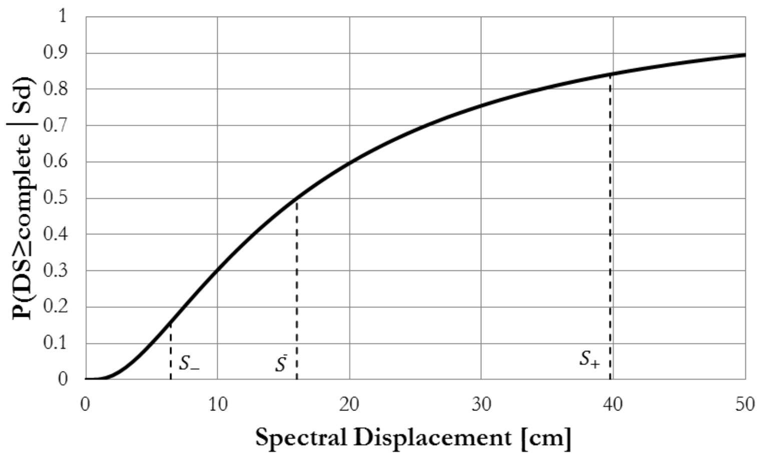


**Figure 6.3.** Sample complete damage state fragility curve (low-rise, low-code CIW building)

## 6.3. Selection of the Seismic Design Level and Benchmark Years

For a given building type, the proposed capacity and fragility curves consider the variability of strength and ductility due to the target seismicity used in the design, but ignore the fact that older buildings, conceived under less stringent building codes, will behave poorly compared to modern buildings. However, the behaviour of these buildings can be captured by assigning them a lower seismic design level. For example, an older building located in a moderate seismic zone can be considered Low-Code or even Pre-Code, if built before any seismic provisions were enforced. Therefore the selection of the appropriate building characterization will be dependent on two factors: the seismicity and the age of the building, related to the seismic provision used in design.

Some guidance is provided in (NIBS, 2003) on how to select appropriate damage functions for the United States. Two benchmark years are defined, 1975 and 1941, although it is cautioned that they are very approximate. In regions of low or moderate seismicity, where seismic codes have not been enforced, these years should be revised.

An example on how buildings are categorised for their seismic screening based on their age and seismicity is given by FEMA154, where the same capacity and fragility curves described above are used. The process is simplified by defining only three seismic zones for the entire US territory: high, moderate and low seismicity. The proposed seismic design levels are presented in **Table 6.3**. The user is asked to define two significant dates: the year when seismic provisions were first adopted and enforced (Pre-Code) and the year when these seismic provisions were significantly updated (Post-Benchmark)[9]. If these parameters are unknown to the user, it is suggested that 1941 is used as Pre-Code year for all LLRS types, except for tilt-up construction, where 1973 is recommended. Post-Benchmark years are proposed based on several seismic design provisions, as the International Conference of Building Officials Uniform Building Code or the National Earthquake Reduction Program FEMA302 Recommended Provisions for the Development of Seismic Regulations for New Buildings. The user is asked to select the appropriate Post-Benchmark years based on the code applied in the jurisdiction where the evaluated buildings are located. Suggested values vary according to the LLRS, and are between 1976 and 1993.

**Table 6.3.** Damage functions as used by FEMA154 (ATC, 2002b)

| Seismicity | Post-Benchmark | | Pre-Code |
|---|---|---|---|
| High | High-Code | Moderate-Code | Pre-Code* |
| Moderate | Moderate-Code | Low-Code | Pre-Code* |
| Low | Low-Code | Pre-Code* | Pre-Code* |

* WLF building type: Low-Code

### *6.3.1. Seismic Design Provisions in Canada*

In Canada, a model national building code, developed by the National Research Council of Canada, is updated approximately every five years. A comprehensive description of the evolution of the seismic provisions of the code was recently done by Mitchell et al (Mitchell et al., 2010). The treatment of seismicity and ductility requirements is briefly discussed in the following paragraphs, since these were identified as key parameters for the selection of benchmark years for Eastern Canada.

[9] For low seismicity regions, the Pre-Code category is not applicable, and the Post-Benchmark refers to the year when seismic codes were first introduced.

Seismic provisions appeared in the appendix of the National Building Code of Canada (NBC) for the first time in 1941, with the lateral force dependant on the soil's bearing capacity and the building's weight. The first seismic zoning map was introduced in 1953. This qualitative map provided four zones of relative seismic intensity. Most of Québec's territory was deemed aseismic, but the Saint Lawrence and Ottawa Rivers valleys were classified as the highest seismic zone (zone 3, also assigned to parts of British Columbia). This seismic zoning remained unchanged until 1970, when the first probabilistic map was presented, giving accelerations with a 100 year return period. On this map virtually the entire province of Québec was considered seismically active (although Montréal's seismic zone was reduced). The seismic maps only changed again in 1985, when seven distinct seismic zones were introduced, giving accelerations and velocities with a probability of exceedance of 10% in 50 years (475 years return period). The latest Canadian seismicity provisions use the uniform hazard spectrum approach, and appeared in 2005 and were slightly modified in 2010. Spectral accelerations with a probability of exceedance of 2% in 50 years (2475 years return period) are presented for specific locations in Canada. These values assume stiff soil (class C) and 5% viscous damping.

The importance of the LLRS was first indirectly acknowledged in the 1965 NBC, where a type of construction factor ($C$) was introduced in the calculation of the minimum seismic shear force. For ductile moment resisting frames and concrete shear walls $C$=0.75, for all other structures $C$=1.25. From 1970 to 1985, the type of construction factor was renamed ($K$), and more construction types were added with values ranging between 0.67 and 2.0. Only in 1990 a factor that directly accounts for the ductility of the LLRS appeared ($R$). This seismic force reduction factor was defined as the capacity of the structure to dissipate energy in the inelastic range, and took values between 1 and 4. It was also the first time clear design and detailing requirements for ductile structures were stipulated in the CSA Standards related to steel and reinforced concrete structural design.

### *6.3.2. Selected Benchmark Years for Seismic Screening in Eastern Canada*

Seismic design levels and damage functions for the seismic screening were chosen based on the seismicity and year of construction as shown in **Table 6.4**. It was deemed that historically the design practices for moderate and high seismic zones in the province are comparable.

**Table 6.4.** Damage functions for seismic screening in Eastern Canada

| **Seismicity*** | **Post-Benchmark (1990)** | | **Pre-Code (1970)** |
|---|---|---|---|
| Moderate and High | Moderate-Code | Low-Code | Pre-Code** |
| Low | Low-Code | Pre-Code** | Pre-Code** |

* See **Section 6.4** for definition of the seismicity regions

** WLF: Low code

Benchmark years were selected based on the seismic provisions evolution, related to NBC release dates[10]. This process is partially judgemental, and several experienced structural engineers where consulted. In case of differences in opinion, a conservative approach with later benchmark years was preferred.

1970 was chosen as the Pre-Code year for all LLRSs mainly based on the introduction of the first probabilistic seismic zoning map. The 1953 NBC was disregarded because of the qualitative nature of the seismic map and the abrupt changes in zones in Eastern Canada, with a boundary between highest and zero seismicity. 1970 was also the first time where the period of the structure was considered in the calculation of the lateral seismic force.

The Post-Benchmark year was defined as 1990, based mainly on the improvement in ductility requirements in the structural steel and reinforced concrete standards. This was the first year the ductility factor *R* appeared. Although some ductility requirements were already included in earlier editions of the code, only in 1990 a clear link between the NBC and the CSA materials standards was made, assuring that the ductility required by the NBC was effectively achieved in practice. The seismic

[10] This model code has to be adopted by provincial authorities to be legally enforced, sometimes with a delay of several years. However, it is common practice of structural engineers to design according to the latest edition NBC as soon as it is released.

zoning had also been updated in 1985 increasing the return period of the maximum design earthquake from 100 to 475 years.

It can be argued that the Post-Benchmark year can be further refined by LLRS type. For ductile concrete moment frame structures, for example, design and detailing provisions were introduced as early as in the 1977 CSA standard. One uniform date was preferred for simplicity, considering that the Post-Benchmark year has low significance in the screening process of schools in Québec. According to a school inventory report from the Québec Ministry of Education, around 75% of them were constructed prior to 1970 (Chagnon, 2006), and therefore belong to the Pre-Code damage functions.

## 6.4. Seismic Zoning and Spectral Acceleration Values

Since it is not feasible to calculate the *BSHs* and score modifiers for the spectral accelerations of all the province's school locations, different seismic zones were introduced. FEMA154 follows the same procedure, and proposes limiting values to define low, moderate and high seismicity regions based on FEMA310, as repeated here in **Table 6.5**. The use of these same zones in Québec is questionable especially due to a 2/3 reduction factor of the spectral acceleration used in the United States but not in Canada. There are also other concerns in relation to the distribution of seismicity and population in the province that would make such a classification irrelevant. Therefore a new criterion and limiting values are proposed.

**Table 6.5.** Criteria specifying seismicity regions of United States based on spectral acceleration values used in FEMA154 (ATC, 2002b)

| Region of Seismicity | Sa(0.2s) | Sa(1.0) |
|---|---|---|
| Low | < 0.167g | < 0.067g |
| Moderate | 0.167g to 0.500g | 0.067g to 0.200g |
| High | ≥ 0.500g | ≥ 0.200g |

### *6.4.1. Classification of the Seismic Zones of Québec*

In Canada, spectral hazard of a specific site is determined based on spectral acceleration (Sa) values with 2% probability in 50 years, given for 0.2, 0.5, 1.0 and

2.0s, Sa(0.2s), Sa(0.5s), Sa(1.0s) and Sa(2.0s). Usually both Sa(0.2s) and Sa(1.0s) are used to characterize a site's seismic hazard, so that ratio between the short and long period response is considered. This is relevant when comparing seismicity in eastern and western Canada, since in western Canada the drop in the spectral acceleration with period is steeper than in western Canada (typical ratios of Sa(0.2)/Sa(1.0) in Eastern Canada are in the order of 4 to 5, for Western Canada they are in the order of 2 to 3).

School buildings are typically low-rise structures, and therefore only short and intermediate period responses should be influential when evaluating their response. More specifically, when applying the capacity spectrum method the most relevant Sa value should be the one closest to the effective period of the structure. Note that the effective period will depend on the capacity and seismic demand spectra and therefore involve a variety of factors, as for example the LLRS type, seismic design level, magnitude of input spectral accelerations and soil amplification factors. From the analysis of a large number of cases it was determined that effective period values are typically between 0.5 and 0.7s. It follows that Sa(0.5s) should be most relevant when applying the capacity spectrum method.

To prove this affirmation, spectral accelerations of the 2010 NBC for 10 locations across the province were selected, covering the entire magnitude range[11]. For each location, *BSHs* were calculated for all 15 building types, assuming the low-code seismic performance level; the results are plotted against the sites spectral acceleration values at different periods, in **Figure 6.4**. Here average *BSHs* for all building types are presented against spectral acceleration at different periods, normalized by their respective maximum value. Clearly it can be seen that Sa(0.5) correlates best with the *BSHs*. A second order polynomial trend line fits with an $R^2$ value of 0.99 (see **Figure 6.4**). Therefore this parameter was chosen to determine the seismic zoning.

---

[11] Selected locations: Rivière-du-Loup, Cap St-Ignace, Rivière-des-Roches, Québec City, Montréal, St-Paul d'Abbotsford, Granby, Sherbrooke, Manawan, and Rouyn-Noranda

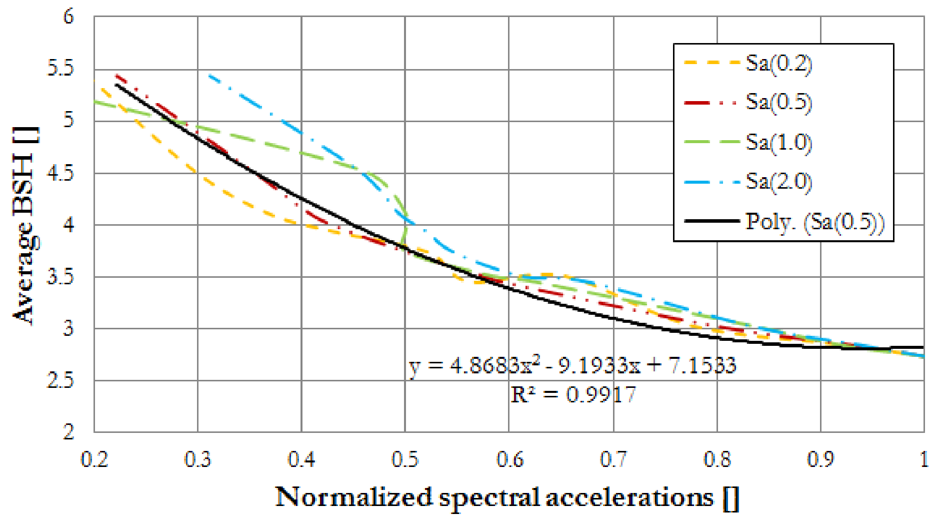


**Figure 6.4.** Average BSHs versus normalized spectral accelerations

### *6.4.2. Selection of Limiting Values for Seismic Zones*

After defining Sa(0.5) as the parameter that will determine the seismic zone, limiting values need to be selected. The seismic zonation should comply with two conditions. First, the different categories should be relevant given the province's particular seismic hazard distribution and it's relation to the demographics. Second, variation of *BSHs* for a given bracket of spectral acceleration values should be limited.

Seismic hazard in Québec is extremely varied as can be seen from the Canadian seismic hazard map presented in **Figure 6.5**. The northern region, covering most of the province's territory, has a very low seismicity. The Saint Lawrence and Ottawa Valley regions to the south are the province's most active seismic zones, with a seismicity that can be considered moderate. They are the province's most densely populated area as well. A very small area is highly active in the Charlevoix region. La Malbaie, located in this zone, is the municipality with highest seismicity in Québec and has spectral accelerations even higher than those of Vancouver or Victoria. Luckily this area is sparsely populated.

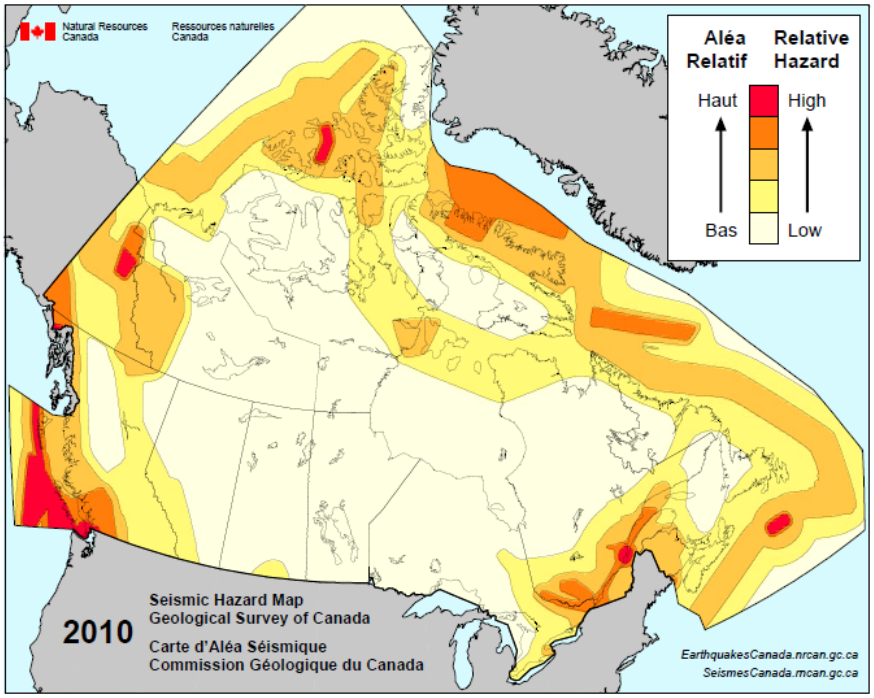


**Figure 6.5.** Simplified seismic hazard map of Canada (NRC, 2010)

Based on statistical data of the Canadian census of 2006, the population distribution for different seismicity levels was defined and results are summarized in **Figure 6.6**. Sa(0.5s) for all cities with a population over 10.000 were determined, covering 75% of the province's total population. It is noteworthy that in Québec, 80% of the population lives in urban or suburban areas. Montréal, the province's largest city, comprises more than 20% of the province's total inhabitants. This and the fact that most of the population lives to the south of the province explains that 83% of the sampled population lives in areas with Sa(0.5s) values between 0.30 and 0.35.

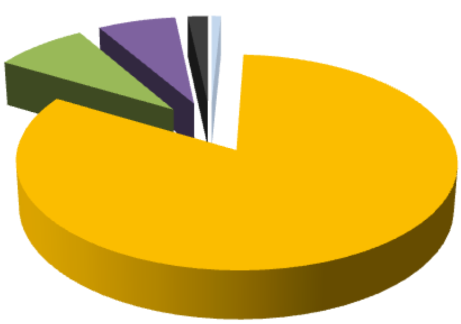

| | |
|---|---|
| Sa(0.5s) > 0.35g | 0.8% |
| 0.30g ≤ Sa(0.5s) < 0.35g | 82.8% |
| 0.25g ≤ Sa(0.5s) < 0.30g | 8.0% |
| 0.20g ≤ Sa(0.5s) < 0.25g | 6.7% |
| Sa(0.5s) < 0.25g | 1.7% |

**Figure 6.6.** Québec's population distribution by Sa(0.5s) values

To determine the effect of the selection of seismicity limits on the *BSHs*, these scores were calculated for each category of **Figure 6.6**, for low-code and pre-code building types. To determine the Sa values to use for each bracket, weighted mean values with respect to the population were calculated. The averaged *BSHs* are presented in **Table 6.6**.

**Table 6.6.** Average *BSHs* calculated for different seismicity levels

| Sa(0.5) [g] | Population[%] | Average *BSH* Low-Code | Average *BSH* Pre-Code |
|---|---|---|---|
| > 0.35 | 0.8 | 3.0 | 2.7 |
| 0.30 – 0.35 | 82.8 | 3.5 | 3.2 |
| 0.25 – 0.30 | 8.0 | 3.6 | 3.3 |
| 0.20 – 0.25 | 6.7 | 3.8 | 3.5 |
| < 0.20 | 1.7 | 5.3 | 4.8 |

### *6.4.3. Seismic Zoning and Spectral Acceleration Values Used*

Based on the findings presented in **Table 6.6**, Sa values in **Table 6.7** were grouped in three seismic zones, using Sa(0.5) as a reference to define seismicity for low-rise school buildings. To calculate the Sa values used for each seismicity region, the weighted mean values with respect to the population were used. Results are presented in **Table 6.8** and **Figure 6.7**.

**Table 6.7.** Seismic zones for seismic screening in Québec

| Seismicity | Sa(0.5) [g] | Population [%] |
|---|---|---|
| High | > 0.35 | 0.8 |
| Moderate | 0.25 – 0.35 | 90.8 |
| Low | < 0.25 | 8.4 |

**Table 6.8.** Spectral acceleration values for each seismic zone

| Seismicity | Sa(0.2) [g] | Sa(0.5) [g] | Sa(1.0) [g] | Sa(2.0) [g] |
|---|---|---|---|---|
| High | 0.79 | 0.45 | 0.20 | 0.07 |
| Moderate | 0.62 | 0.30 | 0.14 | 0.05 |
| Low | 0.55 | 0.13 | 0.06 | 0.03 |

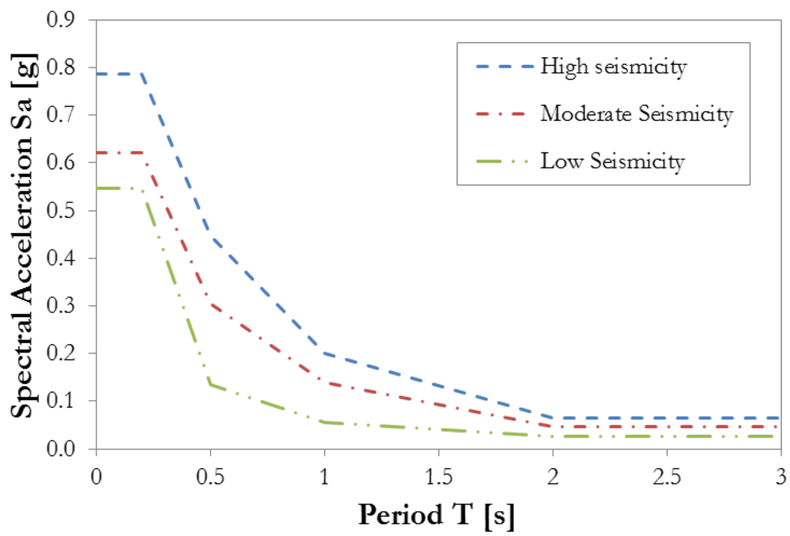


**Figure 6.7.** Spectral acceleration values for each seismic zone

### 6.5. Basic Structural Hazard Scores

To calculate the *BSHs*, soil type C (reference soil) and capacity curves for low rise buildings were used. For the selection of the capacity curves, seismic design levels for buildings constructed between 1970 and 1990 were considered, corresponding to low-code for moderate and high seismicity, and pre-code for low seismicity (see **Table 6.4**). Initial damping was assumed to be 5% for all cases. Having 15 building types and three seismic zones, these calculations yield 45 *BSHs*. These are given in **Table 6.9**.

**Table 6.9.** Basic structural hazard (*BSH*) scores

| | Seismic Zone | | |
|---|---|---|---|
| **Type** | **Low** | **Moderate** | **High** |
| WLF | 5.2 | 4.3 | 3.7 |
| WPB | 5.7 | 4.7 | 4.1 |
| SMF | 4.7 | 3.2 | 2.8 |
| SBF | 4.7 | 3.7 | 3.2 |
| SLF | 4.6 | 3.6 | 3.1 |
| SCW | 4.6 | 3.7 | 3.1 |
| SIW | 4.4 | 3.5 | 3.0 |
| CMF | 4.3 | 3.3 | 2.7 |
| CSW | 4.6 | 3.6 | 3.0 |
| CIW | 4.0 | 3.1 | 2.6 |
| PCW | 4.3 | 3.2 | 2.7 |
| PCF | 3.5 | 3.3 | 2.6 |
| RML | 4.2 | 3.6 | 3.0 |
| RMC | 4.3 | 3.7 | 3.0 |
| URM | 2.6 | 2.5 | 2.1 |

## 6.6. Score Modifier Values

### *6.6.1. Building Height*

Although for most building types capacity and fragility curves for mid- and high-rise buildings are available, score modifiers were only calculated for mid-rise buildings because of the inexistence of high-rise schools. Interim scores were therefore calculated with the provided capacity and fragility curves for mid-rise buildings where applicable, keeping the same seismic design level. The acceleration spectra used were the same as for the *BSHs*. As mentioned before, the score modifiers are the difference between these interim scores and the *BSHs*. The 45 calculated score modifiers for mid-rise buildings are presented in **Table 6.10**.

**Table 6.10.** Score modifiers for mid-rise buildings

| | Seismic Zone | | |
|---|---|---|---|
| **Type** | **Low** | **Moderate** | **High** |
| WLF | N/A | N/A | N/A |
| WPB | N/A | N/A | N/A |
| SMF | 0.4 | 0.3 | -0.3 |
| SBF | 0.0 | -0.1 | -0.2 |
| SLF | N/A | N/A | N/A |
| SCW | 0.2 | 0.0 | 0.0 |
| SIW | 0.1 | 0.0 | -0.1 |
| CMF | 0.2 | 0.1 | -0.1 |
| CSW | 0.1 | 0.0 | 0.0 |
| CIW | 0.0 | 0.0 | 0.1 |
| PCW | N/A | N/A | N/A |
| PCF | 0.1 | 0.1 | -0.1 |
| RML | 0.0 | -0.1 | 0.3 |
| RMC | 0.0 | -0.1 | 0.2 |
| URM | 0.4 | 0.5 | 1.5 |

### *6.6.2. Construction Year*

Two sets of score modifiers were calculated to consider the construction year: pre-code and post-benchmark, as presented in **Table 6.11**. To calculate the interim scores, the same input parameters as for the *BSHs* were used, only modifying the seismic design level as specified in **Table 6.4**. For moderate and high seismicity, post-benchmark interim scores were calculated assuming a moderate-code seismic design level and pre-code interim scores were obtained using the pre-code seismic design level. For low seismicity, post-benchmark interim scores consider a low-code design level, and pre-code interim scores are not applicable. Pre-code score modifier values for moderate seismicity CMF and CWI were modified based on judgement from -0.3 to -1.0, as suggested by (ATC, 2002b). This reflects the poor expected performance of older concrete frame type buildings.

**Table 6.11.** Score modifiers for pre-code and post-benchmark buildings

| Type | Pre-Code | | | Post-Benchmark | | |
|---|---|---|---|---|---|---|
| | Low Seismicity | Moderate Seismicity | High Seismicity | Low Seismicity | Moderate Seismicity | High Seismicity |
| WLF | N/A | 0.0 | 0.0 | 0.0 | 0.0 | 0.0 |
| WPB | N/A | -0.3 | -0.3 | 0.4 | 0.6 | 0.5 |
| SMF | N/A | 0.0 | 0.0 | 0.0 | 1.1 | 0.8 |
| SBF | N/A | -0.3 | -0.3 | 0.4 | 0.7 | 0.6 |
| SLF | N/A | -0.3 | -0.2 | 0.3 | 0.5 | 0.4 |
| SCW | N/A | -0.3 | -0.3 | 0.4 | 0.7 | 0.6 |
| SIW | N/A | -0.3 | -0.3 | 0.4 | N/A | N/A |
| CMF | N/A | -1.0* | -0.3 | 0.4 | 0.8 | 0.6 |
| CSW | N/A | -0.3 | -0.2 | 0.3 | 0.9 | 0.8 |
| CIW | N/A | -1.0* | -0.3 | 0.4 | N/A | N/A |
| PCW | N/A | -0.6 | -0.4 | 0.8 | 0.0 | 0.0 |
| PCF | N/A | -0.2 | -0.2 | 0.2 | 0.9 | 0.7 |
| RML | N/A | -0.4 | -0.3 | 0.5 | 0.2 | 0.4 |
| RMC | N/A | -0.4 | -0.3 | 0.5 | 0.2 | 0.4 |
| URM | N/A | -0.4 | -0.3 | 0.5 | N/A | N/A |

*: values modified based on judgement.

### *6.6.3. Structural weaknesses*

Major changes were introduced in the treatment of irregularities and other features that could affect seismic performance when compared to the FEMA154 procedure, now called structural weaknesses as a more general term. Four separate types were considered: horizontal irregularities, vertical irregularities, deterioration and short concrete columns. Although organized differently than the NRC92 guidelines, where the irregularities are categorized in 7 classes, all the potential weaknesses considered in the NRC92 method are also present in the adapted method. Horizontal irregularities were subdivided into re-entrant corners, asymmetric stairways, asymmetric partition walls, torsion in the lateral load resisting system, diaphragm discontinuity, out of plane offset and others. Vertical irregularities were classified as steps in elevation view, soft storey, building on sloping terrain, change in structural type, and others. These categories were determined to be more likely to occur in school buildings, based on the findings of the initial evaluation exposed in **Chapter 3**, complemented with results of other studies for schools.

The effect of each type of structural weakness on the seismic performance was classified as severe, significant or insignificant, as done as well in the seismic screening method developed by New Zealand Society for Earthquake Engineering, NZSEE (NZSEE, 2006). A chart was developed for the final user to provide guidance on the selection of the severity of the structural weaknesses. The chart was developed by thorough examination of information on irregularities in different building codes and other documents, and reference to these documents is provided. An example of the chart is presented in **Table 6.12**, the complete guide can be found in **Chapter 7**.

**Table 6.12.** Example on the guidance to the selection of the severity of structural weaknesses

<table>
<tr><th rowspan="2">Structural weakness</th><th colspan="3">Effect on seismic performance</th></tr>
<tr><th>Insignificant</th><th>Significant</th><th>Severe</th></tr>
<tr><td rowspan="2">Steps in elevation view</td>
<td>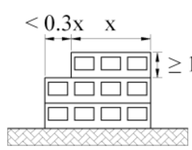
</td>
<td>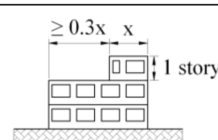
</td>
<td>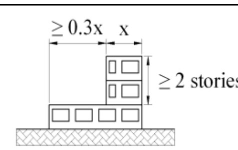
</td></tr>
<tr><td>Horizontal dimension of any storey is less than 130% of that in an adjacent storey.<br>One storey penthouses with less than 10% the weight of the level below (NRC/IRC, 2010a).</td>
<td>Horizontal dimension of any storey is more than 130% of that in an adjacent storey (NRC/IRC, 2010a).</td>
<td>Horizontal dimension of any storey is more than 130% of that in an adjacent storey (NRC/IRC, 2010a) and height above setbacks is at least 2 storeys (McConnell, 2007).</td></tr>
</table>

To account for the effect of the structural weaknesses in a simple manner as needed for seismic screening is not an easy task because the possible defects are so varied, and many parameters influence the building's response. The selected approach was adapted from FEMA154's treatment of horizontal irregularities, characterizing the structural weaknesses as an increase of the spectral acceleration values in the calculation of the interim score. To study the effect that this increase will have on the score modifiers and select appropriate increase levels, the spectral accelerations were augmented up to four times, in increases of 10%, and the score modifiers were calculated for all building types. The spectral accelerations considered were those of the moderate seismic zone, since it is representative of the majority of schools in Québec. Results are presented in **Figure 6.8**.

In **Figure 6.8** the selected increases of spectral acceleration values are marked with vertical lines. Significant irregularity modifiers were calculated based on 150% spectral acceleration values, as proposed for horizontal irregularities in FEMA154. For severe irregularities an increase of 350% was used, so that the average values of the modification factors would be the same as the average of the vertical irregularity modifiers of FEMA154, considered the most severe type of irregularity. This implies that the final scores will be below or close to the cut-off score of 2 if only this score modifier is applicable to a certain building.

The approach was deemed to be consistent with the NZSEE screening method, although the comparison is difficult because of the difference in procedures. In the NZSEE method, the building score is given as the percentage of resistance of a similar building constructed to current standards. Buildings with scores over 67% are deemed to be adequate. For scores between 33% and 67%, buildings are deemed at earthquake risk, and further mitigation actions are recommended. Buildings with scores under 33% are classified as potentially earthquake damage prone, and mitigation actions are mandatory by law. Severe and significant structural weaknesses are considered by reducing the score to 40% and 70% of its original value. Therefore it can be concluded that a building where no other factors are considered, will not be deemed earthquake prone by a significant weakness, but only by a severe one. Similarly, in the adapted method proposed here, the majority of building types will have a score below 2 (considered the cut-off score by FEMA154) only for a severe weakness for high and moderate seismicity. The average percentages of reduction in the scores for these two seismicity cases are 50% and 80% for significant and severe weaknesses, also similar to the values proposed by the NZSEE.

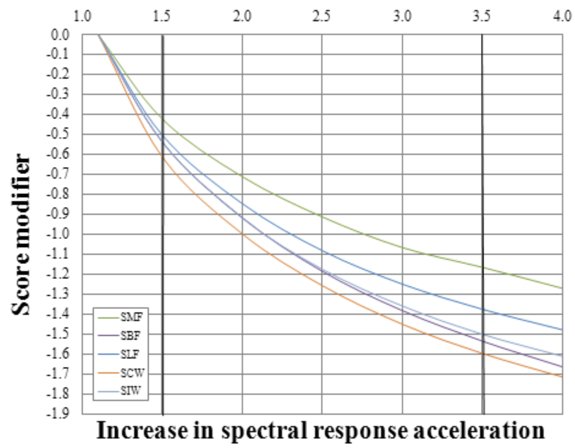


a. Steel structures

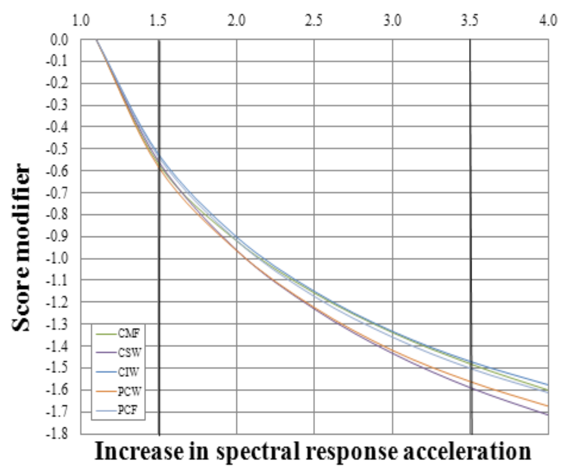


b. Concrete structures

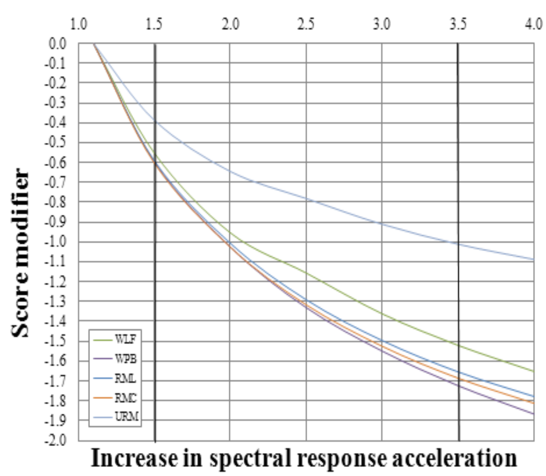


c. Wood and masonry structures

**Figure 6.8.** Effect on the score modifier by the increase of the spectral acceleration values

The calculated score modifiers for significant and severe structural weaknesses are presented in **Table 6.13**. Note that for insignificant weaknesses the *BSH* will not be affected.

**Table 6.13.** Score modifiers for significant and severe structural weaknesses

| Type | Significant Weakness (1.5Sa) | | | Severe Weakness (3.5Sa) | | |
|---|---|---|---|---|---|---|
| | Low Seismicity | Moderate Seismicity | High Seismicity | Low Seismicity | Moderate Seismicity | High Seismicity |
| WLF | -0.6 | -0.6 | -0.6 | -1.5 | -1.6 | -1.5 |
| WPB | -0.6 | -0.6 | -0.6 | -1.9 | -1.8 | -1.6 |
| SMF | -0.7 | -0.4 | -0.4 | -1.8 | -1.2 | -1.0 |
| SBF | -0.5 | -0.6 | -0.6 | -1.7 | -1.6 | -1.4 |
| SLF | -0.5 | -0.5 | -0.5 | -1.7 | -1.5 | -1.2 |
| SCW | -0.5 | -0.7 | -0.6 | -1.8 | -1.7 | -1.4 |
| SIW | -0.5 | -0.6 | -0.6 | -1.7 | -1.6 | -1.4 |
| CMF | -0.7 | -0.6 | -0.5 | -1.8 | -1.6 | -1.3 |
| CSW | -0.5 | -0.6 | -0.6 | -1.8 | -1.7 | -1.5 |
| CIW | -0.5 | -0.6 | -0.6 | -1.6 | -1.6 | -1.4 |
| PCW | -0.4 | -0.7 | -0.5 | -1.4 | -1.6 | -1.4 |
| PCF | -0.5 | -0.6 | -0.6 | -1.8 | -1.7 | -1.3 |
| RML | -0.5 | -0.7 | -0.6 | -1.6 | -1.8 | -1.5 |
| RMC | -0.5 | -0.7 | -0.6 | -1.6 | -1.9 | -1.5 |
| URM | -0.3 | -0.4 | -0.4 | -0.8 | -1.1 | -0.9 |

### *6.6.4. Potential for Pounding*

Guidance for the treatment of pounding of adjacent buildings was taken from the NZSEE proposed screening method (NZSEE, 2006). Again as for structural weaknesses, the potential for pounding was classified as severe, significant or insignificant. The severity was determined by comparing the separation between buildings ($d$) to limiting values related to the building height ($h$):

$d < 0.005h$ : severe effect on seismic performance, (6.5)

$0.005h < d < 0.01h$: significant effect on seismic performance, and (6.6)

$d > 0.01h$ : insignificant effect on seismic performance. (6.7)

Furthermore two independent factors can aggravate pounding: floor misalignment and difference in height (given in number of storeys). Since school buildings are low- and mid-rise buildings, the difference in number of storeys will be limited and this factor will never be dominant. Therefore, only floor misalignment was considered. As for structural weaknesses, score modifiers were calculated based on an interim score obtained by an increased seismic demand. The amplification factors to affect the acceleration response spectrum for each case are presented in **Table 6.14**. Values used were adapted for the NZSEE method, following a similar reasoning as exposed in the previous section.

**Table 6.14.** Increase of the spectral acceleration values for calculation of score modifiers for pounding effects

| | **Effect on seismic performance** | | |
|---|---|---|---|
| | **Severe** | **Significant** | **Insignificant** |
| Vertical misalignment > 20% of storey height | 3.5Sa | 1.5Sa | 1.3Sa |
| Vertical misalignment ≤ 20% of storey height | 1.5Sa | 1.3Sa | 1.0Sa |

The calculated score modifiers for spectral acceleration increases of 150% and 350% are the same as for the structural weaknesses modifier, and can be found in **Table 6.13**. Score modifiers for 130% spectral acceleration are presented in **Table 6.15**.

**Table 6.15.** Score modifiers for pounding with 130% spectral acceleration

| | Seismic Zone | | |
|---|---|---|---|
| **Type** | **Low** | **Moderate** | **High** |
| WLF | -0.4 | -0.4 | -0.4 |
| WPB | -0.4 | -0.5 | -0.4 |
| SMF | -0.4 | -0.3 | -0.3 |
| SBF | -0.3 | -0.3 | -0.4 |
| SLF | -0.3 | -0.3 | -0.3 |
| SCW | -0.3 | -0.4 | -0.4 |
| SIW | -0.3 | -0.3 | -0.4 |
| CMF | -0.4 | -0.4 | -0.3 |
| CSW | -0.4 | -0.4 | -0.4 |
| CIW | -0.3 | -0.3 | -0.4 |
| PCW | -0.3 | -0.5 | -0.3 |
| PCF | -0.3 | -0.3 | -0.4 |
| RML | -0.3 | -0.5 | -0.4 |
| RMC | -0.4 | -0.5 | -0.4 |
| URM | -0.2 | -0.3 | -0.3 |

### *6.6.5. Local Soil Conditions*

For the proposed seismic screening method, score modifiers were calculated for soil class types A to E by applying the corresponding ground motion amplification factors for short and long periods, $F_a$ and $F_v$, to the acceleration spectra for low, moderate and high seismicity, presented in **Table 6.16**. Soil type C has no score modifier associated to it, since it is the reference soil type considered in the *BSH*. Structures located on soil type F cannot be addressed by the screening method, and should be evaluated in consultation with a geotechnical engineer experienced in earthquake engineering. The calculated score modifiers are presented in **Table 6.17** to **6.19**.

**Table 6.16.** Ground motion amplification factors

| Seismicity | Soil Type A | | Soil Type B | | Soil Type D | | Soil Type E | |
|---|---|---|---|---|---|---|---|---|
| | $F_a$ | $F_v$ | $F_a$ | $F_v$ | $F_a$ | $F_v$ | $F_a$ | $F_v$ |
| High | 0.800 | 0.500 | 0.914 | 0.700 | 1.100 | 1.299 | 1.071 | 1.999 |
| Moderate | 0.748 | 0.500 | 0.848 | 0.640 | 1.152 | 1.360 | 1.255 | 2.060 |
| Low | 0.718 | 0.500 | 0.818 | 0.600 | 1.182 | 1.400 | 1.345 | 2.100 |

**Table 6.17.** Soil score modifiers for low seismicity

| Type | Soil Type A | Soil Type B | Soil Type D | Soil Type E |
|---|---|---|---|---|
| WLF | 0.7 | 0.5 | -0.4 | -0.9 |
| WPB | 1.1 | 0.8 | -0.5 | -1.1 |
| SMF | 1.3 | 0.9 | -0.6 | -1.2 |
| SBF | 1.0 | 0.7 | -0.4 | -1.0 |
| SLF | 1.1 | 0.7 | -0.4 | -1.0 |
| SCW | 0.9 | 0.6 | -0.4 | -1.1 |
| SIW | 0.9 | 0.6 | -0.4 | -1.0 |
| CMF | 0.9 | 0.7 | -0.6 | -1.1 |
| CSW | 1.0 | 0.7 | -0.4 | -1.1 |
| CIW | 0.9 | 0.6 | -0.4 | -1.0 |
| PCW | 0.9 | 0.6 | -0.3 | -0.7 |
| PCF | 1.0 | 0.7 | -0.4 | -1.1 |
| RML | 1.0 | 0.7 | -0.4 | -0.9 |
| RMC | 1.0 | 0.7 | -0.4 | -0.9 |
| URM | 0.4 | 0.3 | -0.2 | -0.5 |

**Table 6.18.** Soil score modifiers for moderate seismicity

| Type | Soil Type A | Soil Type B | Soil Type D | Soil Type E |
|---|---|---|---|---|
| WLF | 0.8 | 0.5 | -0.4 | -1.0 |
| WPB | 1.2 | 0.9 | -0.5 | -1.1 |
| SMF | 0.9 | 0.6 | -0.3 | -0.8 |
| SBF | 1.1 | 0.8 | -0.4 | -1.0 |
| SLF | 1.1 | 0.8 | -0.4 | -0.9 |
| SCW | 1.1 | 0.8 | -0.5 | -1.1 |
| SIW | 1.1 | 0.8 | -0.4 | -1.0 |
| CMF | 1.2 | 0.7 | -0.5 | -1.0 |
| CSW | 1.1 | 0.8 | -0.4 | -1.1 |
| CIW | 1.1 | 0.8 | -0.4 | -1.0 |
| PCW | 0.9 | 0.6 | -0.5 | -1.1 |
| PCF | 1.1 | 0.8 | -0.4 | -1.0 |
| RML | 1.0 | 0.6 | -0.6 | -1.2 |
| RMC | 1.0 | 0.7 | -0.6 | -1.2 |
| URM | 0.6 | 0.4 | -0.3 | -0.7 |

**Table 6.19.** Soil score modifiers for high seismicity

| Type | Soil Type A | Soil Type B | Soil Type D | Soil Type E |
|---|---|---|---|---|
| WLF | 0.8 | 0.4 | -0.4 | -0.8 |
| WPB | 1.2 | 0.5 | -0.4 | -1.0 |
| SMF | 0.8 | 0.4 | -0.3 | -0.6 |
| SBF | 1.1 | 0.5 | -0.4 | -0.9 |
| SLF | 1.1 | 0.5 | -0.3 | -0.8 |
| SCW | 1.1 | 0.6 | -0.4 | -0.9 |
| SIW | 1.1 | 0.5 | -0.4 | -0.9 |
| CMF | 1.0 | 0.5 | -0.3 | -0.8 |
| CSW | 1.1 | 0.5 | -0.4 | -0.9 |
| CIW | 1.1 | 0.5 | -0.4 | -0.9 |
| PCW | 1.0 | 0.6 | -0.3 | -0.8 |
| PCF | 1.1 | 0.5 | -0.4 | -0.9 |
| RML | 1.1 | 0.6 | -0.4 | -0.9 |
| RMC | 1.1 | 0.6 | -0.4 | -1.0 |
| URM | 0.6 | 0.3 | -0.3 | -0.6 |

## 6.7. Out-of-Plane Failure of Heavy Infill Walls

The aim of the separate treatment of heavy infill walls is to establish the hazard for their out-of-plane failure. Note that the presence of a weak storey induced by a significant lower amount of walls in one floor compared to other floor levels, and problems related to the uneven distribution of the walls in the building's principal directions, as identified during the survey of the walls discussed in **Chapter 3**, will be addressed by the screening method by including it as a structural weakness. However, these problems will only need to be identified by a visual inspection in further schools to evaluate, since a detailed survey of masonry walls is not feasible in a rapid seismic screening context. It is also important to notice that this same limitation applies to the determination of the risk of out-of-plane failure of the walls: the information required must be relatively fast and easy to collect.

### *6.7.1. Out-of-Plane Behaviour of Unreinforced Infill Walls*

The out-of-plane behaviour of unreinforced masonry walls has not been studied with the wealth of details as their in-plane behaviour, but several studies have been conducted in recent years, see for example (Felice and Giannini, 2001, Meisl et al., 2007, Varela-Rivera et al., 2011). These tests have demonstrated that the out-of-plane behaviour of masonry walls is mainly influenced by the support conditions, aspect ratio (height over length), slenderness ratio (height over thickness), and axial load level and stiffness of the surrounding frame. More recently the out-of-plane behaviour of masonry walls has been studied in more detail for the creation of the seismic retrofit guidelines for British Columbia's schools (APEGBC and UBC, 2011). The discussion of the following paragraphs is largely adapted from the findings of this document.

Unreinforced masonry walls can be classified for the study of their out-of-plane behaviour according to their top and bottom confinement as cantilever walls and laterally supported walls (at top and bottom), if the vertical confining elements are disregarded. The laterally supported walls can further be classified into walls with inadequate or adequate connection at the top. Cantilever walls will rock out-of-plane about the base of the wall, as shown in **Figure 6.9**, and their failure mode is total collapse of the wall. Inadequately supported walls also will act as cantilever walls (see **Figure 6.10**), since the roof or the diaphragm connection at the top does not restrain the wall effectively. However, the top confining element may generate friction or surcharge forces at the top of the wall. The failure mode of this type of wall is total collapse, and can be catastrophic if the wall is load bearing. When the wall is laterally restrained effectively at top and bottom, as shown in **Figure 6.11**, the out-of-plane rocking of the wall will form a hinge approximately at mid-height of the wall. The mode of failure is similar to the one of cantilever walls with surcharge.

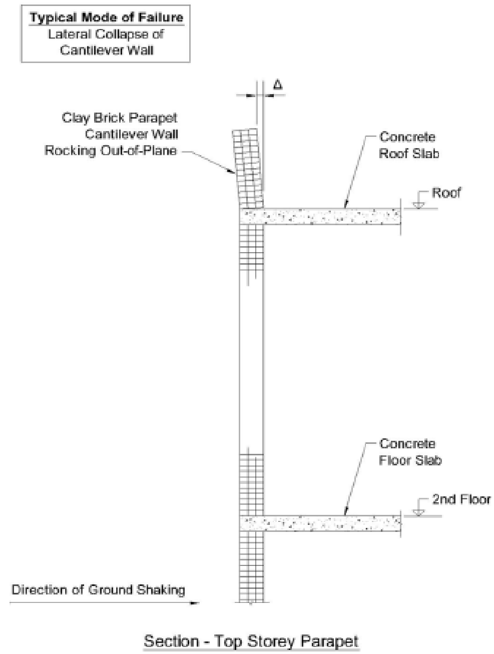


**Figure 6.9.** Out-of-plane behaviour of cantilever walls (APEGBC and UBC, 2011)

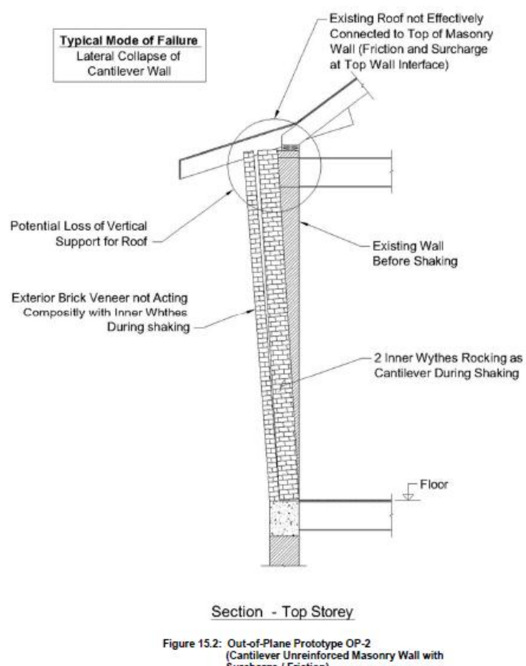


**Figure 6.10.** Out-of-plane behaviour of cantilever walls (APEGBC and UBC, 2011)

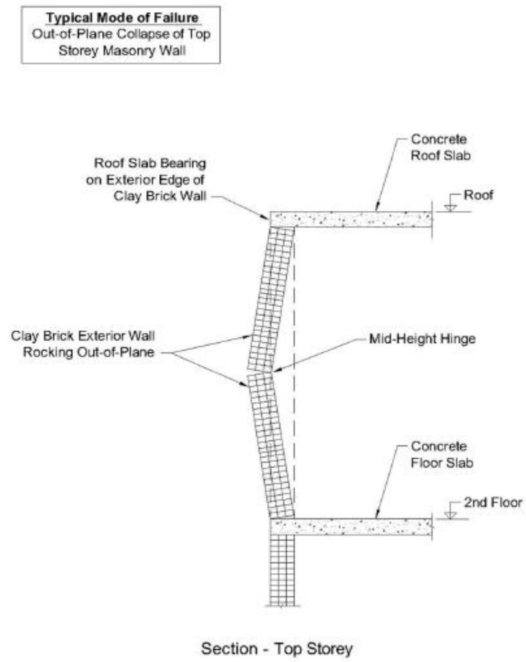


**Figure 6.11.** Out-of-plane behaviour of laterally supported walls (APEGBC and UBC, 2011)

### *6.7.2. Critical Walls to be Identified in the Screening Process*

For all the types of unreinforced walls identified above, the walls will fail out-of-plane if their lateral displacement is excessive. Establishing the probable lateral displacement is not a task simple enough to be performed in a rapid seismic screening context. There are some features however that make walls less likely to have excessive laterally displacements. Therefore it is proposed that the walls that do not conform to these features should be identified in the seismic screening context. It has been noted that walls with reasonably small slenderness ratios that are fully confined at top and bottom generate large vertical restraint forces in the confining elements when rocking out-of-plane. These forces act as surcharge and restrain the out-of-plane movement. This mechanism is effective enough to make the confining of walls an appropriate retrofit solution. To be considered fully confined, the walls need to be confined at the top and bottom by stiff reinforced concrete elements[12]. Their thickness must be at least 140 mm, and their maximum height is limited to 4 m

[12] Note that these requirements were developed considering that there can be a small gap above the masonry wall. However, to be considered confined the top of the wall needs to be grouted to the bottom surface of the slab or beam.

for thicknesses over 150 mm and 3 m for thicknesses between 140 and 150 mm (APEGBC and UBC, 2011). It is therefore proposed that walls that do not comply with these dimensional limitations or that are not confined by reinforced concrete members should be identified as potentially prone to out-of-plane failure in the adapted seismic screening method. However, note that the identification of these walls will not affect the score assigned to a building, but will rather be an independent factor to consider. These specifications are summarized in **Table 6.20**.

**Table 6.20.** Walls potentially prone to out-of-plane collapse

| Parameter | Value |
|---|---|
| Wall thickness, t | t < 140 mm |
| Wall height, h | h > 3 m (if t = 140 to 150 mm)<br>h > 4 m (if t > 150 mm) |
| Confining elements at top and bottom | Not confined with stiff concrete elements, or noticeable gap at the top |

From the data collected on the infill walls in this study it can be concluded that 1.1% of the walls don't comply with the thickness limitation of 140 mm, 10.1% don't comply with the maximum height limitation and 4% have a noticeable gap at the top and therefore are not laterally supported or confined at the top. The type of confining element was not recorded. However, from building plans the probable material for the confining elements could be established for roughly half of the total examined wall length. From these, 28.6% of the walls are confined by steel elements.

## 6.8. Summary

The seismic screening method that was developed is a score assignment procedure, with the final score dependant on the seismicity, lateral load resisting system type, building height, construction year, potential structural weaknesses (horizontal and vertical irregularities, deterioration and short concrete columns), potential for pounding of adjacent buildings and local soil conditions. The methodology is inspired by FEMA154, with scores calculated based on the capacity spectrum method. The adapted method better reflects the specific structural characteristics of school buildings and takes into consideration the province's seismicity and soil classification as stipulated in the 2010 edition of NBC. The application of the method is relatively simple and based on a form that can be filled out relying only on a visual inspection of a building, although inspection of building plans and use of other relevant sources of available information are strongly recommended.

The risk of out-of-plane collapse of unreinforced infill masonry walls was treated independently, identifying walls with geometric properties that make them especially vulnerable. The parameters that need to be evaluated are the walls thickness, height and confining elements at the top and bottom of the walls.

# Chapter 7. Application of the Seismic Screening Method

In this chapter results of the application of the developed adapted seismic screening method are presented. In **Section 7.1** some general remarks on the use of the method are given as guidance for its future application. Final scores obtained when applying the method to the 16 schools (101 individual buildings) designated as post-critical shelters in Montreal, which were described in detail in **Chapters 3** to **5**, are presented in **Section 7.2**. For this evaluation the previously collected information was re-examined to classify the identified structural weaknesses and the potential pounding according to the severity as proposed in **Chapter 6**. The results obtained were also used to analyze each factor that participates in the final score and determine the influence of it, as presented in **Section 7.3**. Finally, the revised data was used to recalculate the scores of FEMA154 and NRC92 and compare them with the adapted seismic screening method, as presented in **Sections 7.4** and **7.5**. This was done to validate the developed method and highlight its advantages over the existing methods. Both FEMA154 and NRC92 have several drawbacks that make their application questionable, as discussed in detail in **Chapter 2**, and that includes for example the treatment of the seismicity and local soil conditions. These drawbacks were already addressed and improved upon in the developed seismic screening method, and won't be mentioned in detail here. Focus will be given on specific conclusions that can be reached from the numeric results calculated. Note that the results are specific for the visited schools and the conclusions reached in this chapter are influenced by the characteristics of them and could vary for another school sample. Finally, since the proposed evaluation of the potential of out-of-plane failure of infill walls is independent and results obtained for the evaluated schools were already presented in **Chapter 6**, they will not be discussed here again.

## 7.1. Procedure for the Application of the Method

The application of the adapted seismic screening method is similar to the one of FEMA154 (ATC, 2002a) and NRC92 (NRC/IRC, 1992), and these documents can be used as reference. The general procedure that should be followed by decision makers to apply the rapid seismic screening method in a cost-effective manner is presented in **Figure 7.1**, and can be divided in two steps: pre-field planning and site visits where the data collection forms are completed and final scores are calculated.

### *7.1.1. Pre-Field Preparation*

In the specific context of the screening of the schools in the Québec, it is responsibility of the province's Ministry of Education (MELS) to establish a cost estimate and budget for the screening process. As for the selection of schools to first retrofit, a conjoint research project between École de Technologie Superior (ETS), Sherbrooke University and McGill University is currently under way to propose a three-tier procedure for the seismic evaluation of schools in Québec. Tier 1 and 2 will identify the schools where a site visit and a more detailed screening, as the one proposed in the present research, should be applied. Tier 1 will rely on the seismic hazards maps of the NBC, together with some very basic information of the schools, as the construction year and number of storeys for example. Tier 2 will classify the buildings identified as critical in tier 1 according to already available, more specific characteristics of the schools. The seismic screening method proposed in the present research could then be applied as the tier 3 to the schools deemed to be vulnerable by tier 2. The procedure will be tested with a sample of schools in 2012.

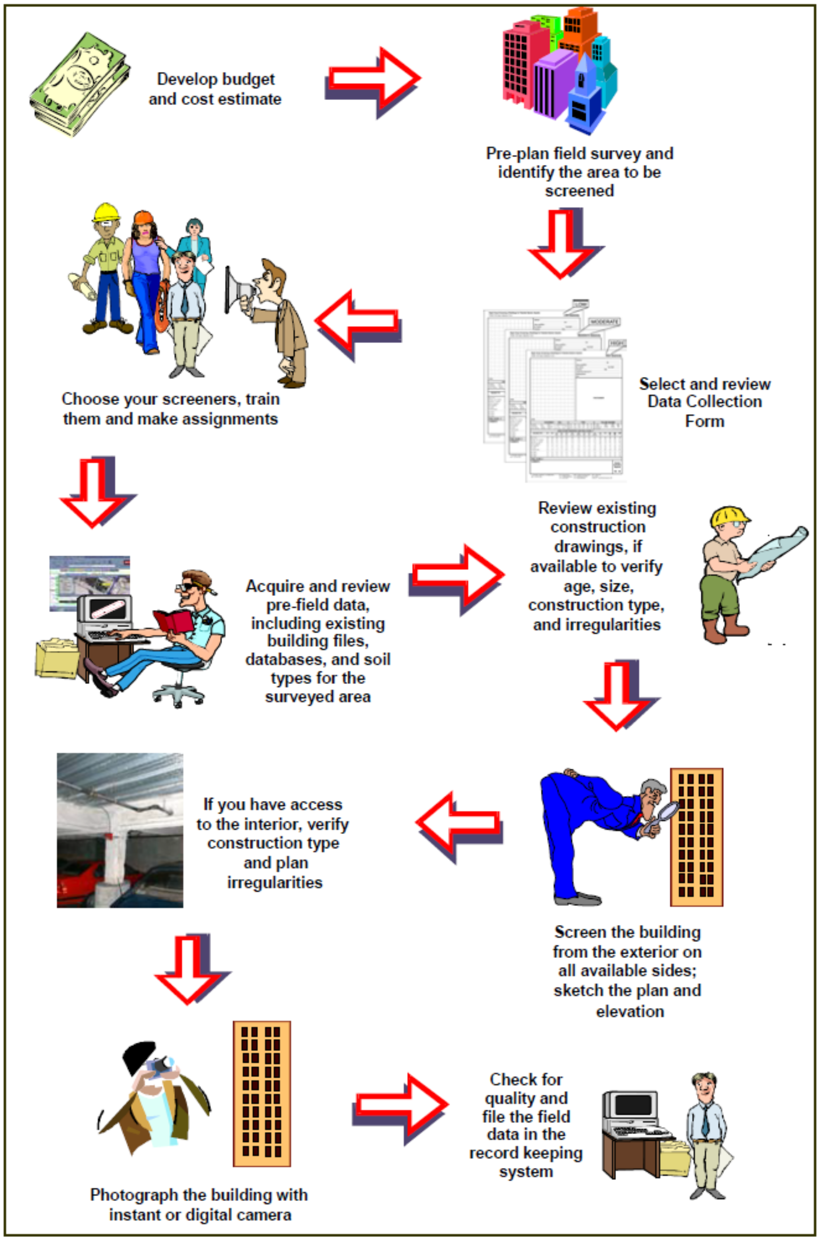


**Figure 7.1.** Rapid visual screening implementation sequence (ATC, 2002a)

Screeners who will apply the adapted seismic screening method must be trained to be familiar with the procedure to follow. Although they don't need to be seismic engineering experts, they should have some background in construction, civil engineering or architecture. It is also important to make some sample assessments and compare results obtained by different screeners, to make sure they are comparable.

Since most schools have building plans available through the school boards, the pre-field data collection will contribute significantly to the screening. From the building plans key characteristics of the schools can be established. Some of the features are much easier identified from plans than from site visits, as the building's age, lateral load resisting system and location of joints. The consultation of the building plans therefore allows for a more accurate screening with reduced time for the site visits.

Whenever possible soil conditions should be established from geotechnical or geological maps or reports prior to the site visit, since identification on site is almost always impossible. If the soil conditions can't be established, soil type E should be assumed. For one or two storey buildings, with a total height less than 7.5 meters, soil type D can be used (ATC, 2002a). In no reliable soil data are available estimation of the soil type based on ambient noise records as discussed in **Chapter 5** can be applied if deemed necessary.

### *7.1.2. Completing the Data Collection Forms (Site visits)*

Data collection forms with the information gathered from pre-field data should be prepared for every individual building to examine. In field, the collected information needs to be verified and complemented and whenever possible pictures should be taken to support the collected data. Special attention should be given to the possible structural weaknesses, since they have a notorious influence on the building's final score. To help the evaluator, a guide for the classification of the structural weaknesses was prepared, as mentioned in **Chapter 6**. The complete guide can be found in **Appendix G**.

Data collection forms for the adapted seismic screening method were developed in Microsoft Excel. These can be printed out, or taken into field on a portable electronic device. A linked score calculation form will calculate the scores and score modifiers for the input automatically. Both forms will make up the final report of the evaluated building. An example of completed data collection and score calculation forms are presented in **Figure 7.2** to **7.4**. The user is allowed to select up to three different structural types. Scores will be calculated for each one given, and the most critical score will be given as the final score. This has demonstrated to be useful in cases where the structural type cannot be established with certainty or where several structural types are combined in one single building (in this case one score is calculated independently for each type). Furthermore, recording the certainty in the selection of the structural type and the structural weaknesses will allow for a better control of the quality of the collected information.

***École secondaire (Name withheld)*** ***Building B1***

| **DATA COLLECTION FORM** | | | **Date:** 09.10.2008 |
|---|---|---|---|
| **School:** École secondaire (Name withheld) | | **Address:** Withheld | **Postal Code:** Withheld |
| **Latitude:** Withheld | **Longitude:** Withheld | **District:** Withheld | |
| **School board:** Withheld | | **Number of students:** 1202 | **Year of construction:** 1973 |
| **Building ID:** B1 | **Number of stories:** 4 | **Floor area:** 2280 $m^2$ | **Inspected by:** H. Tischer |

**Satellite plan view**


**Picture**

| **Structural Type** | | **Choice** | **Certainty [%]** |
|---|---|---|---|
| Wood | WLF | | |
| | WPB | | |
| Steel | SMF | | |
| | SBF | | |
| | SLF | | |
| | SCW | | |
| | SIW | | |
| Concrete | CMF | | |
| | CSW | | |
| | CIW | 1 | 80% |
| | PCF | 2 | 20% |
| | PCW | | |
| Masonry | RML | | |
| | RMC | | |
| | URM | | |

| **Pounding** | | **No pounding:** | |
|---|---|---|---|
| Joint depth, d [cm]: | 2.54 | d/H = | 0.0031 |
| Height of lower building, H [m]: | 8.10 | Effect: | Severe |
| Minimum story height, X [m]: | 3.40 | | |
| Difference in story height y [m]: | 0.64 | | |
| 20% Story height [m]: | 0.68 | | |

| **Soil type** | |
|---|---|
| A | |
| B | |
| C | x |
| D | |
| E | |
| F | |
| Unknown | |

**Comments**

A small part of the building has a basement.

Only a small part of the building is 4 stories high, the rest is 3 stories high.

Prefabricated slabs.

Concrete walls around stairs.

| **Structural Weakness** | **Low** | **Significant** | **Severe** | **Cert.** | **Structural Weakness** | **Low** | **Significant** | **Severe** | **Cert.** |
|---|---|---|---|---|---|---|---|---|---|
| **1. Horizontal Irregularities** | | | | | **2. Vertical Irregularities** | | | | |
| Re-entrant corners | | x | | 100% | Steps in elevation view | | x | | 90% |
| Asymmetric stairways | | | | | Soft Story | | | | |
| Asymmetric partition walls | | | | | Building on Hill | | | | |
| Torsion in LFRS | | | | | Change in structural type | | | | |
| Diaphragm discontinuity | | | | | Other | | | | |
| Out of plane offset | | | | | **3. Deterioration** | | | | |
| Other | | | | | **4. Short Concrete Columns** | | | | |

**Figure 7.2.** Sample data collection form

***École secondaire (Name withheld)*** ***Building B1***

**PHOTOGRAPHIC EVIDENCE**

Re-entrant corners


Steps in elevation view

**Figure 7.3.** Sample photographic evidence form

***École secondaire (Name withheld)*** ***Building B1***

**SCORE CALCULATION FORM**

| | | | |
|---|---|---|---|
| **School:** École secondaire (Name withheld) | | Address: Withheld | Postal Code: Withheld |
| **Latitude:** Withheld | **Longitude:** Withheld | **District:** Withheld | |
| School board: Withheld | | **Number of students:** 1202 | **Year of construction:** 1973 |
| **Building ID:** B1 | **Number of stories:** 4 | **Floor area:** 2280 $m^2$ | |

**Satellite plan view**


**Picture**

**CALCULATIONS**

Seismicity: Moderate

| | Choice | | | Comments |
|---|---|---|---|---|
| | 1 | 2 | 3 | |
| Structural type | CIW | PCF | | |
| Certainty | 80% | 20% | | |
| Basic Structural Hazard Score | 3.1 | 3.2 | | |
| Score Modifiers | | | | |
| Pre-Code | 0.0 | 0.0 | | |
| Post-Benchmark | 0.0 | 0.0 | | |
| Mid Rise Buildings (4 to 7 stories) | 0.0 | 0.1 | | |
| Soil Type | 0.0 | 0.0 | | Soil type: C |
| Horizontal irregularities | -0.6 | -0.6 | | Effect (worst case): Significant |
| Vertical irregularities | -0.6 | -0.6 | | Effect (worst case): Significant |
| Deterioration | 0.0 | 0.0 | | Effect: None |
| Short concrete columns | 0.0 | 0.0 | | Effect: None |
| Pounding effects | | | | Effect: Severe |
| Floor misalignment | -0.6 | -0.6 | | Vertical misalignment ≤ 20% of story height |
| Total Score | 1.3 | 1.5 | | |

**FINAL SCORE**

| | |
|---|---|
| **Structural type:** | **CIW** |
| **Final Score:** | **1.3** |
| **Probability of collapse:** | **≥ 1%** |
| **Collapse potential:** | **Moderate** |

**Figure 7.4.** Sample score calculation form

### *7.1.3. Using the Obtained Results*

The final classification used in (McConnell, 2007) as presented in **Chapter 2** was adopted for the developed seismic screening method, and is repeated here in **Table**

**7.1**. It must be noted that the screening method will identify buildings that are potentially at risk, but to determine if they are truly at risk and if corrective interventions are necessary, a detail analysis must be performed on them.

**Table 7.1.** Proposed ranking of final scores of the adapted seismic screening method (McConnell, 2007)

| Classification | Probability of collapse | Score |
|---|---|---|
| Very high | 100% | ≤ 0.0 |
| High | 10% to 100% | 0.1 – 1.0 |
| Moderate | 1% to 10% | 1.1 – 2.0 |
| Low | below 1% | > 2.0 |

## 7.2. Final Scores of the Evaluated Schools

The adapted seismic screening method was applied to the 16 schools designated as post-critical shelters on the island of Montreal, for a total of 101 buildings evaluated. The distribution of the final scores is presented in **Figure 7.5**, where it can be seen that 18 school buildings are classified as having very high priority for future interventions, 18 as high priority, 44 as moderate priority and 21 as low priority. The average final score obtained was 1.3 with a standard deviation of 1.2. The high standard deviation demonstrates that the developed method is capable of differentiating between the evaluated buildings, which is desirable.

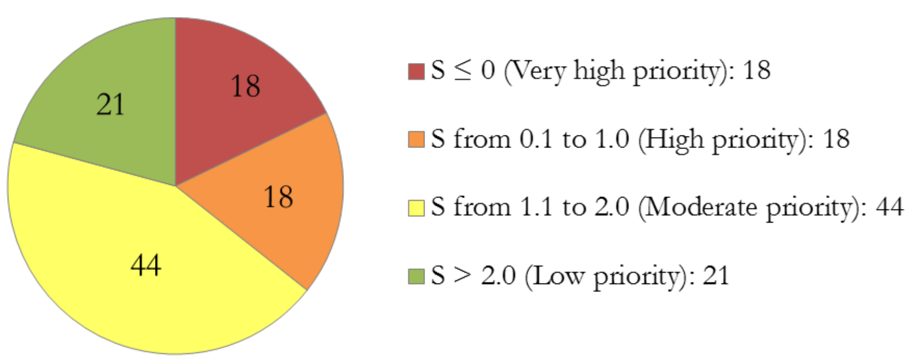


**Figure 7.5.** Final scores of 101 school buildings evaluated with the adapted seismic screening method

Average scores per school sites and the distribution of scores according to severity for the buildings at each site are presented in **Table 7.2**. Clear trends can be established by school site, with significantly different final score averages. This was expected, since several (if not all) buildings located on the same site usually share common features, such as local soil conditions, construction year and lateral load resisting system type. However, it must be noted that individual buildings on the same site have clearly distinctive scores, see for example S2_CL, with 2 buildings classified as having high priority, 4 as moderate priority and 1 as low priority. This supports the need to evaluate each building individually.

**Table 7.2.** Final scores per school site

| School | Average Final Score | No. of Buildings | | | |
|---|---|---|---|---|---|
| | | Very High Priority | High priority | Moderate Priority | Low Priority |
| S1_A | 2.3 | 0 | 0 | 2 | 8 |
| S2_CL | 1.4 | 0 | 2 | 4 | 1 |
| S3_AV | 1.6 | 1 | 1 | 7 | 2 |
| S4_JM | 1.3 | 1 | 0 | 7 | 0 |
| S5_LR | -0.2 | 1 | 0 | 0 | 0 |
| S6_EM | -0.7 | 10 | 0 | 1 | 0 |
| S7_CaL | -0.4 | 4 | 2 | 0 | 0 |
| S8_EAO | 1.8 | 0 | 0 | 2 | 0 |
| S9_R | 2.1 | 0 | 1 | 2 | 4 |
| S10_JG | 1.3 | 0 | 1 | 4 | 0 |
| S11_PD | 1.8 | 0 | 0 | 3 | 1 |
| S12_LM | 1.9 | 0 | 1 | 1 | 2 |
| S13_SE | 2.4 | 0 | 1 | 3 | 3 |
| S14_MR | 0.9 | 1 | 3 | 2 | 0 |
| S15_DJ | 1.0 | 0 | 5 | 2 | 1 |
| S16_PT | 1.8 | 0 | 1 | 1 | 2 |

## 7.3. Influence of BSHs and Score Modifiers on the Final Score

The influence of the *BSHs* and score modifiers on the classification of the buildings was determined by performing analysis of variance (ANOVA) on the numerical values obtained for each of them. This type of analysis allows a comparison of the mean and standard deviation of groups (in this case there are four groups, which are the building's classification according to their final scores) and determine if there is a difference between groups or not. Analysis using ANOVA will identify cases where at least one group is different, therefore independent analyses were performed between all possible pairs of groups for a more specific analysis where deemed necessary. If there is a difference between groups for a given score modifier, it can be then concluded that it is a dominant parameter on the final score. Selected results are presented in **Appendix H**. In the present case, ANOVA is used to determine if BSH and score modifiers individually affect the classification according to the final score. Although these parameters are not random, a positive answer would justify the inclusion of the specific parameter, meanwhile a negative outcome would affirm that the parameter is not essential for the classification. Results for each parameter were then further analyzed to explain the influence or lack of influence of the final score for the evaluated building stock. Post-benchmark, mid-rise, deterioration and short concrete column modifiers were excluded from the analysis because there were too few cases to be significant. In general it was noted that most of the parameters are influential on the final score, which is desirable for a rapid seismic screening tool. Additionally, the classification of the structural weaknesses and the potential for pounding according to their severity demonstrated to be effective to differentiate between the buildings, something that was sought when developing the method because of the high incidence of these parameters in school buildings.

### *7.3.1. Basic Structural Hazard Scores*

The analysis of variance demonstrated that the *BSHs* cannot be differentiated between groups, and are therefore not influential in the classification of the buildings of the evaluated sample. Average and variance values for each group are shown in **Table 7.3**, where it can be seen that the average values for each group are very similar and their difference is not significant considering the variance of the data.

This result was expected because of the limited number of building types and the low variability of the *BSHs* values for the predominant building types, with values between 3.1 and 3.6 for 96% of the total building studied.

**Table 7.3.** Average and variance of *BSHs* by classification of final score

| Classification | Average | Variance |
|---|---|---|
| Very high | 3.16 | 0.03 |
| High | 3.24 | 0.05 |
| Moderate | 3.30 | 0.04 |
| Low | 3.30 | 0.04 |

### *7.3.2. Pre-Code Score Modifier*

The analyses of variance demonstrated that the pre-code score modifier highly influences the final score, excepting the moderate and low priority categories where no difference could be established. The clearly different average values presented in **Table 7.4** confirm this finding. The same conclusion can also be reached from **Figure 7.6**, where the distribution of pre-code buildings versus non pre-code buildings for the different priority classes is shown. This can be partly explained by the high incidence of concrete frame buildings (with and without infill walls) in the visited school buildings, which make up almost 60% of the total sampled schools. Of these, 15 are classified as very high, 9 high, 7 moderate and 2 low priority. These building types have a very low pre-code score modifier of -1.0. For other building type the typical value for the pre-code modifier is -0.3.

**Table 7.4.** Average and variance of pre-code score modifier by classification of final score

| Classification | Average | Variance |
|---|---|---|
| Very high | -0.87 | 0.10 |
| High | -0.53 | 0.24 |
| Moderate | -0.22 | 0.13 |
| Low | -0.13 | 0.09 |

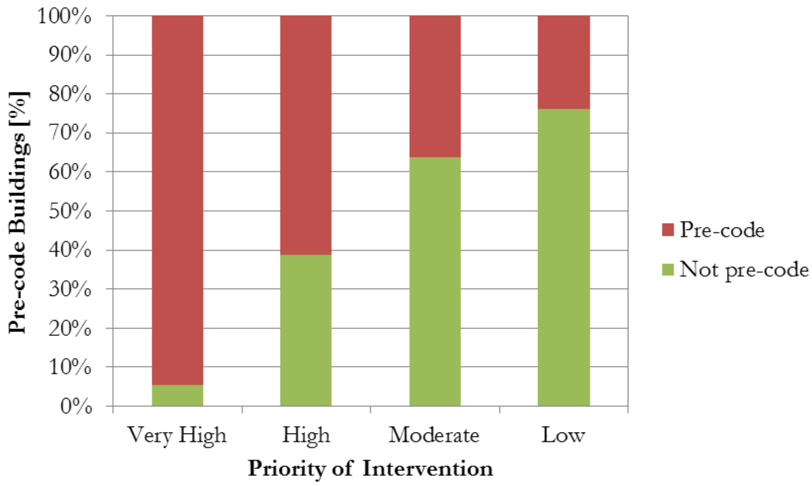


**Figure 7.6.** Distribution of pre-code buildings

### *7.3.3. Soil Type Score Modifier*

The analysis of variance determined that the soil type score modifier is different between groups. However, a more detailed assessment between pairs of groups demonstrated that the very high and low priority categories present no difference. The same is the case for the high and moderate priority groups. Observing the average and variance of this modifier presented in **Table 7.5** this can be confirmed, with the lowest average value obtained for high priority buildings and the highest average value for very high priority buildings. The same can be observed from the distribution of the cases on different soil types according to priority of intervention presented in **Figure 7.7**. Although the soil type score modifier has the potential to be influential on the final score, with high values for soil type A (of around 1.0 for moderate seismicity) and low values for soil type E (of around -1.0 for moderate seismicity), the sampled schools were all located on soil types B to D, which have less significant score modifier values associated to them (about 0.8 for soil type B and -0.5 for soil type D in a moderate seismic zone, soil type C will not affect the score at all). This explains that the influence of the soil type is not penalizing on the schools sampled, combined with the fact that irregularities and pounding are extremely common, and if they are severe their score modifiers are more significant than the soil type score modifier.

**Table 7.5.** Average and variance of soil type score modifier by classification of final score

| Classification | Average | Variance |
|---|---|---|
| Very high | 0.33 | 0.31 |
| High | -0.05 | 0.19 |
| Moderate | 0.06 | 0.18 |
| Low | 0.29 | 0.18 |

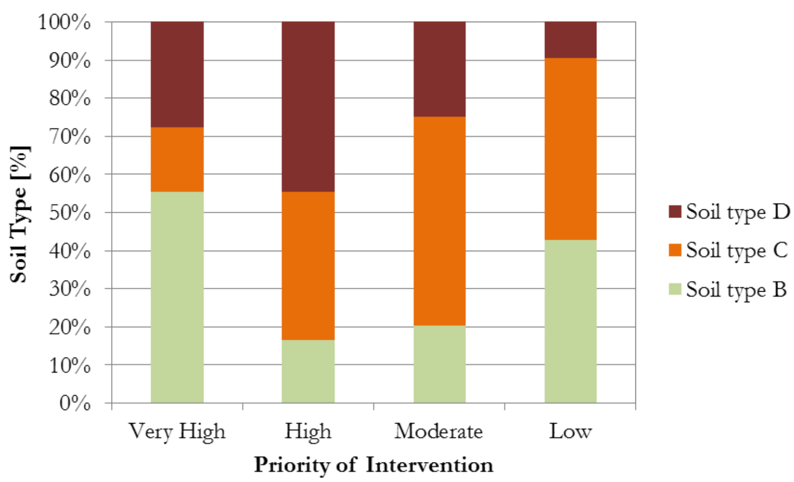


**Figure 7.7.** Distribution of soil types

### *7.3.4. Horizontal Irregularity Score Modifier*

**Table 7.6** shows average and variance for the horizontal irregularity score modifier. These values and the accompanying analyses of variance demonstrated the very high difference of this modifier in the different categories, except between the very high and the high priority and the high and moderate priority groups. The influence of this factor can be partly explained by the high values the horizontal irregularity score modifier can take (of the order of -1.6 for severe and -0.6 for significant irregularities for the studied lateral load resisting types). Furthermore, the classification of the horizontal irregularities in terms of their effect in low, significant and severe allowed for a clear differentiation between buildings. Of the 101 studied cases, 68 presented horizontal irregularities. From these, 22 were classified as having a low, 19 a significant and 27 a severe effect. The ability of the method in differentiating according to the severity of the horizontal irregularities can also be appreciated by analyzing the distribution of cases in the priority classes, as can be seen in **Figure 7.8**.

**Table 7.6.** Average and variance of horizontal irregularity score modifier by classification of final score

| Classification | Average | Variance |
|---|---|---|
| Very high | -1.12 | 0.45 |
| High | -0.67 | 0.53 |
| Moderate | -0.48 | 0.39 |
| Low | -0.03 | 0.02 |

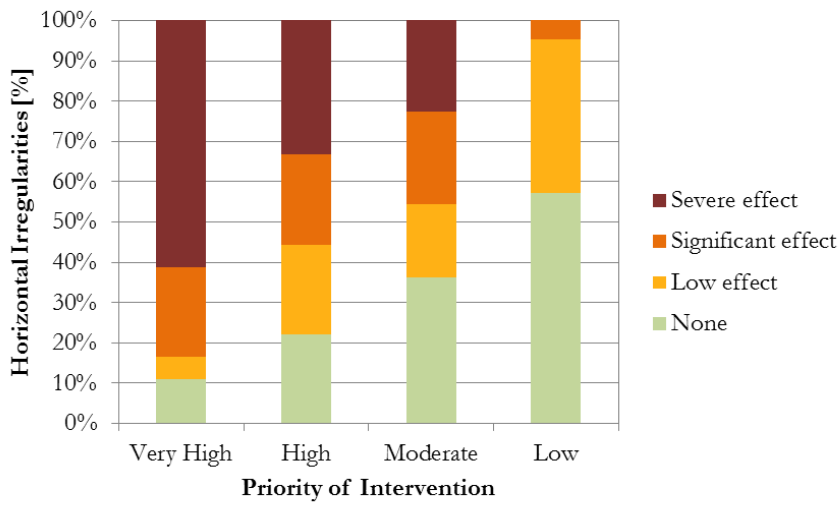


**Figure 7.8.** Distribution of horizontal irregularities classified according to their effect

### *7.3.5. Vertical Irregularity Score Modifier*

Conclusions for the vertical irregularity score modifiers are very similar than those for the horizontal irregularity score modifiers. From the analyses of varaince a very high difference between groups could be established (see also average and variance values in **Table 7.7**), except between the very high and high priority and the moderate and low priority groups. Again this can be explained by the high values this modifier can take and by the well-established differentiation of the vertical irregularities by severity: from the 73 recorded cases 38 were classified as having a low, 15 a significant and 20 a severe effect. The distribution of cases with severe vertical irregularities in the different categories again shows how well the method singles them out, as can be seen in **Figure 7.9**, together with the other severity classes.

**Table 7.7.** Average and variance of vertical irregularity score modifier by classification of final score

| Classification | Average | Variance |
|---|---|---|
| Very high | -1.06 | 0.56 |
| High | -0.61 | 0.42 |
| Moderate | -0.25 | 0.28 |
| Low | -0.03 | 0.02 |

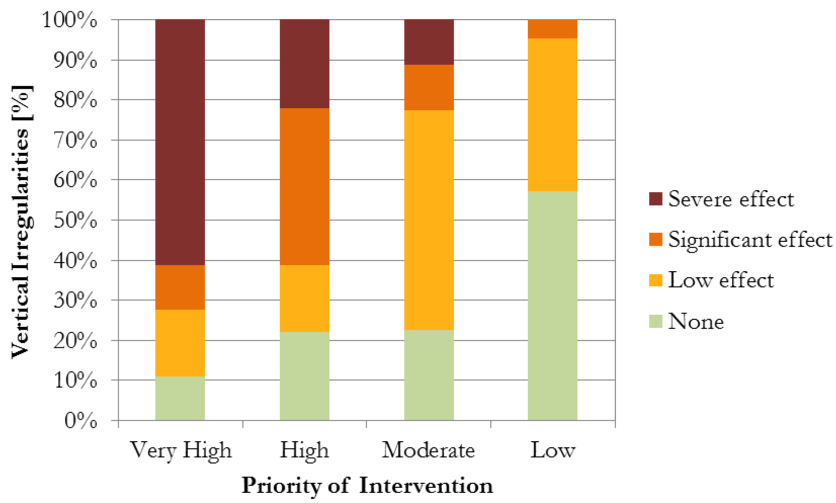


**Figure 7.9.** Distribution of vertical irregularities classified according to their effect

### *7.3.6. Pounding Score Modifier*

The analyses of variance as well as the average and variance values presented in **Table 7.8** demonstrated that there is difference in the pounding score modifier values between the very high priority and all other groups. Values for this score modifier are high for severe cases of pounding, which in part explains the influence of this factor on the final score. The classification of the pounding effect according to the separation between buildings also showed to be effective in differentiating the buildings. A total of 6 cases of no, 24 of significant and 71 of severe pounding were recorded (no insignificant pounding cases were present). **Figure 7.10** shows how they are distributed according to the buildings final classification.

**Table 7.8.** Average and variance of pounding score modifier by classification of final score

| Classification | Average | Variance |
|---|---|---|
| Very high | -1.12 | 0.32 |
| High | -0.72 | 0.17 |
| Moderate | -0.76 | 0.16 |
| Low | -0.55 | 0.27 |

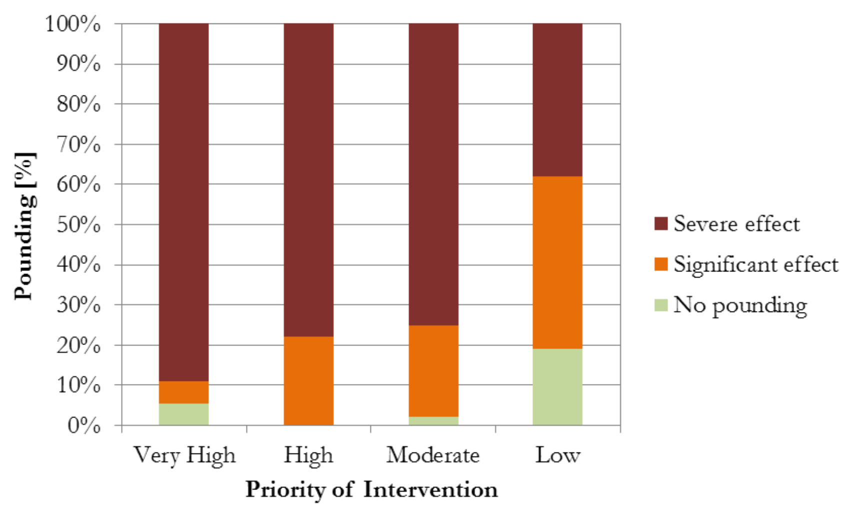


**Figure 7.10.** Distribution of pounding classified according to their effect

## 7.4. FEMA154 Results

### *7.4.1. Final Scores and Influence Factors*

Scores for FEMA154 were recalculated considering the reassessment of the structural weaknesses. It must be noted that score modifiers for vertical and plan irregularities were only applied to cases with these irregularities were identified as having a moderate or high effect. The final scores were classified according to priority in the same manner as for the adapted seismic screening method. The obtained average and standard deviation values were 1.5 and 1.2 respectively. 12

buildings were classified as having very high, 27 has high, 22 as moderate and 40 as low priority for future intervention.

As done for the adapted seismic screening method, the influence of *BSHs* and score modifiers was analyzed. For the *BSHs* and pre-code and soil type score modifiers similar results were obtained as for the adapted seismic screening method. For the vertical score modifier the analyses of variance determined extremely high difference between groups. The further analysis of the results showed that FEMA154 is extremely penalizing when this type of structural weakness is present (with score modifier of the order of -2.0), and that the method is incapable of discerning the severity of this irregularity: no building with a vertical irregularity was classified as having a low priority, and only two as having a moderate priority. On the other hand, all buildings of very high priority and 22 out of 27 of high priority have a vertical irregularity. Plan irregularities on the other hand, even when severe, have a low influence on the final score, with a rather modest score modifier value of -0.5. The highest percentage of cases with horizontal irregularities is found in the moderate priority class, followed by the very high, low and high classes in that order, showing that they are not significant on the final score. These shortcomings in dealing with irregularities are very significant when evaluating schools, where they are extremely common.

### *7.4.2. Comparison between the Adapted Method and FEMA154*

When comparing the adapted seismic screening method and FEMA154, it is noted that the averages and standard deviations obtained are very close. However, the direct comparison is questionable, since FEMA154 does not consider pounding and deterioration, the first of these two factors having a profound impact on the final scores of the adapted method as demonstrated in the previous section. Therefore scores obtained with the adapted seismic screening method were recalculated without considering the score modifiers for pounding and deterioration to allow for a more realistic comparison. In this case, an average of 2.1 for the final scores was obtained, clearly higher than the results for FEMA154. This can also be seen in **Figure 7.11**, where final scores obtained using the adapted method without the pounding and deterioration score modifiers are plotted against final scores obtained using FEMA154. In this graph, more data points lie above the diagonal (plotted with red) indicating higher scores achieved by the adapted method. This result was expected and can be explained by several factors, including the higher *BSHs* obtained because of the update of the underlying capacity spectrum method (see **Chapter 2**), the less penalizing score modifier for moderate effect vertical irregularities and the inappropriate soil classification of the soil in FEMA154 (see again **Chapter 2**).

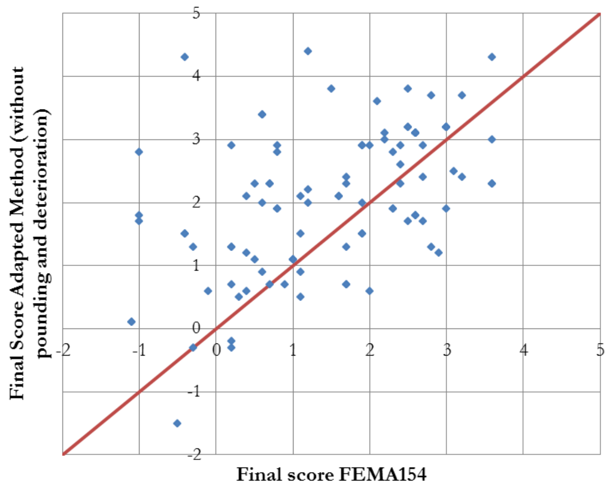


**Figure 7.11.** Final scores of the adapted method (without considering pounding and deterioration score modifiers) against final scores of FEMA154

A comparison of number of buildings in each category is given in **Figure 7.12**. Again, if comparing the adapted seismic screening method directly with FEMA154, the adapted method seems more conservative. However, if pounding and deterioration modifiers are disregarded, it can be seen that the adapted method actually is less conservative.

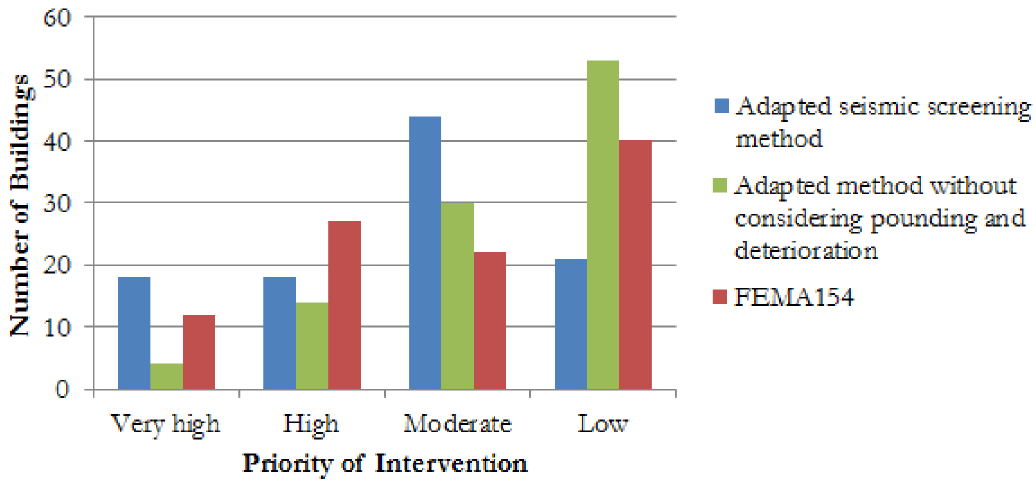


**Figure 7.12.** Number of buildings classified according to priority

Another interesting comparison is the number of cases where buildings are classified as having the same priority of intervention according to the adapted method and according to FEMA154. **Figures 7.13** and **7.14** show this comparison, where the number of buildings in each category is plotted for FEMA154, against the adapted method and the adapted method without considering the pounding and deterioration score modifiers. For these two plots, red columns indicate the number of buildings where the classification for both examined methods is the same, orange columns show the number of buildings where the classification according to FEMA154 is more conservative and violet columns show the number of buildings were the adapted method is more conservative. Both figures show that buildings with radically different final scores are rare (values tend to decrease for columns farther off the red diagonal). Note how **Figure 7.13** is significantly more scattered than **Figure 7.14**, due to the pounding effect that will affect the majority of buildings but is not considered by FEMA154. Finally, **Figure 7.14** again clearly shows how the adapted method is less conservative than FEMA154.

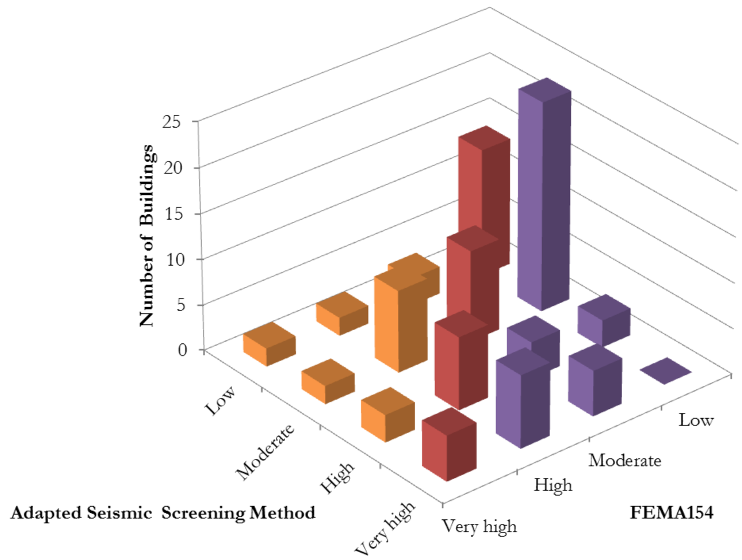


**Figure 7.13.** Comparative distribution of building according classification for the adapted seismic screening method compared to FEMA154

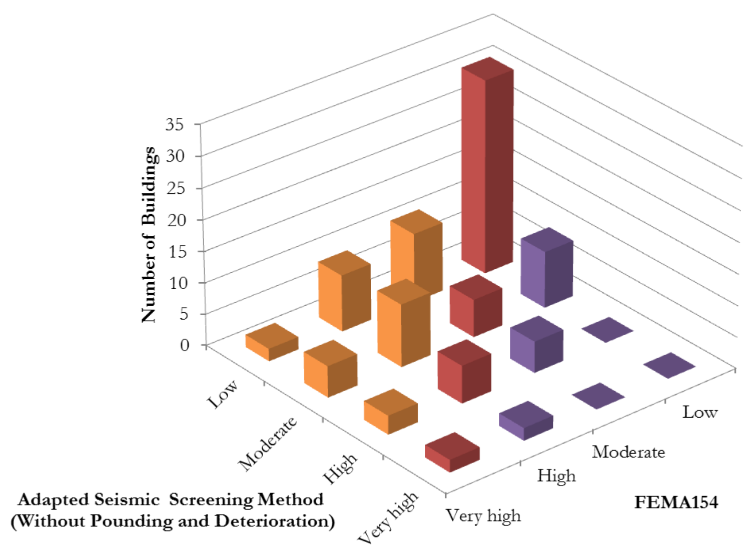


**Figure 7.14.** Comparative distribution of building according classification for the adapted seismic screening method without pounding and deterioration compared to FEMA154

## 7.5. NRC92 Results

### *7.5.1. Final Scores and Influence Factors*

Scores for NRC92 were recalculated considering the reassessment of the structural weaknesses. The average final score was 14.3 and the standard deviation 8.5 (from

**Chapter 2**, it is important to note that opposed to the adapted seismic screening method and FEMA154, high final scores indicate critical buildings in NRC92). 5 buildings were classified as potentially hazardous, 22 as having high, 28 moderate and 46 low priority for future interventions. The parameters that make up the final score (seismicity, soil conditions, type of structure, irregularities, importance and non-structural hazards) were analyzed as done for the other two discussed methods to determine their influence on the final score. General results seem to indicate that each one of these factors has a high influence on the final score (which in the case of seismicity for example is surprising, since all evaluated buildings are located in the same seismic zone). A more careful examination however demonstrated that the NRC92 method clearly singles out older buildings (constructed prior to 1970).

Seismicity and soil condition factors will only take values different than 1 (note that these are multiplicative, therefore a value of 1 will have no effect on the final score) for buildings constructed before 1965. In the sample, 15 buildings were constructed before that date. Of the 5 buildings classified as potentially hazardous, all are pre-1965 buildings, as well as 8 high priority and 2 moderate priority buildings. When taking only these buildings into account, neither the seismicity nor the soil condition factors exhibit any difference between groups, and therefore do not influence the final score.

Values of all other factors will be different for pre- and post-1970 buildings. Clearly pre-1970 buildings fare worse in the final score, with all buildings classified as potentially hazardous and high priority being pre-1970. In comparison, 57% of moderate priority and only 26% of low priority are pre-1970. When doing analyses of variance for the type of structure, presence of irregularities and non-structural hazard factors independently for pre- and post-1970 buildings, it was found that there is a clear difference between groups for the type of structure and the non-structural hazard factors. For the irregularities factor, there is no difference between groups for the pre-1970 buildings. Finally, the importance factor will be the same for all buildings of the sample evaluated for construction before or after 1970, and therefore only the construction year is penalized.

### *7.5.2. Comparison between Adapted Method and NRC92*

Comparison between the adapted seismic screening method and NRC92 is not as straight forward as seen with FEMA154, since they are different in methodology and final score values. However, they can be compared based on the classification of the final score according to the priority of future intervention, as can be seen in **Figure 7.15**. In general terms the adapted method is more conservative than the NRC92 method for the sampled buildings.

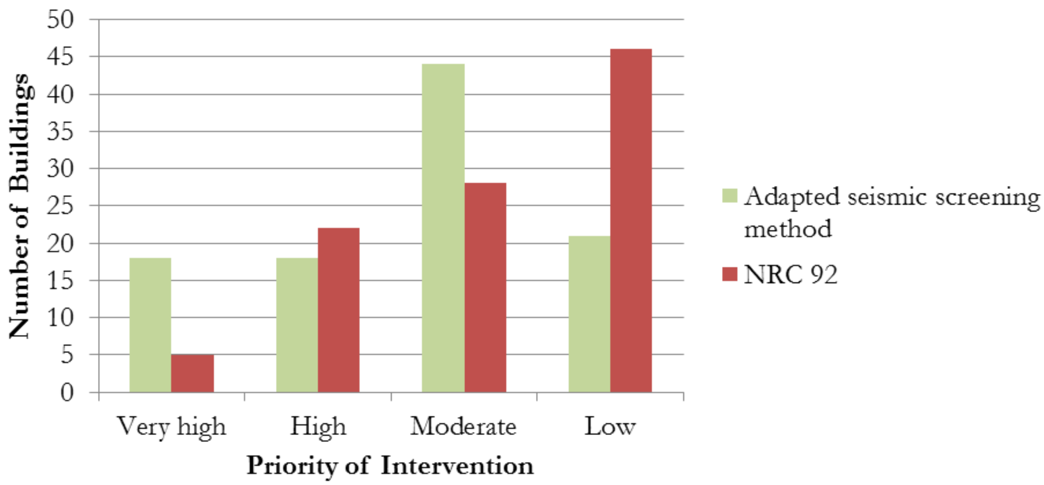


**Figure 7.15.** Number of buildings classified according to priority

**Figure 7.16** shows the building by building agreement in final classification of the buildings. Again, on this plot red columns indicate the number of buildings where the classification for both methods examined is the same, orange columns show the number of buildings where the classification according to NRC92 is more conservative and violet columns show the number of buildings were the adapted method is more conservative. The scatter between the results is significant, which can be explained by the different parameters that single out critical buildings for both cases.

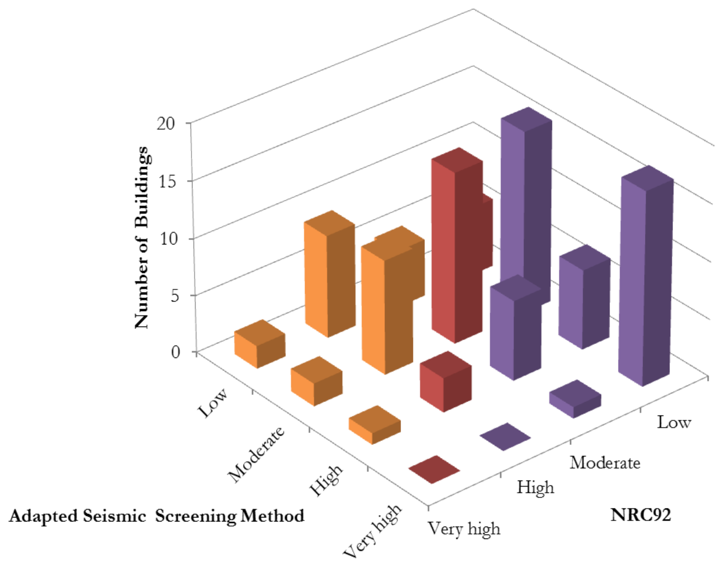


**Figure 7.16.** Comparative distribution of building according classification for the adapted seismic screening method compared to NRC92

### 7.6. Summary

The adapted seismic screening method was tested by applying it to 101 individual school buildings at 16 different sites. Results indicated that 18 school buildings had very high priority for future interventions, 18 high priority, 44 moderate priority and 21 low priority, with an average final score of 1.3. A high standard deviation of 1.2 on the final scores shows how the method developed is capable of differentiating between the buildings evaluated, which is a desirable feature for screening.

The influence of the BSHs and score modifiers on the classification of the buildings was determined by performing analysis of variance (ANOVA) on the numerical values obtained for each of them, excluding score modifiers where the low number of attained cases made the analysis irrelevant. Results showed that the BSHs cannot be differentiated between groups, and are therefore not influential in the classification of the buildings of the evaluated sample. However, most of the other evaluated parameters showed a high influence on the final score, including the pre-code, horizontal irregularities, vertical irregularities and potential for pounding modifiers.

To highlight the advantages of the developed method when compared with existing procedures, scores were also calculated using FEMA154 and NRC92. Average and standard deviations obtained with the adapted seismic screening method and FEMA154 are very close. However, such a direct comparison is questionable, since FEMA154 does not consider pounding and deterioration. When scores obtained with the adapted seismic screening method were recalculated without considering these two modifiers for a more realistic comparison, clearly higher scores (less conservative) were achieved by the adapted method with a consistent building-by-building agreement. Comparison between the adapted screening method and NRC92 is not as straight forward, since they are different in methodology and final score values. However, they can be compared based on the classification of the final score according to the priority of future intervention. In general terms the adapted method is more conservative than NRC92 for the sampled buildings, but the building-by-building agreement is very poor. The scatter between the results can be explained by the different parameters that single out critical buildings for both cases.

The influence of the different parameters that make up the final score of FEMA154 and NRC92 was also analysed using ANOVA. It was shown that FEMA154 does not properly capture the adverse effects of vertical and horizontal irregularities. The method is extremely penalizing when vertical irregularities are present, and is incapable of discerning the severity of this irregularity. Plan irregularities on the other hand, even when severe, have no influence on the final score. These shortcomings of FEMA154 in dealing with irregularities are very significant when evaluating schools, where they are extremely common. The analysis of the NRC92 scores demonstrated that the method tends to systematically penalize older buildings. Clearly pre-1970 buildings fare worse in the final score, with all buildings classified as having very high (potentially hazardous) or high priority for future intervention. When performing ANOVA for the LLRS type, presence of irregularities and non-structural hazard factors independently for pre- and post-1970 buildings, it was found that there is a clear difference between groups for the LLRS type and the non-structural hazard factors. For the irregularities factor however, there is no difference between groups for the pre-1970 buildings.

# Chapter 8. Summary and Conclusions

## 8.1. General

The main objective of this dissertation was to develop a rapid seismic screening method adapted to school buildings of the province of Québec. Sixteen schools (comprising 101 individual buildings) designated as post-critical shelters on the island of Montréal were studied to determine the specific characteristics of the schools and to identify the factors that need to be considered by the adapted seismic screening method. This allowed fulfilling a secondary objective of the research, which was to determine the probable seismic behaviour and adequacy of these buildings to serve as emergency shelters after a strong, design-level earthquake. A summary of the main conclusions of the research are given in the next sections.

## 8.2. Adapted Seismic Screening Method

The developed adapted seismic screening method is a score assignment procedure, based on the framework proposed by the FEMA154 methodology (ATC, 2002a), with the final score for each building calculated as the sum of the basic structural hazard score ($BSH$) dependant on the lateral load resisting system and several score modifiers that reflect each building's specific characteristics. Score modifiers to account for building height, construction year, structural weaknesses (horizontal and vertical irregularities, deterioration and short concrete columns), potential for pounding and local soil conditions were considered. The province of Québec was divided into three seismic regions, of low, moderate and high seismicity, and sets of $BSHs$ and score modifiers for each region were calculated. The application of the method is relatively simple, and its practical implementation is based on a data collection and a data analysis form conveniently implemented in a Microsoft Excel dynamic format. Although these forms can be filled out relying only on a visual inspection of a building, it is strongly recommended that building plans and other relevant sources of information available be consulted.

The main innovations and advantages of the developed seismic screening method can be summarized in the following points:

- The method was developed after collecting an extensive database on the characteristics of school buildings in Quebec, based on the examination of 101 individual school buildings. This strong experimental foundation assures that the method is able to represent buildings with the special characteristics of schools in an adequate manner.
- The calculation of the *BSHs* and score modifiers is based on a nonlinear static analysis procedure called the capacity spectrum method. This approach, based on the FEMA154 methodology, provides a clear and rational foundation, allowing future users to understand the assumptions made to obtain the final score. The detailed documentation of the proposed method as presented in this thesis enables its users to better interpret the calculated scores, and also allows for the method to be modified if necessary to be used outside of its intended scope.
- Regions of low, moderate and high seismicity were selected based on the province's demographics and seismicity, as given by the 2010 edition of the National Building Code (NBC). The method is therefore "up-to-date". The method can also be modified easily should the seismicity be modified in future editions of the NBC.
- The parameter used to classify the seismic zones, namely the spectral acceleration value for a period of 0.5 s, was selected based on the characteristics of school buildings, namely that they are low-rise structures with effective periods close to 0.5s.
- Benchmark years, related to quality of construction, were determined based on the evolution of the NBC and Quebec's construction practices.
- The generic capacity curves used to characterize the two most common building types in the sample of evaluated school buildings (namely concrete shear walls and concrete frames with infill unreinforced masonry walls) were validated by comparing their elastic range with the in-situ dynamic properties obtained from ambient vibration testing.
- The building features likely to increase seismic vulnerability, such as the presence of horizontal and vertical irregularities, general level of material deterioration, and potential for pounding of adjacent buildings with insufficient separation, were

classified according to their severity and detailed guidance on how to categorize these features was provided. Different score modifiers were assigned for insignificant, significant and severe structural deficiency features. This more detailed treatment of these aspects of school buildings proved crucial in the development of the adapted method because these features are extremely common in school buildings. A new score modifier for the potential of pounding was introduced, classifying its severity based on the separation between adjacent buildings. Furthermore, floor misalignment was considered as an aggravating factor for pounding. Potential for pounding was present at almost each school site in the evaluated sample, making this score modifier significant.

- Local soil conditions were taken into consideration by using the 2010 NBC ground motion amplification factors. A simple in-situ test for determining soil conditions was tried and deemed appropriate for its use in a rapid seismic assessment context for cases where no reliable geotechnical information is available, especially if poor conditions are suspected.
- Based on the final score, a classification system according to the priority for future intervention (detailed assessment and seismic retrofit programs) was implemented, providing four categories: very high, high, moderate and low. This was inspired by the application of FEMA154 in the state of Oregon (McConnell, 2007).

The application of the developed method to 101 individual school buildings highlighted its advantages. The statistical significance of the influence of the BSHs and score modifiers on the classification of the buildings was determined by means of analysis of variance. In general it was found that most of the selected parameters significantly influence the final score, which is desirable for a rapid seismic screening tool. Additionally, the classification of the structural weaknesses and the potential for pounding according to their severity proved effective to differentiate the buildings, a key goal in the development of the method because of the high incidence of these features in school buildings.

Furthermore, comparison of the results of the adapted seismic screening method to those obtained using the two existing seismic screening methods most relevant in the given context (NRC92 and FEMA154), clearly showed the advantages of the adapted method developed here. It was shown that FEMA154 is more conservative than the developed method and it is very penalizing for buildings with vertical irregularities, while plan irregularities have a low effect on the final score, even if they are severe. Note that potential for pounding is ignored by FEMA154 while it was found influential in the adapted method. Results of NRC92 showed that it is strongly biased to single out older building constructed prior to 1970. In general the adapted method is found to be more conservative than NRC92 for the buildings studied.

Independently from the scoring procedure, the research also provides guidance on how to identify buildings where out-of-plane failure of infill walls is likely under strong shaking. The user is asked to identify key characteristics and dimensions that make unreinforced masonry walls vulnerable. They include walls with thickness under 140 mm, walls with height over 3 m (for thickness between 140 and 150 mm) and over 4 m (for thickness over 150 mm) or walls that are not confined by stiff concrete elements on their perimeter. These characteristics can be identified during the same site visit necessary for seismic screening. The importance of evaluating the risk of out-of-plane failure of heavy unreinforced masonry walls was demonstrated in past earthquakes, where this type of failure was relatively common.

## 8.3. Seismic Vulnerability of Schools Designated as Emergency Shelters in Montréal

Great interest was expressed by officials of Montréal's civil security Centre (*Centre de Securité Civile de Montréal*) in the seismic assessment of schools designated as post-critical shelters. More specifically, an evaluation of the different parts of the school was requested, to be able to know in advance which services and rooms (as for example the cafeteria or large assembly areas as a gymnasium) will likely be available and functional after a design-level earthquake and enable the school to function according to its classification as a shelter.

The application of the developed seismic screening method to each individual building at each school designated as shelter fulfills this need, and therefore this project will have a direct and important impact on the city's earthquake preparedness program. It was found that 18 buildings have a very high, 18 a high, 44 a moderate and 21 a low priority for future intervention. Furthermore, average scores and classifications per school site allowed the determination of which sites are more suitable than others as shelters after an earthquake (school S1_A for example, with an average final score of 2.3 and 2 buildings of moderate and 8 of low priority should fare significantly better than S6_EM, with an average final score of -0.7 and 10 buildings of very high and one of moderate priority). With respect to the identification of heavy unreinforced masonry walls prone to out-of-plane collapse, it was found that only about 1% of the walls do not comply with the thickness limitation of 140 mm, 10% do not comply with the maximum height limitation and 4% have a noticeable gap at the top and are therefore not confined or laterally supported. The type of confining element was not recorded during the surveys, but could be assessed from the structural drawings for roughly half the total examined wall length. From these, it was found that nearly 30% of the walls are confined by steel elements.

A wealth of information was collected through the study of the building plans, site visits, ambient vibration measurements on the buildings and on the ground, Montréal's microzonation map and the collection of a detailed database of the infill walls. This information will also be valuable for several projects related to the seismic vulnerability of schools in Québec that are currently being carried out by the École de Technologie Supérieure (ETS), Sherbrooke University and McGill University in collaboration with the province's Ministry of Education (MELS). If in the future a more detailed assessment and retrofit of one of these schools should be carried out, the information collected will be very useful. The data is organized per school building in a seismic portfolio, which will be made available to the relevant technical personnel, through a separate confidential publication for each school board involved.

## 8.4. Dynamic Properties of Low-Rise Buildings

The experimental program of this research included the evaluation of the dynamic properties of the 101 school buildings using ambient vibration measurements. In-situ properties of low-rise buildings have not been extensively studied, mainly because of the difficulties associated with the modal analysis of the low amplitude records obtained and the potentially high influence of soil-structure interaction in some cases.

Fundamental modes of vibration could be clearly identified for 77 of the studied buildings, while two translational and one torsional mode were determined only for 28 buildings. For other cases either one or two modes were identified. One main outcome of the data analysis is the characterization of the evaluated schools for the seismic portfolio of each school. In particular, for two types of lateral load resisting systems -concrete shear walls (C2) and concrete frames with unreinforced masonry infill walls (C3), the database was extensive enough to do some further analysis (with 22 buildings for C2 and 32 for C3). For these, the approximate NBC formulae for fundamental period were evaluated, and the elastic part of the capacity curves used for the adapted seismic screening method were compared to the experimental data. Further, the first torsional mode periods and damping ratios were also analyzed.

The fit between the recorded data and the NBC expressions for the fundamental period is poor. By means of multiple linear regressions, expressions that significantly improve the predictions were determined. Experimental frequencies were always higher than the ones obtained from the theoretical capacity curves (as expected), with differences between 35% and 50%. Measured frequency values seem to be slightly high but generally in good agreement with the capacity curves. Experimental torsional periods were related to the building height and the fundamental period, obtaining a very poor fit. The large data dispersion is in agreement with the high incidence of irregularities in the studied buildings. Although the scatter of experimental viscous damping ratios is considerable, average values (of the order of 1% to 2%) are significantly lower than the customary 5% viscous damping commonly used for seismic design.

## 8.5. Statement of Originality

The following summarizes the original contributions of this research project:

- A seismic screening method adapted for schools in Québec was developed. The method considers the specific structural characteristics of school buildings, the province's seismicity and demographics, and it is up to date with the 2010 edition of NBC. Its framework is based on the FEMA154 methodology. It was validated by an extensive literature review and a comprehensive experimental program that included structural inspections and ambient vibration measurements in 101 buildings. Comparison with NRC92 and FEMA rapid screening methods clearly highlights the improvements of the developed method.
- The seismic vulnerability of 16 school campuses, comprising 101 individual buildings, was assessed using the developed method. So far this is the province's most extensive database, and gives a clear insight of the expected performance of school buildings in strong seismic events. Since the evaluated schools were designated as post-disaster shelters, their seismic screening is very important to assess which facilities can really fulfill this function without any special seismic retrofitting.
- As part of the experimental characterization of the 101 school buildings, a detailed database on the characteristics of the heavy, unreinforced masonry infill walls was compiled. These walls are very common in school buildings and their out-of-plane failure can compromise the life safety of the occupants either directly or by blocking egress routes.
- A database of the natural periods, mode shapes and corresponding equivalent modal viscous damping ratio was compiled for 77 low-rise school buildings. From these, 22 were reinforced concrete shear wall buildings (C2) and 32 reinforced concrete frames with unreinforced masonry infill walls (C3). To the author's knowledge, this is the most extensive such database for low rise buildings in Canada.
- Simplified expressions for the determination of the approximate period of concrete shear walls and concrete frame buildings as presented in the NBC were compared to the period determined from ambient vibration records to evaluate their validity for low-rise buildings. Better fitting expressions were derived based on the experimental data.

- The elastic part of the generic capacity curves used for the development of the adapted seismic screening method were compared to the period determined from ambient vibration testing for C2 and C3 buildings.
- Average experimental viscous damping values obtained from ambient vibration measurements of low-rise buildings were compared to recommendations on viscous damping of the NBC.

## 8.6. Research Limitations and Recommendations for Future Work

The present research involved the development of a rapid seismic assessment tool and therefore has the limitations intrinsic to these types of methodologies. As their name indicates, rapid seismic assessment tools are used to evaluate a large building stock, where resources and time per building evaluation need to be limited. A trade-off between the accuracy of the evaluation and the complexity of the application needs to be made, resulting in an approximate estimation of the expected seismic behaviour of each individual building. Detailed assessment is therefore still required to confirm the actual expected behaviour of buildings deemed to be at high or very risk, before retrofit solutions can be engineered, if and when needed. It must be understood that the proposed method is not intended for the rigorous seismic vulnerability assessment of a single building (or a reduced number of buildings), but rather for the evaluation of a large building stock, to roughly assess the relative vulnerability of buildings in order to prioritize future interventions.

The determination of the expected seismic performance of a building is based on the evaluation of its probability of collapse under the maximum considered earthquake. To this end, building types were characterized by capacity and fragility curves, as well as estimates of the fraction of the buildings in complete damage state that are expected to collapse. Generic curves and estimates developed in and for the United States were used, as per *Hazus-MH MR4 Technical Manual* (NIBS, 2003). Although an effort was made to validate the generic capacity curves, using in-situ dynamic properties of concrete shear wall (C2) and concrete frame buildings with unreinforced masonry infill walls (C3), the development of specific curves for school buildings in Québec or the validation of the existing curves for other common lateral load resisting types is strongly advisable. Specific curves can be developed for example by performing incremental dynamic analysis on relevant prototypes, as has been done for schools in British Columbia (APEGBC and UBC, 2011).

The schools that were studied were not randomly selected and they are not statistically representative of Québec's entire inventory of school buildings. As a matter of fact, school shelters were exclusively large high schools with a higher than average floor area, a more recent average construction year, and possibly different predominant lateral load resisting systems when compared to the entire building stock under the responsibility of the Ministry of Education. The evaluation of other, randomly selected schools is therefore strongly advisable to validate the methodology and modify it if deemed necessary.

As part of the experimental schedule of the present research project ambient vibration measurements were taken at all school buildings to determine their dynamic properties. The general limitations of ambient vibration tests therefore also apply to the results and conclusions obtained from the gathered data. Ambient vibration measurements rely on very small excitations, and it has been demonstrated in the past that the dynamic properties of buildings vary with the amplitude and duration of the shaking, especially when structural damage is progressively incurred. Monitoring results from damaged instrumented buildings subjected to earthquakes have indicated that their fundamental frequency could be reduced by a factor of as much as 3.5 (Trifunac et al., 2001a, Trifunac et al., 2001b). It is acknowledged that natural frequencies determined from ambient vibration measurements are not equivalent to the frequencies of the deformed structure under strong shaking, especially if the structure suffers permanent damage. There is also not a clear consensus on the factor to relate both, although some ranges and maximum values have been proposed.

Furthermore, although the collected database of dynamic properties is extensive compared with past research on low-rise buildings (especially in Canada), it is still too limited to generalize conclusions based on our observations regarding approximate period equations, damping estimates and validation of the elastic range of generic capacity curves for C2 and C3 buildings.

# Appendix A. Performance of Schools in Past Earthquakes and Seismic Mitigation Programs

## App. A.1. Performance of schools in past earthquakes

| Location | Date | Earthquake | Weekday, Time | Effects |
|---|---|---|---|---|
| Virginia, USA [1] | 23/08/11 | 5.8 $M_w$ Virginia | Tuesday, 1:51pm, schools in session | Two schools came close to collapse. One of the schools was the county's only high school. |
| New Zealand [2] | 04/09/2010 | 7.1 $M_w$ Canterbury | Saturday, 4:35am, schools not in session | Public schools performed well given the magnitude of the event. Only one school was significantly damaged, mainly due to soil liquefaction. Damage to other public schools was relatively low. |
| Haiti [3, 4] | 12/01/10 | 7.0 $M_w$ Haiti | Tuesday, 4:53pm, schools not in session. | Educational system totally collapsed. More than 1.300 schools were destroyed, and about half the nation's 15.000 primary and 1.500 secondary schools were affected. Although not specific estimates were found, many children were killed. |
| Sichuan, China [5] | 12/05/08 | 8.0 $M_w$ Sichuan (or Wenchuan) | Monday, 2:28pm, schools in session | Over 7000 schoolrooms collapsed. About 10.000 school children were killed. |
| Pakistan [6] | 08/10/05 | 7.8 $M_w$ Kashmir | Saturday, 8:50am, children in schools | More than 18.000 children were killed in school collapses.<br>More than 50.000 children seriously injured.<br>More than 10.000 schools collapsed. |
| Asia [6] | 26/12/04 | 9. $M_w$ Southeast Asia | Sunday, 00:58UTC | In Indonesia alone 40.900 students and 2.500 school personnel died.<br>Indonesia: more than 750 schools destroyed, 2135 damaged.<br>Sri Lanka: 51 schools destroyed, 100 damaged.<br>Maldives: 51 schools destroyed or damaged.<br>Thailand: 30 schools destroyed. |
| Mexico [7] | 21/01/03 | 7. $M_w$ Colima | Tuesday, 8:07pm | Damage to 387 schools and 94 university buildings. 84.000 students affected.<br>Two major schools had to be demolished. |
| China [6] | 24/02/03 | 6.3 $M_w$ Xinjiang | Monday, 10:03am, children in school | At least 20 children killed. Many more could have died (children were outside for physical education)<br>900 classrooms collapsed. |

| Location | Date | Earthquake | Weekday, Time | Effects |
|---|---|---|---|---|
| Turkey [6, 8-10] | 01/05/03 | 6.4 $M_w$ Bingol | Thursday, 3:20pm, schools not in session | 84 children and 1 teacher were killed in collapsed dormitory.<br>4 school buildings in Bingol collapsed.<br>More than 90% of schools in the area affected. |
| Dominican Republic [6] | 22/09/03 | 6.5 $M_w$ Puerto Plata | Monday, 12:45am, schools not in session | 6 public schools damaged in Puerto Plata.<br>44 damaged schools in Santiago. |
| Algeria [6, 11] | 21/05/03 | 6.8 $M_w$ Boumerdes | Wednesday, 7:48pm, schools not in session | 103 schools damaged beyond repair.<br>753 schools extensively damaged or destroyed. |
| Iran [6] | 22/06/02 | 6.4 $M_w$ Ab Garm | Saturday, 7:28am | 8 school buildings completely destroyed.<br>137 schools damaged. |
| Iran [6] | 26/12/03 | 6.6 $M_w$ Bam | Friday, 5:26am, schools not in session | 67 of 131 schools collapsed. The remaining were severely damaged. |
| Italy [5, 6, 12-14] | 31/10/02 | 5.6 $M_w$ Molise | Thursday, 11:40am, children in school | 27 children and 2 teachers were killed.<br>San Giuliani school collapsed. Out of 300 other schools evaluated, 20% suffered significant damage. |
| El Salvador [6] | 13/01/01 | 7.6 $M_w$ El Salvador | Saturday, 11:33am | 50% of fatalities were children.<br>85 schools damaged beyond repair.<br>279 schools with serious damage<br>1314 schools with slight damage |
| El Salvador [6] | 13/02/01 | 6.6 $M_w$ El Salvador (aftershock) | Tuesday, 8:22am, children in school | 22 preschoolers and their teacher killed. |

| Location | Date | Earthquake | Weekday, Time | Effects |
|---|---|---|---|---|
| India [6, 15] | 26/01/01 | 7.7 $M_w$ Bhuj | Friday, 8:16am, school not in session | 971 children and 31 teachers killed.<br>1051 elementary school students and 95 teachers seriously injured.<br>At least 1884 school buildings collapsed.<br>11761 school buildings suffered major to minor damage. |
| Peru [6, 9, 16] | 23/06/01 | 8.4 $M_w$ Arequipa | Saturday, 3:33pm | 98 school buildings severely damaged. |
| Colombia [6] | 25/01/99 | 6.2 $M_w$ Quindio | Monday, 1:19pm, semester break | Almost all schools in affected area damaged or destroyed.<br>35% of public schools in Armenia destroyed<br>74% of schools in Armenia and Pereira damaged. |
| Turkey [5, 6, 8, 9, 17] | 17/08/99 | 7.4 $M_w$ Kocaeli | Tuesday, 3:02am, schools not in session | 43 schools damaged beyond repair.<br>381 schools with minor or moderate damage.<br>50% of schools in Istanbul sustained some damage. |
| Taiwan [6] | 21/09/99 | 7.6 $M_w$ Chi-Chi | Tuesday, 1:47am, schools not in session | 51 schools collapsed.<br>786 schools were damaged.<br>22% of elementary, middle and high schools damaged.<br>71% of post-secondary institutions damaged.<br>Schools more severely impacted than other structures due to short column effects and cantilevered corridors at upper floors. |
| Mexico [7] | 30/09/99 | 7.4 $M_w$ Oaxaca | Thursday, 11:31am | 2.000 classrooms and 56.000 students affected. 451 Schools with minor damage, 17 schools with major damage. 5% of schools were demolished. |
| Portugal [6, 18] | 09/07/98 | 5.6 $M_w$ Faial, Azores | Thursday, 5:19am, schools not in session | Kindergarten severely damaged. |
| Iran [6] | 10/05/97 | 7.4 $M_w$ Ardekul | Saturday, 12:57pm | 110 girls killed in an elementary school collapse. |
| Venezuela [6, 19, 20] | 09/07/97 | 6.8 $M_w$ Cariaco | Monday, 3:24pm, children in school | 46 students were killed.<br>40% of collapsed buildings were schools. |

| Location | Date | Earthquake | Weekday, Time | Effects |
|---|---|---|---|---|
| Peru [6] | 12/11/96 | 7.5 $M_w$ Nazca | Tuesday, 3:33pm, schools not in session | 93 school buildings severely damaged. |
| Japan [6] | 17/01/94 | Hanshin-Awaji | Tuesday, 5:46am, schools not in session | Earthquake shaking and fire destroyed schools. Significant non-structural damage. |
| Oregon, USA [6] | 25/03/93 | 5.6 $M_w$ Scott Mills | Spring break | Molalla and Mount Angel High schools severely damaged. |
| Costa Rica [21] | 22/04/91 | 7.4 $M_w$ Talamanca | Monday, 3:57pm | 250 small schools were damaged. |
| Nepal [6] | 20/08/88 | 6.6 $M_w$ Bihar | Saturday, 4:39am, schools not in session | 950 school buildings were damaged. |
| Quebec, Canada [22, 23] | 25/11/88 | 6.0 $M_w$ Saguenay | Friday, 6:46pm | 16 of the 25 schools of the Chicoutimi School Commission suffered architectural damage, with repairs and retrofit costing 3 million Canadian dollars 2.8 million dollars in architectural damage to all 17 schools of the Baie des Ha! Ha! School Board. |
| Armenia [6] | 07/12/88 | 6.9 $M_w$ Spitak | Wednesday, 11:41am, children in school | An estimated 16000 children died. 380 children and youth institutions were destroyed. In Spitak and Leninakin 105 of 131 schools and kindergartens were destroyed. |
| Mexico [6, 24] | 19/09/85 | 8.1 $M_w$ Mexico City | Thursday, 7:17am, schools not in session | Many school buildings collapsed. |
| California, USA [25] | 24/04/84 | 6.2 $M_w$ Morgan Hill | Tuesday, 1:15pm | 6 schools constructed under the Field Act provisions were evaluated and no significant damage was found. |

| Location | Date | Earthquake | Weekday, Time | Effects |
|---|---|---|---|---|
| Idaho, USA [26] | 28/10/83 | 7.3 $M_w$ Borah Peak | Friday, 8:07am | Three schools with major damage, two of which had to be completely demolished. |
| California, USA [27] | 02/05/83 | 6.7 $M_w$ Coalinga | Monday, 11:42pm | 77 Field Act and 2 pre-Field Act school buildings affected (at 9 school sites). Pre-Field Act buildings had to be demolished. Field Act buildings performed well. |
| California, USA [27] | 25/05/80 | 6.2 $M_w$ Mammoth Lake | Sunday, 4:33pm | Two school sites affected with non-structural damage. |
| Algeria [6] | 10/10/80 | 7.3 $M_w$ El Asnam | Friday, 1:25pm, schools not in session | 85 schools collapsed.<br>70% of schools extensively damaged or destroyed.<br>Disproportionate damage to schools. |
| China [6] | 27/07/76 | 8.2 $M_w$ Tangshan | Wednesday, 3:42am, schools not in session | 2000 students killed in the dormitory of the College Mining Institute<br>Most school buildings in Tangshan destroyed. |
| Australia [6] | 02/06/79 | 6.1 $M_w$ Cadoux | Saturday, 9:48am | Brick chimneys fell though roof of school. |
| Ecuador [6] | 09/04/76 | 6.7 $M_w$ Esmeraldas | Friday | Severe damage to exterior of one school. |
| Guatemala [6] | 04/02/76 | 7.5 $M_w$ Guatemala City | Wednesday, 3:01am | Damage to non-structural wall at Universidad el Valle de Guatemala y Colegio Americano de Guatemala. |
| Turkey [6] | 06/09/75 | 6.8 $M_w$ Lice | Saturday, 12:20pm | One school heavily damaged. |
| Peru [6] | 03/10/74 | Lima | Wednesday, 9:21am | One classroom at the Agricultural University destroyed. |
| Mexico [6] | 28/08/73 | Veracruz | Tuesday, 3:51am | Heavy damages in the states of Morelos and Veracruz.<br>One school severely damaged. |
| California, USA [27, 28] | 09/02/71 | 6.6 $M_w$ San Fernando | Tuesday, 6:00am | Two school sites evaluated. All pre-Field Act buildings damaged beyond repair. Damage to post-Field Act very limited. |

| Location | Date | Earthquake | Weekday, Time | Effects |
|---|---|---|---|---|
| Peru [6] | 31/05/70 | 7.8 $M_w$ Peru | Sunday, 4:23pm, schools not in session | 6730 classrooms collapsed and hundreds seriously damaged. |
| Alaska, USA [6] | 27/03/64 | 9.2 $M_w$ Anchorage | Good Friday, schools not in session | Half of Anchorage's schools significantly damaged. One school destroyed. |
| Yugoslavia [6, 29] | 21/07/63 | 5.1 $M_w$ Skopje | Sunday, 5:17am, schools not in session | 44 schools destroyed. 40% of primary schools and 43% of secondary schools severely damaged. |
| California, USA [6, 27] | 21/07/52 | 7.5 $M_w$ Kern Country | Monday, 4:52am, schools not in session | 20 schools damaged or destroyed. Post 1933 Field Act buildings only suffered minor damages. |
| Japan [6] | 04/03/52 | Hokkaido | Tuesday | 400 schools collapsed. |
| Washington, USA [6] | 13/04/49 | M7.1 $M_w$ Olympia | Wednesday, noon, schools not in session | 2 children killed at school. 10 schools destroyed. 30 schools were damaged. 10.000 students affected. |
| Japan [6] | 28/06/48 | 7.3 $M_w$ Fukui | Monday, 5:13pm | School collapsed. |
| Canada [6] | 23/06/46 | 7.3 $M_w$ Vancouver Island | Sunday, 10:15am, schools not in session | Courtnay Elementary School damaged. |
| Quebec, Canada [30] | 05/09/44 | 5.6 $M_w$ Cornwall-Massena | Tuesday, 12:38pm | Considerable damage reported to one Collegiate and Vocational School in Cornwall. |
| California, USA [27] | 18/05/40 | 7.1 $M_w$ Imperial Valley | Saturday, 8:37pm | Nine school sites affected. Some severe damages to pre-Field Act buildings. Field Act buildings with no significant damage. |

| Location | Date | Earthquake | Weekday, Time | Effects |
|---|---|---|---|---|
| Montana, USA [6] | 31/10/35 | 6.0 $M_w$ Helena | Thursday, 9:48pm, schools not in session | 2 students killed. |
| California, USA [6, 27] | 10/03/33 | 6.3 $M_w$ Long Beach | Friday, 5:54pm, schools not in session | 2 school children were killed in collapsed gymnasium.<br>70 schools were collapsed.<br>120 schools were damaged. |
| New Zealand [6] | 17/06/29 | 7.8 $M_w$ Murchison | Monday, 10:17am | Nelson College damaged. |
| Montana, USA [6] | 27/06/25 | Helena | Saturday, 6:21p | Damage to High school in Three Forks.<br>Damage to Manhattan School. |
| California, USA [6] | 18/04/1906 | 8.3 $M_w$ San Francisco | Wednesday, 5:12am, schools not in session | 28 schools in burned area.<br>41 city schools sustained moderate to total loss damage. |
| South Carolina, USA [6] | 31/08/1886 | Charleston | Tuesday, 1:29pm | Damage to Charleston College |

## App. A.2. Seismic Mitigation Projects

| Location | Date | Number of buildings | Objectives | Outcome |
|---|---|---|---|---|
| British Columbia [31, 32] | 2004 | Over 850 schools | Screen all schools in high or moderate seismic zones. | About 750 schools have one or more building components rated at moderate to high risk. A method was developed to do a rapid, but conservative first estimation of the state of the schools (UBC100). The result of this project led to the BC school mitigation program. |
| British Columbia [32-43] | 2004-2019 | Around 750 (expected) | Assess and retrofit all at-risk schools | Retrofit in progress. Initial budget of 1.5 billion Canadian Dollars. Guidelines for the performance-based seismic retrofit of BC school buildings (assessment and retrofit) were developed. The evaluation is based on the toolbox method, a simplified procedure that allows combining the resistance of different lateral load resisting systems (hybrid systems). |
| Oregon, USA [44, 45] | 2007 | 1101 schools and 179 colleges | Seismic screening of essential facilities | 31% of the evaluated educational facilities have a low, 22% a moderate, 35% a high and 12% a very high collapse potential in a design-level earthquake. |
| San Remo, Italy [46] | Published in 2004 | 35 schools | Evaluate the vulnerability of the city's schools | Schools with mixed structural types, indicating a change of use of the building, were amongst the buildings found to be most vulnerable. Other buildings evaluated were either reinforced concrete or masonry constructions, being masonry more vulnerable. An integrated, multi-phase evaluation procedure was proposed and used to evaluate the vulnerability of the schools. |
| Potenza, Italy [13] | Published in 2004 | All the province's schools | Evaluate the vulnerability of schools | Proposed a screening method and used it to evaluate the schools of the province of Potenza. The first phase of the screening procedure is the estimation of the vulnerability of each building based on data already available to government agencies. The second phase is the evaluation of buildings identified in phase one, doing non-destructive testing, as ambient vibration testing, and collecting more detailed information. Finally the third phase is the detailed evaluation and retrofit of buildings where necessary |

| Location | Date | Number of buildings | Objectives | Outcome |
|---|---|---|---|---|
| Italy [47] | In progress | Approx. 50.000 school buildings | Develop a nationwide prioritisation procedure for the retrofit of school buildings | A two-phase procedure has been proposed. The first phase considers only some key characteristics of the structures, already collected by the Italian Ministry of Education. The second phase takes into consideration more specific characteristics of each school. It has only been applied locally, since the detailed information needed has only been collected for a limited number of masonry structures |
| Iran | 2002 to 2010 | 150 schools to strengthen (phase 1), 257.945 classrooms to reconstruct and strengthen (phase 2) | Strengthen schools and classrooms. | 131.935 classrooms need to be reconstructed, 126.010 classrooms need strengthening, 39% of schools are unsafe. In 2002 the strengthening of 150 schools begun. In 2006 the School Safety Act was passed in the Parliament to reconstruct 257.945 classrooms in 4 years. Budget: 4 billion US Dollars to strengthen 39% of the total vulnerable classrooms. |
| Algeria [11] | 2003 | 1800 schools inspected | Reconstruct or retrofit schools affected by the Bourmedes earthquake. | 122 schools had to be rebuilt and 560 were seriously damaged. Budget: US$ 70 million (estimated). |
| Berkeley, California [48] | 1992-2003 | 16 | Assess and retrofit all the community's schools. | 7 schools were found to pose serious life threats to students. The project was triggered by parents' concerns after the effects of the 1989 Loma Prieta earthquake. All schools have been intervened, 2 being rebuilt. Budget: 158 million US Dollars. |

| Location | Date | Number of buildings | Objectives | Outcome |
| --- | --- | --- | --- | --- |
| New Zealand [49, 50] | 1998-2001 | 21.100 buildings at 2.361 state schools. | Evaluate non-masonry buildings | Schools had been checked and retrofitted over the years, but no solid information existed. For that reason this project was carried out. The Ministry of Education adopted a national standard to evaluate all existing school buildings. Masonry buildings had been evaluated and retrofitted or demolished over the years, so they were excluded from the study. School buildings generally in good structural conditions. Only 4 buildings were found to have unacceptable level of risk. 11% of the buildings were found to have at least one structural defect. |
| Turkey [51] | 1999 | 2250 | Retrofit of Pre-code buildings (pre 1998) | Included assessment of schools, replacement and retrofit program. 80% of the screened buildings must be retrofitted or replaced. The project included non-structural mitigation and building maintenance, training for implementation and enforcement of construction standards and basic disaster awareness education. Budget of $US 320 million to retrofit and replace more than 1800 buildings. |
| Quito, Ecuador [52] | 1992-1994 | 340 schools for evaluation, 15 for retrofit. | Evaluate the vulnerability of public schools, strengthen sample of schools. | 60 school buildings were identified to be the most vulnerable. Three stages: First visit and determination of most vulnerable schools, rapid visual screening, detailed analysis. Budget: Retrofit cost between $US 7.000 and $US 244.000 for each school. |
| Venezuela [19, 20, 53] | In progress | All the country's schools | Assess and retrofit all the country's schools. | A general national school survey found that 46% of buildings were built before 1982 with deficient seismic design practices. A more detailed evaluation based on a data collection form was performed on a sample of 284 schools and a risk index was calculated. Detailed studies were conducted at 10 schools, including ambient vibration tests. |
| Greece [54] | Projected, estimated duration 15 years | Not determined. | Seismic assessment of schools. | Three-stage process proposed: rapid visual screening, approximate seismic evaluation, more detailed assessment. |

## App. A.3. References for App. A.1 and App A.2


[1] Caldwell, P. and Beavers, J. (2011). *Email: Central Virginia M5.8 earthquake update*.

[2] Mitchell, B. (2010). "The impact of the Canterbury (New Zealand) earthquake on schools." Available online at http://www.oecd.org (November 8, 2011).

[3] Save the Children (2010). "Helping Haiti's children the first three months of Save the children's earthquake response." Available online at http://www.savethechildren.org (December 8, 2011).

[4] Cawthorne, A. (2010). "Interview - Haitian education system 'totally collapsed'." *Reuters*, Available online at http://uk.reuters.com (December 8, 2011).

[5] OECD (2009). "Rebuilding schools after the Wenchuan Earthquake: China visits OECD, Italy and Turkey." *International Training Program on the Post-Earthquake Reconstruction of Public Facilities*, Paris, Italy and Turkey, December 1-11, 9 p.

[6] Risk RED, Petal, M., and Kunz, C. (2006). "Coalition for Global School Safety Mother Slide Show." *School disaster risk reduction: Think globally, act locally*, Available online at http://www.interragate.info/cogss/mothershow (February 5, 2011).

[7] de la Garza Reyna, J. (2004). "Earthquakes and educational infrastructure policy in Mexico." *Keeping schools safe in earthquakes, ad hoc experts' group meeting on earthquake safety in schools*, Paris, February 9-11, 140-146.

[8] Gur, T., Pay, A.C., Ramirez, J.A., Sozen, M.A., Irfanoglu, A., Bobet, A., and Johnson, A.M. (2009). "Performance of school buildings in Turkey during the 1999 Düzce and the 2003 Bingöl earthquakes." *Earthquake Spectra*, **25**(2): 239-256.

[9] Irfanoglu, A. (2009). "Performance of template school buildings during earthquakes in Turkey and Peru." *Journal of Performance of Constructed Facilities*, **23**(1): 5-14.

[10] Gülkan, P. (2004). "Obstacles to improving seismic safety of school buildings in Turkey." *Keeping schools safe in earthquakes, ad hoc experts' group meeting on earthquake safety in schools*, Paris, February 9-11, 64-87.

[11] Bendimerad, F. (2004). "Earthquake vulnerability of school buildings in Algeria." *Keeping schools safe in earthquakes, ad hoc experts' group meeting on earthquake safety in schools*, Paris, February 9-11, 35-51.

[12] Augenti, N., Cosenza, E., Dolce, M., Manfredi, G., Masi, A., and Samela, L. (2004). "Performance of school buildings during the 2002 Molise, Italy, earthquake." *Earthquake Spectra*, **20**(S1): 257-270.

[13] Dolce, M., Masi, A., Moroni, C., Liberatore, D., Laterza, M., Ponzo, F., Cacosso, G., D'Alessandro, G., Faggalla, M., Gilgliotti, R., Perillo, G.,

Samela, L., Santarsiero, G., Spera, G., Suanno, P., and Vona, M. (2004). "Valutazione della vulnerabilità sismica di edifici scolastici della Provincia di Potenza (in Italian)." *XI Congresso Nazionale, L'ingegneria Sismica in Italia*, Genova, Italy, January 25-29, 13 p.

[14] Dolce, M. (2004). "Seismic safety of schools in Italy." *Keeping schools safe in earthquakes, ad hoc experts' group meeting on earthquake safety in schools*, Paris, February 9-11, 52-63.

[15] Rai, D.C., Prasad, A.M., Jain, S.K., Rao, G., and Patel, P. (2002). "Hospitals and Schools." *Earthquake Spectra*, **18**(S1): 265-277.

[16] EERI (2001). "Preliminary observations on the southern Peru earthquake of June 23, 2001 " EERI Special Earthquake Report, Earthquake Engineering Research Institute, Oakland, CA.

[17] Yüzügüllü, Ö., Barbarosgoglu, G., and Erdik, M. (2004). "Seismic risk mitigation practices in school buildings in Istambul, Turkey." *Keeping schools safe in earthquakes, ad hoc experts' group meeting on earthquake safety in schools*, Paris, February 9-11, 88-100.

[18] Proença, J.M. (2004). "Damage in schools in the 1998 Faial earthquake in the Azores Islands, Portugal." *Keeping schools safe in earthquakes, ad hoc experts' group meeting on earthquake safety in schools*, Paris, February 9-11, 131-139.

[19] López, O.A., Hernández, J.J., Del Re, G., and Puig, J. (2004). "Seismic risk in schools: The Venezuelan project." *Keeping schools safe in earthquakes, ad hoc experts' group meeting on earthquake safety in schools*, Paris, February 9-11, 88-100.

[20] López, O.A., Hernández, J.J., Del Re, G., and Puig, J. (2004). "Reducción del riesgo sísmico en escuelas de Venezuela (in Spanish)." *IMME*, **42**(3): 33-56.

[21] Mitchell, D. and Tinawi, R. (1992). "Structural damage due to the April 22, 1991, Costa Rican earthquake." *Canadian Journal of Civil Engineering*, **19**(4): 586-605.

[22] Tinawi, R. and Mitchell, D. (1990). "1988 Saguenay earthquake. Damage to schools and post-disaster buildings." *Engineering in our Environment: CSCE Annual Conference and 1st Biennial Environmental Speciality Conference*, Hamilton, ON, May 16-18, 573-590.

[23] Mitchell, D., Tinawi, R., and Law, T. (1989). "The 1988 Saguenay earthquake - A site visit report." Canadian National Comittee on Earthquake Engineering, Open File Report #1999.

[24] Mitchell, D., Adams, J., DeVall, R.H., Lo, R.C., and Weichert, D. (1986). "Lessons from the 1985 Mexican earthquake." *Canadian Journal of Civil Engineering*, **13**(5): 535-557.

[25] Meehan, J.F. (1985). "The Morgan Hill Earthquake of April 24, 1984: Effects on Hospitals and Public School Buildings." *Earthquake Spectra*, **1**(3): 575-577.

[26] Adham, S.A. and Ballif, B. (1985). "Borah Peak, Idaho earthquake of October 28, 1983: Buildings and schools." *Earthquake Spectra*, **2**(1): 169-182.

[27] Jephcott, D.K. (1986). "50-Year record of Field Act seismic building standards for California schools." *Earthquake Spectra*, **2**(3): 621-629.

[28] Jephcott, D.K. and Hudson, D.E. (1974). "The performance of public school plants during the San Fernando earthquake." California Institute of Technology, Pasadena, CA.

[29] Milutinovic, Z. (2004). "Towards effective mitigation and emergency response in the former Yugoslav Republic of Macedonia." *Keeping schools safe in earthquakes, ad hoc experts' group meeting on earthquake safety in schools*, Paris, February 9-11, 88-100.

[30] Bruneau, M. and Lamontagne, M. (1994). "Damage from 20th century earthquakes in eastern Canada and seismic vulnerability of unreinforced masonry buildings." *Canadian Journal of Civil Engineering*, **21**(4): 643-662.

[31] Ventura, C.E., Taylor, G., White, T., Clement, G., Weichert, D., and Mill, A. (2004). "User guide for UBC-21 low-rise buildings, rapid seismic risk assessment software for British Columbia buildings." University of British Columbia, Vancouver, BC.

[32] Pandey, B. and Ventura, C.E. (2010). "The BC seismic retrofit program - Lessons learnt and application of innovations." *9th US National and 10th Canadian Conference on Earthquake Engineering: Reaching Beyond Borders*, Toronto, ON, July 25-29, Paper No. 1047.

[33] Taylor, G.W., White, T.W., and Ventura, C.E. (2006). "British Columbia school seismic mitigation program: performance-based school retrofit guidelines." *8th U.S. National Conference on Earthquake Engineering*, San Francisco, CA, April 18-22, 10 p.

[34] APEGBC and UBC (2005). "Bridging guidelines for the performance-based seismic retrofit of British Columbia school buildings." Association of Professional Engineers and Geoscientists of British Columbia, University of British Columbia and British Columbia Ministry of Education, Vancouver, BC.

[35] APEGBC and UBC (2005). "Commentary on bridging guidelines for the performance-based seismic retrofit of British Columbia school buildings." Association of Professional Engineers and Geoscientists of British Columbia, University of British Columbia and British Columbia Ministry of Education, Vancouver, BC.

[36] APEGBC and UBC (2005). "Supplement to bridging guidelines for the performance-based seismic retrofit of British Columbia school buildings." Association of Professional Engineers and Geoscientists of British Columbia, University of British Columbia and British Columbia Ministry of Education, Vancouver, BC.

[37] Pina, F. (2011). "Methodology for the seismic risk assessment of low-rise school buildings in British Columbia." Ph.D. thesis, Department of Civil Engineering, University of British Columbia, Vancouver. Available online at https://circle.ubc.ca/.

[38] Ventura, C.E., Taylor, G., Finn, W.D.L., and Pina, F. (2010). "Performance-based approach for seismic retrofit of schools in British Columbia." *9th US National and 10th Canadian Conference on Earthquake Engineering: Reaching Beyond Borders*, Toronto, July 25-29, Paper No. 1670.

[39] Sherstobitoff, J., Taylor, G., and Shuttleworth, J. (2010). "Seismic retrofit strategies for historical clay brick masonry school buildings; British Columbia, Canada " *9th US National and 10th Canadian Conference on Earthquake Engineering: Reaching Beyond Borders*, Toronto, July 25-29, Paper No. 1676.

[40] Pina, F., Taylor, G., Ventura, C.E., and Finn, W.D.L. (2010). "Seismic risk assessment tool for seismic mitigation of schools in British Columbia." *9th US National and 10th Canadian Conference on Earthquake Engineering: Reaching Beyond Borders*, Toronto, July 25-29, Paper No. 1193.

[41] Pina, F., Ventura, C.E., Taylor, G., and Finn, W.D.L. (2010). "Selection of ground motions for the seismic risk assessment of schools in British Columbia, Canada." *9th US National and 10th Canadian Conference on Earthquake Engineering: Reaching Beyond Borders*, Toronto, July 25-29, Paper No. 1624.

[42] Pina, F., Taylor, G., Ventura, C.E., and Finn, W.D.L. (2010). "Site response analysis for the seismic risk assessment of schools in British Columbia, Canada." *9th US National and 10th Canadian Conference on Earthquake Engineering: Reaching Beyond Borders*, Toronto, July 25-29, Paper No. 1154.

[43] APEGBC and UBC (2011). "Seismic retrofit guidelines." Association of Professional Engineers and Geoscientists of British Columbia, University of British Columbia and British Columbia Ministry of Education, Vancouver, BC.

[44] McConnell, V.S. (2007). "Statewide seismic needs assessment: Implementation of Oregon 2005 Senate Bill 2 relating to public safety, earthquakes, and seismic rehabilitation of public buildings." State of Oregon, Department of Geology and Mineral Industries, Portland, OR. Available online at http://www.oregongeology.org/sub/projects/rvs/default.htm.

[45] Tesfamariam, S., Wang, Y., and Saatcioglu, M. (2010). "Risk-based seismic retrofit prioritization of reinforced concrete civic infrastructure: Case study for state of Oregon schools and emergency facilities." *9th US National and 10th Canadian Conference on Earthquake Engineering: Reaching Beyond Borders*, Toronto, July 25-29, Paper No. 1507.

[46] Balbi, A., Frumento, S., Lagomarsino, S., and Penna, A. (2004). "Una procedura integrata per la valutazione della vulnerabilità sismica degli edifici scolastici (in Italian)." *XI Congresso Nazionale, L'ingegneria Sismica in Italia*, Genova, Italy, January 25-29, 21 p.

[47] Borzi, B., Ceresa, P., Faravelli, M., Fiorini, E., and Onida, M. (2011). "Definition of a prioritisation procedure for structural retrofitting of Italian school buildings." *COMPDYN 2011, III ECCOMAS Thematic Conference on Computational Methods in Structural Dynamics and Earthquake Engineering*, Corfu, Greece, May 26–28, Paper No. 302.

[48] Chakos, A. (2004). "Learning about seismic safety of schools from community experience in Berkeley, California." *Keeping schools safe in earthquakes, ad hoc experts' group meeting on earthquake safety in schools*, Paris, February 9-11, 45-51.

[49] Mitchell, B. (2004). "Making schools safer: The New Zealand experience." *Keeping schools safe in earthquakes, ad hoc experts' group meeting on earthquake safety in schools*, Paris, February 9-11, 119-130.

[50] Connell Wagner Limited (2003). "Technical Guidelines for Structural Mitigation Work." Connell Wagner Limited, New Zealand. Available online at http://www.minedu.govt.nz.

[51] COGSS (2007). "Schools disaster risk reduction: Think globally, act locally. Case Study: Turkey." The Coalition for Global School Safety Disaster Prevention Education. Available online at www.interragate.info/cogss/case-studies/turkey (October 1, 2009).

[52] EPN and GHI (1995). "The Quito, Ecuador, school earthquake safety project: Investing in Quito's future." Escuela Politécnica Nacional, GeoHazard International, Stanford, CA.

[53] Lopez, O., Marinilli, A., Bonilla, R., Fernandez, N., Dominguez, J., Coronel, G., Rodriguez, D., Tenreiro, E., and Vielma, R. (2010). "Seismic risk reduction in Venezuelan schools." *9th US National and 10th Canadian Conference on Earthquake Engineering: Reaching Beyond Borders*, Toronto, July 25-29, Paper No. 1014.

[54] Spence, R. (2004). "Strengthening school buildings to resist earthquakes: Progress in european countries." *Keeping schools safe in earthquakes, ad hoc experts' group meeting on earthquake safety in schools*, Paris, February 9-11, 217-228.

# Appendix B. Sample Report of the Dynamic Characteristics of a School Building

**6 - SCHOOL NAME WITHHELD**

**General Information**

| | | | |
|---|---|---|---|
| **Address:** | Withheld | | |
| **School Board:** | Withheld | | |
| **Number of Buildings:** | 11 | **Number of Students:** | 1511 |

**Location Plan:**

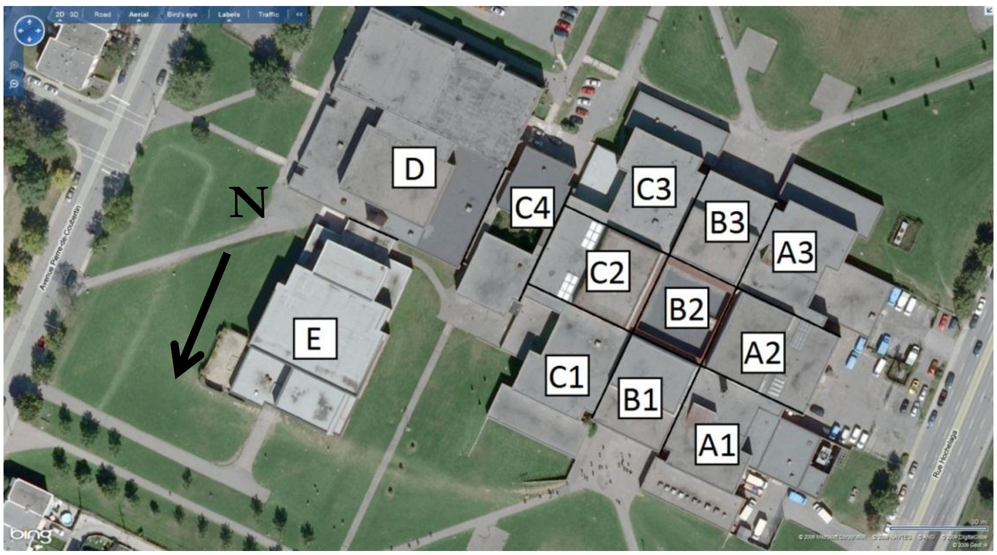


**Summary of Results**

| Building ID | 1st Translational NS Mode | | 1st Translational EW Mode | | 1st Torsional Mode* | |
|---|---|---|---|---|---|---|
| | Freq. [Hz] | Damp. [%] | Freq. [Hz] | Damp. [%] | Freq. [Hz] | Damp. [%] |
| A1 | 4.95 | 1.3 | 4.61 | 1.7 | 5.21 | 1.3 |
| A2 | 4.96 | 1.2 | 4.62 | 1.2 | - | - |
| A3 | 4.94 | 0.9 | 4.61 | 1.5 | 5.20 | 0.7 |
| B1 | 5.21 | 1.8 | 4.62 | 1.8 | 6.08 | 0.2 |
| B2 | - | - | - | - | - | - |
| B3 | 5.22 | 1.2 | 4.63 | 2.1 | 6.06 | 1.9 |
| C1 | - | - | 4.59 | 1.3 | - | - |
| C2 | - | - | 4.58 | 1.3 | - | - |
| C3 | - | - | 4.62 | 1.5 | - | - |
| C4 | - | - | 4.59 | 1.6 | - | - |
| D | - | - | - | - | - | - |

Note: The third mode of buildings A1 and B3 in the NS direction.

| **Building A1** | | | |
|---|---|---|---|
| **General Information** | | | |
| **ID:** | EM_BldA1 | **Height** | 9.1m |
| **Year of construction:** | 1967 | **Width NS dir.** | 42m |
| **Number of Storeys:** | 3 | **Width EW dir.** | 34m |
| **Structural System:** | Concrete frames with infill masonry shear walls | | |

**Typical Plan View**

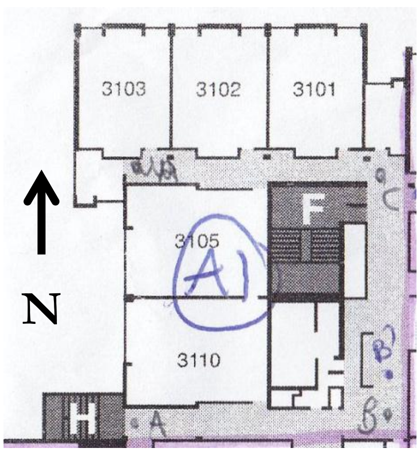


**Elevation View**

**Test Setup**

| **Date** | August 16 and 18 2010 | **Length of measurements** | 8min |
|---|---|---|---|
| **Staff** | H. Tischer, D. Hausfather | **Sampling frequency** | 128Hz |
| **Equipment** | 5 Micromed Tromino ENGYN PLUS tromographs | | |

**DOF Information**

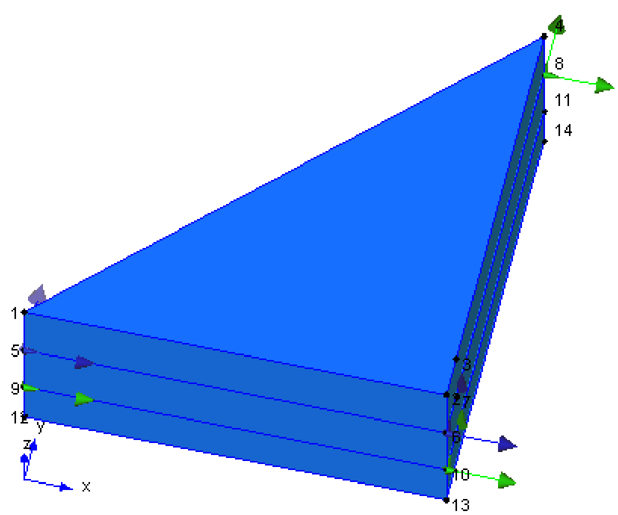

| **Building A1** | | | | | |
|---|---|---|---|---|---|
| **Modal Parameters** | | | | | |
| Mode ID | Direction | F (Hz) | Std. F (Hz) | ξ (%) | Std ξ (%) |
| 1 | EW | 4.61 | 0.01 | 1.7 | 0.2 |
| 2 | NS | 4.95 | 0.03 | 1.3 | 0.4 |
| 3 | NS | 5.21 | 0.01 | 1.3 | 0.1 |

**Singular Value Plot**

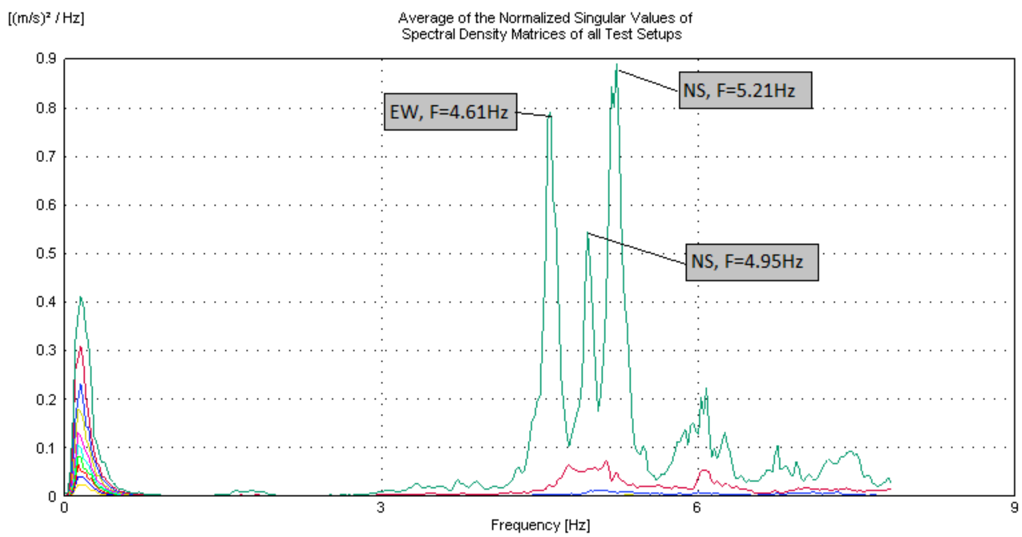


**Spectral Analysis Configuration:**

Number of frequency lines: 512
Sampling Frequency: 25.6Hz
Nyquist Frequency: 12.8Hz
Frequency Line Spacing: 0.025 Hz
Overlap: 66.67 %

**Comments**

- Height measured from ground floor (el. 69’ 96”) to main roof (el. 106’10”).
- Due to problems with the records on the roof, the movement of the roof was modeled to be the same as that of the third floor.
- Building E is not part of the school and was not tested.

## Building A1

### Modal Parameters

| Mode ID | Direction | F (Hz) | Std. F (Hz) | ξ (%) | Std ξ (%) |
|---|---|---|---|---|---|
| 1 | EW | 4.61 | 0.01 | 1.7 | 0.2 |
| 2 | NS | 4.95 | 0.03 | 1.3 | 0.4 |
| 3 | NS | 5.21 | 0.01 | 1.3 | 0.1 |

### Mode Shapes

**Mode 1 - EW**

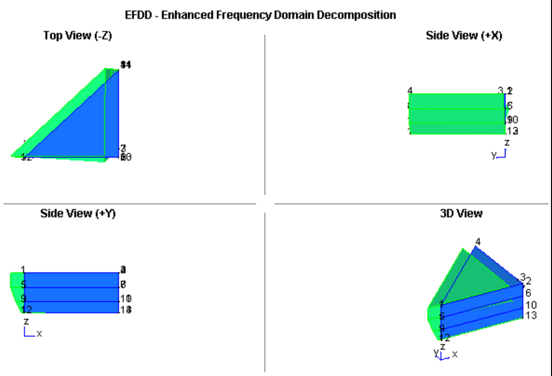


Notes: From EFDD.

**Mode 2 – NS**

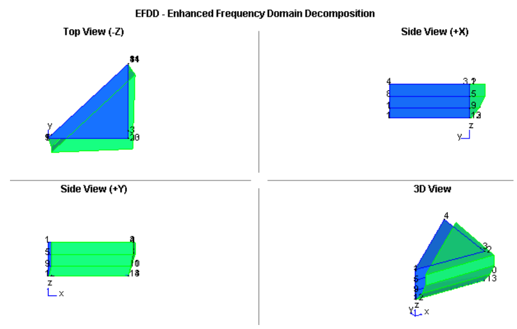


Notes: From EFDD. This mode has a slight EW component.

**Mode 3 - NS**

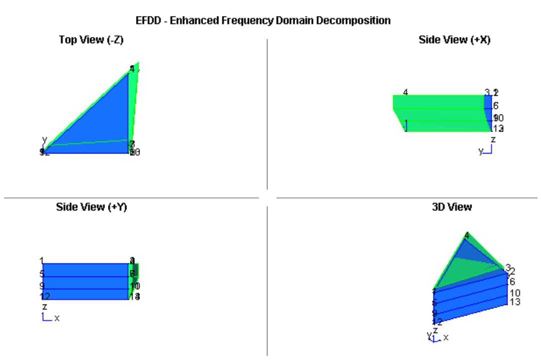


Notes: From EFDD. This mode has an EW component.

# Appendix C. Experimental Dynamic Properties of Buildings

## App. C.1. Concrete Shear Wall Buildings (C2)

**Table C.1.** General characteristics

| ID | Number of storeys | Height [m] | Width [m] | |
|---|---|---|---|---|
| | | | Transversal | Longitudinal |
| JM_BldT | 4 | 12.5 | 28 | 36 |
| JM_BldV | 4 | 12.5 | 36 | 45 |
| JM_BldW | 4 | 12.5 | 36 | 50 |
| JM_BldX | 4 | 12.5 | 40 | 60 |
| JM_BldY | 1 | 8.0 | 25 | 31 |
| JM_BldZ | 1 | 8.0 | 25 | 31 |
| JM_BldS | 1 | 12.5 | 50 | 50 |
| CaL_Bld1 | 6 | 21.0 | 22 | 25 |
| CaL_Bld3 | 6 | 21.0 | 22 | 25 |
| CaL_Bld4 | 2 | 9.0 | 34 | 40 |
| CaL_Bld5 | 5 | 21.0 | 45 | 55 |
| CaL_Bld6 | 3 | 12.0 | 23 | 63 |
| PD_BldA | 4 | 13.4 | 60 | 62 |
| PD_BldC | 4 | 13.4 | 40 | 62 |
| PD_BldD | 1 | 4.6 | 44 | 73 |
| SE_BldB | 2 | 7.3 | 55 | 90 |
| SE_BldD | 1 | 4.9 | 54 | 71 |
| MR_BldC | 2 | 10.6 | 60 | 64 |
| MR_BldC' | 2 | 12.0 | 37 | 55 |
| MR_BldD | 1 | 12.0 | 30 | 38 |
| PT_BldA | 3 | 11.2 | 33 | 58 |
| PT_BldB | 3 | 11.2 | 38 | 58 |

**Table C.2.** Experimental dynamic properties

| ID | Transversal Mode | | | | | Longitudinal Mode | | | | | Torsional Mode | | | | |
|---|---|---|---|---|---|---|---|---|---|---|---|---|---|---|---|
| | **F [Hz]** | **Std F [Hz]** | **ξ [%]** | **Std ξ [%]** | **T [s]** | **F [Hz]** | **Std F [Hz]** | **ξ [%]** | **Std ξ [%]** | **T [s]** | **F [Hz]** | **Std F [Hz]** | **ξ [%]** | **Std ξ [%]** | **T [s]** |
| JM_BldT | 3.54 | 0.02 | 1.2 | 0.2 | 0.28 | 3.69 | N/A | N/A | N/A | 0.27 | 5.94 | N/A | N/A | N/A | 0.17 |
| JM_BldV | 3.45 | 0.03 | 3.1 | 0.4 | 0.29 | 3.48 | 0.22 | 4.1 | 0.2 | 0.29 | 6.50 | 0.00 | 0.2 | 0.0 | 0.15 |
| JM_BldW | N/A | N/A | N/A | N/A | N/A | 3.49 | N/A | 4.3 | N/A | 0.29 | N/A | N/A | N/A | N/A | N/A |
| JM_BldX | 3.63 | 0.12 | 5.6 | 1.3 | 0.28 | 3.65 | 0.01 | 6.2 | 1.1 | 0.27 | N/A | N/A | N/A | N/A | N/A |
| JM_BldY | 6.49 | N/A | 6.1 | N/A | 0.15 | 7.45 | N/A | 3.1 | N/A | 0.13 | 8.07 | N/A | 0.1 | N/A | 0.12 |
| JM_BldZ | 4.32 | N/A | 2.6 | N/A | 0.23 | 3.70 | N/A | 1.8 | N/A | 0.27 | N/A | N/A | N/A | N/A | N/A |
| JM_BldS | 4.60 | N/A | 1.5 | N/A | 0.22 | 4.73 | N/A | 2.0 | N/A | 0.21 | 5.04 | N/A | 1.2 | N/A | 0.20 |
| CaL_Bld1 | 2.99 | 0.00 | 1.1 | 0.4 | 0.33 | 3.33 | 0.08 | 1.3 | 1.3 | 0.30 | 5.23 | N/A | 0.5 | N/A | 0.19 |
| CaL_Bld3 | 2.97 | 0.00 | 1.7 | 0.2 | 0.34 | 3.99 | 0.01 | 1.8 | 0.7 | 0.25 | 3.29 | N/A | 0.7 | N/A | 0.30 |
| CaL_Bld4 | 3.29 | N/A | 0.2 | N/A | 0.30 | 2.99 | N/A | 1.4 | N/A | 0.33 | 7.57 | N/A | 0.1 | N/A | 0.13 |
| CaL_Bld5 | 3.00 | 0.01 | 1.4 | 0.1 | 0.33 | 3.29 | 0.00 | 0.3 | 0.0 | 0.30 | 7.57 | 0.00 | 0.1 | 0.0 | 0.13 |
| CaL_Bld6 | 3.00 | N/A | 0.7 | N/A | 0.33 | 3.29 | N/A | 0.3 | N/A | 0.30 | 7.92 | N/A | 1.4 | N/A | 0.13 |
| PD_BldA | 3.84 | 0.03 | 1.1 | 0.6 | 0.26 | N/A | N/A | N/A | N/A | N/A | 4.73 | 0.02 | 1.8 | 0.4 | 0.21 |
| PD_BldC | 3.83 | 0.02 | 1.7 | 0.4 | 0.26 | N/A | N/A | N/A | N/A | N/A | 7.28 | 0.00 | 0.0 | 0.1 | 0.14 |
| PD_BldD | 7.28 | 0.00 | 0.1 | 0.0 | 0.14 | N/A | N/A | N/A | N/A | N/A | N/A | N/A | N/A | N/A | N/A |
| SE_BldB | 6.33 | N/A | 0.2 | N/A | 0.16 | 7.83 | N/A | 0.2 | N/A | 0.13 | N/A | N/A | N/A | N/A | N/A |
| SE_BldD | N/A | N/A | N/A | N/A | N/A | 8.63 | N/A | 0.1 | N/A | 0.12 | N/A | N/A | N/A | N/A | N/A |
| MR_BldC | 4.16 | 0.02 | 1.7 | 0.7 | 0.24 | 3.67 | 0.04 | 0.6 | 0.6 | 0.27 | 7.10 | 0.02 | 0.6 | 0.5 | 0.14 |
| MR_BldC' | 5.00 | 0.02 | 1.8 | 2.0 | 0.20 | 5.03 | 0.05 | 2.3 | 3.0 | 0.20 | N/A | N/A | N/A | N/A | N/A |
| MR_BldD | 6.06 | 1.05 | 4.4 | 1.0 | 0.17 | 5.00 | 0.00 | 0.2 | 0.0 | 0.20 | 12.93 | 0.00 | 0.1 | 0.0 | 0.08 |
| PT_BldA | 4.42 | N/A | 2.5 | N/A | 0.23 | 4.03 | N/A | 1.1 | N/A | 0.25 | N/A | N/A | N/A | N/A | N/A |
| PT_BldB | 6.25 | N/A | 2.6 | N/A | 0.16 | 4.41 | N/A | 1.4 | N/A | 0.23 | 11.46 | N/A | 0.5 | N/A | 0.09 |

F: Frequency Std F: Standard deviation of frequency ξ: Viscous damping Std ξ: Standard deviation of viscous damping T: Period

## App. C.2. Concrete Frame Buildings with Unreinforced Masonry Infill Walls (C3)

**Table C.3.** General characteristics

| ID | Number of storeys | Height [m] | Width [m] | |
|---|---|---|---|---|
| | | | Transversal | Longitudinal |
| A_BldA1 | 2 | 8.1 | 38 | 56 |
| A_BldA2 | 2 | 8.1 | 38 | 56 |
| A_BldA3 | 1 | 4.1 | 27 | 74 |
| A_BldA4 | 1 | 4.1 | 27 | 70 |
| A_BldB1 | 3 | 16.7 | 38 | 50 |
| A_BldB2 | 3 | 16.7 | 38 | 50 |
| CL_BldA1 | 2 | 7.1 | 62 | 62 |
| CL_BldB2 | 1 | 5.1 | 33 | 33 |
| CL_BldC | 2 | 7.1 | 53 | 53 |
| AV_Bld1A | 3 | 7.8 | 41 | 48 |
| AV_Bld1B | 2 | 7.6 | 20 | 36 |
| AV_Bld1C | 2 | 7.6 | 20 | 36 |
| EM_BldA1 | 3 | 9.1 | 34 | 42 |
| EM_BldA2 | 3 | 12.3 | 27 | 35 |
| EM_BldA3 | 3 | 9.1 | 34 | 42 |
| EM_BldB1 | 3 | 13.0 | 23 | 28 |
| EM_BldB3 | 3 | 13.0 | 23 | 28 |
| EM_BldC1 | 3 | 13.0 | 34 | 42 |
| EM_BldC2 | 3 | 13.0 | 26 | 34 |
| EM_BldC3 | 3 | 9.7 | 34 | 42 |
| EM_BldC4 | 2 | 6.5 | 18 | 51 |
| CaL_Bld2 | 6 | 21.0 | 48 | 58 |
| EAO_Bld2 | 3 | 11.8 | 17 | 17 |
| JG_BldA | 2 | 6.9 | 49 | 55 |
| JG_BldB | 2 | 10.5 | 46 | 65 |
| JG_BldD | 2 | 9.5 | 42 | 45 |
| SE_BldA | 2 | 7.3 | 32 | 50 |
| SE_BldC | 2 | 7.2 | 48 | 50 |
| SE_BldE | 2 | 11.7 | 50 | 66 |
| MR_BldA | 2 | 10.6 | 49 | 78 |
| MR_BldB | 2 | 10.6 | 60 | 78 |
| MR_BldB' | 2 | 10.6 | 18 | 74 |

**Table C.4.** Experimental dynamic properties

| ID | Transversal Mode | | | | | Longitudinal Mode | | | | | Torsional Mode | | | | |
|---|---|---|---|---|---|---|---|---|---|---|---|---|---|---|---|
| | **F [Hz]** | **Std F [Hz]** | **ξ [%]** | **Std ξ [%]** | **T [s]** | **F [Hz]** | **Std F [Hz]** | **ξ [%]** | **Std ξ [%]** | **T [s]** | **F [Hz]** | **Std F [Hz]** | **ξ [%]** | **Std ξ [%]** | **T [s]** |
| A_BldA1 | 4.90 | 0.00 | 1.4 | 0.2 | 0.20 | N/A | N/A | N/A | N/A | N/A | 5.65 | 0.05 | 0.5 | 0.6 | 0.18 |
| A_BldA2 | 4.86 | 0.02 | 1.7 | 0.2 | 0.21 | N/A | N/A | N/A | N/A | N/A | N/A | N/A | N/A | N/A | N/A |
| A_BldA3 | 10.05 | 0.00 | 2.4 | 0.0 | 0.10 | 14.62 | 0.00 | 0.1 | 0.0 | 0.07 | N/A | N/A | N/A | N/A | N/A |
| A_BldA4 | N/A | N/A | N/A | N/A | N/A | N/A | N/A | N/A | N/A | N/A | 11.22 | N/A | 0.2 | N/A | 0.09 |
| A_BldB1 | 4.86 | 0.03 | 2.2 | 1.0 | 0.21 | N/A | N/A | N/A | N/A | N/A | 5.68 | 0.03 | 0.6 | 0.0 | 0.18 |
| A_BldB2 | 3.87 | 0.01 | 2.1 | 0.7 | 0.26 | N/A | N/A | N/A | N/A | N/A | N/A | N/A | N/A | N/A | N/A |
| CL_BldA1 | 4.67 | N/A | 0.6 | N/A | 0.21 | 5.23 | N/A | 0.3 | N/A | 0.19 | 7.43 | N/A | 0.1 | N/A | 0.13 |
| CL_BldB2 | 9.07 | N/A | 0.3 | N/A | 0.11 | 9.08 | N/A | 0.1 | N/A | 0.11 | N/A | N/A | N/A | N/A | N/A |
| CL_BldC | 4.19 | 0.06 | 1.0 | 1.0 | 0.24 | 5.15 | 0.01 | 0.6 | 0.3 | 0.19 | N/A | N/A | N/A | N/A | N/A |
| AV_Bld1A | 4.92 | 0.01 | 1.2 | 0.3 | 0.20 | 6.34 | 0.04 | 1.6 | 0.1 | 0.16 | 8.74 | 0.08 | 0.4 | 0.1 | 0.11 |
| AV_Bld1B | 7.70 | 0.12 | 1.2 | 0.2 | 0.13 | 5.55 | 0.05 | 2.5 | 0.2 | 0.18 | N/A | N/A | N/A | N/A | N/A |
| AV_Bld1C | 6.95 | 0.05 | 2.1 | 0.2 | 0.14 | 5.62 | 0.16 | 3.2 | 0.6 | 0.18 | 8.89 | 0.02 | 2.1 | 1.5 | 0.11 |
| EM_BldA1 | 4.61 | 0.01 | 1.7 | 0.2 | 0.22 | 4.95 | 0.03 | 1.3 | 0.4 | 0.20 | 5.21 | 0.00 | 1.3 | 0.1 | 0.19 |
| EM_BldA2 | 4.96 | 0.03 | 1.2 | 0.2 | 0.20 | 4.62 | 0.01 | 1.2 | 0.1 | 0.22 | N/A | N/A | N/A | N/A | N/A |
| EM_BldA3 | 4.61 | 0.01 | 1.5 | 0.0 | 0.22 | 4.94 | 0.01 | 0.9 | 0.2 | 0.20 | 5.20 | 0.02 | 0.7 | 0.4 | 0.19 |
| EM_BldB1 | 4.62 | 0.01 | 1.8 | 0.2 | 0.22 | 5.21 | 0.00 | 1.0 | 0.1 | 0.19 | 6.08 | 0.00 | 0.2 | 0.1 | 0.16 |
| EM_BldB3 | 4.63 | 0.02 | 2.1 | 0.3 | 0.22 | 5.22 | 0.01 | 1.2 | 0.1 | 0.19 | 6.06 | 0.04 | 1.9 | 2.2 | 0.17 |
| EM_BldC1 | 4.59 | 0.05 | 1.3 | 0.4 | 0.22 | N/A | N/A | N/A | N/A | N/A | N/A | N/A | N/A | N/A | N/A |
| EM_BldC2 | N/A | N/A | N/A | N/A | N/A | 4.58 | 0.01 | 1.3 | 0.5 | 0.22 | N/A | N/A | N/A | N/A | N/A |
| EM_BldC3 | 4.62 | 0.01 | 1.5 | 0.0 | 0.22 | N/A | N/A | N/A | N/A | N/A | N/A | N/A | N/A | N/A | N/A |
| EM_BldC4 | 4.59 | 0.01 | 1.6 | 0.7 | 0.22 | N/A | N/A | N/A | N/A | N/A | N/A | N/A | N/A | N/A | N/A |
| CaL_Bld2 | 3.29 | 0.00 | 0.6 | 0.0 | 0.30 | 2.98 | 0.00 | 1.5 | 0.1 | 0.34 | 3.97 | 0.03 | 2.1 | 0.5 | 0.25 |
| EAO_Bld2 | 7.02 | 0.00 | 0.1 | 0.0 | 0.14 | 7.02 | 0.00 | 0.1 | 0.0 | 0.14 | 8.47 | 0.02 | 0.1 | 0.0 | 0.12 |

| | | | | | | | | | | | | | | | |
|---|---|---|---|---|---|---|---|---|---|---|---|---|---|---|---|
| JG_BldA | N/A | N/A | N/A | N/A | N/A | 8.09 | N/A | 0.2 | N/A | 0.12 | N/A | N/A | N/A | N/A | N/A |
| JG_BldB | 4.73 | N/A | 2.1 | N/A | 0.21 | 5.27 | N/A | 1.9 | N/A | 0.19 | N/A | N/A | N/A | N/A | N/A |
| JG_BldD | 7.23 | N/A | 0.7 | N/A | 0.14 | 7.18 | N/A | 0.7 | N/A | 0.14 | N/A | N/A | N/A | N/A | N/A |
| SE_BldA | N/A | N/A | N/A | N/A | N/A | 8.07 | N/A | 2.7 | N/A | 0.12 | N/A | N/A | N/A | N/A | N/A |
| SE_BldC | N/A | N/A | N/A | N/A | N/A | 5.82 | N/A | 2.7 | N/A | 0.17 | 7.90 | N/A | 0.2 | N/A | 0.13 |
| SE_BldE | 5.06 | N/A | 0.8 | N/A | 0.20 | 7.65 | N/A | 0.3 | N/A | 0.13 | N/A | N/A | N/A | N/A | N/A |
| MR_BldA | 5.00 | 0.00 | 0.2 | 0.0 | 0.20 | 3.86 | 0.01 | 0.7 | 0.5 | 0.26 | N/A | N/A | N/A | N/A | N/A |
| MR_BldB | 3.74 | 0.03 | 0.8 | 0.5 | 0.27 | 4.11 | 0.04 | 0.9 | N/A | 0.24 | N/A | N/A | N/A | N/A | N/A |
| MR_BldB' | 3.78 | 0.02 | 1.1 | 0.6 | 0.26 | 4.19 | 0.02 | 2.0 | 0.7 | 0.24 | 8.06 | 0.00 | 0.1 | 0.0 | 0.12 |

F: Frequency     Std F: Standard deviation of frequency     $\xi$: Viscous damping     Std $\xi$: Standard deviation of viscous damping     T: Period

# Appendix D. Linear Regression Analyses for Fundamental Period Data

## App. D.1. Procedure

To perform the linear regressions, data were first linearized by applying the natural logarithm to the $T_o$ expression above, obtaining:

$$y = \alpha + bx \tag{D.1}$$

Where $y = \ln(T_o)$, $x = ln(h)$ and $\alpha = ln(a)$.

While the parameter $b$ was obtained from the conditions set above, the parameter $\alpha$ was calculated from **Equation D.2** to obtain the best fit, where $\bar{y}$ and $\bar{x}$ are the mean values of $y$ and $x$.

$$\alpha = \bar{y} - b\bar{x} \tag{D.2}$$

Two measures were used to determine the quality of the fit: the coefficient of determination $R^2$and the standard error estimate $s_e$, applied to the linearized data. Note that the standard deviation of the sample can also be estimated by $s_e$. For a sample of $n$ data points, $R^2$and $s_e$ are calculated according to **Equations D.3** and **D.4**. To improve the fit, two outliers were removed from the C2 and three from the C3 data sets. These were selected according to the changes between the regression using the full data set and the regression without an outlier candidate.

$$R^2 = 1 - \frac{SS_{err}}{SS_{tot}} \tag{D.3}$$

$$s_e = \sqrt{\frac{SS_{err}}{n-2}} \tag{D.4}$$

Where

$$SS_{err} = \sum_{i=1}^{n}[y_i - (\alpha + bx_i)]^2 \tag{D.5}$$

$$SS_{tot} = \sum_{i=1}^{n}[y_i - \bar{y}]^2 \tag{D.6}$$

## App. D.2. Concrete Shear Wall Buildings (C2)

**Table D.1.** Results of regression analyses for C2 buildings with outlier

| Type | Coefficient b | Coefficient a | $s_e$ | $R^2$ |
|---|---|---|---|---|
| Unconstrained | 0.58 | 0.052 | 0.212 | 0.525 |
| Constrained | 0.75 | 0.036 | 0.222 | 0.482 |
| Constrained | 1.00 | 0.020 | 0.267 | 0.251 |

**Table D.2.** Results of regression analyses for C2 buildings without outlier

| Type | Coefficient b | Coefficient a | $s_e$ | $R^2$ |
|---|---|---|---|---|
| Unconstrained | 0.66 | 0.043 | 0.181 | 0.674 |
| Constrained | 0.75 | 0.035 | 0.184 | 0.662 |
| Constrained | 1.00 | 0.020 | 0.225 | 0.495 |

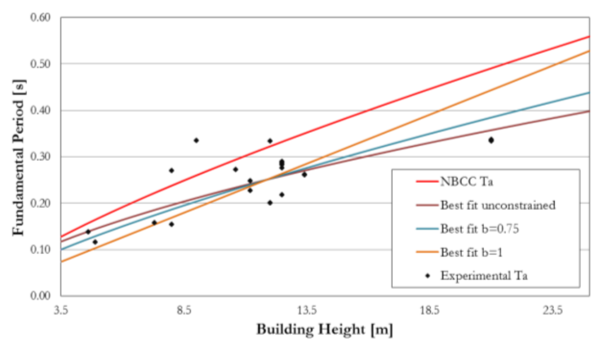


**Figure D.1.** Regression analyses for C2 buildings with outliers

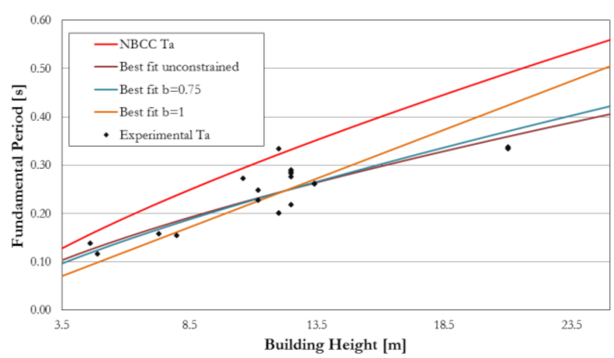


**Figure D.2.** Regression analyses for C2 buildings without outliers

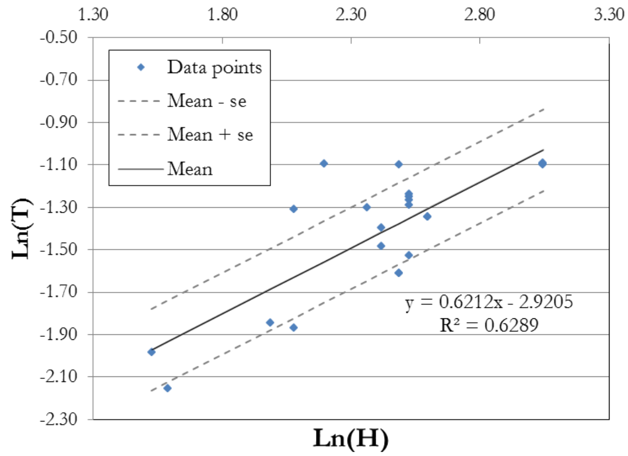


**Figure D.3.** Best fit unconstrained with outlier for C2

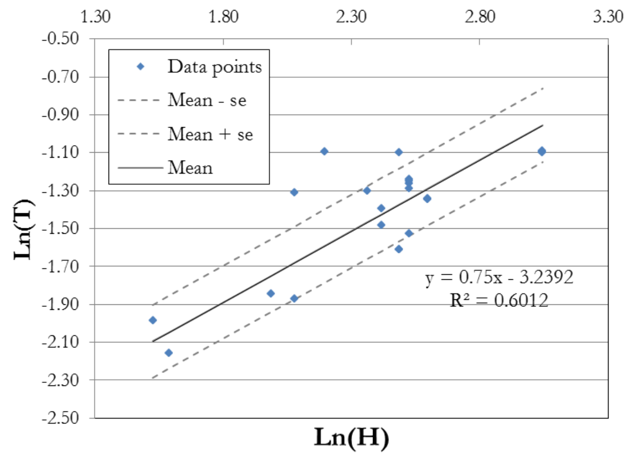


**Figure D.4.** Best fit b=0.75 with outlier for C2

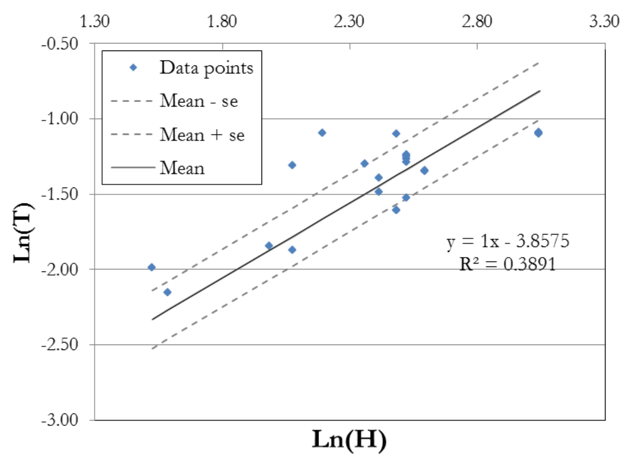


**Figure D.5.** Best fit b=1.0 with outlier for C2

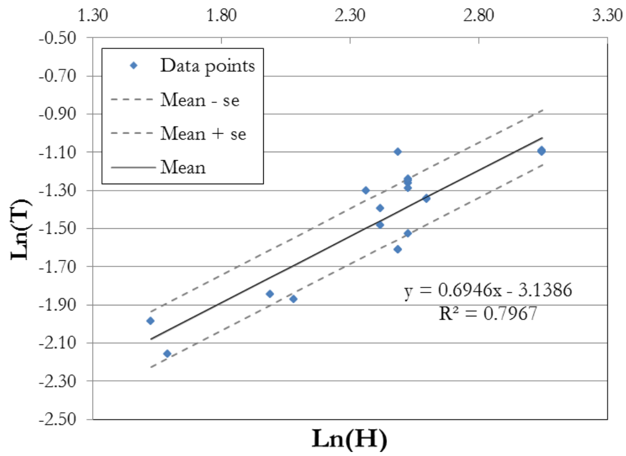


**Figure D.6.** Best fit unconstrained without outlier for C2

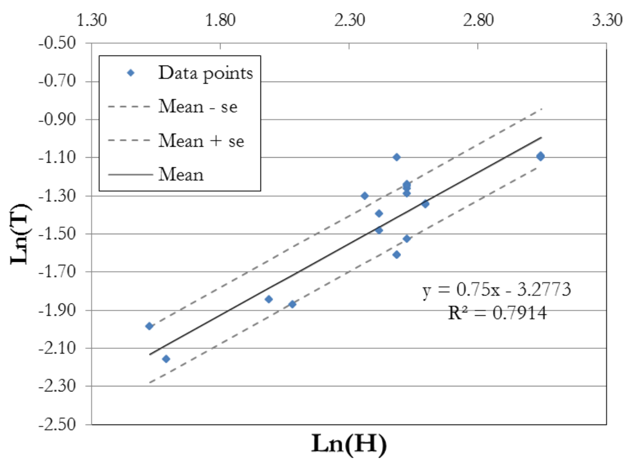


**Figure D.7.** Best fit b=0.75 without outlier for C2.

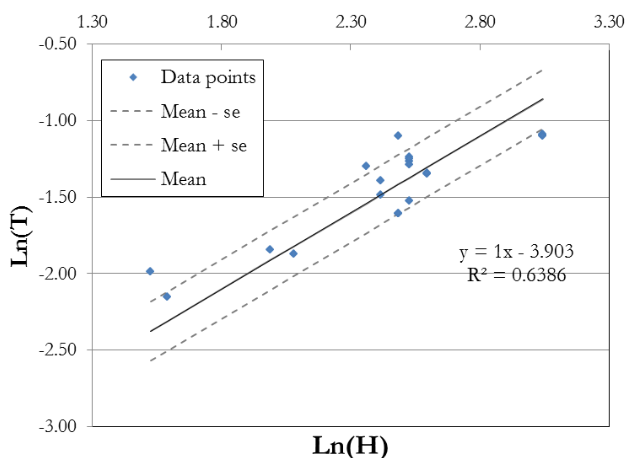


**Figure D.8.** Best fit b=1.0 without outlier for C2

## App. D.3. Concrete Frame Buildings with Unreinforced Masonry Infill Walls (C3)

**Table D.3.** Results of regression analyses for C3 buildings with outlier

| Type | Coefficient b | Coefficient a | $s_e$ | $R^2$ |
|---|---|---|---|---|
| Unconstrained | 0.62 | 0.054 | 0.193 | 0.629 |
| Constrained | 0.75 | 0.039 | 0.200 | 0.601 |
| Constrained | 1.00 | 0.021 | 0.247 | 0.389 |

**Table D.4.** Results of regression analyses for C3 buildings without outlier

| Type | Coefficient b | Coefficient a | $s_e$ | $R^2$ |
|---|---|---|---|---|
| Unconstrained | 0.69 | 0.043 | 0.145 | 0.797 |
| Constrained | 0.75 | 0.038 | 0.147 | 0.791 |
| Constrained | 1.00 | 0.020 | 0.194 | 0.639 |

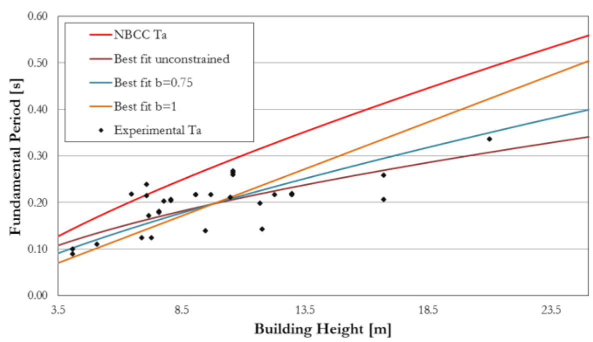


**Figure D.9.** Regression analyses for C3 buildings with outliers

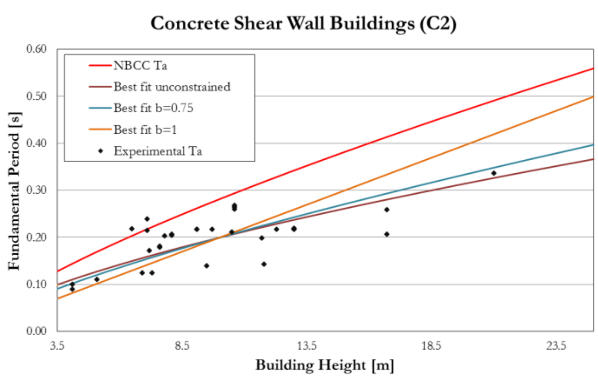


**Figure D.10.** Regression analyses for C3 buildings without outliers

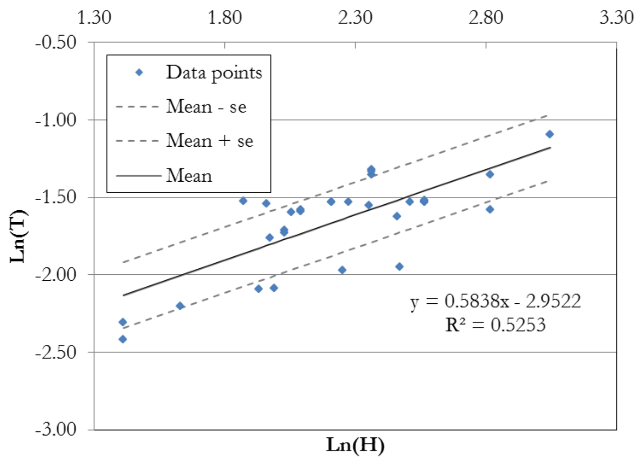


**Figure D.11.** Best fit unconstrained with outlier for C3

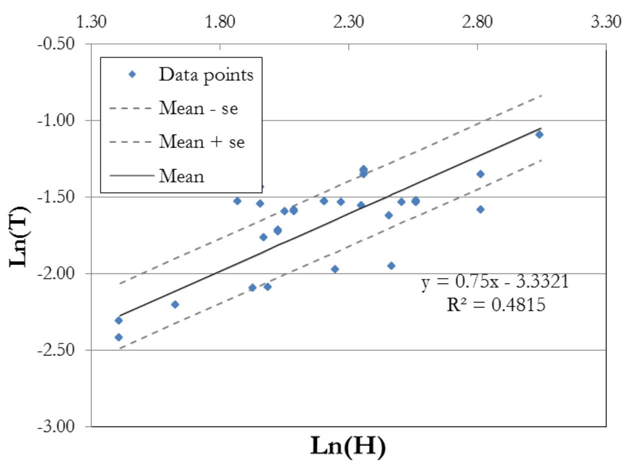


**Figure D.12.** Best fit b=0.75 with outlier for C3

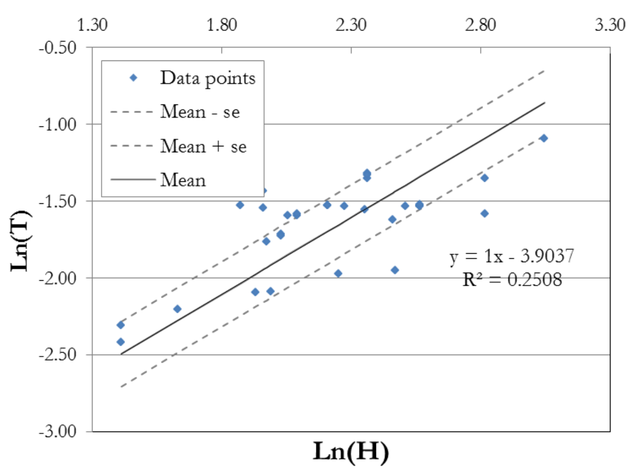


**Figure D.13.** Best fit b=1.0 with outlier for C3

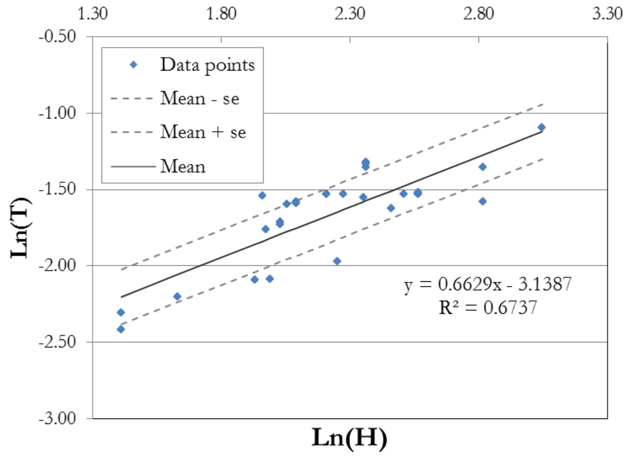


**Figure D.14.** Best fit unconstrained without outlier for C3

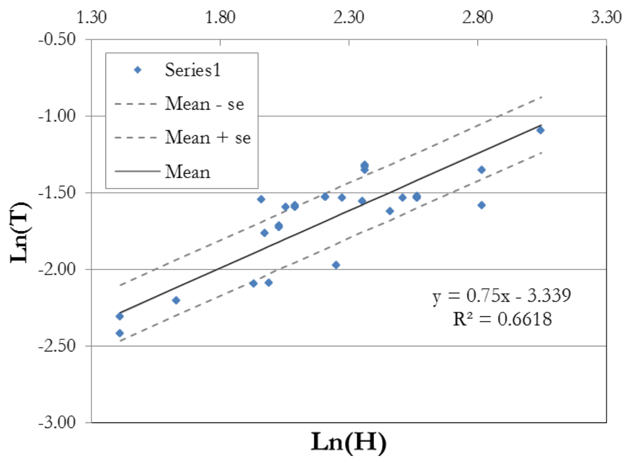


**Figure D.15.** Best fit b=0.75 without outlier for C3

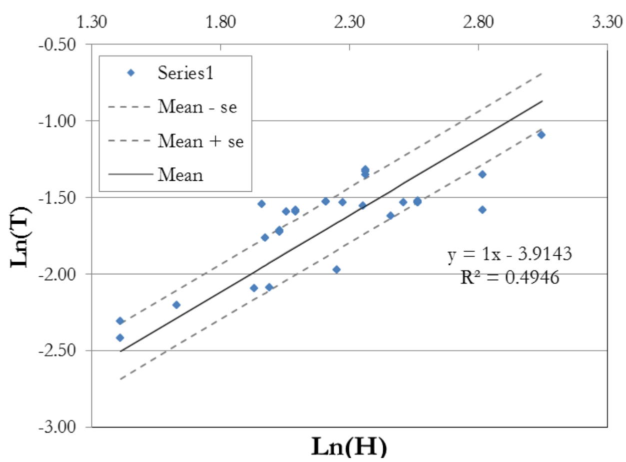


**Figure D.16.** Best fit b=1.0 without outlier for C3

# Appendix E. NBC Soil Type Estimates from Ambient Noise Data

## App. E.1. Natural Frequency Estimates

Natural frequency estimates, f, and their standard deviation, Std, are presented in **Table E.1**. These values were calculated from one record of ambient data per site, with f and Std calculated using the Micromed Grilla software, as exposed in **Chapter 5**. Values of the natural frequency minus one standard deviation and plus one standard deviation are also recorded in **Table E.1**, identified as fmin and fmax respectively.

**Table E.1.** Natural frequency estimates

| School | f [Hz] | Std [Hz] | fmin [Hz] | fmax [Hz] |
|---|---|---|---|---|
| S1_A | 10.31 | 0.07 | 10.2 | 10.4 |
| S2_CL | 17.56 | 4.55 | 13.0 | 22.1 |
| S3_AV | 14.38 | 0.56 | 13.8 | 14.9 |
| S4_JM | 3.72 | 0.06 | 3.7 | 3.8 |
| S5_LR | 16.72 | 4.95 | 11.8 | 21.7 |
| S6_EM | 51.56 | 0.19 | 51.4 | 51.8 |
| S7_CaL | 3.09 | 0.64 | 2.5 | 3.7 |
| S8_EAO | 16.88 | 5.69 | 11.2 | 22.6 |
| S9_R | 29.30 | 10.50 | 18.8 | 39.8 |
| S10_JG | 23.09 | 5.67 | 17.4 | 28.8 |
| S11_PD | 14.48 | 0.08 | 14.4 | 14.6 |
| S12_LM | 37.81 | 0.15 | 37.7 | 38.0 |
| S13_SE | 42.78 | 0.08 | 42.7 | 42.9 |
| S14_MR | 5.31 | 1.40 | 3.9 | 6.7 |
| S15_DJ | 36.25 | 0.06 | 36.2 | 36.3 |
| S16_PT | 1.88 | 0.02 | 1.9 | 1.9 |

## App. E.2. Rock Depth and Shear Wave Velocity Estimates

Rock depth estimates, h, are presented in **Table E.2**. Lower bounds and upper bounds are identified as hmin and hmax, and their average value was calculated. Finally, the estimates of the shear wave velocity, $V_{s\,rock}$, are presented.

**Table E.2.** Rock depth and shear wave velocity estimates

| School | hmin [m] | hmax [m] | Average h [m] | $V_{s\,rock}$ [m/s] |
|---|---|---|---|---|
| S1_A | 15.7 | 21.0 | 18.4 | 2200 |
| S2_CL | 10.5 | 15.7 | 13.1 | 1400 |
| S3_AV | 5.3 | 10.5 | 7.9 | 2200 |
| S4_JM | 5.3 | 10.5 | 7.9 | 2200 |
| S5_LR | 0.0 | 5.3 | 2.6 | 2200 |
| S6_EM | 0.0 | 5.3 | 2.6 | 2200 |
| S7_CaL | 5.3 | 10.5 | 7.9 | 2200 |
| S8_EAO | 0.0 | 5.3 | 2.6 | 2200 |
| S9_R | 0.0 | 5.3 | 2.6 | 2200 |
| S10_JG | 5.3 | 10.5 | 7.9 | 2200 |
| S11_PD | 5.3 | 10.5 | 7.9 | 2200 |
| S12_LM | 0.0 | 5.3 | 2.6 | 2200 |
| S13_SE | 0.0 | 5.3 | 2.6 | 2200 |
| S14_MR | 10.5 | 15.7 | 13.1 | 1400 |
| S15_DJ | 10.5 | 15.7 | 13.1 | 1000 |
| S16_PT | 21.0 | 26.2 | 23.6 | 1000 |

## App. E.3. Soil Shear Wave Velocity Estimates

Soil shear wave velocities were estimated considering the upper and lower bound estimates of the rock depth, hmin and hmax, as well as the natural frequency plus or minus its standard deviation, fmin and fmax. The obtained results for each case, as well as the average values, are recorded in **Table E.3**.

**Table E.3.** Soil shear wave velocity estimates

| School | Soil shear wave velocity, $V_{s\ soil}$ [m/s] | | | | |
|---|---|---|---|---|---|
| | hmin, fmin | hmin, fmax | hmax, fmin | hmax, fmax | Average |
| S1_A | 644 | 653 | 859 | 871 | 757 |
| S2_CL | 546 | 928 | 819 | 1391 | 969 |
| S3_AV | 290 | 314 | 580 | 627 | 459 |
| S4_JM | 77 | 79 | 154 | 159 | 118 |
| S5_LR | N/A | N/A | 247 | 455 | 351 |
| S6_EM | N/A | N/A | 1079 | 1087 | 1083 |
| S7_CaL | 51 | 78 | 103 | 157 | 104 |
| S8_EAO | N/A | N/A | 235 | 474 | 354 |
| S9_R | N/A | N/A | 395 | 836 | 615 |
| S10_JG | 366 | 604 | 731 | 1207 | 786 |
| S11_PD | 302 | 306 | 604 | 611 | 457 |
| S12_LM | N/A | N/A | 791 | 797 | 794 |
| S13_SE | N/A | N/A | 897 | 900 | 898 |
| S14_MR | 164 | 282 | 246 | 422 | 293 |
| S15_DJ | 1519 | 1524 | 2277 | 2285 | 1902 |
| S16_PT | 156 | 159 | 195 | 199 | 178 |

N/A: not possible to calculate values because rock depth equal to zero.

## App. E.4. Weighted Average Shear Wave Velocity Estimates

**Table E.4** shows the weighted shear wave velocity estimates, $V_{s30}$. These were calculated with the same considerations as the soil shear wave velocity estimates.

**Table E.4.** Weight average shear wave velocity estimates

| School | Weight average shear wave velocity, $V_{s30}$ [m/s] | | | | |
|---|---|---|---|---|---|
| | hmin, fmin | hmin, fmax | hmax, fmin | hmax, fmax | Average |
| S1_A | 971 | 981 | 1052 | 1064 | 1018 |
| S2_CL | 905 | 1188 | 1020 | 1395 | 1150 |
| S3_AV | 1023 | 1072 | 1113 | 1172 | 1097 |
| S4_JM | 377 | 388 | 389 | 400 | 389 |
| S5_LR | 2200 | 2200 | 923 | 1317 | 1562 |
| S6_EM | 2200 | 2200 | 1861 | 1866 | 2031 |
| S7_CaL | 265 | 383 | 270 | 395 | 330 |
| S8_EAO | 2200 | 2200 | 893 | 1344 | 1547 |
| S9_R | 2200 | 2200 | 1222 | 1711 | 1711 |
| S10_JG | 1172 | 1504 | 1292 | 1708 | 1440 |
| S11_PD | 1049 | 1056 | 1144 | 1152 | 1100 |
| S12_LM | 2200 | 2200 | 1677 | 1682 | 1939 |
| S13_SE | 2200 | 2200 | 1754 | 1756 | 1977 |
| S14_MR | 385 | 586 | 405 | 632 | 509 |
| S15_DJ | 1136 | 1137 | 1417 | 1418 | 1277 |
| S16_PT | 209 | 213 | 217 | 222 | 215 |

## App. E.5. NBC Soil Type Estimates

Considering the limiting values given in the NBC, the soil type was established for each $V_{s30}$ value presented in **Table E.4**. Upper and lower bound are presented in **Table E.5**, as well as the values obtained using the average $V_{s30}$ estimates. Finally, the values were adapted considering two conditions. First, categories A and B can only be used if the distance between the foundation and the rock depth is less than 3 m, even if $V_{s30}$ is higher than 760 m/s (NRC/IRC, 2010b). Second, for three schools the $V_{s30}$ value was slightly above a limit value. In these cases the lower soil type category was assumed. Both modifications are identified in **Table E.5** as corrected values.

**Table E.5.** NBC soil type estimates

| School | NBC soil type estimate | | | |
|---|---|---|---|---|
| | **Upper bound** | **Lower bound** | **Average** | **Corrected** |
| S1_A | B | B | B | C |
| S2_CL | B | B | B | C |
| S3_AV | B | B | B | C |
| S4_JM | C | C | C | D |
| S5_LR | A | B | A | B |
| S6_EM | A | A | A | A |
| S7_CaL | C | D | D | D |
| S8_EAO | A | B | A | B |
| S9_R | A | B | A | A |
| S10_JG | A | B | B | C |
| S11_PD | B | B | B | C |
| S12_LM | A | A | A | A |
| S13_SE | A | A | A | A |
| S14_MR | C | C | C | C |
| S15_DJ | B | B | B | C |
| S16_PT | D | D | D | D |

# Appendix F. Lateral Load Resisting System Types Descriptors

## App. F.1. Capacity Curves

**Table F.1.** Code building capacity curves – Moderate-code seismic design level, from (NIBS, 2003)

| Type* | Yield Capacity Point | | Ultimate Capacity Point | |
|---|---|---|---|---|
| | Dy (cm) | Ay (g) | Dy (cm) | Ay (g) |
| WLF | 0.91 | 0.300 | 16.46 | 0.900 |
| WPB | 0.79 | 0.200 | 11.94 | 0.500 |
| SMF-L | 0.79 | 0.125 | 13.97 | 0.375 |
| SMF-M | 2.26 | 0.078 | 27.05 | 0.234 |
| SBF-L | 0.79 | 0.200 | 9.55 | 0.400 |
| SBF-M | 3.07 | 0.167 | 24.64 | 0.333 |
| SLF | 0.79 | 0.200 | 9.55 | 0.400 |
| SCW-L | 0.48 | 0.160 | 6.58 | 0.360 |
| SCW-M | 1.40 | 0.133 | 12.47 | 0.300 |
| SIW-L | - | - | - | - |
| SIW-M | - | - | - | - |
| CMF-L | 0.51 | 0.125 | 8.94 | 0.375 |
| CMF-M | 1.47 | 0.104 | 17.55 | 0.312 |
| CSW-L | - | 0.200 | - | 0.500 |
| CSW-M | 1.32 | 0.167 | 13.18 | 0.417 |
| CIW-L | - | - | - | - |
| CIW-M | - | - | - | - |
| PCW | 0.91 | 0.300 | 10.97 | 0.600 |
| PCF-L | 0.61 | 0.200 | 7.32 | 0.400 |
| PCF-M | 1.32 | 0.167 | 10.54 | 0.333 |
| RML-L | 0.81 | 0.267 | 9.75 | 0.533 |
| RML-M | 1.75 | 0.222 | 14.07 | 0.444 |
| RMC-L | 0.81 | 0.267 | 9.75 | 0.533 |
| RMC-M | 1.75 | 0.222 | 14.07 | 0.444 |
| URM-L | - | - | - | - |
| URM-M | - | - | - | - |

* L: Low rise, M: Medium rise

**Table F.2.** Code building capacity curves – Low-code seismic design level, from (NIBS, 2003)

| Type* | Yield Capacity Point | | Ultimate Capacity Point | |
|---|---|---|---|---|
| | Dy (cm) | Ay (g) | Dy (cm) | Ay (g) |
| WLF | 0.61 | 0.200 | 10.97 | 0.600 |
| WPB | 0.41 | 0.100 | 5.97 | 0.250 |
| SMF-L | 0.38 | 0.062 | 5.82 | 0.187 |
| SMF-M | 1.12 | 0.039 | 11.28 | 0.117 |
| SBF-L | 0.41 | 0.100 | 3.99 | 0.200 |
| SBF-M | 1.55 | 0.083 | 10.26 | 0.167 |
| SLF | 0.41 | 0.100 | 3.99 | 0.200 |
| SCW-L | 0.25 | 0.080 | 2.74 | 0.180 |
| SCW-M | 0.69 | 0.067 | 5.21 | 0.150 |
| SIW-L | 0.30 | 0.100 | 3.05 | 0.200 |
| SIW-M | 0.86 | 0.083 | 5.77 | 0.167 |
| CMF-L | 0.25 | 0.062 | 3.73 | 0.187 |
| CMF-M | 0.74 | 0.052 | 7.32 | 0.156 |
| CSW-L | 0.30 | 0.100 | 3.81 | 0.250 |
| CSW-M | 0.66 | 0.083 | 5.49 | 0.208 |
| CIW-L | 0.30 | 0.100 | 3.43 | 0.225 |
| CIW-M | 0.66 | 0.083 | 4.95 | 0.188 |
| PCW | 0.46 | 0.150 | 4.57 | 0.300 |
| PCF-L | 0.30 | 0.100 | 3.05 | 0.200 |
| PCF-M | 0.66 | 0.083 | 4.39 | 0.167 |
| RML-L | 0.41 | 0.133 | 4.06 | 0.267 |
| RML-M | 0.89 | 0.111 | 5.87 | 0.222 |
| RMC-L | 0.41 | 0.133 | 4.06 | 0.267 |
| RMC-M | 0.89 | 0.111 | 5.87 | 0.222 |
| URM-L | 0.61 | 0.200 | 6.10 | 0.400 |
| URM-M | 0.69 | 0.111 | 4.60 | 0.222 |

* L: Low rise, M: Medium rise

**Table F.3.** Code building capacity curves – Pre-code seismic design level, from (NIBS, 2003)

| Type* | Yield Capacity Point | | Ultimate Capacity Point | |
|---|---|---|---|---|
| | Dy (cm) | Ay (g) | Dy (cm) | Ay (g) |
| WLF | 0.61 | 0.200 | 10.97 | 0.600 |
| WPB | 0.41 | 0.100 | 5.97 | 0.250 |
| SMF-L | 0.38 | 0.062 | 6.99 | 0.187 |
| SMF-M | 1.12 | 0.039 | 13.54 | 0.117 |
| SBF-L | 0.41 | 0.100 | 4.78 | 0.200 |
| SBF-M | 1.55 | 0.083 | 12.32 | 0.167 |
| SLF | 0.41 | 0.100 | 4.78 | 0.200 |
| SCW-L | 0.25 | 0.080 | 3.30 | 0.180 |
| SCW-M | 0.69 | 0.067 | 6.25 | 0.150 |
| SIW-L | 0.30 | 0.100 | 3.05 | 0.200 |
| SIW-M | 0.86 | 0.083 | 5.77 | 0.167 |
| CMF-L | 0.25 | 0.062 | 4.47 | 0.187 |
| CMF-M | 0.74 | 0.052 | 8.79 | 0.156 |
| CSW-L | 0.30 | 0.100 | 4.57 | 0.250 |
| CSW-M | 0.66 | 0.083 | 6.60 | 0.208 |
| CIW-L | 0.30 | 0.100 | 3.43 | 0.225 |
| CIW-M | 0.66 | 0.083 | 4.95 | 0.188 |
| PCW | 0.46 | 0.150 | 5.49 | 0.300 |
| PCF-L | 0.30 | 0.100 | 3.66 | 0.200 |
| PCF-M | 0.66 | 0.083 | 5.28 | 0.167 |
| RML-L | 0.41 | 0.133 | 4.88 | 0.267 |
| RML-M | 0.89 | 0.111 | 7.04 | 0.222 |
| RMC-L | 0.41 | 0.133 | 4.88 | 0.267 |
| RMC-M | 0.89 | 0.111 | 7.04 | 0.222 |
| URM-L | 0.61 | 0.200 | 6.10 | 0.400 |
| URM-M | 0.69 | 0.111 | 4.60 | 0.222 |

* L: Low rise, M: Medium rise

## App. F.2. Structural fragility Curves

**Table F.4.** Structural fragility curve parameters, from (NIBS, 2003)

| Type* | Moderate-code | | Low-code | | Pre-code | |
|---|---|---|---|---|---|---|
| | Median (cm) | Beta | Median (cm) | Beta | Median (cm) | Beta |
| WLF | 24.00 | 1.04 | 24.00 | 0.99 | 19.20 | 1.06 |
| WPB | 41.15 | 0.92 | 41.15 | 0.99 | 32.92 | 0.99 |
| SMF-L | 32.92 | 0.88 | 27.43 | 0.96 | 21.95 | 0.95 |
| SMF-M | 54.86 | 0.87 | 45.72 | 0.98 | 36.58 | 0.98 |
| SBF-L | 32.92 | 0.93 | 27.43 | 0.98 | 21.95 | 0.98 |
| SBF-M | 54.86 | 0.89 | 45.72 | 0.98 | 36.58 | 0.98 |
| SLF | 18.01 | 0.89 | 15.01 | 0.90 | 12.01 | 0.89 |
| SCW-L | 28.80 | 0.92 | 24.00 | 0.98 | 19.20 | 0.98 |
| SCW-M | 48.01 | 0.94 | 40.01 | 0.99 | 32.00 | 1.00 |
| SIW-L | - | - | 19.20 | 0.95 | 15.37 | 0.95 |
| SIW-M | - | - | 32.00 | 0.98 | 25.60 | 0.99 |
| CMF-L | 27.43 | 0.89 | 22.86 | 0.97 | 18.29 | 0.97 |
| CMF-M | 45.72 | 0.89 | 38.10 | 0.98 | 30.48 | 0.98 |
| CSW-L | 27.43 | 0.87 | 22.86 | 0.95 | 18.29 | 0.93 |
| CSW-M | 45.72 | 0.91 | 38.10 | 0.99 | 30.48 | 0.98 |
| CIW-L | - | - | 16.00 | 0.91 | 12.80 | 0.92 |
| CIW-M | - | - | 26.67 | 0.98 | 21.34 | 0.96 |
| PCW | 18.01 | 1.04 | 15.01 | 0.89 | 12.01 | 0.98 |
| PCF-L | 24.00 | 0.88 | 20.02 | 0.96 | 16.00 | 0.93 |
| PCF-M | 40.01 | 0.93 | 33.32 | 0.99 | 26.67 | 1.00 |
| RML-L | 24.00 | 0.94 | 20.02 | 0.92 | 16.00 | 0.94 |
| RML-M | 40.01 | 0.89 | 33.32 | 0.96 | 26.67 | 0.96 |
| RMC-L | 24.00 | 0.93 | 20.02 | 0.91 | 16.00 | 0.92 |
| RMC-M | 40.01 | 0.88 | 33.32 | 0.96 | 26.67 | 0.96 |
| URM-L | - | - | 12.01 | 1.08 | 9.60 | 1.18 |
| URM-M | - | - | 18.67 | 0.91 | 14.94 | 0.88 |

* L: Low rise, M: Medium rise

## App.F.3. Collapse rates

**Table F.7.** Collapse rates by model building type for complete structural damage, from (NIBS, 2003)

| Type* | Probability of collapse given complete damage state |
|---|---|
| WLF | 0.03 |
| WPB | 0.03 |
| SMF-L | 0.08 |
| SMF-M | 0.05 |
| SBF-L | 0.08 |
| SBF-M | 0.05 |
| SLF | 0.03 |
| SCW-L | 0.08 |
| SCW-M | 0.05 |
| SIW-L | 0.08 |
| SIW-M | 0.05 |
| CMF-L | 0.13 |
| CMF-M | 0.10 |
| CSW-L | 0.13 |
| CSW-M | 0.10 |
| CIW-L | 0.15 |
| CIW-M | 0.13 |
| PCW | 0.15 |
| PCF-L | 0.15 |
| PCF-M | 0.13 |
| RML-L | 0.13 |
| RML-M | 0.10 |
| RMC-L | 0.13 |
| RMC-M | 0.10 |
| URM-L | 0.15 |
| URM-M | 0.15 |

* L: Low rise, M: Medium rise

# Appendix G. Guidance on the classification of the severity of the structural weaknesses

## Guidance to severity of most common structural weaknesses

| Structural weakness | Effect on seismic performance | | |
|---|---|---|---|
| | **Low**<br>**1.0Sa** | **Significant**<br>**1.5Sa** | **Severe**<br>**3.5Sa** |
| **1. Horizontal irregularity** | | | |
| Re-entrant corners, L-, T-, E-, H-, U-shape | 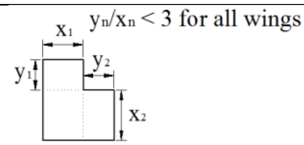 <br>All wings length/width ≤ 3.0 [1]<br><br>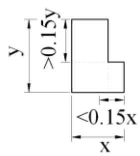 <br>Only one projection is greater than 15% of the total length in that direction. | 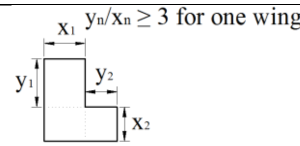 <br>One wing length/width > 3.0 [1]<br><br>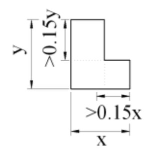 <br>Both projections are greater than 15% of the total length in that direction [2-4]. | 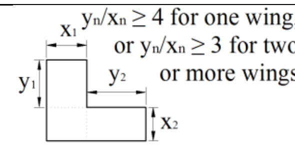 <br>Two or more wings length/width > 3.0 or one wing length/width > 4.0 [1]<br><br>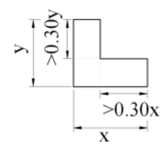 <br>Both projections are greater than 30% of the total length in that direction. |
| Torsion due to asymmetrical stairways<br><br>Note: Only applies to buildings with rigid or semi-rigid diaphragms [4]. | 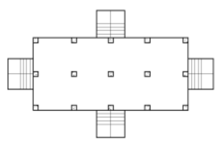<br>Rigidly connected stairways are placed symmetrically. | 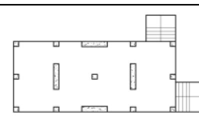<br>Rigidly connected stairways are placed asymmetrically in a relative rigid building. | 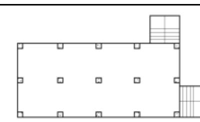<br>Rigidly connected stairways are placed asymmetrically in a relative light building [5]. |
| Torsion due to partition walls<br><br>Note: Only applies to buildings with rigid or semi-rigid diaphragms [4]. | 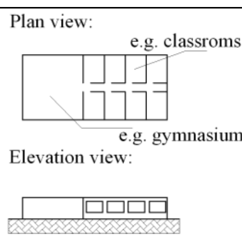 <br>One storey building with large open multipurpose rooms used along smaller classroom areas with relatively rigid interior walls [5] and the clear height of the open space one storey only. | 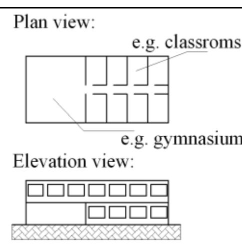 <br>Large open multipurpose rooms used along smaller classroom areas with relatively rigid interior walls [5] and the clear height of the open space one storey only. | 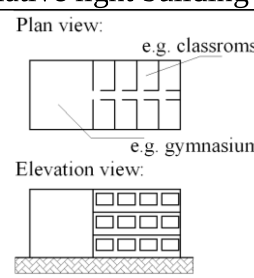 <br>Large open multipurpose rooms used along smaller classroom areas with relatively rigid interior walls [5] and the clear height of the open space more than one storey. |

| | | | |
|---|---|---|---|
| Torsion due to location of lateral force resisting system<br><br>Note: Only applies to buildings with rigid or semi-rigid diaphragms [4]. | | 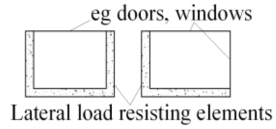<br>Primary lateral load resisting elements are at 90 degrees and at least one is non-parallel (elements have a C or L shape) [2, 3]. | |
| Diaphragm discontinuity | 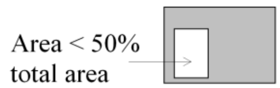<br>Opening is less than 50% of the gross enclosed diaphragm area. | 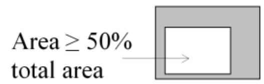<br>Opening is greater than 50% of the gross enclosed diaphragm area [2-4]. | <br>Opening is greater than 70% of the gross enclosed diaphragm area. |
| Out of plane offset | 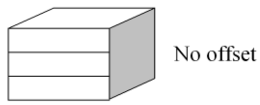<br>No discontinuity of vertical element of the lateral force resistant path. | 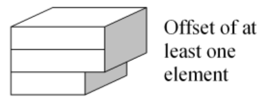<br>Discontinuity of at least one vertical element of the lateral force resistant path [4].<br>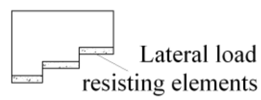<br>[2] | 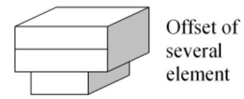<br>Discontinuity of several vertical element of the lateral force resistant path. |
| **2. Vertical Irregularities** | | | |
| Steps in elevation view | 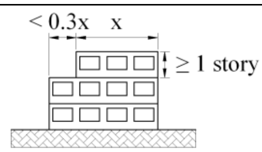<br>Horizontal dimension of any storey is less than 130% of that in an adjacent storey.<br>One storey penthouses with less than 10% the weight of the level below [6]. | 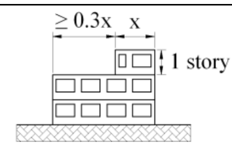<br>Horizontal dimension of any storey is more than 130% of that in an adjacent storey [6]. | 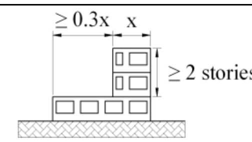<br>Horizontal dimension of any storey is more than 130% of that in an adjacent storey [6] and height above setbacks is at least 2 storeys [2]. |
| Soft storey | | | 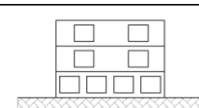<br>Stiffness of one storey is dramatically less than most other storeys [2, 5]. |

| | | | |
|---|---|---|---|
| Sloping terrain | 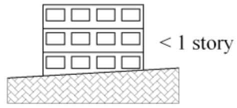<br>Slope rises less than 1 storey. | 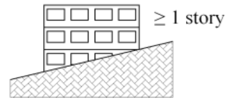<br>Slope rises at least one storey[2, 3, 7, 8]. | 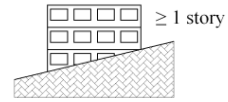<br>Slope rises more than 1.5 storeys [2, 3]. |
| Vertical change in structural type | The different lateral load resisting systems are of similar stiffness. | Soft over stiff lateral load resisting system. | Stiff over soft lateral load resisting system. |
| **3. Short concrete columns**<br>Columns < 70% storey height between floors clear of confining infill, beams or spandrels [1] | 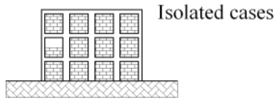<br>No, or only isolated, short columns [1]. | 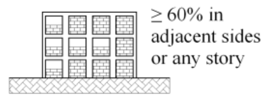<br>≥ 60% short columns in adjacent sides or<br>≥ 60% short columns<br>In one storey [1]. | 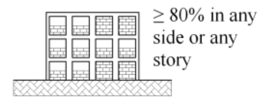<br>≥ 80% short columns in any one side or<br>≥ 80% short columns in any storey [1]. |
| **5. Pounding**<br>H is the level of the floor being considered or the height of the lower building [1].<br><br>Note: See details for Sa amplification factors. | 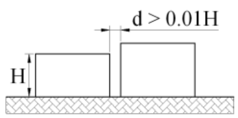<br>[1] | 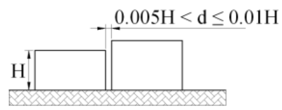<br>[1] | 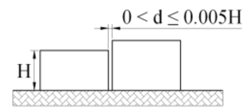<br>[1] |
| **6. Deterioration** | Damage or poor condition of non-structural elements only. | Damage or poor condition of view structural elements. | Generalized damage or poor condition of structural elements [8]. |

# Guidance to severity of other structural weaknesses

| Structural weakness | Effect on seismic performance | | |
|---|---|---|---|
| | **Low**<br>**1.0Sa** | **Significant**<br>**1.5Sa** | **Severe**<br>**3.5Sa** |
| **1. Vertical Irregularities** | | | |
| Mass irregularity<br><br>Note: roofs with significantly less mass than the storeys below are excluded [6]. | 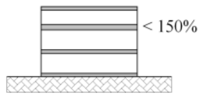<br>Effective mass of storey less than 150% effective mass of adjacent storey. | 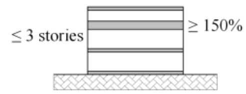<br>Effective mass of storey more than 150% effective mass of adjacent storey [2-4]. | 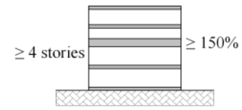<br>Effective mass of storey more than 150% effective mass of adjacent storey [2-4] and building has 4 storeys or more [2]. |
| In-plane discontinuity in vertical lateral load resisting elements | 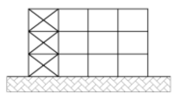<br>Horizontal offset distance less than the horizontal length of the vertical lateral force resistant element | 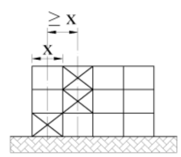<br>Horizontal offset distance at least the horizontal length of the vertical lateral force resistant element [2, 3] | 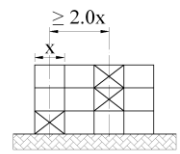<br>Horizontal offset distance at least twice the horizontal length of the vertical lateral force resistant element [2] |
| Cripple walls | | | 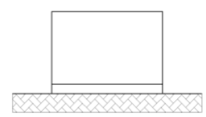<br>The building has cripple walls [2, 7]. |
| Sloped or inclined walls | 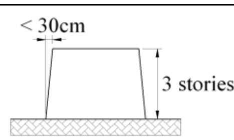<br>Walls have an out of plane slope less than 30cm per 3 storeys. | 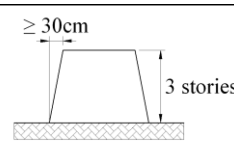<br>Walls have an out of plane slope greater than 30cm per 3 storeys [2]. | 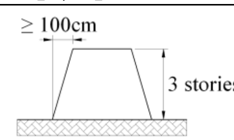<br>Walls have an out of plane slope greater than 100cm per 3 storeys [2]. |
| **2. Horizontal irregularity** | | | |
| Good lateral resistance in one direction but not in the other direction | | 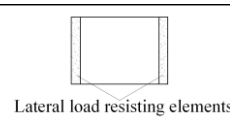<br>Lateral force resistance is in one direction only. | |
| Nonparallel system | | 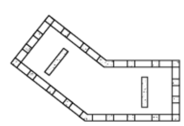<br>Some vertical lateral | |

| | | | |
|---|---|---|---|
| | | force resisting elements are not parallel to the major orthogonal axes of the system [2, 4, 6]. | |
| Long, narrow buildings | 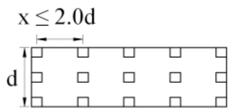<br>Spacing of lateral load resisting elements is < 2.0 building width [1]. | 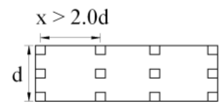<br>Spacing of lateral load resisting elements is > 2.0 building width [1]. | 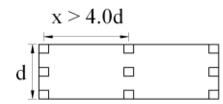<br>Spacing of lateral load resisting elements is > 4.0 building width [1]. |
| **Mayor modifications** | | | Any change in function, use or addition to the building, which results in significant increase in loading or weight [8]. |

**References**


[1] NZSEE (2006). "Assessment and improvement of the structural performance of buildings in earthquakes." New Zealand Society for Earthquake Engineering, Wellington, New Zealand. Available online at http://www.nzsee.org.nz.

[2] McConnell, V.S. (2007). "Statewide seismic needs assessment: Implementation of Oregon 2005 Senate Bill 2 relating to public safety, earthquakes, and seismic rehabilitation of public buildings." State of Oregon, Department of Geology and Mineral Industries, Portland, OR. Available online at http://www.oregongeology.org/sub/projects/rvs/default.htm.

[3] ICC (2006). "International Building Code." International Code Council, Country Club Hills, IL.

[4] ASCE (2010). "Minimum design loads for buildings and other structures (ASCE/SEI 7-10)." Structural Engineering Institute, American Society of Civil Engineers, Reston, VA.

[5] BSSC (1990). "FEMA149 Seismic considerations - Elementary and secondary schools." Building Seismic Safety Council, Federal Emergency Management Agency, Washington D.C.

[6] NRC/IRC (2010). "National Building Code of Canada 2010." National Research Council of Canada, Institute for Research in Construction, Ottawa, ON.

[7] ATC (2002). "FEMA154 Rapid visual screening of buildings for potential seismic hazard: A handbook." Applied Technology Council, Redwood, CA.

[8] NRC/IRC (1992). "Manual for screening of buildings for seismic investigation." National Research Council of Canada, Institute for Research in Construction, Ottawa, ON.

# Appendix H. Selected analyses of variance (ANOVA) for BSHs and Score Modifier Values Obtained from the Evaluation of the Sample of Schools

## App. H.1. Definitions

*SS*: sum of squares

*Df*: degrees of freedom

*MS*: mean square

*F*: calculated F-value

*P-value*: Probability to obtain a F-value greater or equal to the one actually observed

*F crit*: critical F-value corresponding to a *P-value* of 0.05 (significance level)

## App. H.2. Basic Structural Hazard Scores

Anova: Single Factor

SUMMARY

| *Groups* | *Count* | *Sum* | *Average* | *Variance* |
|---|---|---|---|---|
| Very High | 18 | 56.9 | 3.16 | 0.03 |
| High | 18 | 58.4 | 3.24 | 0.05 |
| Moderate | 44 | 145.2 | 3.30 | 0.04 |
| Low | 21 | 69.2 | 3.30 | 0.04 |

ANOVA

| *Source of Variation* | *SS* | *df* | *MS* | *F* | *P-value* | *F crit* |
|---|---|---|---|---|---|---|
| Between Groups | 0.27 | 3 | 0.092 | 2.26 | 0.09 | 2.70 |
| Within Groups | 3.94 | 97 | 0.041 | | | |
| | | | | | | |
| Total | 4.21 | 100 | | | | |

**Conclusion:**
No difference between groups

## App. H.3. Pre-Code Score Modifier

Anova: Single Factor

SUMMARY

| Groups | Count | Sum | Average | Variance |
|---|---|---|---|---|
| Very High | 18 | -15.6 | -0.87 | 0.10 |
| High | 18 | -9.6 | -0.53 | 0.24 |
| Moderate | 44 | -9.6 | -0.22 | 0.13 |
| Low | 21 | -2.8 | -0.13 | 0.09 |

ANOVA

| Source of Variation | SS | df | MS | F | P-value | F crit |
|---|---|---|---|---|---|---|
| Between Groups | 7.11 | 3 | 2.370 | 17.37 | 4.17E-09 | 2.70 |
| Within Groups | 13.23 | 97 | 0.136 | | | |
| | | | | | | |
| Total | 20.34 | 100 | | | | |

**Conclusion:**
High difference between groups

## App. H.4. Soil Type Score Modifier

Anova: Single Factor

SUMMARY

| Groups | Count | Sum | Average | Variance |
|---|---|---|---|---|
| Very High | 18 | 6 | 0.33 | 0.31 |
| High | 18 | -0.9 | -0.05 | 0.19 |
| Moderate | 44 | 2.6 | 0.06 | 0.18 |
| Low | 21 | 6.1 | 0.29 | 0.18 |

ANOVA

| Source of Variation | SS | df | MS | F | P-value | F crit |
|---|---|---|---|---|---|---|
| Between Groups | 2.08 | 3 | 0.695 | 3.43 | 0.02 | 2.70 |
| Within Groups | 19.65 | 97 | 0.203 | | | |
| | | | | | | |
| Total | 21.73 | 100 | | | | |

**Conclusion:**
Difference between groups

## App. H.5. Horizontal Irregularity Score Modifier

Anova: Single Factor

SUMMARY

| *Groups* | *Count* | *Sum* | *Average* | *Variance* |
|---|---|---|---|---|
| Very High | 18 | -20.2 | -1.12 | 0.45 |
| High | 18 | -12.1 | -0.67 | 0.53 |
| Moderate | 44 | -21.3 | -0.48 | 0.39 |
| Low | 21 | -0.6 | -0.03 | 0.02 |

ANOVA

| *Source of Variation* | *SS* | *df* | *MS* | *F* | *P-value* | *F crit* |
|---|---|---|---|---|---|---|
| Between Groups | 12.05 | 3 | 4.015 | 11.49 | 1.65E-06 | 2.70 |
| Within Groups | 33.91 | 97 | 0.350 | | | |
| | | | | | | |
| Total | 45.95 | 100 | | | | |

**Conclusion:**
Extremely high difference between groups

## App. H.6. Vertical Irregularity Score Modifier

Anova: Single Factor

SUMMARY

| *Groups* | *Count* | *Sum* | *Average* | *Variance* |
|---|---|---|---|---|
| Very High | 18 | -19 | -1.06 | 0.56 |
| High | 18 | -10.9 | -0.61 | 0.42 |
| Moderate | 44 | -11 | -0.25 | 0.28 |
| Low | 21 | -0.6 | -0.03 | 0.02 |

ANOVA

| *Source of Variation* | *SS* | *df* | *MS* | *F* | *P-value* | *F crit* |
|---|---|---|---|---|---|---|
| Between Groups | 12.37 | 3 | 4.124 | 13.88 | 1.34E-07 | 2.70 |
| Within Groups | 28.83 | 97 | 0.297 | | | |
| | | | | | | |
| Total | 41.20 | 100 | | | | |

**Conclusion:**
Extremely high difference between groups

## App. H.7. Pounding Score Modifier

Anova: Single Factor

SUMMARY

| *Groups* | *Count* | *Sum* | *Average* | *Variance* |
|---|---|---|---|---|
| Very High | 18 | -20.2 | -1.12 | 0.32 |
| High | 18 | -13 | -0.72 | 0.17 |
| Moderate | 44 | -33.4 | -0.76 | 0.16 |
| Low | 21 | -11.6 | -0.55 | 0.27 |

ANOVA

| *Source of Variation* | *SS* | *df* | *MS* | *F* | *P-value* | *F crit* |
|---|---|---|---|---|---|---|
| Between Groups | 3.27 | 3 | 1.091 | 5.11 | 2.52E-03 | 2.70 |
| Within Groups | 20.70 | 97 | 0.213 | | | |
| | | | | | | |
| Total | 23.97 | 100 | | | | |

**Conclusion:**
Difference between groups

# References

Adams, J., and Atkinson, G. (2003). "Development of seismic hazard maps for the proposed 2005 edition of the National Building Code of Canada." *Canadian Journal of Civil Engineering*, **30**(2): 255-271.

Akkar, S. D., and Miranda, E. (2005). "Statistical evaluation of approximate methods for estimating deformation demands on existing structures." *ASCE Journal of Structural Engineering*, **131**(1): 160-172.

Anagnostopoulos, S. A. (1996). "Building pounding re-examined: How serious a problem is it?" *11th Word Conference on Earthquake Engineering*, Acapulco, México, 1996, Paper No. 2108.

APEGBC, and UBC (2005). "Bridging guidelines for the performance-based seismic retrofit of British Columbia school buildings." Association of Professional Engineers and Geoscientists of British Columbia, University of British Columbia and British Columbia Ministry of Education, Vancouver, BC.

APEGBC, and UBC (2011). "Seismic retrofit guidelines." Association of Professional Engineers and Geoscientists of British Columbia, University of British Columbia and British Columbia Ministry of Education, Vancouver, BC.

ASCE (1998). "FEMA310 Handbook for the seismic evaluation of buildings: A prestandard." Federal Emergency Management Agency, Washington D.C.

ATC (1985). "ATC-13 Earthquake damage evaluation data for California." Applied Technology Council, Redwood, CA.

ATC (1988a). "FEMA154 Rapid visual screening of buildings for potential seismic hazard: A handbook." Applied Technology Council, Redwood, CA.

ATC (1988b). "FEMA155 Rapid visual screening of buildings for potential seismic hazard: supporting documentation." Applied Technology Council, Redwood, CA.

ATC (1996). "ATC-40 Seismic evaluation and retrofit of concrete buildings." Applied Technology Council, Redwood, CA.

ATC (2002a). "FEMA154 Rapid visual screening of buildings for potential seismic hazard: A handbook." Applied Technology Council, Redwood, CA.

ATC (2002b). "FEMA155 Rapid visual screening of buildings for potential seismic hazard: Supporting documentation." Applied Technology Council, Redwood, CA.

ATC (2004). "FEMA424 Design guide for improving school safety in earthquakes, floods, and high winds." Applied Technology Council, Redwood, CA.

ATC (2005). "FEMA440 Improvement of nonlinear static seismic analysis procedures." Applied Technology Council, Redwood, CA.

Augenti, N., Cosenza, E., Dolce, M., Manfredi, G., Masi, A., and Samela, L. (2004). "Performance of school buildings during the 2002 Molise, Italy, earthquake." *Earthquake Spectra*, **20**(S1): 257-270.

Balbi, A., Frumento, S., Lagomarsino, S., and Penna, A. (2004). "Una procedura integrata per la valutazione della vulnerabilità sismica degli edifici scolastici (in Italian)." *XI Congresso Nazionale, L'ingegneria Sismica in Italia*, Genova, Italy, January 25-29, 21 p.

Bendat, J. S., and Piersol, A. G. (1993). *Engineering applications of correlation and spectral analysis*, 2nd ed., Wiley, New York.

Borzi, B., Ceresa, P., Faravelli, M., Fiorini, E., and Onida, M. (2011). "Definition of a prioritisation procedure for structural retrofitting of Italian school buildings." *COMPDYN 2011, III ECCOMAS Thematic Conference on Computational Methods in Structural Dynamics and Earthquake Engineering*, Corfu, Greece, May 26–28, Paper No. 302.

Brayard, P. (2008). "Étude du comportement sismique des écoles typiques du Québec (in French)." Master's thesis, Département de Génie de la Construction, École de Technologie Supérieure, Montréal, QC. Available online at http://espace.etsmtl.ca/.

Brincker, R., Zhang, L., and Andersen, P. (2001). "Modal identification of output-only systems using frequency domain decomposition." *Smart Materials and Structures*, **20**: 441-445.

Brownjohn, J. M. W. (2003). "Ambient vibration studies for system identification of tall buildings." *Earthquake Engineering & Structural Dynamics*, **32**: 71-96.

Bruneau, M., and Lamontagne, M. (1994). "Damage from 20th century earthquakes in eastern Canada and seismic vulnerability of unreinforced masonry buildings." *Canadian Journal of Civil Engineering*, **21**(4): 643-662.

BSSC (1998). "FEMA302 NEHRP Recommended provisions for seismic regulations for new buildings and other structures,." Building Seismic Safety Council, Washington, D.C.

BSSC (2009). "FEMA P-750 NEHRP Recommended provisions for seismic regulations for new buildings and other structures." Building Seismic Safety Council, Washington, D.C.

Bulut, S., Bulut, S., and Tayli, A. (2005). "The dose of exposure and prevalence rates of post traumatic stress disorder in a sample of Turkish children eleven months after the 1999 Marmara earthquakes." *School Psychology International*, **26**(1): 55-70.

Calvi, G. M., Pinho, R., Magenes, G., Bommer, J. J., Restrepo-Vélez, L. F., and Crowley, H. (2006). "Development of seismic vulnerability assessment methodologies over the past 30 years." *ISET Journal of Earthquake Technology*, **43**(3): 75-104.

Castellaro, S., and Mulargia, F. (2009). "$V_{30}$ estimates using constrained H/V measurements." *Bulletin of the Seismological Society of America*, **99**(2 A): 761-773.

Castellaro, S., and Mulargia, F. (2010). "How far from a building does the ground-motion free-field start? The cases of three famous towers and a modern building." *Bulletin - Seismological Society of America*, **100**(5): 2080-2094.

Chagnon, D. (2006). "Parc immobilier scolaire / portrait des principales caractéristiques pour une étude de résistance aux secousses sismiques." Ministère de l'Éducation, des Loisirs et du Sport (MÉLS) - Direction Générale du Financement et de l'Équipement - Direction de l'Équipement Scolaire. Internal report, Québec, QC.

Chakos, A. (2004). "Learning about seismic safety of schools from community experience in Berkeley, California." *Keeping schools safe in earthquakes, ad hoc experts' group meeting on earthquake safety in schools*, Paris, February 9-11, 45-51.

Chang, S. E., McDaniels, T. L., Mikawoz, J., and Peterson, K. (2007). "Infrastructure failure interdependencies in extreme events: Power outage consequences in the 1998 Ice Storm." *Natural Hazards*, **41**(2): 337-358.

Choi, H. I., and Williams, W. J. (1989). "Improved time-frequency representation of multicomponent signals using exponential kernels." *Acoustics, Speech and Signal Processing, IEEE Transactions on*, **37**(6): 862-871.

Chopra, A. K. (1995). *Dynamics of structures: Theory and applications to earthquake engineering*, 1st ed., Prentice Hall, Englewood Cliffs, NJ.

Chopra, A. K., and Goel, R. K. (2000). "Evaluation of NSP to estimate seismic deformation: SDOF systems." *ASCE Journal of Structural Engineering*, **126**(4): 482-489.

Connell Wagner Limited (2003). "Technical Guidelines for Structural Mitigation Work." Connell Wagner Limited, New Zealand. Available online at http://www.minedu.govt.nz.

Cooley, J. W., and Tukey, J. W. (1965). "An Algorithm for the Machine Calculation of Complex Fourier Series." *Mathematics of Computation*, **19**(90): 297-301.

CSA (2006). "Seismic risk reduction of operational and functional components (OFCs) of buildings, CAN/CSA-S832-06 (R11)." Canadian Standards Association, Rexdale, ON.

De Roeck, G. B. P., and Ren, W. X. (2000). "Benchmark study on system identification through ambient vibration measurements." *IMAC 18, the International Modal Analysis Conference*, San Antonio, Texas, February, 1106-1112.

Dolce, M. (2004). "Seismic safety of schools in Italy." *Keeping schools safe in earthquakes, ad hoc experts' group meeting on earthquake safety in schools*, Paris, February 9-11, 52-63.

Dolce, M., Masi, A., Moroni, C., Liberatore, D., Laterza, M., Ponzo, F., Cacosso, G., D'Alessandro, G., Faggalla, M., Gilgliotti, R., Perillo, G., Samela, L., Santarsiero, G., Spera, G., Suanno, P., and Vona, M. (2004). "Valutazione della vulnerabilità sismica di edifici scolastici della Provincia di Potenza (in Italian)." *XI Congresso Nazionale, L'ingegneria Sismica in Italia*, Genova, Italy, January 25-29, 13 p.

Faccioli, E., Pessina, V., Calvi, G. M., and Borzi, B. (1999). "A study on damage scenarios for residential buildings in Catania city." *Journal of Seismology*, **3**(3): 327-343.

Felice, G. d., and Giannini, R. (2001). "Out-of-Plane Seismic Resistance of Masonry Walls." *Journal of Earthquake Engineering*, **5**(2): 253-271.

Figueiredo, A. C. A., Nave, M. F. F., and Contributors of JET-EFDA (2004a). "Time–Frequency analysis of non-stationary signals in fusion plasmas using the Choi-Williams distribution." *Nuclear Fusion* **44**(10): L17-L20.

Figueiredo, A. C. A., Nave, M. F. F., and Contributors of JET-EFDA (2004b). "Time–Frequency analysis of nonstationary fusion plasma signals: A comparison between the Choi-Williams distribution and Wavelets." *Review of Scientific Instruments*, **75**(10): 4268-4270.

Finn, W. D. L., and Wightman, A. (2003). "Ground motion amplification factors for the proposed 2005 edition of the National Building Code of Canada." *Canadian Journal of Civil Engineering*, **30**(2): 272-278.

Gilles, D. (2011). "In situ dynamic characteristics of reinforced concrete shear wall buildings." Ph.D. thesis, Department of Civil Engineering and Applied Mechanics, McGill University, Montréal, QC. Available online at http://digitool.library.mcgill.ca/.

Gilles, D., McClure, G., and Chouinard, L. E. (2011). "Uncertainty in fundamental period estimates leads to inaccurate design seismic loads." *Canadian Journal of Civil Engineering*, **38**(8): 870-880.

Goel, R. K., and Chopra, A. K. (1998). "Period formulas for concrete shear wall buildings." *ASCE Journal of Structural Engineering*, **124**(4): 426-433.

Hans, S., Boutin, C., Ibraim, E., and Roussillon, P. (2005). "In situ experiments and seismic analysis of existing buildings. Part I: Experimental investigations." *Earthquake Engineering & Structural Dynamics*, **34**(12): 1513-1530.

Hong, L. L., and Hwang, W. L. (2000). "Empirical formula for fundamental vibration periods of reinforced concrete buildings in Taiwan." *Earthquake Engineering & Structural Dynamics*, **29**: 327-338.

Ingham, J. M. (2011). "Building performance in the 2010/2011 Canterbury earthquake swarm." *COMPDYN 2011, III ECCOMAS Thematic Conference on Computational Methods in Structural Dynamics and Earthquake Engineering*, Corfu, Greece, May 26–28, Paper No. 687.

Ivanovic, S. S., Trufinac, M. D., and Todorovska, M. I. (2000). "Ambient vibration tests of structures - A review." *ISET Journal of Earthquake Technology*, **37**(4): 165-197.

Jeng, V., and Tzeng, W. L. (2000). "Assessment of seismic pounding hazard for Taipei City." *Engineering Structures*, **22**(5): 459-471.

Jephcott, D. K. (1986). "50-Year record of Field Act seismic building standards for California schools." *Earthquake Spectra*, **2**(3): 621-629.

Joshi, G. C., and Kumar, R. (2010). "Preliminary seismic vulnerability assessment of Mussoorie Town, Uttarakhand (India)." *Journal of Building Appraisal*, **5**(4): 357-368.

Karbassi, A., and Nollet, M.-J. (2008). "Development of an index assignment procedure compatible with the regional seismicity in the province of Quebec for the rapid visual screening of existing buildings." *Canadian Journal of Civil Engineering*, **35**(9): 925-937.

Lang, K. (2002). "Seismic vulnerability of existing buildings." Ph.D. Thesis, Institute of Structural Engineering, Swiss Federal Institute of Technology, Zürich, Switzerland. Available online at http://e-collection.library.ethz.ch/.

Lin, L., and Adams, J. (2011). "Engineering caracteristics of ground motion records of the Val-des-Bois, Quebec, earthquake of June 23, 2010." *CSCE 2011 General Conference*, Ottawa, ON, June 14-17, Paper No. 092.

López, O. A., Hernández, J. J., Del Re, G., and Puig, J. (2004a). "Reducción del riesgo sísmico en escuelas de Venezuela (in Spanish)." *IMME*, **42**(3): 33-56.

López, O. A., Hernández, J. J., Del Re, G., and Puig, J. (2004b). "Seismic risk in schools: The Venezuelan project." *Keeping schools safe in earthquakes, ad hoc experts' group meeting on earthquake safety in schools*, Paris, February 9-11, 88-100.

Lord, J.-F., Ventura, C. E., and Dascotte, E. (2004). "Automated model updating using ambient vibration data from a 48-storey building in Vancouver." *22th International Modal Analysis Conference (IMAC)*, Detroit, Michigan, January 26 - 29, 7 p.

Lu, K. C., Wang, Y., Lynch, J. P., Loh, C. H., Chen, Y. J., Lin, P. Y., and Lee, Z. K. (2006). "Ambient vibration study of Gi-Lu cable-stay bridge: application of wireless sensing units [6174-46]." *Proceedings - SPIE The International Society for Optical Engineering*, **6174**: 61741.

MathWorks, Inc. (2011). "Matlab (Version R2011a) [Software]".

McClure, G., Cappai, J., Shapiro, R., Li, M., Dunlop-Brère, G., and Keller, P. (2010). "Assessing the post-earthquake functionality of critical buildings in Montréal." *9th U.S. National and 10th Canadian Conference on Earthquake Engineering*, Toronto, ON, July 25-29, Paper No. 993.

McConnell, V. S. (2007). "Statewide seismic needs assessment: Implementation of Oregon 2005 Senate Bill 2 relating to public safety, earthquakes, and seismic rehabilitation of public buildings." State of Oregon, Department of Geology and Mineral Industries, Portland, OR. Available online at http://www.oregongeology.org/sub/projects/rvs/default.htm.

Meehan, J. F. (1985). "The Morgan Hill Earthquake of April 24, 1984: Effects on Hospitals and Public School Buildings." *Earthquake Spectra*, **1**(3): 575-577.

Meisl, C. S., Elwood, K. J., and Ventura, C. E. (2007). "Shake table tests on the out-of-plane response of unreinforced masonry walls." *Canadian Journal of Civil Engineering*, **34**(11): 1381-1392.

Mendes-Victor, L. A., Oliveira, C. S., Azevedo, J., Ribeiro, A., Elnashai, A. S., and Jeong, S. H. (2009). *Rapid probabilistic assessment of structural systems in earthquake regions*, The 1755 Lisbon Earthquake: Revisited, 1st ed., Springer Netherlands, Dordrecht.

Michel, C., Lestuzzi, P., Gueguen, P., and Bard, P. Y. (2010). "Comparison between seismic vulnerability models and experimental dynamic properties of existing buildings in France." *Bulletin of Earthquake Engineering*, **8**(6): 1295-1307.

Micromed S.p.A. (2011). "Grilla (Version 6.1) [Software]".

Mitchell, B. (2004). "Making schools safer: The New Zealand experience." *Keeping schools safe in earthquakes, ad hoc experts' group meeting on earthquake safety in schools*, Paris, February 9-11, 119-130.

Mitchell, D., Paultre, P., Tinawi, R., Saatcioglu, M., Tremblay, R., Elwood, K., Adams, J., and DeVall, R. (2010). "Evolution of seismic design provisions in the National Building Code of Canada." *Canadian Journal of Civil Engineering*, **37**(9): 1157-1170.

Mitchell, D., Tinawi, R., and Law, T. (1989). "The 1988 Saguenay earthquake - A site visit report." Canadian National Comittee on Earthquake Engineering, Open File Report #1999.

Montalvão, D., Maia, N., and Ribeiro, A. (2006). "A review of vibration-based structural health monitoring with special emphasis on composite materials." *The Shock and Vibration Digest*, **38**(4): 295-324.

Mujumdar, V., and McGavin, G. (1999). "Field Act public schools... A need for safety reviews." *Earthquake Spectra*, **15**(3): 585-596.

Nakamura, Y. (2000). "Clear identification of fundamental idea of Nakamura's technique and its applications." *12th World Conference on Earthquake Engineering*, Auckland, New Zealand, January 30 - February 4, Paper No. 2656.

NIBS (2003). "Hazus MH MR4 Technical Manual." National Institute of Building Sciences, Department of Homeland Security, Emergency Preparedness and Response Directorate, Washington, D.C.

NRC (2009). "Earthquakes Canada." Available online at http://earthquakescanada.nrcan.gc.ca/index-eng.php (September 1, 2009).

NRC (2010). "2010 Simplified seismic hazard map for Canada, Geological Survey of Canada." Available online at.

NRC/IRC (1990). "National Building Code of Canada 1990." National Research Council of Canada, Institute for Research in Construction, Ottawa, ON.

NRC/IRC (1992). "Manual for screening of buildings for seismic investigation." National Research Council of Canada, Institute for Research in Construction, Ottawa, ON.

NRC/IRC (2010a). "National Building Code of Canada 2010." National Research Council of Canada, Institute for Research in Construction, Ottawa, ON.

NRC/IRC (2010b). "User's Guide - NBC 2010 Structural Commentaries (Part 4 of Division B)." National Research Council of Canada, Institute for Research in Construction, Ottawa, ON.

NZSEE (2006). "Assessment and improvement of the structural performance of buildings in earthquakes." New Zealand Society for Earthquake Engineering, Wellington, New Zealand. Available online at http://www.nzsee.org.nz.

OECD (2005). "OECD Recommendation concerning guidelines on earthquake safety in schools,." Organisation for Economic Co-operation and Development, Paris, France. Available online at http://www.oecd.org/dataoecd/11/45/31968539.pdf.

Olshansky, R. B., and Wu, Y. (2004). "Evaluating earthquake safety in Mid-American communities." *Natural Hazards Review*, **5**(2): 71-81.

Oppenheim, A. V., and Schafer, R. W. (2010). *Discrete-time signal processing*, 3rd ed., Pearson, Upper Saddle River.

Pandey, B., and Ventura, C. E. (2010). "The BC seismic retrofit program - Lessons learnt and application of innovations." *9th US National and 10th Canadian Conference on Earthquake Engineering: Reaching Beyond Borders*, Toronto, ON, July 25-29, Paper No. 1047.

Prest, V. K., and Hode Keyser, J. (1962). "Surficial geology and soils, Montréal area, Québec." Department of Public Words, City of Montréal, Montréal, QC.

Proakis, J. G., and Manolakis, D. G. (1996). *Digital signal processing: Principles, algorithms, and applications*, 3rd ed., Prentice Hall, Upper Saddle River, N.J.

Rainieri, C., Fabbrocino, G., and Cosenza, E. (2010). "Some remarks on experimental estimation of damping for seismic design of civil constructions." *The Shock and Vibration Digest*, **17**(4-5): 383-395.

Revkin, A. C. (2008). "Earthquake in China highlights the vulnerability of schools in many countries." *The New York Times*, Available online at http://www.nytimes.com.

Rosset, P., Bour, M., and Chouinard, L. (2011). "Estimation and comparison of Vs30 microzonation maps for Montreal using multiple sources of information." *Submitted to Earthquake Spectra, December 2011*.

Saatcioglu, M., Shooshtari, M., and Foo, S. (2010). "Seismic screening of buildings in Canada." *9th U.S. National and 10th Canadian Conference on Earthquake Engineering*, Toronto, ON, July 25-29, Paper No. 1239.

Spence, R. (2004). "Strengthening school buildings to resist earthquakes: Progress in european countries." *Keeping schools safe in earthquakes, ad hoc experts' group meeting on earthquake safety in schools*, Paris, February 9-11, 217-228.

Structural Vibration Solutions A/S. (2010a). "ARTeMIS Extractor Handy (Version 5.0) [Software]".

Structural Vibration Solutions A/S (2010b). "User's guide to ARTeMIS Extractor Handy (Version 5.0)."

Taylor, G. W., White, T. W., and Ventura, C. E. (2006). "British Columbia school seismic mitigation program: performance-based school retrofit guidelines." *8th U.S. National Conference on Earthquake Engineering*, San Francisco, CA, April 18-22, 10 p.

Tinawi, R., and Mitchell, D. (1990). "1988 Saguenay earthquake. Damage to schools and post-disaster buildings." *Engineering in our Environment: CSCE Annual Conference and 1st Biennial Environmental Speciality Conference*, Hamilton, ON, May 16-18, 573-590.

Tischer, H. (2007). "Evaluation of dynamic effectiveness of building seismic retrofitting (in Spanish)." Escuela de Ingeniería Civil y Geomática, Universidad del Valle, Cali, Colombia. Available online at

Tischer, H., Marulanda, J., and Thomson, P. (2006). "Effect of the seismic retrofit on the dymanic properties of a building affected by the Pizarro earthquake (in Spanish)." *Ingeniería y Competitividad*, **8**(2): 101-111.

Tischer, H., Marulanda, J., and Thomson, P. (2007). "Comparison of three transforms for time-frequency distributions from their application to ambient vibration records (in Spanish)." *Ingeniería y Competitividad*, **9**(2): 21-32.

Tischer, H., Mitchell, D., and McClure, G. (2011). "Comparison of seismic screening methods for schools in a moderate seismic zone." *COMPDYN 2011, III ECCOMAS Thematic Conference on Computational Methods in Structural Dynamics and Earthquake Engineering*, Corfu, Greece, May 26–28, Paper No. 275.

Tobita, J., Fukuwa, N., and Yagi, S. (2000). "Experimental evaluation of dynamic characteristics of low and medium-rise buildings with soil-structure interaction." *12th World Conference on Earthquake Engineering (12WCEE)*, Auckland, New Zealand, January 30 - February 4, Paper No. 2244.

Trifunac, M. D. (1972). "Comparisons between ambient and forced vibration experiments." *Earthquake Engineering & Structural Dynamics*, **1**(2): 133-150.

Trifunac, M. D., Ivanovic, S. S., and Todorovska, M. I. (2001a). "Apparent Periods of a Building. I: Fourier Analysis." *ASCE Journal of Structural Engineering*, **127**(5): 517-526.

Trifunac, M. D., Ivanovic, S. S., and Todorovska, M. I. (2001b). "Apparent Periods of a Building. II: Time-Frequency Analysis." *ASCE Journal of Structural Engineering*, **127**(5): 527-537.

Van Overschee, P. (1993). "Subspace algorithms for the stochastic identification problem." *Automatica*, **29**(3): 649-660.

Varela-Rivera, J. L., Navarrete-Macias, D., Fernandez-Baqueiro, L. E., and Moreno, E. I. (2011). "Out-of-plane behaviour of confined masonry walls." *Engineering Structures*, **33**(5): 1734-1741.

Ventura, C. E., Taylor, G., White, T., Clement, G., Weichert, D., and Mill, A. (2004). "User guide for UBC-21 low-rise buildings, rapid seismic risk assessment software for British Columbia buildings." University of British Columbia, Vancouver, BC.